Universidad de Concepción

Facultad de Ciencias Naturales y Oceanográficas

Doctorado en Sistemática y Biodiversidad

STRESS MEMORY IN THE OFFSPRING OF *CHENOPODIUM QUINOA* WILLD (AMARANTHACEAE) EXPOSED TO NITROGEN DEFICIENCY

Tesis presentada a la Facultad de Ciencias Naturales y Oceanográficas de la Universidad de Concepción para optar al grado académico de Doctora en Sistemática y Biodiversidad.

POR: CATALINA JAVEIRA CASTRO OÑATE

PROFESORA GUÍA: LUISA BASCUÑAN GODOY

PROFESOR CO-GUÍA: TEODORO COBA DE LA PEÑA

Junio 2025

Concepción, Chile

AGRADECIMIENTOS

Quisiera agradecer a mi Directora de tesis, la Dra. Luisa Bascuñan-Godoy, por la guía en este proceso, no solo en el ámbito académico y profesional, sino también en lo personal. Gracias por la comprensión y paciencia durante este periodo, además del apoyo incondicional, y darme oportunidades y herramientas para desempeñarme en el futuro. También me gustaría agradecer a mi Co-Director, el Dr. Teodoro Coba de la Peña, por aceptar colaborar en este trabajo y su apoyo a la distancia.

Gracias a todos los miembros del Laboratorio de Fisiología Vegetal de la Universidad de Concepción por la ayuda que me brindaron y los desayunos que compartimos. En especial a Elizabeth, José, María Paz y Enrique por los aportes a este trabajo y el apoyo en cada momento.

Gracias a mi familia y amigos por el apoyo entregado estos 5 años. A mis padres Rosa y Hugo, que siempre me han apoyado en todo lo que me he propuesto, y a mis hermanos en especial a Constanza por el cariño y la contención en momentos de estrés. Quisiera agradecer a Solange y Dieter, amigos que han estado incondicionalmente subiéndome el ánimo y por todos los años de amistad que van. Finalmente, agradecer a mis mascotas, Simba y Emi por estar conmigo y mantenerme cuerda durante este proceso.

Este trabajo no hubiera sido posible sin el financiamiento de ANID Becas/Doctorado Nacional 21201031, ANID Fondecyt Regula 1220589 y ANID Fondecyt Regular 1211473.

TABLE OF CONTENTS

LIST OF TABLES

LIST OF FIGURES

RESUMEN

Las plantas han desarrollado variadas estrategias para lidiar con el estrés abiótico a lo largo de sus vidas, sin embargo, el estrés ambiental puede tener efectos duraderos, modificando positivamente las respuestas fisiológicas de las plantas a los siguientes episodios de estrés. Esto se ha denominado pre-acondicionamiento o memoria del estrés. Interesantemente, esta memoria puede incluso ser transmitida a su descendencia, denominándose "memoria inter o transgeneracional".

Chenopodium quinoa Willd (Amaranthaceae) es una especie que se caracteriza por una gran tolerancia a múltiples estreses, incluyendo el déficit de N. En esta tesis hipotetizamos que *C. quinoa* es capaz de transferir una "memoria" a su descendencia, inducida por déficit de N. Esta "memoria" es abordada través del estudio del fenotipo y características fisiológicas, bioquímicas y moleculares de plantas madre (F0) hacia su descendencia (F1 y F2) crecidas bajo condiciones óptimas (HN) y deficientes de N (LN).

Las plantas madre (F0) crecidas bajo condiciones de LN mostraron una reducción significativa de la fotosíntesis y un incremento de la disipación térmica de la energía, que se asoció con reducciones del rendimiento. Además, se observaron cambios en la composición metabólica de las semillas, que se asociaron a una germinación acelerada comparada a semillas provenientes de plantas crecidas a HN.

Respecto a las respuestas biométricas y fisiológicas de las plántulas F1 (hijas), descendientes de plantas LN y crecidas en LN ($LN_{F0}LN_{F1}$), estas presentaron una mayor biomasa y número de raíces secundarias, lo que se relacionó positivamente con un aumento en la fotosíntesis y conductancia estomática. Al igual que en F1, las descendientes de LN en F2 (nietas) presentaron una mayor biomasa área y radicular cuando fueron crecidas en LN, sin distinción de en qué condición crecieron sus respectivas madres (F1) ($LN_{F0}HN_{F1}LN_{F2}$ o $LN_{F0}LN_{F1}LN_{F2}$). Interesantemente, en F2 si bien no se

observaron cambios en la fotosíntesis, la reducción de la disipación térmica y aumento de la eficiencia fotoquímica (también observado en F1) sugieren un ajuste transgeneracional en los mecanismos de uso y disipación de la energía.

Estudios metabólicos adicionales en F1 y F2 indicaron un mayor contenido de almidón, terpenos, lípidos y flavonoides en plántulas descendientes de LN, sugiriendo una mayor ganancia de C por unidad de N que las plantas descendientes de HN. Los cambios en F2 no mostraron distinción de la condición de N de la F1, sugiriendo que el ambiente ancestral (plantas abuelas) y no sólo el materno, están jugando un papel clave en el desempeño de la descendencia.

Finalmente, identificamos genes diferencialmente expresados influenciados predominantemente por las condiciones de N de la F0. Entre estos se genes relacionados con la adquisición de N y metilación del ADN (*NRT1.1*, *GLR2.1*, *SAM-dependent MTasa*, *QR*, *E2F TF3* y *GRAS*), los cuales se encuentran up-regulados en la descendencia de madres crecidas a LN_{F0} en ambas generaciones (F1 y F2). Los cambios de expresión de estos genes fueron relacionados con las modificaciones fisiológicas a través de las generaciones. Adicionalmente, a través del estudio de redes de coexpresión se sugieren genes regulatorios clave que modulan la expresión de genes relacionados a la persistencia y reversión de la memoria.

En conjunto, los resultados de esta tesis demuestran un desempeño diferencial entre la descendencia de plantas F0 crecidas a HN o LN. Concluimos que *C. quinoa* es capaz de transmitir una "memoria del estrés" a su descendencia, modulando sus respuestas fisiológicas, metabólicas y de expresión de genes, con implicancias en su resistencia frente a condiciones limitantes de N.

ABSTRACT

Plants have developed various strategies to cope with abiotic stress throughout their lives; however, environmental stress can have lasting effects, positively modifying the physiological responses of plants to subsequent stress episodes. This phenomenon known as preconditioning or stress memory. Interestingly, this memory can even be transmitted to their offspring, referred to as "intergenerational" or "transgenerational" stress memory.

Chenopodium quinoa Willd. (Amaranthaceae) is a species known for its high tolerance to multiple stresses, including N deficit. In this thesis, we hypothesize that *C. quinoa* is able of transfer a "stress memory" to its offspring, induced by N deficiency. This "stress memory" is addressed through the study of the phenotype and physiological, biochemical, and molecular traits of mother plants (F0) and their progeny (F1 and F2) grown under optimal (HN) and deficient (LN) N conditions.

The mother plants (F0) grown under LN conditions showed a significant reduction of photosynthesis and an increase in thermal dissipation, which was associated with yield reductions. In addition, changes in the metabolic composition of seeds were observed, which were associated with accelerated germination compared to seeds from plants grown at HN.

Regarding the biometric and physiological responses of F1 seedlings (daughters), descendants of LN plants grown in LN ($LN_{F0}LN_{F1}$) presented a greater biomass and higher number of secondary roots, which were positively related to increased photosynthesis and stomatal conductance. Similarly, in the F2 generation (granddaughters), descendants of LN plants also showed greater shoot and root biomass when grown at LN, regardless of N conditions of their respective mother (F1) were grown ($LN_{F0}HN_{F1}LN_{F2}$ or $LN_{F0}LN_{F1}LN_{F2}$). Interestingly, in F2 although no changes in photosynthesis were observed, the reduction in thermal dissipation and the increase in

photochemical efficiency (also observed in F1) suggests a transgenerational adjustment in energy use and dissipation mechanisms.

Additional metabolomic studies in F1 and F2 highlighted a higher starch, terpene, lipid and flavonoid content in seedlings descended from LN plants, suggesting a greater C per unit of N than those descended from HN plants. The changes observed in F2 did not vary according to N condition of F1, suggesting that the ancestral environment (grandmother plants), and not only the maternal environment is playing a key role in offspring performance.

Finally, we identified differentially expressed genes predominantly influenced by F0 N conditions. These include genes related to N acquisition and DNA methylation (*NRT1.1*, *GLR2.1*, *SAM-dependent MTasa*, *QR*, *E2F TF3* and *GRAS*), which were up-regulated in the offspring of LN_{F0} mother plants in both generations (F1 and F2). The changes in the expression were related to physiological responses across generations. Additionally, through co-expression networks studies, key regulatory genes that modulate the expression of genes related to memory persistence and reversion were suggested.

Taking together, the findings of this thesis reveal a differential performance between the offspring of F0 plants grown at optimal (HN) or low nitrogen (LN) conditions. These results support the conclusion that *C. quinoa* is capable of transmitting a "stress memory" to its progeny, modulating their physiological, metabolic, and transcriptomic responses. This inherited memory enhances the offspring's capacity to cope with N deficient environments.

INTRODUCTION

Transgenerational memory in plants

Plants must respond to adverse biotic and abiotic conditions of the local environment, adjusting their physiological responses (acclimation) to cope with environmental stresses. Most of these stresses are transitory, like extreme temperatures, drought, insect attack or microbial infections, and once these finish, plants can recover and re-establish their physiological parameters. However, several environmental stresses have lasting effects in the plant, positively modifying its physiological response to following stress episodes, which have been called **pre-conditioning** and/or **stress memory** (Bruce et al., 2007). This stress memory can be extended even to the descendance, where the term "**transgenerational memory**" or "**transgenerational plasticity**" has been used. Here, the environmental condition of the ancestors affects the performance of the offspring to a specific stress. This could enable plants to anticipate environmental stresses

based on ancestors' experiences enhancing survival and reproductive success of the descendants (Lämke and Bäurle, 2017; Kambona et al., 2023).

Diverse mechanisms have been proposed to explain this responses: 1) Epigenetic changes associated to methylation and acetylation of DNA and histones, that modify genetic expression levels without altering the DNA sequence; 2) Accumulation of signaling proteins or transcription factors, where the result is changes in the abundance of transcriptions; 3) Memory mechanisms mediated by symbionts; and 4) Sustained alterations in metabolite levels (Bruce et al., 2007; Gamir et al., 2014; Gundel et al., 2017). The metabolic levels as a mediator of pre-conditioning has been largely unexplored, despite that a large part of the metabolism is affected by stress conditions (Herman and Sultan, 2011, Pissolato et al., 2024).

There is known that plants show a distinctive response to subsequent stress compared to the first time, and specific genes related to stress response pathways, hormone signaling and transcription factors are activated more quickly and strongly in plants with stress memory (Alves de Freitas Guedes

et al., 2019). The long-term memory refers to the maintenance of stress-responsive genes in a partially activated state after the stress is removed, enabling a faster and more robust reactivation upon subsequent exposure. Understanding how gene expressions respond to environmental conditions across generations is crucial for knowing the molecular basis of plant stress adaptation.

The adaptative value of transgenerational effects has been a discussion and controversy topic in the last few years, since they can remain if the stress conditions persist, but they can revert if the stress dissipates (Lämke and Bäurle, 2017). In fact, “transgenerational memory” overlaps with the concept of maternal effect, known for decades and define as the effects of paternal (generally maternal) environmental stress on the size and development of the descendance. Quantitative geneticists interested in plant breeding and evolutionary biologist that study change by natural selection, they considered that these induced hereditary effects were “a frequent and often problematic source of environmental similarity" (Falconer, 1981) that masked genetically inherited variants. This vision of

transgenerational environmental effects as a “concern” lead to the design of experiments that minimized the chance to detect those effects, that were treated as experimental error. This approach shifted in the end of the 80s and 90s, when a series of fundamental reviews and empirical researches re-conceptualized these effects as a transgenerational form of individual phenotypical plasticity, and, therefore, a source of potential ecological variation and of evolutionary significance (Donohue and Schmitt, 1998; for a general description of studies in plants and animals, see Mousseau and Fox, 1998; Roach and Wulff, 1987; Sultan, 1996). The multigenerational approach has led to a differentiation between intergenerational and transgenerational memory, where intergenerational memory is directly transmitted from the parents to the first-generation, and the transgenerational memory becomes evident after a stress-free generation (Kambona et al., 2023; Pissolato et al., 2024).

Transgenerational memory has been described in various organisms facing different types of stress. Yin et al. (2019) analyzed 139 published papers on annual and perennial plants, and vertebrate and invertebrate animals,

revealing a positive transgenerational effect, suggesting that ancestral environments generally improve offspring performance. Interestingly, they found that transgenerational effects under stressful conditions were strongly positive only in annual plants and invertebrates, where these types of organisms had a greater capacity to generate transgenerational memory. Specific examples of transgenerational memory in animals have been reported, for example, in *Pocillopora damicornis*, where the high temperature negatively affected adult performance, offspring larvae had better metabolic performance when exposed to heat, than those from non-stressed parents (Putnam and Gates, 2015).

Recent studies have shown different strategies about how plants retain stress memory across generations. In the offspring of mother plants of *Arabidopsis thaliana* and *Solanum lycopersicum* subjected to herbivory exhibit resistance to this stress, associated with jasmonic acid (JA) -dependent defense responses (Rasmann et al., 2012). Other examples have been observed in *Oryza sativa* L., where mother plants exposed to high concentrations of heavy metals inherit a greater resistance capacity to their offspring through

upregulation of genes associated with ion transport and sequestration (Cong et al., 2019). Other work in rice links nitrogen (N) deficiency with changes in DNA methylation in offspring, resulting in an increased ability to grow under conditions of low N availability (Kou et al., 2011). Lamelas et al. (2024) investigated the transgenerational memory of cross tolerance between drought and heat stress, demonstrating that seedlings from previous stress generation retain key protein that contributed to heat stress tolerance. Seeds from stressed parents displayed differential gene expression, particularly microRNAs and stress-responsive genes, along with higher levels of starch and secondary metabolites, which may function as biomarkers for stress memory. López et al. (2024) studied the epigenomic and transcriptomic persistence of stress memory in *Fragaria vesca*, revealing that heat-stress induces DNA methylation changes, which were linked to transcriptional alterations in stress-response genes. The review by Avramova (2019) provides strong evidence that plant stress memory is regulated by transcriptional and epigenetic mechanisms, mainly through the abscisic acid (ABA) and JA signaling pathways.

Different studies have highlighted the importance of transcription factors not only in the initial stress response, but also in how stressful experiences are remembered and transmitted to future generations.

Research on both intergenerational and transgenerational memory related to N limitation has been scantily documented. In *Arabidopsis thaliana*, it has been shown that exposure to multigenerational stress enhances the nitrate uptake ability, triggering a suite of responses to N-deficiency (Massaro et al., 2019). Additionally, Liu et al. (2021) showed cross-stress effects, demonstrating that progeny from water-stressed plants exhibited increased resistance to N starvation compared to offspring from well-watered plants. Zhao et al. (2024) transcription analysis showed upregulation of N transport-related proteins to increase the N absorption of plants, and found various transcription factors including *GRAS*, *MYB*, and *WRKY* upregulated to enhanced N uptake by expanding root absorption area. Also, *WRKY* transcription factors are crucial for defense responses in plants (Bakshi and Oelmüller, 2014), while other key transcription factors such as *Cytokinin response factors* (*CRFs*) are important in regulating plant development in

response to oxidative stress and redox status (Gentile et al., 2024). Li et al. (2022) examined transgenerational plasticity in gene expression of *Thlaspi arvense* under cadmium stress. It was found that certain genes, in the second generations, maintained similar expression levels to those observed in Cd-stressed parental plants, even under non-stress conditions. This sustained expression pattern suggests a potential role in transgenerational memory.

In plants, changes at the transcriptomic and epigenetic level have been widely reported in many species. However, the metabolic level as a mediator of pre-conditioning and transgenerational memory has remained largely unexplored, despite the fact that much of the metabolism is altered during stress. The identification of metabolic pathways, associated to gene expression patterns and their link to environmental stress response is crucial to understanding the molecular and biological processes underpinning transgenerational memory (Fraire-Velázquez and Balderas-Hernández, 2013; Krasensky and Jonak, 2012; Schmidt and Baldwin, 2006).

Nitrogen metabolism in plants

Nitrogen (N) is a vital nutrient for plants, since it plays an important role in metabolism during seed germination, seedling establishment, development and senescence (Gaufichon et al., 2010; Marschner, 2012). It is considered a macronutrient and forms part of amino acids, proteins, nucleic acids, phospholipids and pigments like chlorophyll, among other molecules, and it's a limiting factor in growth and plant yield (Moll et al., 1982; O'Brien et al., 2016).

N is absorbed by roots in plants mainly in its inorganic forms like nitrate (NO_3^-) and ammonium (NH_4^+), which represent a 2% of soil N. This absorption occurs through N transporters located in plasma membrane, to then be incorporated into amino acids and/or distributed to the rest of the plant (Crawford and Forde, 2002).

N uptake is carried out through an active transport system at root level. For both NO_3^- and NH_4^+, there are 2 types of transporters, classified on its N affinity: Low and High (Rawat et al. 1999; Wang et al., 1993). Low Affinity

Transporters (LATs) have constitutive expression and are up regulated when there is a high external N concentration (>0.5 mM). NO_3^- transporters correspond to the *NRT1* family and NH_4^+ transporters, to the *AMT2* family (Raven and Farquhar, 1981; Von Wirén et al., 1997; Wang et al., 1993). High Affinity Transporters (HATs) allow N transport when it's at a low external concentration (<0.5 mM) and its expression is inducible in external N presence. HATs for NO_3^- are form the *NRT2* family, and for NH_4^+, the *AMT1* family (Ullrich et al., 1984; Lee and Rudge, 1986; Mäck and Tischner, 1994; Wang et al., 1993; Kronzucker et al., 1998; Gazzarini et al.,1999; Rawal et al., 1999; Miller et al., 2007).

The assimilation process followed the N uptake by the roots, where N is incorporated into organic molecules. This process occurs in roots, stems, and leaves and involves various enzymes such as nitrate reductase (NR, EC 1.7.99.4), which catalyzes a cytoplasmic reaction to reduce nitrate to nitrite (NO_2^-). NO_2^- is then translocated to the chloroplast where it is reduced to NH_4^+ by the enzyme nitrite reductase (NiR, EC 1.7.2.1). Finally, NH_4^+ is assimilated in the glutamine synthetase/glutamate synthase cycle

(GS/GOGAT; EC GS 6.3.1.2; EC GOGAT 1.4.7.1) in the chloroplasts (Lea and Forde, 1994; Liss and Slater, 1974). While NO_3^- needs to be transformed by NR and NiR to be assimilated into amino acids, NH_4^+ is directly transported to different organs of the plant by the xylem to become part of proteins, and/or assimilated by the GS-GOGAT cycle (Lea and Miflin, 2011).

Interestingly, more than half of the total N content in the leaves of C3 plants is stored as the chloroplast protein RuBisCO, which is the most important and abundant protein determining CO_2 fixation (Mu et al., 2018). This is reflected in the strong correlation between CO_2 fixation and plant productivity (Masclaux-Daubresse et al., 2010).

The RuBisCO protein plays another central role in N metabolism that occurs during senescence, the final stage of plant development (Gan and Amasino, 1997; Shahri, 2011). Here, chloroplast dismantling impacts RuBisCO degradation and, consequently, CO_2 fixation, remobilizing more than 70% of the captured N (Marek and Stewart, 1992). N remobilization is essential for the reassimilation processes associated with seed filling. During this process,

nutrients stored as proteins in the RuBisCO enzyme and other proteins that make up photosystem II (PSII) in mature leaves are mobilized to the remaining organs and to the seeds or grains of the plant (Bascuñán-Godoy et al., 2018a).

Environmental stress conditions, such as low nitrogen content, could induce accelerated senescence, reducing the time for nutrient mobilization and resulting in deterioration of seed yield and quality (Masclaux-Daubresse et al., 2010).

Physiological Responses to N Deficit

Plants employ a wide variety of strategies to cope with N deficiency or heterogeneity in the soil. These strategies include morphological, biochemical, and molecular responses, including altered root architecture, decreased chlorophyll production, changes in N distribution within the plant, and induction of early senescence (Chapin et al., 1987; Ciampitti et al., 2013). Changes in root architecture are very important, as has been observed in

various species, including *Arabidopsis* and maize, which increase root length (in search of the nutrient) and increase the number of secondary roots in N patches (Crawford and Forde, 2002). These changes in root biomass and architecture, the regulation of the expression of high-affinity NO_3^- and NH_4^+ transporters, and of assimilation-related enzymes (NR, NiR, GS, and GDH) play a key role in the efficiency of N assimilation under conditions of low N availability (Gu et al., 2013; Krapp et al., 2011). NH_4^+ re-assimilation contributes significantly to N balance under low N conditions, where the enzyme GS catalyzes its incorporation into glutamine. The GS overexpression promotes physiological improvements in photosynthesis and growth under N-limiting conditions (Fuentes et al., 2001; Masclaux-Daubresse et al., 2010).

Under N-deficit conditions, many plants undergo proteolysis with the consequent release of NH_4^+ (Liu and von Wirén, 2017). The incorporation of NH_4^+ into amino acids and other nitrogenous compounds is very important to avoid toxicity, therefore, an increase in compounds such as amino acids, especially Glutamine and Proline, and others such as Betalains and

anthocyanins has been observed under stress conditions (Li et al., 2019; Naing and Kim, 2021). The incorporation of NH_4^+ into organic compounds is related to the cytosolic isoform of GS and not chloroplast, since N deficiency causes accelerated senescence and dismantling of chloroplasts. It should be noted that N deficiency affects all components of the seeds and their size, volume and weight characteristics (Fenner, 2010; Brevedan, 1980).

Nitrogen and Seed Germination

Reserve materials play a vital role in plant life (Soriano et al., 2011), and germination is affected by their use and storage (Bewley, 1997; Borisjuk et al., 2004; Fait et al., 2006). From a plant nutritional perspective, deficiencies in important macronutrients such as nitrogen cause changes in endosperm structure, influencing seed moisture and seed coat thickness, and, therefore, later germination stages (Wen et al., 2017).

During the early germination stage, N is necessary to meet the seed's amino acid requirements for protein synthesis (Soriano et al., 2011). Some studies on *Cupressus sempervirens* (common cypress) and black pine have shown

that seed N content stimulates germination speed (Caliskan and Makineci, 2015, 2020). N content has also been shown to promote germination in Mediterranean species, such as *Pinus halapensis*, which have limited seed reserve materials (Broncano et al., 1998; Thanos and Rundel, 1995). Other authors determined that the relationship between N and germination percentage in corn seeds is because proteins can absorb more water than polysaccharides and lipids, promoting seed germination (Bedi et al., 2009; Hara and Toriyama, 1998). Early seed germination is often advantageous in competitive environments for nutrient acquisition, allowing seeds to reach available nutrients before other competitors (Caliskan and Makineci, 2020). However, how seed N content affects performance in later plant stages has been poorly reported.

Chenopodium quinoa **Willd (*Amaranthaceae*) as a biological model of transgenerational resistance**

Chenopodium quinoa Willd (quinoa) is a pseudocereal of the *Amaranthaceae* family and *Chenopodiaceae* subfamily. It is cultivated primarily in the Andean regions of South America. It is characterized by its high nitrogen use

efficiency and high tolerance to various types of abiotic stress, such as low temperatures, soil salinity, and aridity (Bascuñán-Godoy et al., 2016). Furthermore, quinoa has been selected by the Food and Agriculture Organization of the United Nations (FAO) as a crop that will provide food security for this century. This is due to its high protein content, in addition to its presence of all the essential amino acids (Abugoch, 2009; Bazule et al., 2014; INIA, 2015; Nowak et al., 2016).

There is a great diversity of quinoa genotypes that can be classified into five specific agroecological zones: Sierra (also known as Altiplano type); Inter-Andean Valleys (with a cold semi-dry climate, rainfall of 450–600 mm, and temperatures ranging from 4 to 15˚C); Yungas (cultivated under tropical conditions); Salares (high-altitude salt lakes characterized by growth under limited annual rainfall (150–300 mm)); and Coasts/Lowlands (where annual rainfall ranges between 500 and 1500 mm) (Bazile et al., 2014; Martínez et al., 2009). Among these ecotypes, coastal/lowland varieties are particularly important due to their wide longitudinal geographic expansion, which allows for greater adaptation to photoperiod, making them highly suitable for the

spread of quinoa cultivation in different climatic areas (Bendevis et al., 2014; Jacobsen et al., 1997; Jacobsen and Stølen, 1993). In fact, Chilean coastal landraces were used as elite accessions for European quinoa breeding programs (Jacobsen et al., 1997; Jacobsen and Stølen, 1993).

Berti et al. (2000) worked with two Chilean landraces, Faro and UdeC9, at different N concentrations (using $NaNO_3$ as the source): High, Sufficient, Moderate-Low, and Very Low (225, 150, 75, and 0 kg ha^{-1}, respectively). At high N supply (150 N kg ha^{-1}), Faro showed a nitrogen use efficiency (NUE), defined as the yield produced per unit of N applied, of 30 kg kg^{-1}, similarly to that reported for other described varieties and landraces. At moderately low N supply (70 kg kg^{-1}), Faro's NUE increased to 56.5 kg kg^{-1}, while other varieties and landraces remained at 30 kg kg^{-1}, despite changes in N supply. Considering these values for the breed varieties, it is interesting that Faro, a genotype from South-Central Chile, showed a large increase in NUE at moderate and low nitrogen levels. Currently, the information available on quinoa NUE is very limited, and the description of the physiological,

biochemical, and molecular processes underlying the contrasting NUE values for different varieties is in its initial stages.

In quinoa seeds, the embryo surrounds the perisperm (originating in the nucellus, 2n), while the endosperm is minimal (Burrieza et al., 2014; López-Fernández and Maldonado, 2013). N (as proteins and amino acids) is mainly stored in the embryo, while carbon (as starch) is stored in the perisperm (Gargiulo et al., 2019). Under Low Nitrogen (LN) conditions, the fate of seed N in proteins or free amino acids differs between genotypes (Bascuñán-Godoy et al., 2018b). Under LN, mature Faro seeds had reduced protein content and increased free amino acids (compared to High Nitrogen (HN)), whereas UdeC9 increased proteins and strongly reduced free amino acids (Bascuñán-Godoy et al., 2018b). However, the effect of LN on germination or how these changes might affect tolerance to N limitation during establishment or development has not been studied.

The inherited ability to withstand low nitrogen availability in daughter plants from mothers raised under LN conditions has been reported in *O. sativa* L.,

where they link N deficiency with changes in DNA methylation in the offspring, resulting in an increased ability to grow under N-limiting conditions (Kou et al., 2011). However, in *C. quinoa*, there is no history of transgenerational memory that helps offspring cope with stressful conditions experienced by the mother plants.

Considering the robust capacity to cope with low N availability of the Faro genotype of *C. quinoa*, we wondered whether reduced N supplementation in mother plants conditions the offspring to better physiological performance under N-limiting conditions.

Hypothesis:

Mother plants of *C. quinoa* subjected to N deficiency are capable of transferring a "stress memory" to their descendants, enhancing their nitrogen utilization compared to the offspring of mother plants grown under optimal N conditions.

Prediction:

Maternal N deficiency modulates the physiological performance of their descendants, expressed through phenotypic, metabolic and transcriptomic adjustments.

General aim:

Determine the presence of "stress memory" in the offspring of *C. quinoa* plants grown at N-deficiency conditions, using physiological, metabolic and molecular approaches.

Specific objectives:

1. To study the effect of N availability in the physiological characteristics of mother plants (F0) and its impact on seed metabolic composition and germination (F1 and F2): Chapter 1 and Chapter 2
2. To evaluate the effects of maternal N conditions in the physiology, biochemic and metabolic profile of their offspring (F1 and F2) during establishment stage: Chapter 2
3. To study the transcriptomic profile of seedlings (F1 and F2) descendants of mother plants grown at HN and LN: Chapter 3

4. To establish relations between results to elucidate the effects of nitrogen deficiency on potential intergenerational (F1) and transgenerational (F2) memory: Integration of Chapter 1, 2 and 3

CHAPTER 1:

Intergenerational stress memory at establishment stage: Effects of maternal N on offspring first stages of development

Nitrogen Stress Memory in Quinoa: Maternal Effects on Seed Metabolism and Offspring Growth and Physiology

Authors and addresses:

Catalina Castro[1], Javiera Rojas[1], José Ortíz[1], Rodrigo Sanhueza-Lepe[1], Alexander Vergara[2], Francisco Poblete[1], Elizabeth Escobar[1], Teodoro Coba de la Peña[3], Enrique Ostria-Gallardo[1], Luisa Bascuñan-Godoy[1]

[1]Laboratorio de Fisiología Vegetal, Departamento de Botánica, Facultad de Ciencias Naturales y Oceanográficas, Universidad de Concepción, Concepción, Chile

[2]Department of Plant Physiology, Umeå Plant Science Centre, Umeå University, Umeå, SE, Sweden

[3]Laboratorio de Recursos Naturales y Fitorremediación, Centro de Estudios Avanzados en Zonas Áridas (CEAZA), La Serena, Chile

Manuscript published in Physiologia Plantarum:

Castro, C., Rojas, J., Ortíz, J., Sanhueza-Lepe, R., Vergara, A., Poblete, F., Escobar, E., Coba de la Peña T., Ostria-Gallardo, E., Bascuñan-Godoy, L. (2024). Nitrogen Stress Memory in Quinoa: Maternal Effects on Seed Metabolism and Offspring Growth and Physiology. *Physiol Plant.* 176(6):e14614. doi: 10.1111/ppl.14614. PMID: 39513412.

ABSTRACT

Plants have developed various strategies to deal with abiotic stress throughout their lifetimes. However, environmental stress can have long-lasting effects, positively modifying plant physiological responses to subsequent stress episodes, a phenomenon known as preconditioning or stress memory. Intriguingly, this memory can even be transmitted to offspring, referred to as “inter- or transgenerational memory”.

Chenopodium quinoa is a pseudocereal that can withstand several abiotic stresses, including nitrogen (N) limitation. This research highlights the critical role of maternal N conditions in shaping the physiological and metabolic responses of their offspring. Mother quinoa plants (F0) were grown under High N (HN) or Low N (LN) conditions. LN_{F0} plants exhibited lower panicle biomass, net photosynthesis, and yield compared to HN_{F0} plants. Seeds from LNF0 retained proteins, reduced amino acids’ levels, and increased lipids (such as PI 34:2), especially phosphatidylcholines, and their

unsaturation level, which was associated with faster germination compared to HN_{F0} seeds. Offsprings seedlings (F1) grown under either HN or LN had similar proteins and amino acid proportions of their seeds. However, $LN_{F0}LN_{F1}$ seedlings displayed significantly higher biomass and number of root tips. These changes were significantly correlated with transpiration, net photosynthesis, and stomatal conductance, as well as with starch content, suggesting higher CO_2 fixation at the whole plant level in $LN_{F0}LN_{F1}$ plants.

Our findings suggest that quinoa transmits maternal environmental stress information to its offspring, modulating their resilience. This work underscores the potential of utilizing maternal environmental conditions as a natural priming tool to enhance crop resilience against nutritional stress.

Keywords: Nitrogen stress, Stress memory, imprinting, metabolomic memory, Seed germination, Lipids, Offspring tolerance

INTRODUCTION

It is well-established that stressed plants can undergo metabolic and genetic changes to resist various stresses. Furthermore, recent studies have indicated that traits of stressed plants can be transmitted to the next generation. This "stress memory" involves positive changes in the offspring, enhancing their resistance to stresses experienced by the mother plants (Herman and Sultan, 2011; Holeski et al., 2012, Sharma et al., 2023). Among the most studied mechanisms of this response are epigenetic modifications, such as histone acetylation and DNA methylation. However, other mechanisms may also play a role in the inheritance of stress memory, including the alterations of metabolic profile and metabolite levels (Bruce et al., 2007; Gamir et al., 2014; Gundel et al., 2017, Kambona et al., 2023, Siddique et al., 2024). Despite the significant impact of stress conditions on metabolite levels, the role of the metabolic profile as a mediator of preconditioning remains underexplored (Herman and Sultan, 2011).

Nitrogen (N) is a critical macronutrient for plants, and its deficiency constitutes one of the most significant abiotic stress factors for plant development (Ye et al., 2022). Research on both intergenerational and transgenerational memory related to N limitation has been scantily documented. In *Arabidopsis thaliana*, it has been shown that exposure to multigenerational stress enhances the nitrate uptake ability, triggering a suite of responses to N-deficiency (Massaro et al., 2019). Additionally, Liu et al. (2021) showed cross-stress effects, demonstrating that progeny from water stressed plants exhibited increased resistance to N starvation compared to offspring from well-watered plants.

Several authors studying drought stress memory in various plant species, including *Arachis hypogaea* L. (Racette et al., 2020), *Brassica napus* L. (Hatzig et al., 2018) and *Triticum aestivum* L. (Wang et al., 2018), have suggested that the increased stress tolerance in progeny might be linked to metabolite changes at the seed level, particularly involving shifts in fatty acid patterns. It is well-established that seed lipid concentrations and fatty acid compositions are influenced by various abiotic environmental factors such as

temperature, CO_2 concentration, and nutrient availability (Thomas et al., 2003; Edwards and Hertel, 2011; Rondanini et al., 2011; Trentacoste et al., 2012; McNaughton et al., 2015). For example, in sunflowers, an increase in oleic acid and a reduction in linoleic acid has been observed in seeds when mother plants were subjected to high temperatures during seed filling, affecting germination performance (Izquierdo and Aguirrezabal, 2008).

Considering that N plays a central role in plant metabolism, understanding how N affects maternal plant performance and thus, seed development, carbon (C) allocation and storage, metabolic profile, and performance is crucial to better understand N stress tolerance in offspring.

Chenopodium quinoa Willd. (Amaranthaceae), a pseudocereal native to the Andean regions of South America, has demonstrated considerable resilience to numerous abiotic stresses, including a notable tolerance to N deficiency (Bascunan-Godoy et al., 2018). Quinoa seeds have remarkable nutritional properties that include high protein content and the presence of all essential amino acids. This has led to its selection by the FAO as a crop with significant

potential to contribute to global food security (Abugoch, 2009; Bazule et al., 2014; INIA, 2015; Nowak et al., 2016). Considering its role in food security, the potential for enhancing N deficit resistance through intergenerational memory in quinoa is of high importance.

To explore the potential inheritance of stress memory in quinoa, this study examined how N deficiency in mother plants affects the metabolomic pattern of seeds, and growth and physiological traits in offspring. We hypothesize that mother plants subjected to N deficiency transfer environmental information to their offspring enhancing performance when facing N deficit. Our results provide valuable insights into nitrogen dynamics and related tolerance in offspring of quinoa under stress conditions.

MATERIAL AND METHODS

Plant material and growth conditions of mother plants (F0)

Faro, a lowland quinoa genotype known for its high Nitrogen Use Efficiency (NUE; Bascuñan-Godoy et al., 2018) was selected for this study. Seeds were obtained at the National Institute of Agriculture Research (http://163.247.128.32/gringlobal/search.aspx, INIA-Intihuasi Vicuña, Chile), previously collected in summer in Chillan at "El Nogal Experimental Station" (36_35' 43.2" S, 72_04' 39.9" Wand 140 m.a.s.l) of Central Chile.

The experiments were conducted in pots from September 2021 until February 2022 under greenhouse conditions. The environmental conditions were: 1200 μmol m-2 s-1 PAR at noon (natural light), maximum and minimum temperatures (daily ranges) of 23 °C and 17 °C, respectively, 12 h day length, and 80% relative humidity. Seeds were directly germinated in pots of 10 L filled with 5 kg of substrate consisting of 80% sand and 20% perlite. Three

supplementations with modified MS culture medium (Murashige and Skoog, 1962) without N were administrated: initially at sowing, subsequently when plants developed 4 true leaves, and finally at the 8-true-leaf stage. The substrate was supplemented with NH_4NO_3 to reach two N-level treatments at the same times as the MS supplementation: high nitrogen (HN_{F0}: 0.6 g of N per pot), which is the optimal N level for quinoa growth, and low nitrogen (LN_{F0}: 0.3 g N per pot) (See Pinto-Irish et al., 2020 for details about optimal and deficient N level for quinoa growth). Plants (one per pot of 10 L) were irrigated to field capacity with water every three days, maintaining optimal soil moisture until the seed maturation stage. The experiment was conducted using a completely randomized design, with additional plants placed to mitigate border effects. Measurements of biomass, gas exchange, and chlorophyll *a* fluorescence parameters were performed after two weeks of panicle initiation (December, grain filling stage). Yield measurements were taken at the end of the life cycle (3 weeks after panicle initiation).

Offsprings (F1 seedling) growth conditions

Offsprings (F1 seedlings) were grown in 1 L pots within a growth chamber configured to simulate the greenhouse conditions mentioned above. The growth chamber was provided with LED lamps that closely replicate the sunlight spectrum to minimize differences between generations. Set conditions were: 700-800 μmol m^{-2} s^{-1} PAR, maximum and minimum temperatures of 25 °C and 17 °C, respectively, 16/8 h day/night, and 80% relative humidity. Seeds were germinated directly in the substrate (1 kg, same as the F0). At sowing, one supplementation of modified MS culture medium (Murashige and Skoog, 1962) without N was applied. The soil in the pots was supplemented with NH_4NO_3 as N source, one supplementation at sowing, to reach two N-level treatments: high nitrogen (HN: 0.6 g of N per pot), which is the optimal N level for quinoa growth, and low nitrogen (LN: 0.3 g N per pot); and 4 groups conditions were obtained: 1) Offspring of HN mother plants, grown at HN ($HN_{F0}HN_{F1}$); 2) Offspring of HN mother plants, grown at LN ($HN_{F0}LN_{F1}$); 3) Offspring of LN mother plants, grown at HN ($LN_{F0}HN_{F1}$); and 4) Offspring of LN mother plants, grown at LN ($LN_{F0}LN_{F1}$). Plants (one per pot of 1 L) were irrigated at field capacity every three days with water to maintain optimal soil moisture until they had 4 true leaves (~20

days of growth). At this time, measurements were performed, and samples were collected.

Biomass and yield

The dry weight of leaves, panicles and roots was determined by drying the tissue at 60 °C for 48 h until a constant weight was reached. Grain yield was determined as the total grain weight per plant at the end of the growth season.

Gas exchange measurements

Photosynthetic gas exchange measurements were conducted in healthy, fully expanded leaves (third leaf from the top) using a CIRAS-2 infrared gas analyzer system (PP SYSTEMS). Leaves were first equilibrated at a photon density flux of 1,200 μmol m^2 s^{-1} (slightly higher than light saturation point) for at least 10 min. CO_2 concentration was set at 400 ppm. Leaf temperature was maintained at 28 °C, and the leaf-to-air vapor pressure deficit was kept

between 1 and 1.3 kPa. Under these chamber conditions, we determined net photosynthesis (Pn), stomatal conductance (g_s), and intrinsic water use efficiency (iWUE). iWUE was calculated as the ratio Pn/g_s.

Chlorophyll fluorescence measurements

Chlorophyll (Chl) fluorescence measurements were conducted with a portable fluorimeter (FMS 2, Hansatech Instruments Ltd., Norfolk, United Kingdom). Leaves from plants (third leaf from the top) of each group (n=4) were dark-adapted at ambient temperature for 30 min prior to measurements. The actinic light used for measurements was of 1,200 μmol photons m^2 s^{-1} following Bascuñán-Godoy et al. (2015). The fluorescence parameters, including maximum photochemical efficiency of PSII (Fv/Fm) and non-photochemical quenching (NPQ), were calculated according to Maxwell and Johnson (2000), and the photochemical quenching (qL, which estimates the fraction of open PSII) according to Kramer et al. (2004). The data was obtained using the following formulas: $F_v/F_m = (F_m - F_O)/F_m$; $qL = ((F'_m - F_s)/(F'_m - F'_O)) \cdot (F'_O/F_s)$; $NPQ = (F_m - F'_m)/F'_m$.

Seed characteristics

Seed weight and seed number per cm^2 were determined and used as proxy of yield for each treatment. Seed weight was determined by measuring the weight of 1000 oven-dried seeds and seed number per cm^2 by counting the number of seeds per square centimeter, from 6 plants of each group (n=6).

Seed germination parameters

50 seeds from 5 different individuals from each treatment were placed in Petri dishes with tissue paper; 5 mL of distilled water was added as needed to maintain adequate moisture for germination. Seeds were incubated for 24 h at 25°C in the dark. The number of germinated seedlings was recorded every 2 h. Germination was considered completed when the radicle emerged from the seed. Germination percentage ([number of germinated seeds/number of total seeds] *100) was determined according to Scott et al. (1984). Mean

germination time ($\sum_{i=1}^{k} ni * ti \,/\, \sum_{i=1}^{k} ni$; where ti = time since the beginning of the experiment; ni = number of germinated seeds at i time; and k = last germination time) was determined according to Ranal and Santana (2006).

Biochemical characterization of seeds and seedlings (F1)

For biochemical determinations, 100 seeds per treatment (n=5) and 5 seedlings per treatment (n=5) were utilized. Protein quantification was performed using the Bradford method (1976), using BSA as standard protein. Total free amino acid content was determined by ninhydrin method, according to Sun et al. (2006). Total soluble sugars (TSS) were extracted with a methanol-chloroform-water solution (12:5:3 v:v:v) according to Dickinson (1979) and determined according to Chow and Landhäusser (2004) using phenol 2% and sulfuric acid. Starch content was determined according to Smith and Zeeman (2006) by solubilizing the starch, converting it quantitatively to glucose and assaying the glucose. Ammonium content was determined according to Forster (1995), and nitrate content was determined by reducing nitrate to nitrite using vanadium chloride (III) (VCl_3), followed

by addition of sulfanilamide and dichloroiodate de N-(1-naftil)-ethylenediamine (NEDD) (Doane and Horwáth, 2003).

Metabolomic analyses of seeds (F1)

For the metabolomic profile analyses, seeds from mother plants were frozen, ground to powder and lyophilized to generate 20 mg/sample of both treatments (HN and LN), with each treatment conducted in triplicate. Metabolite profiling and analysis was performed at Mass Spectrometry and Sequencing Unit (PUC, Santiago, Chile) using an untargeted global metabolomic platform that combined Gas Chromatography – Mass Spectrometry (GC-MS) and Ultra Performance Liquid Chromatography – Tandem Mass Spectrometer (UPLC/MS/MS) analyses. The general extraction was performed with 80% methanol, LC-MS grade. 300 µL of cold methanol were added to each sample, then mixed in vortex for 10 sec and 5 min in ultrasound. Samples were incubated in a cold bath for 30 min, then centrifuged for 5 min at 10000 g to obtain the supernatant, which was transferred to an HPLC vial. The chromatography was performed in a

Kinetex C18 column of 2.1 mm x 100 mm, and the solvents were water + 0.1% formic acid and 90% acetonitrile + 0.1% formic acid. Metabolites were identified using the Fiehnlib libraries (https://fiehnlab.ucdavis.edu/projects/fiehnlib). Metabolite processing and statistical analysis were performed using MetaboScape 4.0 software (Bruker Daltonics). A custom Perl script was used to preprocess the normalized data for subsequent analysis. The *pheatmap* R package with the default clustering method, complete linkage, was applied to cluster the metabolites based on their z-score normalized expression levels across different samples. The ClassyFire online platform was used to assign the metabolites to a class according to their chemical properties. (Djoumbou Feunang et al., 2016).

F1 seedling biomass, and morphometric analyses

Dry weights of shoots and roots (n = 5 plants of each treatment) were determined by drying the tissues at 60 °C for 48 h until constant weight. Root parameters (total root length, number of tips) were determined by image analysis using RhizoVision Explorer v2.0.2. Roots were scanned in Epson

perfection v850 pro, with the following parameters: professional mode, gray 16-bit image, 600 resolution pixels per mm, Shine -50, Contrast 85. Gas exchange measurements were performed in the first true leaf (n = 5) in the same conditions previously stated (Materials and methods 2.3) for the determination of CO_2 Net photosynthesis (Pn), stomatal conductance (g_s), transpiration rate (E), and intrinsic water use efficiency (iWUE).

Statistical analysis

One-way ANOVA was conducted to determine the effects of N in mother plants (F0). Two-way ANOVA was used to study the effect of N supply in mothers (F0) and their impact on the offspring (F1) growing at different N conditions. For the assumption checking, Kolmogorov-Smirnov test was used for the normality testing and the equal variance was tested by checking the variability in the group means. Tukey HSD test (level of significance $p < 0.05$) was used as a post-hoc test, to explore evidence of significant differences. The statistical analyses were performed using the STATISTICA 6.0 software (StatSoft Inc., Tulsa, OK, USA). Principal Component Analysis

(PCA) was conducted using *prcomp* function in R to facilitate the computation of PCA. Visualization was achieved through *ggplot2* for the distribution by treatments on the principal components and *factoextra* for the variable contributions.

RESULTS

Yield and biomass of mother plants under different N supplies

The biomass of shoots and roots of mother plants (F0) was similar between the treatments (Fig. 1). However, LN conditions significantly affected the biomass of the panicle and yield ($p < 0.05$); they were reduced by -48.7% and -52.4%, respectively, compared to plants at HN conditions (Fig. 1B, C). Seed weight was also significantly reduced by LN conditions (20%), while seed size was similar between treatments (Fig. S1).

N supplementation effect on photosynthesis and chlorophyll *a* fluorescence parameter in mother plants

Plants subjected to LN conditions exhibited significant reduction in Pn and stomatal conductance (gs) (-63.3% and -76.2%, respectively) compared to

HN conditions (Fig. 2A, B). iWUE values were similar in both treatments (Fig. 2C).

The Maximum quantum efficiency (Fv/Fm) and the photochemical quenching (qL) were not affected by N supply (Fig. 3A, 3B). However, N affects thermal dissipation: the nonphotochemical quenching (NPQ) increased by about 2.4 times under LN compared to HN conditions (Fig. 3C).

Maternal N supply impact seed metabolites.

Both starch and total soluble sugars (TSS) contents were significantly higher in seeds of LN_{F0} plants than in seeds of HN_{F0} plants (Fig. 4A, 4D). There were no significant differences in total protein content of seeds between treatments (Fig. 4B). However, total amino acid content was lower in seeds produced by LN_{F0} plants than HN_{F0} plants (Fig. 4C). Additionally, in seeds from LN_{F0} plants, the nitrate content was significantly lower (Fig. 4E), while

the ammonium content was significantly higher (Fig. 4F) than those observed in seeds from HN_{F0} plants.

Change in the metabolomics pattern of seeds.

The metabolomic profile of seeds from HN_{F0} and LN_{F0} plants yielded a total of 95 known metabolites. Metabolites showing differences in abundance between the HN and LN conditions were categorized into six classes (Fig. 5): Carbohydrates, Flavonoids, Lipids, Nucleotides, Terpenes, and Others. Additionally, the heat map was divided into six clusters to facilitate a more detailed description of the results. Notably, the analysis indicates high variability among samples of seeds from HN-treated plants, whereas samples of seeds from plants grown in LN condition exhibited low variability. In cluster I, HN seeds showed a higher accumulation of metabolites, including lipids like monoolein, Sphingolipid HexCer 18:2;2O/14:0;O, a triterpenoid saponin (NCGC00180494-03_C42H66O14_1-O-[(3beta,5xi,9xi,18xi)-3-(beta-D-Glucopyranuro-nosyloxy)-28-oxoolean-12-en-28-yl]-beta-D-glucopyranose), a nucleoside (xanthosine), sucrose and some other

metabolites like Di−n−butyl phthalate (DBP), canrenone (a precursor of Spironolactone), and erucamide (primary fatty amide resulting from the formal condensation of the carboxy group of erucic acid with ammonia). Cluster II showed most of the consistent changes observed between treatments, with a higher quantity of metabolites with high reproducibility. This cluster indicated that LN seeds had a higher quantity of lipids than HN seeds, with special emphasis on phospholipids. Among them, phosphatidylethanolamine (PE), phosphatidylcholine (PC), and phosphatidylinositol (PI) were the ones that changed the most (Fig. 5). The metabolomic analysis also found an increase of both diacylglycerols (DG18:2 18:3) and phosphatidylinositol (PI 34:2) in LN seeds.

In addition to lipids, terpenoid metabolism changed with LN supply. Both terpene_6 (a triterpenoid saponin) and canrenone (steroidal triterpene lactone) were reduced under LN. We observed a high increase of terpenes under LN (Fig. 6, cluster II). LN treatment in mother plants also reduces both Dodecylbenzene sulfonic acid and Di-n-butyl phthalate (cluster I) in seeds.

It was observed that in cluster III, which only contained lipids and a flavonoid, there is a variability between replicates and there was no clear pattern between treatments; nevertheless, some metabolites changed with less variation (for example: PI 34:2, which corresponds to 1-phosphatidyl-1D-*myo*-inositol). A replicate of LN seed in cluster IV showed a much higher quantity of metabolites, mostly lipids and two flavonoids. In cluster V, a replicate of HN showed a higher quantity of metabolites than the others, indicating no clear pattern of differentiation between treatments. Finally, in cluster VI there were no evident differences or consistent changes between treatments.

N supply in mother plants affect the germination parameters of their offspring

The seeds (F1) of mother plants submitted to both treatments reached 100% germination (Fig. 6A); however, most of the offspring of plants grown at LN_{F0} germinated faster than the offspring of plants grown at HN_{F0} (Fig. 6B).

Effect of N treatment in F0 mother plants on F1 seedling growth at different N treatments

Regarding F1 seedlings, the descendants of LN_{F0} plants had significantly higher shoot biomass than the descendants of HN_{F0} in both HN and LN conditions. Also, F1 seedlings (from both types of F0 mother plants) had significant higher shoot biomass when grown at LN than at HN conditions (Fig. 7A). There were no significant differences in root biomass between offsprings from either HN_{F0} or LN_{F0} plants that grew in HN_{F1} conditions. A significant difference in root biomass is observed in descendants of LN_{F0}, where seedlings grown at LN_{F1} had higher root biomass than those grown at HN_{F1} (Fig. 7B).

Offsprings of both HN_{F0} and LN_{F0} mother plants showed a significant increase in total root length when grown at LN_{F1}, compared to those plants grown at HN_{F1} conditions (Fig. 7C). In the same way, a significant increase in this parameter was observed in offspring of LN_{F0} plants grown at LN_{F1} conditions (Fig. 7C, 7E). Besides, the descendants of LN_{F0} plants had a

significantly higher number of root tips when grown at LN_{F1} compared to all the other treatments (Fig. 7D).

The increased number of tips was highly correlated with plant transpiration (r=0.81) (Fig. S2)

Maternal N supply induces changes in photosynthesis and metabolites in their offspring.

Offspring of LN_{F0} had significantly higher Pn (51% when grown at HN_{F1} and 35% when grown at LN_{F1}) than the HN_{F0} descendants (Fig. 8A). Also, offspring of LN_{F0} significantly increased gs and E when grown at LN_{F1} (50% higher for gs and 40% higher for E) (Fig. 8B, 8C).

Offspring of LN_{F0} plants significantly increased their starch content in shoot when grown at LN_{F1}, compared to those grown at HN_{F1}, and to the offspring from HN_{F0} grown in both conditions (Fig. 9A). Offsprings from LN_{F0} and

HN_{F0} showed an increase in shoot TSS under LN conditions (Fig. 9B). Total soluble protein content was similar between offspring of HN_{F0} and LN_{F0} at LN_{F1}. However, offspring from HN_{F0} showed a significant higher total protein content than offspring from LN_{F0} plants at HN growth conditions (Fig. 9C). Finally, offsprings of both HN_{F0} and LN_{F0} mother plants display a decrease in free amino acid content at LN conditions, in comparison with HN conditions, this decrease is significant for descendants of HN_{F0} plants, but not for descendants of LN_{F0} plants (Fig. 9D).

We observed distinct grouping patterns among F1 seedling features in the PCA (Fig. 10A). Principal Component 1 (PC1) explains a significant 51.84% of the variability, while Principal Component 2 (PC2) accounts for 22.48%. The treatments showed differential clustering primarily along the PC1 axis, with a less pronounced separation along the PC2 axis. The contributing factors are shown in the PCA biplot (Fig. 10B), where the variables of gs, E and root tips show a strong contribution to the treatment differentiation, implying a high degree of correlation among these characteristics. TSS,

amino acids, total protein and root biomass appeared to be less influential on the primary trend but contributed to the variability explained by PC2.

DISCUSSION

Effects of Nitrogen supply over physiological traits of mother plants

Our results regarding the penalty in biomass, photosynthesis and changes in the use of energy during N limitation (Fig. 1A, B, 2 and 3) are consistent with previous studies (Ruiz et al., 2014; Bascunan-Godoy et al., 2016; Bascunan-Godoy et al., 2018; Manaa et al., 2019). It highlights the maintenance of Fv/Fm and qL at LN, which are related to the increase of thermal dissipation (measured as NPQ) (Fig. 3), suggesting that PSII is managing energy excess under LN conditions. This increase in NPQ may be related to reductions in Pn and gs (Fig. 2), suggesting a lower proportion of energy used for photosynthesis at LN. Furthermore, this is also related to the fact that, during senescence, photosynthetic-related proteins are the mayor N-source for remobilization (Masclaux-Daubresse et al., 2010). This reduction of CO_2 fixation under LN also affected panicle biomass, seed yield, but not seed size (Fig. 1C; Suppl. Fig. 1).

Effects of Nitrogen supply on seeds and offspring

Carbon is stored in the form of carbohydrates, lipids and storage proteins, the latter enabling in addition the storage of nitrogen, which together determines the weight of seeds (Makino, 2011; Hou et al., 2012; Zhang et al. 2016; Wen et al., 2018). Inorganic N remobilization during leaf senescence likely occurs and is dependent on the size of the inorganic N pools stored in the leaves prior to the onset of senescence (Havé et al., 2017). Several studies provide molecular and physiological evidence that, under N-limitation, vigorous senescence and N remobilization modify N allocation to seeds (Lemaitre et al., 2008; Masclaux-Daubresse et al., 2010). In fact, in wheat and *A. thaliana*, N remobilization contributes about two times more to grain N content at LN compared to HN (Le Gouis et al., 2007). In quinoa seeds from LN conditions, lower levels of total free amino acids were observed, yet protein levels remain comparable to those in HN seeds (Fig. 4B, 4C). This suggests that under N-limitation, proteolysis supports rapid protein turnover and continuous N recycling for protein neo-synthesis in seeds (Lemaitre et al., 2008).

Additionally, the contrasting contents of NO_3^- and NH_4^+ in seeds (Fig. 4F) may reflect varying physiological processes occurring in leaves of mother plants, such as recycling of N molecules. The reduction in NO_3^-, amino acids and purine metabolites, such as xanthosine, aligns with the N-limitation, and would not be directly related with downregulation of NRT1.1 transporter (Loqué et al., 2003). Conversely, the increased level of protein and amino acid degradation, and enhanced photorespiration in leaves have been linked to elevated NH_4^+ (Hildebrandt et al., 2015; Bascunan-Godoy et al., 2018). The elevated NH_4^+ level acts as a gas-transmitter, accelerating seed germination, breaking dormancy, and stimulating growth processes necessary for seedling emergence (Li et al., 2023). This is in agreement with our results in germination speed, where LN seeds germinated faster than HN seeds (Fig. 5B).

Consistently with other works, LN induced a significant increase in seed carbohydrates (starch and TSS) (Fig. 4A, 4D). This response is linked with changes in the activity of C- related enzymes within the endosperm, as observed in other crops (Midorikawa et al., 2014). Interestingly, sucrose was

the only sugar that decreased in seeds from LN plants. Sucrose serves as precursor of fatty acids and lipids, through its conversion to pyruvate, acetyl-CoA and then malonyl-CoA in amyloplast. Studies had shown that the physical properties of the membrane can be modified by altering the proportion of different lipid classes (Botella et al., 2017). We found significant lipid changes, especially in phosphatidylethanolamines (PEs) (Fig. 6 B), which are associated with enhanced nutrient remobilization efficiency (Fan et al., 2020). Additionally, we observed variations in phosphatidylinositol (PI 34:2), which plays a key role in rice seed germination by enhancing the activity of NADPH oxidase (Liu et al., 2012), and diacylglycerols (DG 18:2 18:3), which are important in gametogenesis and subsequent leaf and root growth (Angkawijaya et al., 2020).

Beside the metabolic functions and membrane dynamics modifications, phospholipids also play a crucial role in stress signaling and acclimatation. In fact, PE lyso 18:1, which is produced by the hydrolyzation of structural PE by phospholipase A2, was found to increase under LN. This lipid metabolite can directly stimulate the mitogen-activated protein (MAP)-

kinase signaling cascades and promote the activation of extracellular acid invertase (Cowan, 2009). Such processes are potentially related to higher C content in seeds and offspring of LN plants. Also, lipids compete with Terpenoids for primary substrates in biosynthesis (acetyl-CoA and pyruvate) used in the methylerythritol 4-phosphate or in the mevalonate pathway. Some terpenoids have antifungal protective activity (such as saponin and lactone), whereas others, such as Canrenone, have antioxidant activity (Boncan et al., 2020; Tewari et al., 2021). Canrenone accumulation, especially in $HN_{F0}LN_{F1}$ plants, would be a response to mitigate the oxidative stress generated by the nitrogen deficiency (Tewary et al., 2021; Boncan et al., 2020). Terpenoids also play a role in hormone production, including abscisic acid (ABA) and Gibberellins (GA), which are crucial in plant resistance and growth.

We propose that the observed increase in terpenoids and lipids, particularly phospholipids, and the change in their unsaturation levels, such as the reduction of PC 18:2 18:2 and the increase of PC 18:1 18:2 and PC 18:1 18:1 under LN, reflect changes not only in the endosperm but also in the embryo constitution (Fig. 6). These lipids may serve as critical sources of energy and

carbon for the respiratory processes, thereby facilitating faster seed germination (Ali and Elozeiri, 2017; Kim, 2020). Furthermore, they likely influence accelerated water uptake and post-germinative growth by altering the composition and permeability of cell walls (Wen et al., 2017; Jang et al., 2019; Mironenka et al., 2020). For example, suberin, a root apoplastic barrier predominantly composed of fatty acids, exhibits compositional changes under low N supply altering root architecture in several species (Grünhofer et al., 2021).

To avoid strong differences of temperature that can affect the performance of seedlings, our F1 studies were conducted under controlled conditions, which also included a lower light intensity compared to mothers F0. It is well established that changes in light intensity influence the use of different N sources by plants, affecting NR activity and chlorophyll content, which in turn may impact photosynthetic rates and leaf area ratio (Debiasi et al., 2021). In that case, those changes are expected to affect plants grown under HN conditions more than those grown under LN conditions. However, we used saturating light for all seedlings treatments (800 μmol m^2 s^{-1}); therefore, we

expected that the differences observed among groups (with same F0 treatment) would be maintained.

In F1 seedlings, consistent with the limiting N supply, we observed a physiological adjustment accounting for the similarities in the content of proteins between HN and LN offspring, but not in amino acids levels (Fig. 9C, D). Interestingly, protein and amino acids in seedlings resembled seeds N proportions, reinforcing the role of metabolic remobilization during senescence. However, the greater biomass observed in $LN_{F0}LN_{F1}$ suggests a more successful nutrient acquisition under N-limited conditions compared to other conditions. Alterations in root characteristics in the $LN_{F0}LN_{F1}$ seedlings, such as maintenance of root length with an increased number of tips (Fig. 7D) has been linked with a differential N transport to cell root system (Luo et al., 2013). In our study, the number of tips was highly correlated with plant transpiration (E), and positively associated with stomatal conductance, net photosynthesis, and starch accumulation (Fig. 10, Suppl. Fig. 2). It is well-established that transpiration enhances the mass flow of water and dissolved nutrients towards root surfaces, thereby increasing

NO_3^- concentration in-and-around the rhizosphere (Matimati et al., 2014). Moreover, carbohydrate accumulation in $LN_{F0}LN_{F1}$ seedlings may act as an osmolyte (Fig. 9A), contributing to plant water potential, favoring water uptake. In the same line, the higher number of root tips in $LN_{F0}LN_{F1}$ plants, might facilitate extensive soil exploration and enhance water transport, as inferred by the transpiration rate observed in $LN_{F0}LN_{F1}$ seedlings (Fig. 8C). This mechanism, which keeps stomata open (higher gs), would contribute to CO_2 fixation and assimilation at the whole plant level (Fig. 8A).

In conclusion, the nitrogen status of mother plants significantly influences the metabolic profile of seeds, as well as the physiological and growth responses of the offspring to N supply. A deeper understanding of the molecular mechanisms that control nutrient and water mass flow is essential to understand the change in N deficit resistance in offspring. These physiological responses are crucial considering the future nutrients and water scarcity challenges.

AUTHOR CONTRIBUTIONS

CC and LBG designed the assays and led the writing of the manuscript. CC, JR, JO, RSL, FP, AV and EE performed the assays, measurements and data analysis. EOG, TCP and LBG edited the manuscript. All authors contributed to the article and approved the final version of the manuscript.

FUNDING

This work was supported by ANID BECAS/DOCTORADO NACIONAL grant 21201031, ANID FONDECYT REGULAR 1220589 and ANID FONDECYT REGULAR N 1211473.

DATA AVAILABILITY STATEMENT

The data that support the findings of this study are available from the corresponding author upon reasonable request.

REFERENCES

Abugoch, L. (2009). Quinoa (Chenopodium quinoa Willd.): Composition, Chemistry, Nutritional, and Functional Properties. In *Advances in Food and Nutrition Research* (Vol. 58, pp. 1–31). Elsevier. https://doi.org/10.1016/S1043-4526(09)58001-1

Angkawijaya, A.E., Nguyen, V.C., Gunawan, F. and Nakamura, Y. (2020). A Pair of Arabidopsis Diacylglycerol Kinases Essential for Gametogenesis and Endoplasmic

Reticulum Phospholipid Metabolism in Leaves and Flowers. *Plant Cell* **32**(8):2602-2620. doi: 10.1105/tpc.20.00251.

Ali, A. S., and Elozeiri, A. A. (2017). Metabolic Processes During Seed Germination. InTech. doi: 10.5772/intechopen.70653

Bascuñán-Godoy, L., Alcaino, C., Carvajal, D. E., Sanhueza, C., Montecinos, S., and Maldonado, A. (2015). Ecophysiological responses to drought followed by re-watering of two native Chilean swamp forest plants: Myrceugenia exsucca (DC.) O. Berg and Luma chequen (Molina) A. Gray. *Gayana Bot*, **72**, 203–212. https://doi.org/10.4067/S0717-66432015000200004

Bascuñán-Godoy, L., Reguera, M. M., Abdel-Tawab, Y. M., and Blumwald, E. (2016). Water deficit stress-induced changes in carbon and nitrogen partitioning in Chenopodium quinoa Willd. *Planta*, **243**(3), 591–603. https://doi.org/10.1007/s00425-015-2424-z

Bascuñán-Godoy, L., Sanhueza, C., Hernández, C. E., Cifuentes, L., Pinto, K., Álvarez, R., González-Teuber, M., and Bravo, L. A. (2018). Nitrogen Supply Affects Photosynthesis and Photoprotective Attributes During Drought-Induced Senescence in Quinoa. *Front Plant Sci*, **9**, 1–14. https://doi.org/10.3389/fpls.2018.00994

Bazule, D., Bertero, D., and Nieto, C. (2014). Estado del arte de la quinua en el mundo en 2013. In *FAO (Santiago, Chile) CIRAD (Montpellier, France)*. https://doi.org/10.1016/0006-2952(67)90244-4

Boncan, D. A. T., Tsang, S. S. K., Li, C., Lee, I. H. T., Lam, H. M., Chan, T. F., and Hui, J. H. L. (2020). Terpenes and Terpenoids in Plants: Interactions with Environment and Insects. *Int J Mol Sci*, **6**; 21(19):7382. doi: 10.3390/ijms21197382

Botella, C., Jouhet, J., and Block, M. A. (2017). Importance of phosphatidylcholine on the chloroplast surface. *Prog Lipid Res* **65** 12–23. 10.1016/j.plipres.2016.11.001

Bradford, M. M. (1976). A Rapid and Sensitive Method for the Quantitation of Microgram Quiantities of Protein Utilizing the Principle of Protein-Dye Binding. *Anal Biochem*, **72**, 248–254.

Bruce, T. J. A., Matthes, M. C., Napier, J. A., and Pickett, J. A. (2007). Stressful "memories" of plants: Evidence and possible mechanisms. *Plant Sci*, **173**(6), 603–608. https://doi.org/10.1016/j.plantsci.2007.09.002

Chow, P. S., and Landhäusser, S. M. (2004). A method for routine measurements of total sugar and starch content in woody plant tissues. *Tree Physiology*, **24**(10), 1129–1136. https://doi.org/10.1093/treephys/24.10.1129

Cowan, A. (2009). Plant growth promotion by 18:0- lyso -phosphatidylethanolamine involves senescence delay. *Plant signaling and behavior* **4**: 324-7. 10.4161/psb.4.4.8188.

Debiasi, T. V., Calzavara, A. K., Sodek, L. and Oliveira, H. C. (2021). Nitrogen use plasticity in response to light intensity in neotropical tree species of distinct functional groups. *Physiologia Plantarum* **172**(4), 2226–2237. https://doi.org/10.1111/ppl.13470

Dickinson, R. E. (1979). Analytical procedures for the sequential extraction of 14C-labeled constituents from leaves, bark and wood of cottonwood plants. *Physiologia Plantarum* **45**, 480-488. https://doi.org/10.1111/j.1399-3054.1979.tb02618.x

Djoumbou Feunang, Y., Eisner, R., Knox, C., Chepelev, L., Hastings, J., Owen, G., Fahy, E., Steinbeck, C., Subramanian, S., Bolton, E., Greiner, R., Wishart, D. S. (2016). ClassyFire: automated chemical classification with a comprehensive, computable taxonomy. *J Cheminform* **8**, 61. https://doi.org/10.1186/s13321-016-0174-y

Doane, T. A., and Horwáth, W. R. (2003). Spectrophotometric determination of nitrate with a single reagent. *Analytical Letters*, **36**(12), 2713–2722. https://doi.org/10.1081/AL-120024647

Edwards, J., and Hertel, K. (2011). Reproductive development. In: Edwards J (ed.), PROCROP: Canola Growth and Development, Department of Primary Industries, New South Wales, pp. 51–64.

Fan, T., Yang, W., Zeng, X., Xu, X., Xu, Y., Fan, X., Luo, M., Tian, C., Xia, K., and Zhang, M. (2020). A Rice Autophagy Gene OsATG8b Is Involved in Nitrogen Remobilization and Control of Grain Quality. *Front Plant Sci* **11**:588. doi: 10.3389/fpls.2020.00588. PMID: 32582228.

Forster, J. C. (1995). Soil sampling, handling, storage and analysis. In K. Alef and P. Nannipieri (Eds.), *Methods in Applied Soil Microbiology and Biochemistry* (pp. 49–121). Academic Press Ltd. https://doi.org/10.1016/b978-012513840-6/50018-5

Gamir, J., Sánchez-Bel, P., and Flors, V. (2014). Molecular and physiological stages of priming: how plants prepare for environmental challenges. *Plant Cell Reports*, **33**(12), 1935–1949. https://doi.org/10.1007/s00299-014-1665-9

Grünhofer, P., Schreiber, L., and Kreszies, T. (2021). Suberin in Monocotyledonous Crop Plants: Structure and Function in Response to Abiotic Stresses. In: Mukherjee, S., Baluška, F. (eds) Rhizobiology: Molecular Physiology of Plant Roots. Signaling and Communication in Plants. Springer, Cham. https://doi.org/10.1007/978-3-030-84985-6_19

Gundel, P. E., Rudgers, J. A., and Whitney, K. D. (2017). Vertically transmitted symbionts as mechanisms of transgenerational effects. *American J Bot*, **104**(5), 787–792. https://doi.org/10.3732/ajb.1700036

Hatzig, S. V., Nuppenau, J. N., Snowdon, R. J., and Schießl, S. V. (2018). Drought stress has transgenerational effects on seeds and seedlings in winter oilseed rape (Brassica napus L.). *BMC Plant Biol*, **18**(1). https://doi.org/10.1186/s12870-018-1531-y

Havé, M., Marmagne, A., Chardon, F., and Masclaux-Daubresse, C. (2017). Nitrogen remobilization during leaf senescence: lessons from Arabidopsis to crops. *Journal of Experimental Botany*. **68(10)**, 2513–2529. https://doi.org/10.1093/jxb/erw365

Herman, J. J., and Sultan, S. E. (2011). Adaptive transgenerational plasticity in plants: Case studies, mechanisms, and implications for natural populations. *Front Plant Sci*, **2**, 1–10. https://doi.org/10.3389/fpls.2011.00102

Holeski, L. M., Jander, G., and Agrawal, A. A. (2012). Transgenerational defense induction and epigenetic inheritance in plants. *Trends in Ecology and Evolution*, **27**(11), 618–626. https://doi.org/10.1016/j.tree.2012.07.011

Hou, P., Gao, Q., Xie, R., Li, S., Meng, Q., Kirkby, E. A., Römheld, V., Müller, T., Zhang, F., Cui, Z., et al. (2012). Grain yields in relation to N requirement: Optimizing nitrogen management for spring maize grown in China. *Field Crop Res,* **129**:1–6. doi: 10.1016/j.fcr.2012.01.006.

INIA. (2015). Quínoa: Un súper Alimento Para Chile y el Mundo. *Tierra Adentro*, *N° 108*, 84. http://biblioteca.inia.cl/medios/revista-tierra-adentro/Tierra_Adentro_1_diciembre-Especial-Quinoa.pdf

Izquierdo, N. G., and Aguirrezábal, L. A. N. (2008). Genetic variability in the response of fatty acid composition to minimum night temperature during grain filling in sunflower. *Field Crops Research*, 106(2), 116-125.

Jang, J., Bae, E., Choi, Y., and Lee, O. (2019). Ginseng-derived patatin-related phospholipase PgpPLAIIIβ alters plant growth and lignification of xylem in hybrid poplars. *Plant science: an international journal of experimental plant biology* **288**, pp. 110224. https://doi.org/10.1016/J.PLANTSCI.2019.110224.

Kambona, C. M., Koua, P. A., Léon, J., and Ballvora, A. (2023). Stress memory and its regularion in plants experiencing recurrent drought conditions. *Theoretical and Applied Genetics* **136**, 26. https://doi.org/10.1007/s00122-023-04313-1Murphy, D., Rawsthorne, S., and Hills, M. (1993). Storage lipid formation in seeds. *Seed Science Research*, **3**(2), 79-95. doi:10.1017/S096025850000163X

Kramer, D. M., Johnson, G., Kiirats, O., and Edwards, G. E. (2004). New fluorescence parameters for the determination of QA redox state and excitation energy fluxes. *Photosynth Res*, **79**, 209–218. https://doi.org/doi:10.1023/B:PRES.0000015391.99477.0d

Kim, H. U. (2020). Lipid Metabolism in Plants. *Plants (Basel)* **9**(7):871. doi: 10.3390/plants9070871.

Lemaître, T., Gaufichon, L., Boutet-Mercey, S., Christ, A., and Masclaux-Daubresse, S. (2008). Enzymatic and Metabolic Diagnostic of Nitrogen Deficiency in *Arabidopsis thaliana Wassileskija* Accession. *Plant and Cell Physiology* **49**(7) 1056–1065. https://doi.org/10.1093/pcp/pcn081

Li, Z. G., Lu, X. Q., and Chen, J. (2023). Gasotransmitter ammonia accelerates seed germination, seedling growth, and thermotolerance acquirement in maize. *Plant Signal Behav* **18**(1): 2163338. doi: 10.1080/15592324.2022.2163338

Liu, H. P., Able, A. J., and Able, J. A. (2021) Nitrogen Starvation-Responsive MicroRNAs Are Affected by Transgenerational Stress in Durum Wheat Seedlings. *Plant (Basel)*, **10**(5), 826. doi: 10.3390/plants10050826

Liu, J., Zhou, J., and Xing, Da. (2012). Phosphatidylinositol 3-Kinase Plays a Vital Role in Regulation of Rice Seed Vigor via Altering NADPH Oxidase Activity. *PLoS ONE* **7**(3): e33817. DOI: 10.1371/journal.pone.0033817

Loqué, D., Pascal, T., Gojon, A., and Lepetit, M. (2003). Gene Expression of the NO3– Transporter NRT1.1 and the Nitrate Reductase NIA1 Is Repressed in Arabidopsis Roots by NO2–, the Product of NO3– Reduction. *Plant physiology* **132**. 958-67. 10.1104/pp.102.018523.

Lu, Y., Gao, L., Hu, J., Liu, X., Jiang, D., Cao, W., Dai, T., and Tian, Z. (2024). Low nitrogen priming improves nitrogen uptake and assimilation adaptation to nitrogen deficit stress in wheat seedling. *Planta*, **259**, 107. https://doi.org/10.1007/s00425-024-04385-3

Luo, J., Li, H., Liu, T., Polle, A., Peng, C., and Luo, Z. B. (2013). Nitrogen metabolism of two contrasting poplar species during acclimation to limiting nitrogen availability. *Journal of Experimental Botany* **64**(14), 4207–4224. https://doi.org/10.1093/jxb/ert234

McNaughton, A. J., Shelp, B. J., and Rajcan, I. (2015). Impact of temperature on the expression of Kennedy Pathway genes in developing soybean seeds. *Can J Plant* Sci **95**: 87–101. https://doi.org/10.4141/cjps-2014-261

Makino, A. (2011) Photosynthesis, grain yield, and nitrogen utilization in rice and wheat. *Plant Physiol,* **155**:125–129. doi: 10.1104/pp.110.165076.

Manaa, A., Goussi, R., Derbali, W., Cantamessa, S., Abdelly, C., and Barbato, R. (2019). Salinity tolerance of quinoa (*Chenopodium quinoa* Willd) as assessed by chloroplast ultrastructure and photosynthetic performance. *Environ Exp Bot*, **162**, 103-114. doi: 10.1016/j.envexpbot.2019.02.012

Massaro, M., De Paoli, E., Tomasi, N., Morgante, M., Pinton, R., and Zanin, L. (2019). Transgenerational Response to Nitrogen Deprivation in *Arabidopsis thaliana*. *Int J Mol Sci,* **20**, 5587. doi: 10.3390/ijms20225587

Masclaux-Daubresse, C., Daniel-Vedele, F., Dechorgnat, J., Chardon, F., Gaufichon, L., and Suzuki, A. (2010). Nitrogen uptake, assimilation and remobilization in plants: Challenges for sustainable and productive agriculture. *Annals of Botany*, **105**(7), 1141–1157. https://doi.org/10.1093/aob/mcq028

Matimati, I., Verboom, G. A., and Cramer, M. D. (2014). Nitrogen regulation of transpiration controls mass-flow acquisition of nutrients. *J Exp Bot* **65**(1):159-68. doi: 10.1093/jxb/ert367

Maxwell, K., and Johnson, G. N. (2000). Chlorophyll fluorescence - a practical guide. *J Exp Bot*, **51**, 659–668. https://doi.org/doi: 10.1093/jexbot/51.345.659

Midorikawa, K., Kuroda, M., Terauchi, K., Hoshi, M., Ikenaga, S., et al. (2014). Additional Nitrogen Fertilization at Heading Time of Rice Down-Regulates Cellulose Synthesis in Seed Endosperm. *PLOS ONE* **9**(6): e98738. https://doi.org/10.1371/journal.pone.0098738

Mironenka, J., Różalska, S., Soboń, A., and Bernat, P. (2020). Lipids, proteins and extracellular metabolites of Trichoderma harzianum modifications caused by 2,4-dichlorophenoxyacetic acid as a plant growth stimulator. *Ecotoxicology and environmental safety* **194**, 110383. https://doi.org/10.1016/j.ecoenv.2020.110383.

Murashige, T. and Skoog, F. (1962), A Revised Medium for Rapid Growth and Bio Assays with Tobacco Tissue Cultures. *Physiologia Plantarum* **15**: 473-497. https://doi.org/10.1111/j.1399-3054.1962.tb08052.x

Nowak, V., Du, J., and Charrondière, U. R. (2016). Assessment of the nutritional composition of quinoa (Chenopodium quinoa Willd.). *Food Chem*, **193**, 47–54. https://doi.org/10.1016/j.foodchem.2015.02.111

Racette, K., Zurweller, B., Tillman, B., and Rowland, D. (2020). Transgenerational stress memory of water deficit in peanut production. *Field Crops Research*, ***248***. https://doi.org/10.1016/j.fcr.2019.107712

Ranal, M. A., and Santana, D. G. (2006). How and why to measure the germination process? *Brazilian J Botany*, **29**, 1–11. https://doi.org/10.1590/S0100-84042006000100002

Rondanini, D., Castro, D., Searles, P. S., and Rousseaux, M. C. (2011). Fatty acid profiles of varietal virgin olive oils (*Olea europaea* L.) from mature orchards in warm arid valleys of Northwestern Argentina (La Rioja). *Grasas Aceites* **62**: 399–409. doi: 10.3989/gya.125110

Ruiz, K. B., Biondi, S., Oses, R., Acuña-Rodríguez, I. S., Antognoni, F., Martinez-Mosqueira, E. A., ... and Molina-Montenegro, M. A. (2014). Quinoa biodiversity and sustainability for food security under climate change. A review. *Agronomy for sustainable development*, **34**, 349-359.

Scott, S. J., Jones, R. A., and Williams, W. A. (1984). Review of Data Analysis Methods for Seed Germination. *Crop Science*, **24**, 1192–1199.

Sharma, M., Kumar, P., Verma, V., Sharma, R., Bhargava, B., and Irfan, M. (2022). Understanding plant stress memory response for abiotic stress resilience: Molecular insights and prospects. *Plant Physiol and Biochem* **179**, 10-24. https://doi.org/10.1016/j.plaphy.2022.03.004

Siddique, A. B., Parveen, S., Rahman, Z., and Rahman, J. (2024). Revisiting plant stress memory: mechanisms and contribution to stress adaptation. *Physiol and Mol Biol of Plants* **30**(2), 349-367. https://doi.org/10.1007/s12298-024-01422-z

Sun, S. W., Lin, Y. C., Weng, Y. M., and Chen, M. J. (2006). Efficiency improvements on ninhydrin method for amino acid quantification. *Journal of Food Composition and Analysis*, **19**(2–3), 112–117. https://doi.org/10.1016/j.jfca.2005.04.006

Hildebrandt, T. M., Nunes Nesi, A., Araújo, W. L., and Braun, H. -P. (2015). Amino Acid Catabolism in Plants. *Molecular Plant* **8**(11), 1563-1579. https://doi.org/10.1016/j.molp.2015.09.005.

Tewari, R. K., Yadav, N., Gupta, R. *et al.* (2021). Oxidative Stress Under Macronutrient Deficiency in Plants. *J Soil Sci Plant Nutr* **21**, 832–859. https://doi.org/10.1007/s42729-020-00405-9

Thomas, J., Boote, K, Allen, L., Gallo-Meagher, M., and Davis, J. (2003). Elevated temperature and carbon dioxide effects on soybean seed composition and transcript abundance. *Crop Sci* **43**: 1548–1557. https://doi.org/10.2135/cropsci2003.1548

Trentacoste, E. R., Puertas, C. M., and Sadras, V. O. (2012). Modelling the intraspecific variation in the dynamics of fruit growth, oil and water concentration in olive (*Olea europaea* L.). *Eur J Agron* **38**: 83–93. https://doi.org/10.1016/j.eja.2012.01.001

Wang, X., Zhang, X., Chen, J., Wang, X., Cai, J., Zhou, Q., Dai, T., Cao, W., and Jiang, D. (2018) Parental Drought-Priming Enhances Tolerance to Post-anthesis Drought in Offspring of Wheat. *Front Plant Sci*, **9**:261. doi:10.3389/fpls.2018.00261

Wen, D., Xu, H., Xie, L., He, M., Hou, H., and Zhang, C. (2017). A loose endosperm structure of wheat seed produced under low nitrogen level promotes early germination by accelerating water uptake. *Scientific Reports*, *7*(1), 1–11. https://doi.org/10.1038/s41598-017-03333-4

Wen, D., Xu, H., Xie, L., He, M., Hou, H., Wu, C., Li, Y., and Zhang, C. (2018). Effects of Nitrogen Level during Seed Production on Wheat Seed Vigor and Seedling Establishment at the Transcriptome Level. *Int J Mol Sci.* **19**(11):3417. doi: 10.3390/ijms19113417.

Ye, J. Y., Tian, W. H. and Jin, C. W. (2022). Nitrogen in plants: from nutrition to the modulation of abiotic stress adaptation. *Stress Biology.* 2, 4. https://doi.org/10.1007/s44154-021-00030-1

Zhang, Y., Dai, X., Jia, D., Li, H., Wang, Y., Li, C., Xu, H., and He, M. (2016). Effects of plant density on grain yield, protein size distribution, and breadmaking quality of winter wheat grown under two nitrogen fertilization rates. *Eur J Agron.* **73**:1–10. doi: 10.1016/j.eja.2015.11.015.

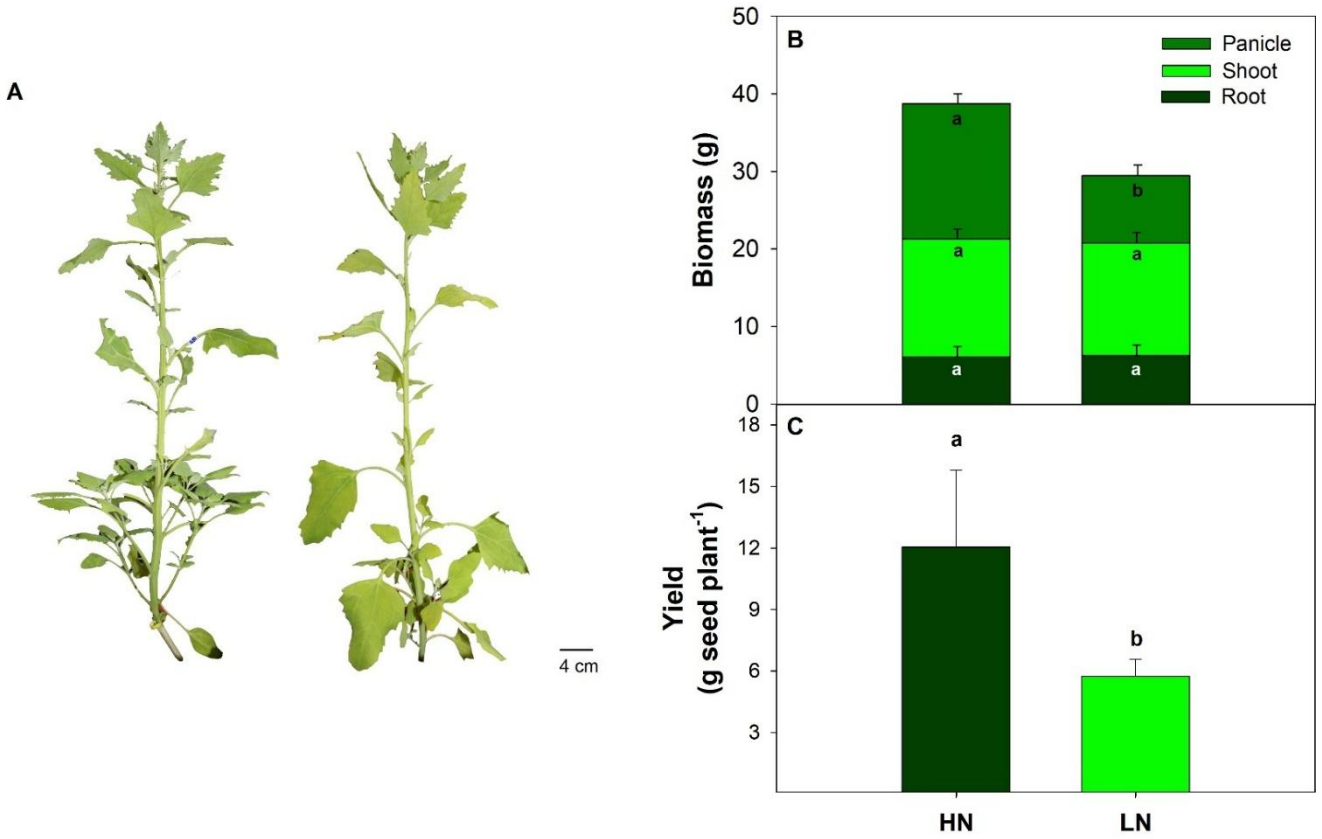

Figure 1.1. Phenotype, biomass, and yield of Faro genotype of *C. quinoa* growing under HN and LN conditions. A. Four-month-old mother plants (F0) grown at High Nitrogen (HN) and Low Nitrogen (LN) supplies. **B.** Biomass of different parts of the plant. **C.** Yield. Bars show mean values ± SE (n=5). Common letters indicate no significant differences among tissues (B) and treatments (B and C) using one-way ANOVA. Tukey HSD was used as a post hoc test ($p < 0.05$).

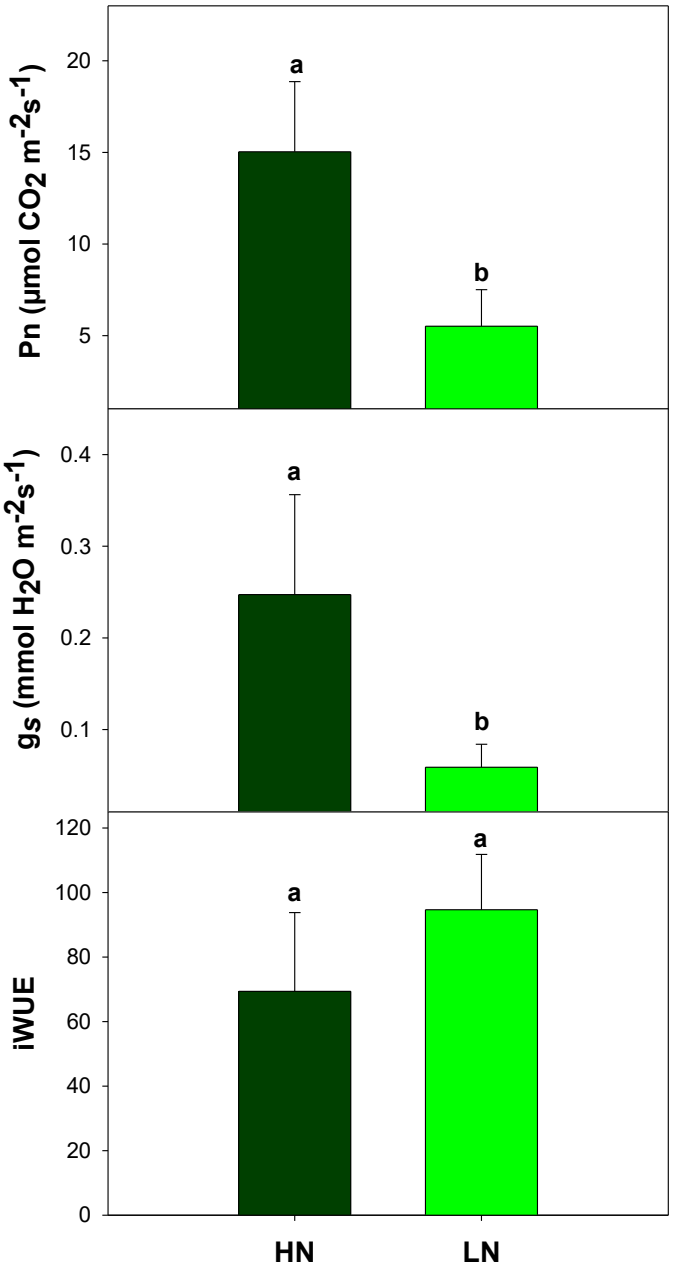

Figure 1.2. Photosynthetic parameters determined in *C. quinoa* at HN and LN conditions. A. Net photosynthetic rate (Pn). **B.** Stomatal conductance (gs). **C.** Intrinsic water use efficiency (iWUE) of mother plants (F0) measured after two weeks of panicle initiation. Bars show mean values ± SE (n=4). Common letters indicate no significant differences among treatments using one-way ANOVA. Tukey HSD was used as a post hoc test ($p < 0.05$).

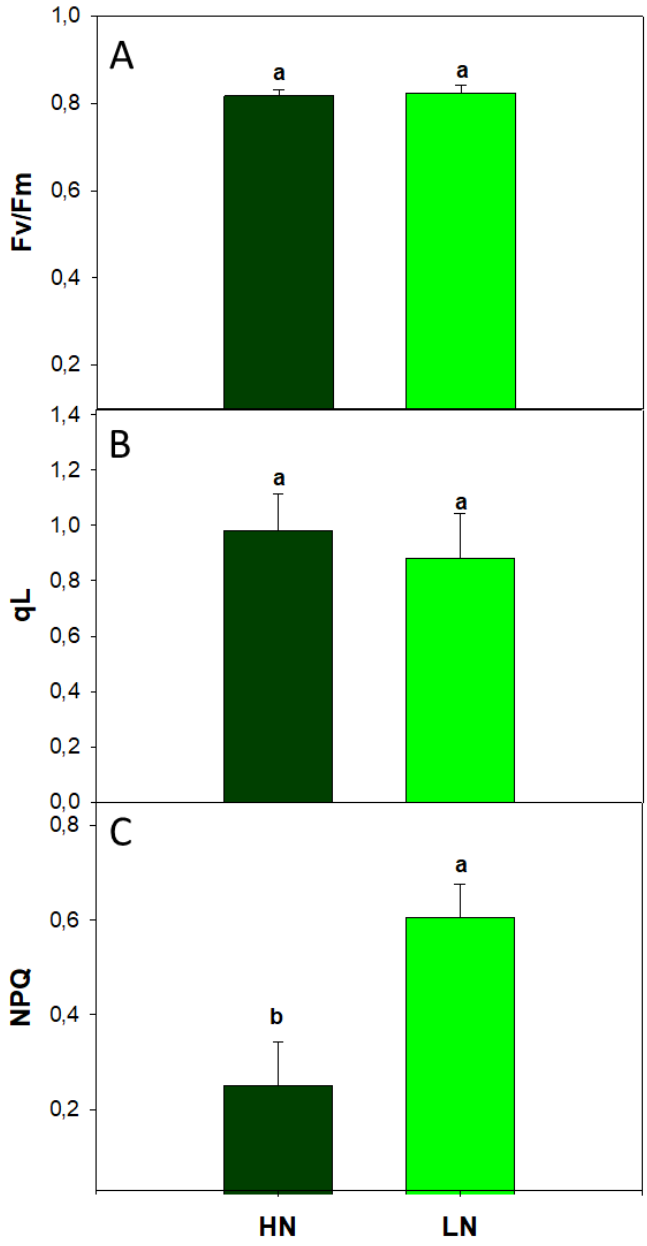

Figure 1.3. Photochemical and non-photochemical fluorescence parameters during grain filling in genotype Faro of quinoa at HN and LN. A. Maximum quantum efficiency (Fv/Fm). B**.** Photochemical quenching (qL). **C.** Nonphotochemical quenching (NPQ). Results were calculated from four independent measurements of different individuals. Bars show mean values ± SE (n = 4). Common letters indicate no significant differences between treatments using one-way ANOVA. Tukey HSD was used as a post hoc test ($p < 0.05$).

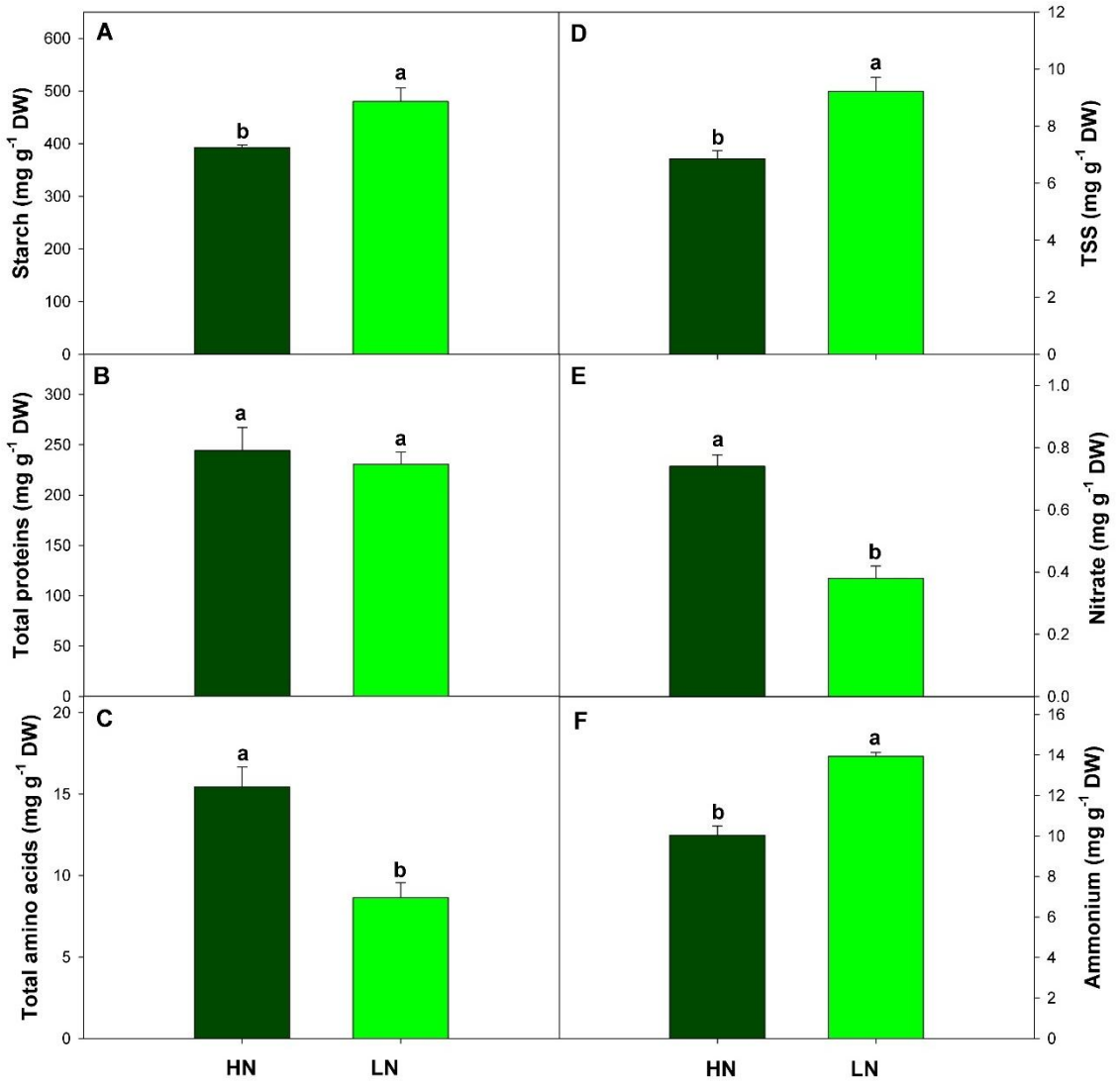

Figure 1.4. Carbohydrates and nitrogen compounds and molecules in seeds of mother plants grown in HN and LN conditions. A. Starch content. **B.** Total proteins. **C.** Total amino acids. **D.** Total soluble sugars**. E.** Nitrate content**. F.** Ammonium content. Bars show mean values ± SE (n=5). Common letters indicate no significant differences between treatments using one-way ANOVA. Tukey HSD was used as a post hoc test ($p < 0.05$).

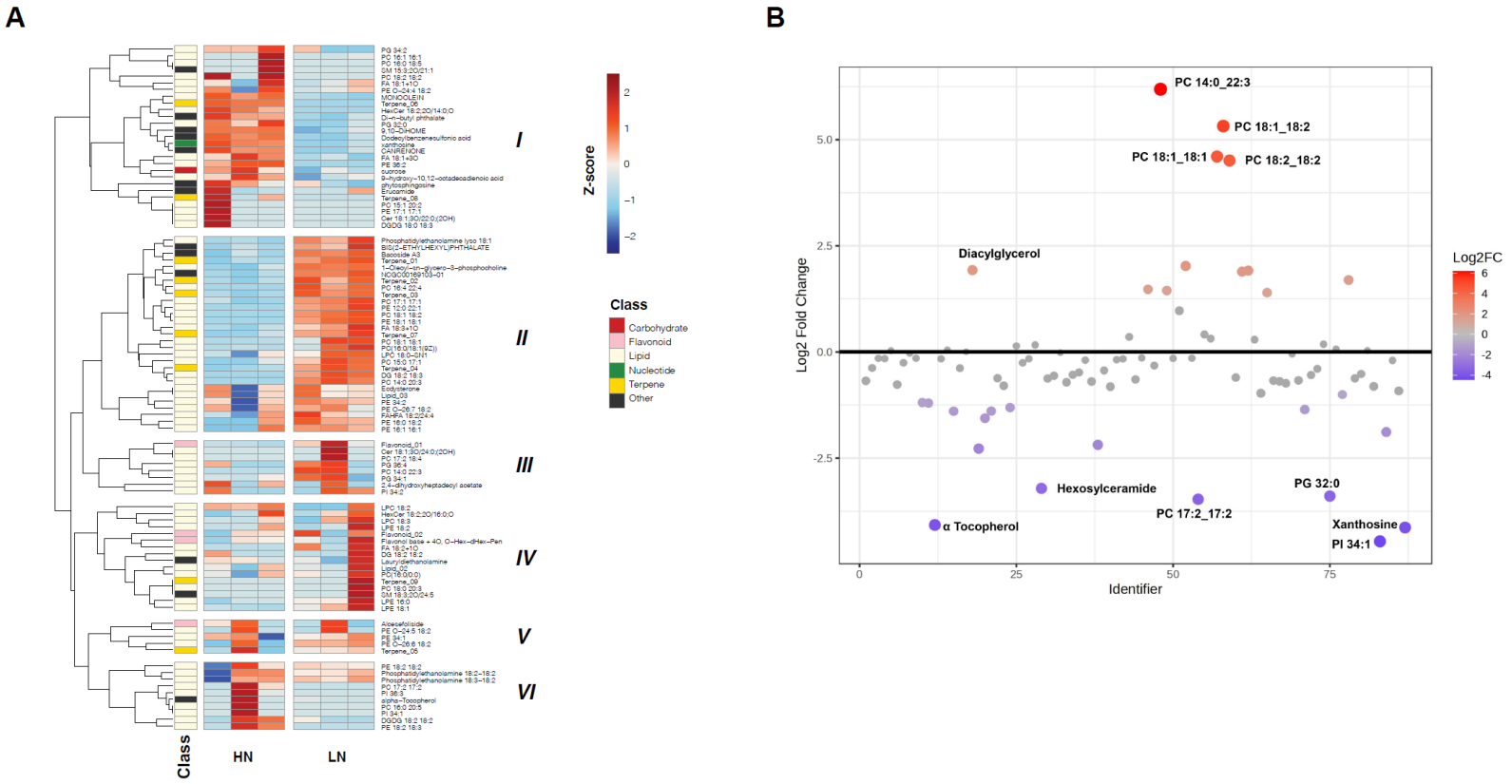

Figure 1.5. Heat map of metabolites found by metabolomics analysis in F1 seeds offspring of plants of HN and LN conditions. Metabolomics analysis. Heatmap of metabolites detected in High Nitrogen (HN) and Low Nitrogen (LN) concentration treatments. Normalized measurements were scaled using Z-scores and analyzed using heatmap and hierarchical clustering. Clusters are indicated with Roman numerals on the right. A file containing detailed information for metabolites and their aliases is available in Table S1.

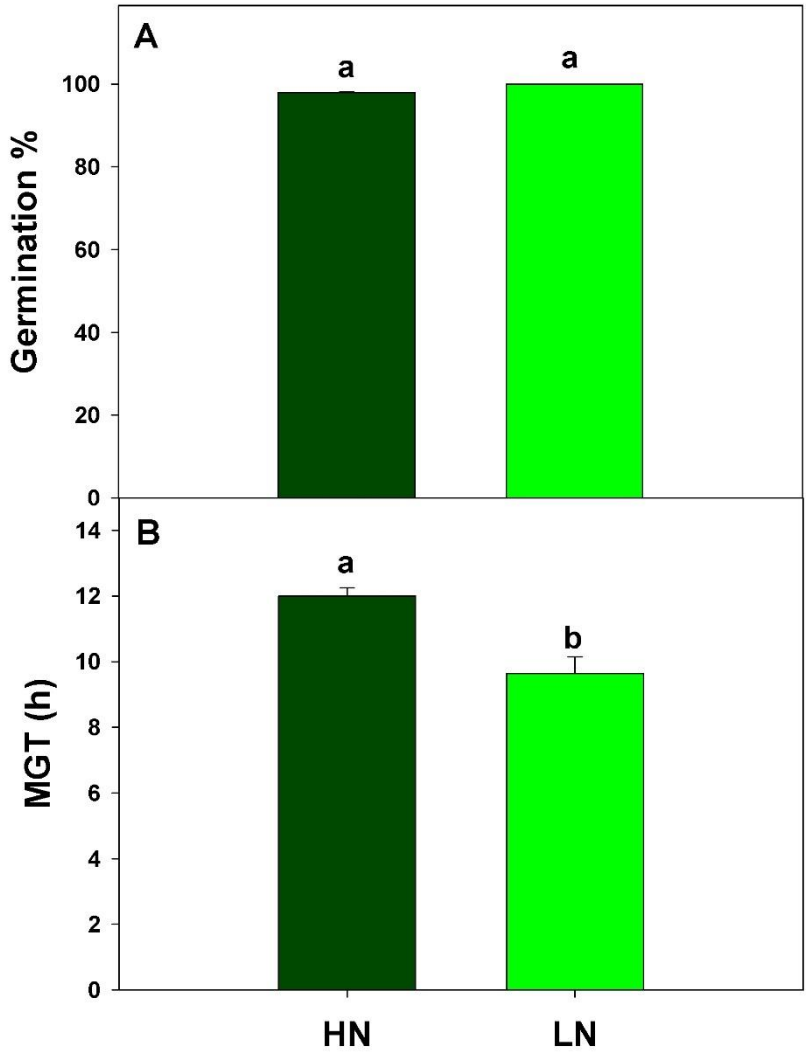

Figure 1.6. Germination parameters of the offspring of quinoa grown at HN and LN. **A.** Germination percentage. **B.** Mean germination time (MGT). Graphic shows the results from 50 seeds (distributed in 5 Petri dishes, with 10 seeds in each). Bars show mean values ± SE (n=5). Common letters indicate no significant differences between treatments using one-way ANOVA. Tukey HSD was used as a post hoc test ($p < 0.05$).

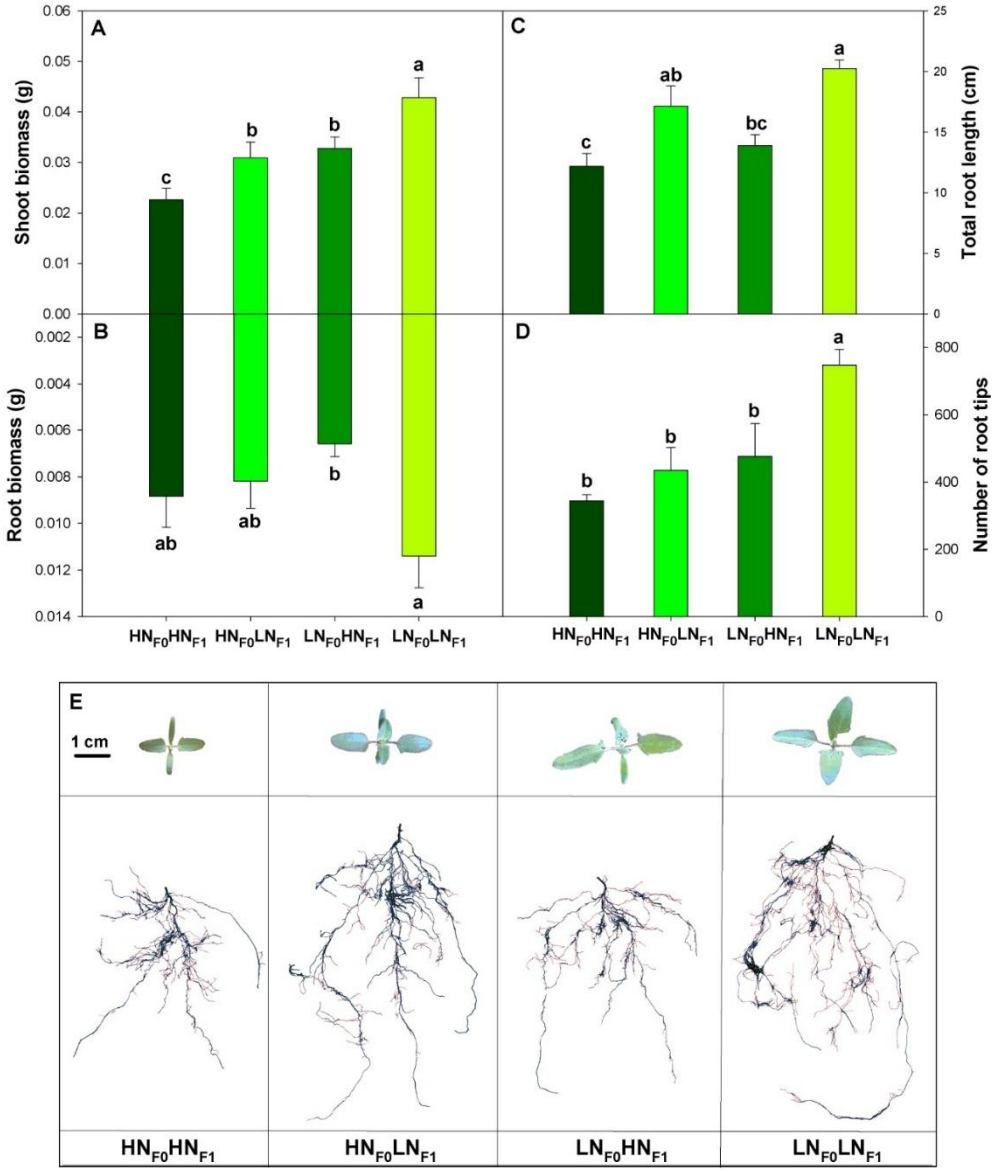

Figure 1.7. Biomass and architecture of 20-day-old F1 seedlings (descendants of F0 mother plants grown at HN and LN) grown in HN and LN conditions. A. Shoot biomass. **B.** Root biomass. **C.** Root length. **D.** Number of root tips. **E.** Architecture of leaves and roots. $HN_{F0}HN_{F1}$: Descendants of HN mother plants, grown at HN; $HN_{F0}LN_{F1}$: Descendants of HN mother plants, grown at LN; $LN_{F0}HN_{F1}$: Descendants of LN mother plants, grown at HN; $LN_{F0}LN_{F1}$: Descendants of LN mother plants, grown at LN. Bars show mean values ± SE (n=5). Common letters indicate no significant differences between treatments using two-way ANOVA, which factors were N supply in F0 and N supply in seedlings. Tukey HSD was used as a post hoc test ($p < 0.05$).

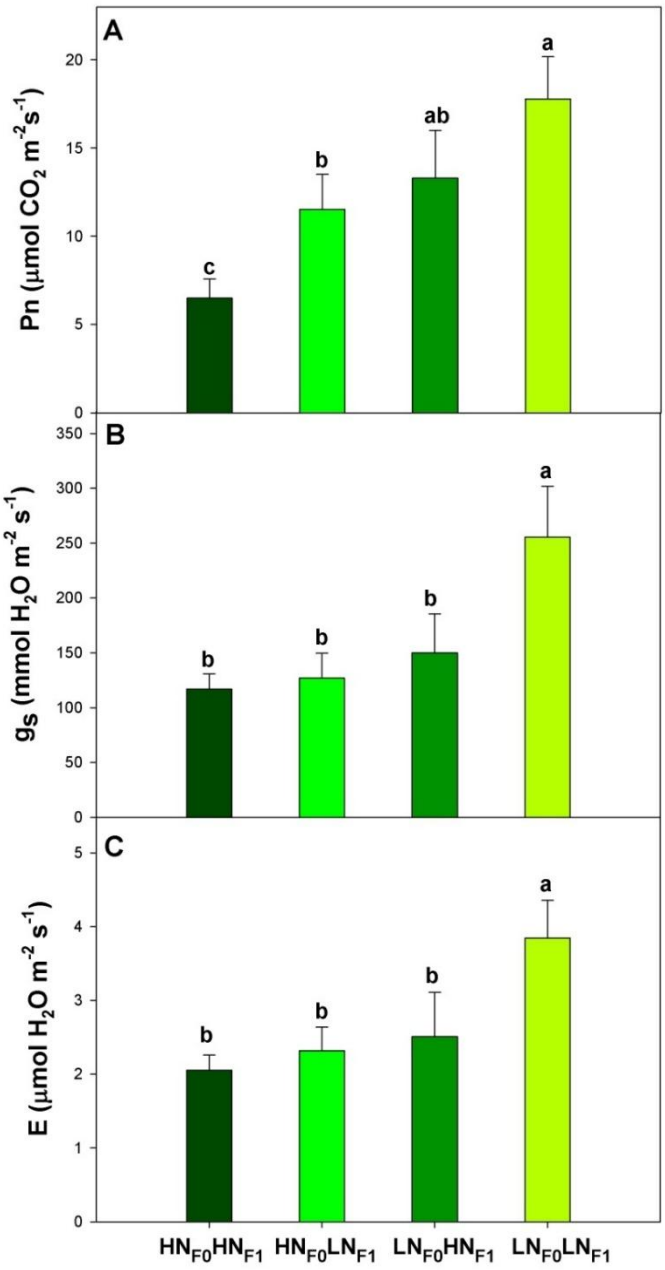

Figure 1.8. Photosynthetic parameters of 20-day-old F1 seedlings (descendants of F0 mother plants grown at HN and LN) grown in HN and LN conditions. A. Net photosynthetic rate (Pn). **B.** Stomatal conductance (gs). **C.** Transpiration rate (E). Bars show mean values ± SE (n=5). Common letters indicate no significant differences between treatments using two-way ANOVA, which factors were N supply in F0 and N supply in seedlings. Tukey HSD was used as a post hoc test ($p < 0.05$).

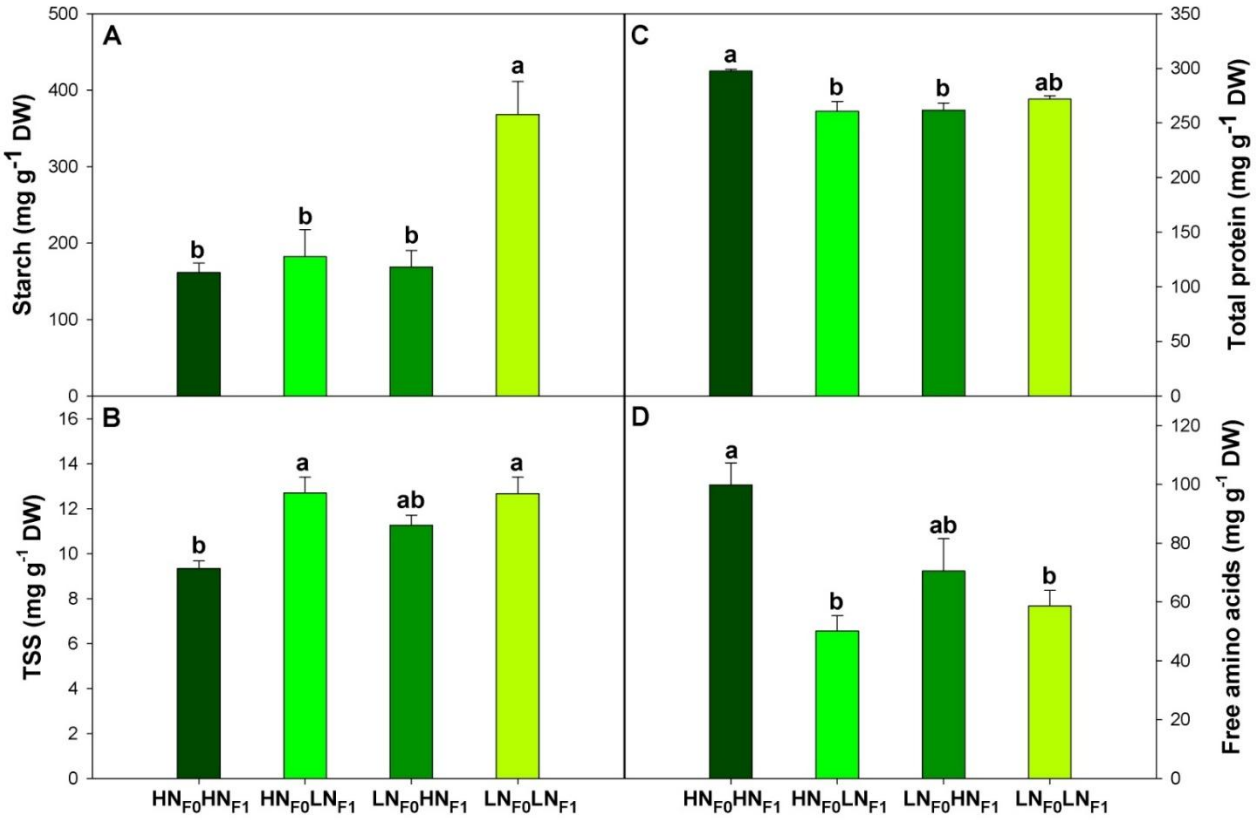

Figure 1.9. Carbohydrates and nitrogen compounds in shoot of 20-day-old F1 seedlings (descendants of HN_{F0} and LN_{F0} mother plants) grown in HN and LN conditions. A. Starch content. **B.** Total soluble sugars (TSS). **C.** Total protein. **D.** Free amino acids. Bars show mean values ± SE (n=5). Common letters indicate no significant differences between treatments using two-way ANOVA, which factors were N supply in F0 and N supply in seedlings. Tukey HSD was used as a post hoc test ($p < 0.05$).

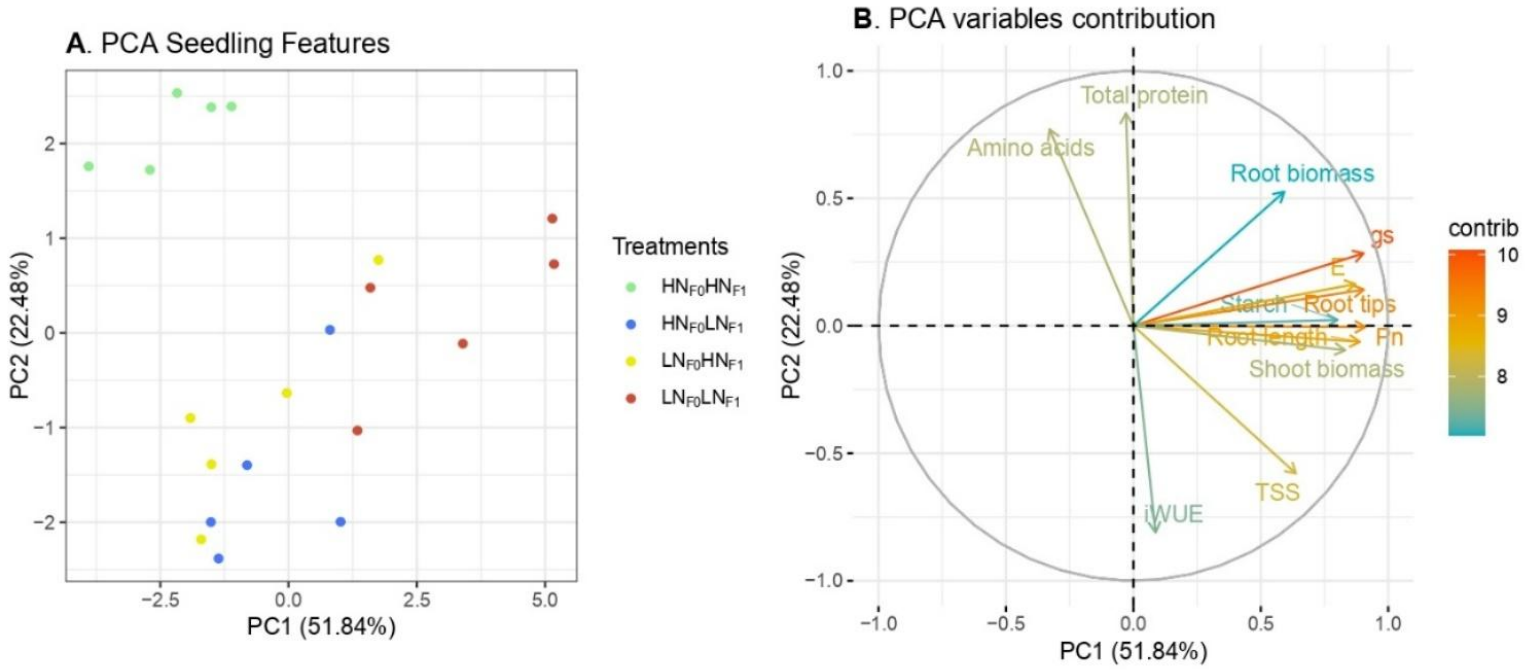

Figure 1.10. Principal Component Analysis (PCA) of seedling features and variable contributions. The percentages indicate the explained variation by each axis. A. Principal Component Analysis (PCA) of F1 seedling features, distinct colors indicate different treatments. **B.** Biplot of Variables contributions to the PCA distribution, each vector's length and direction represents the impact and correlation of the variable with the PCA axes: positive correlated variables point to the same side of the plot and negative correlated variables point to opposite sides of the plot. Colors represent distinct levels of contribution to the PC.

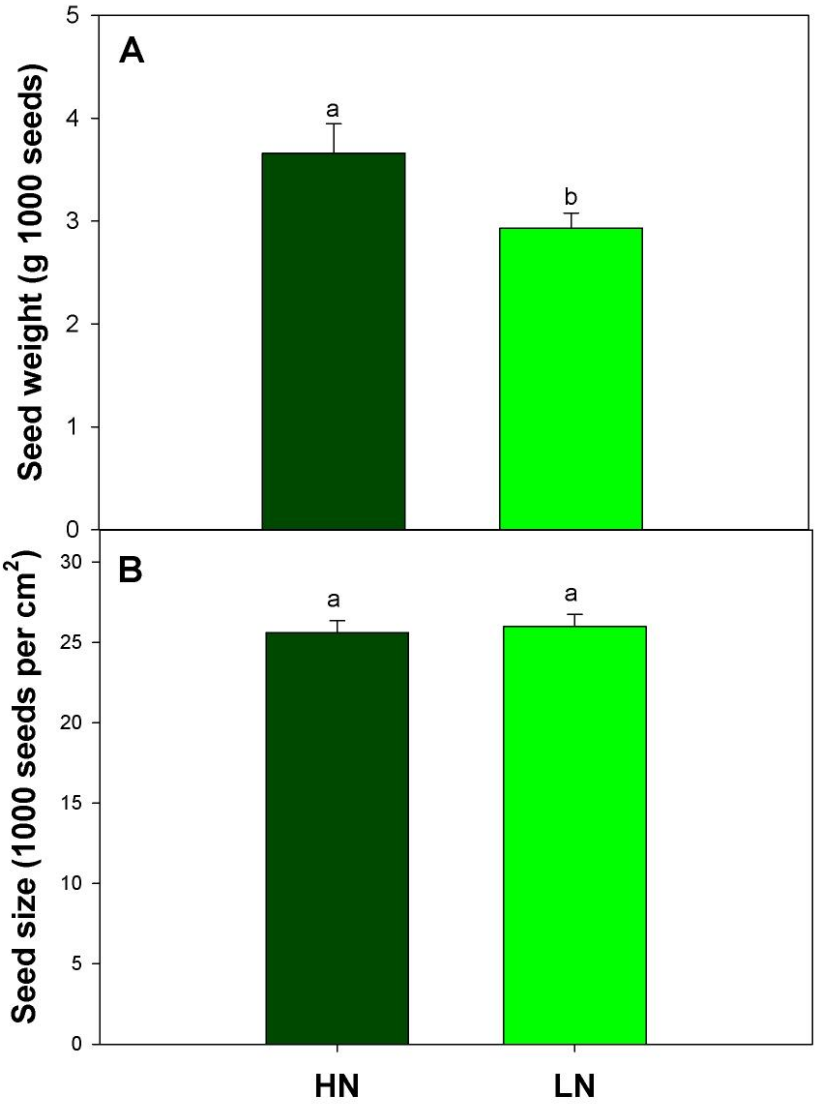

Supplemental Figure 1.1. Seed-related parameters of quinoa subjected to different N supplies. A. Number of seeds per m^2**. B.** Weight of 1000 seeds. Bars show mean values ± SE (n=6). Common letters indicate no significant differences between treatments using one-way ANOVA. Tukey HSD was used as a post hoc test ($p < 0.05$).

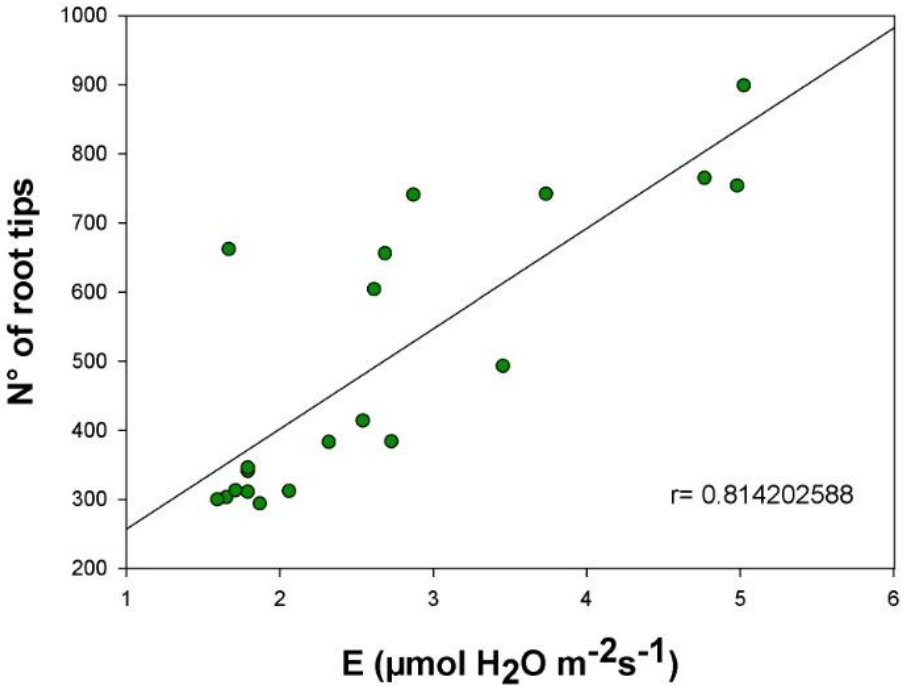

Supplemental Figure 1.1. Correlation analysis of number of tips and transpiration rate in 20 days old F1 seedlings (descendants of F0 mother plants grown at HN and LN) grown in HN and LN conditions. Linear Pearson's correlation coefficient (*r*) was used to examine the correlations.

Supplemental Table 1.1. Metabolites and their aliases for F1 seed metabolomic heatmap

Metabolite	***Class***	***Aliases***
(2S,3R,5R,10R,13R,14S,17S)-2,3,14-trihydroxy-10,13-dimethyl-17-[(2R,3R)-2,3,6-trihydroxy-6-methylheptan-2-yl]-2,3,4,5,9,11,12,15,16,17-decahydro-1H-cyclopenta[a]phenanthren-6-one	Lipid	Ecdysterone
(2S,3S,4S,5R,6R)-6-[[(3S,4R,6aR,6bS,8aS,14bR)-4-(hydroxymethyl)-4,6a,6b,11,11,14b-hexamethyl-8a-[(2S,3R,4S,5S,6R)-3,4,5-trihydroxy-6-(hydroxymethyl)oxan-2-yl]oxycarbonyl-1,2,3,4a,5,6,7,8,9,10,12,12a,14,14a-tetradecahydropicen-3-yl]oxy]-3,4,5-trihydroxyoxane-2-carboxylic acid	Amino acid	Aminoacid_02
(2S,3S,4S,5R,6R)-6-[[(3S,6aR,6bS,8aS,14bR)-4,4,6a,6b,11,11,14b-heptamethyl-8a-[(2S,3R,4S,5S,6R)-3,4,5-trihydroxy-6-(hydroxymethyl)oxan-2-yl]oxycarbonyl-1,2,3,4a,5,6,7,8,9,10,12,12a,14,14a-tetradecahydropicen-3-yl]oxy]-3,4,5-trihydroxyoxane-2-carboxylic acid	Amino acid	Aminoacid_01
(2S,3S,4S,5R,6R)-6-[[(3S,6aR,6bS,8aS,14bR)-8a-carboxy-4,4,6a,6b,11,11,14b-heptamethyl-1,2,3,4a,5,6,7,8,9,10,12,12a,14,14a-tetradecahydropicen-3-yl]oxy]-3,4,5-trihydroxyoxane-2-carboxylic acid	Flavonoid	Flavonoid_01
1-Oleoyl-sn-glycero-3-phosphocholine	Lipid	
1-palmitoyl-2-hydroxy-sn-glycero-3-phosphoethanolamine	Lipid	Lipid_02
2-(3,4-dihydroxyphenyl)-3-[(2S,3R,4S,5S,6R)-4,5-dihydroxy-3-[(2R,3R,4R,5R,6S)-3,4,5-trihydroxy-6-methyloxan-2-yl]oxy-6-[[(2R,3R,4R,5R,6S)-3,4,5-trihydroxy-6-methyloxan-2-yl]oxymethyl]oxan-2-yl]oxy-5,7-dihydroxychromen-4-one	Flavonoid	Flavonoid_02
2-(3,4-dihydroxyphenyl)-5,7-dihydroxy-3-[(2S,3R,4S,5S,6R)-3,4,5-trihydroxy-6-[[(2S,3R,4S,5R)-3,4,5-trihydroxyoxan-2-yl]oxymethyl]oxan-2-yl]oxychromen-4-one	Flavonoid	Flavonoid_03
2S,3R,5R,10R,13R,14S,17S)-2,3,14-trihydroxy-10,13-dimethyl-17-[(2R,3R)-2,3,6-trihydroxy-6-methylheptan-2-yl]-2,3,4,5,9,11,12,15,16,17-decahydro-1H-cyclopenta[a]phenanthren-6-one	Lipid	Lipid_03
6-[[(3S,6aR,6bS,8aS,14bR)-4,4,6a,6b,11,11,14b-heptamethyl-8a-[3,4,5-trihydroxy-6-(hydroxymethyl)oxan-2-yl]oxycarbonyl-1,2,3,4a,5,6,7,8,9,10,12,12a,14,14a-	Lipid	Lipid_01

tetradecahydropicen-3-yl]oxy]-3,5-dihydroxy-4-[3,4,5-trihydroxy-6-(hydroxymethyl)oxan-2-yl]oxyoxane-2-carboxylic acid	
9-hydroxy-10,12-octadecadienoic acid	Lipid
9,10-DiHOME	Other
alpha-Tocopherol	Other
Bacoside A3	Other
BIS(2-ETHYLHEXYL)PHTHALATE	Other
CANRENONE	Other
Cer 18:1;3O/22:0;(2OH)	Lipid
Cer 18:1;3O/24:0;(2OH)	Lipid
DG 18:2 18:2	Lipid
DG 18:2 18:3	Lipid
DGDG 18:0 18:3	Lipid
DGDG 18:2 18:2	Lipid
Di-n-butyl phthalate	Other
Dodecylbenzenesulfonic acid	Other
Erucamide	Other
FA 18:1+1O	Lipid
FA 18:1+3O	Lipid
FA 18:2+1O	Lipid
FA 18:3+1O	Lipid
FAHFA 18:2/24:4	Lipid
Flavonol base + 4O, O-Hex-dHex-Pen	Flavonoid
HexCer 18:2;2O/14:0;O	Lipid
HexCer 18:2;2O/16:0;O	Lipid
Lauryldiethanolamine	Other

LPC 18:0-SN1	Lipid	
LPC 18:2	Lipid	
LPC 18:3	Lipid	
LPE 16:0	Lipid	
LPE 18:1	Lipid	
LPE 18:2	Lipid	
MONOOLEIN	Lipid	
NCGC00169103-03 C19H18O6 Benz[3,4]anthra[1,2-b]oxirene-5,6-dione, 1a,2,3,4,5b,11,11a,11b-octahydro-10,11,11a-trihydroxy-3-methyl-	Other	NCGC00169103-01
NCGC00178646-02!2,4-dihydroxyheptadecyl acetate	Lipid	2,4-dihydroxyheptadecyl acetate
NCGC00347643-02 C30H46O3 (5xi,9xi,13xi,18xi,19beta)-3-Oxolup-20(29)-en-28-oic acid	Terpene	Terpene_01
NCGC00347737-02 C41H66O13 Olean-12-en-28-oic acid, 3-[(2-O-beta-D-glucopyranosyl-alpha-L-arabinopyranosyl)oxy]-23-hydroxy-, (5xi,9xi)-	Terpene	Terpene_02
NCGC00380944-01 C30H46O3 (3beta,5xi,9xi,13alpha,17alpha,18xi)-3-Hydroxy-13,28-epoxyurs-11-en-28-	Terpene	Terpene_03
NCGC00385094-01!2-(3,4-dihydroxyphenyl)-3-[(2S,3R,4S,5R,6R)-4,5-dihydroxy-3-[(2R,3R,4R,5R,6S)-3,4,5-trihydroxy-6-methyloxan-2-yl]oxy-6-[[(2R,3R,4R,5R,6S)-3,4,5-trihydroxy-6-methyloxan-2-yl]oxymethyl]oxan-2-yl]oxy-5,7-dihydroxychromen-4-one	Flavonoid	Alcesefoliside
NCGC00385211-01 C42H66O14 Olean-12-en-28-oic acid, 3-[(3-O-beta-D-glucopyranosyl-beta-D-glucopyranuronosyl)oxy]-, (3beta)-	Terpene	Terpene_04
NCGC00385302-01 C42H68O14 (3beta,5xi,9xi)-3-{[2-O-(beta-D-Glucopyranosyl)-beta-D-glucopyranosyl]oxy}-23-hydroxyolean-12-en-28-oic acid	Terpene	NCGC00385302-01
PC 14:0 20:3	Lipid	
PC 14:0 22:3	Lipid	
PC 15:0 17:1	Lipid	

PC 15:1 20:2	Lipid
PC 16:0 18:5	Lipid
PC 16:0 20:5	Lipid
PC 16:1 16:1	Lipid
PC 16:4 22:4	Lipid
PC 17:1 17:1	Lipid
PC 17:2 17:2	Lipid
PC 17:2 18:4	Lipid
PC 18:0 20:3	Lipid
PC 18:1 18:1	Lipid
PC 18:1 18:2	Lipid
PC 18:2 18:2	Lipid
PC(16:0/0:0)	Lipid
PC(16:0/18:1(9Z))	Lipid
PE 12:0 22:1	Lipid
PE 16:0 18:2	Lipid
PE 16:1 16:1	Lipid
PE 17:1 17:1	Lipid
PE 18:1 18:1	Lipid
PE 18:2 18:2	Lipid
PE 18:2 18:3	Lipid
PE 34:1	Lipid
PE 34:2	Lipid
PE 36:2	Lipid
PE O-24:4 18:2	Lipid
PE O-24:5 18:2	Lipid

PE O-26:6 18:2	Lipid
PE O-26:7 18:2	Lipid
PG 32:0	Lipid
PG 34:1	Lipid
PG 34:2	Lipid
PG 36:4	Lipid
Phosphatidylethanolamine 18:2-18:2	Lipid
Phosphatidylethanolamine 18:3-18:2	Lipid
Phosphatidylethanolamine lyso 18:1	Lipid
phytosphingosine	Other
PI 34:1	Lipid
PI 34:2	Lipid
PI 36:3	Lipid
SM 15:3;2O/21:1	Other
SM 18:3;2O/24:5	Other
sucrose	Carbohydrate
xanthosine	Nucleotide

CHAPTER 2:

Intergenerational and transgenerational stress memory in F1 and F2: Effects of maternal and grandmaternal N status on the early development of offspring

Metabolic imprint of sustained nitrogen deficiency stress across F1 and F2 generations in *Chenopodium quinoa* Willd (Amaranthaceae)

Authors and addresses:

Catalina Castro[1], Rodrigo Sanhueza-Lepe[1], Felipe Asalgado[1], José Ortíz[1], M. Paz Jeréz[1], Elizabeth Escobar[1], Teodoro Coba de la Peña[2], Enrique Ostria-Gallardo[1], Luisa Bascuñan-Godoy[1]*

[1]Laboratorio de Fisiología Vegetal, Departamento de Botánica, Facultad de Ciencias Naturales y Oceanográficas, Universidad de Concepción, Concepción, Chile

[2]Laboratorio de Recursos Naturales y Fitorremediación, Centro de Estudios Avanzados en Zonas Áridas (CEAZA), La Serena, Chile

ABSTRACT

Plants can develop stress memory, a phenomenon in which environmental stress experienced by mother plants improves the resilience of their offspring. While epigenetic mechanisms have been widely studied, the role of metabolism in inter- and transgenerational stress memory remains underexplored. In this study, we investigated the impact of maternal nitrogen (N) deficiency on the physiological and metabolic responses of *Chenopodium quinoa* offspring across two generations.

Our results show that maternal N-deficiency (LN_{F0}) enhances seed germination, seedling biomass, and stomatal conductance in F1 under N-limiting conditions. These responses were associated with higher starch content, lower amino acid levels, and the accumulation of lipids and flavonoids. In F2, despite limited changes in photosynthetic rates, descendants of LN_{F0} exhibited an accelerated growth, with higher shoot and root biomass under low N. Notably, consistent reductions in non-

photochemical quenching (NPQ) and increased photochemical efficiency across generations suggest a transgenerational adjustment in energy dissipation mechanisms. The metabolomic data revealed specific clustering patterns indicating stress-induced metabolic reprogramming, with LN_{F0}-derived offspring showing membrane-stabilizing lipids and antioxidant compounds, increased terpenes, carbohydrates, and N-use efficiency traits.

These findings highlight that maternal N deficiency in quinoa primes metabolic and physiological traits in subsequent generations, supporting the existence of transgenerational stress memory. Such plasticity offers potential applications for improving crop performance under nutrient-poor conditions through preconditioning strategies.

INTRODUCTION

It is known that stressed plants can display metabolic and genetic changes to resist various stresses; besides, it has been reported lately that several attributes could be inherited to the next generation. In this sense, this "stress memory" involves positive changes in the offspring to resist the stresses to which mother plants were exposed (Herman and Sultan, 2011; Holeski et al., 2012, Sharma et al., 2022). Among the most studied mechanisms of this response are epigenetic changes (histone acetylation and DNA methylation). However, other mechanisms could contribute to explaining the inheritance of stress memory, including the alterations of metabolite profile and metabolite levels (Bruce et al., 2007; Gamir et al., 2014; Gundel et al., 2017, Kambona et al., 2023, Siddique et al., 2024). Despite the significant impact of stress conditions on metabolite levels, the role of the metabolic profile as a mediator for preconditioning remains underexplored (Herman and Sultan, 2011).

Nitrogen (N) is essential for optimal plant function, and its deficiency is one of the most significant abiotic stress factors for plant development (Ye et al., 2022). Recent evidence suggests that parental nutrient availability not only

influences the current generation but also affects the progeny through mechanisms of transgenerational memory (Massaro et al. 2020, Castro et al. 2024). This enables plants to anticipate environmental stress based on ancestors' experiences to enhance their survival and reproductive success. Research on both intergenerational and transgenerational memory related to N limitation has been scantily documented. In *Arabidopsis thaliana*, it has been shown that exposure to multigenerational stress enhances the nitrate uptake ability, triggering a suite of responses to N-deficiency (Massaro et al., 2020). Additionally, Liu et al. (2021) showed cross-stress effects, demonstrating that progeny from water-stressed plants exhibited increased resistance to N starvation compared to offspring from well-watered plants. Other examples were reported in peanuts (Racette et al., 2020), *Brassica napus* L. (Hatzig et al., 2018) and *Triticum aestivum* L. (Wang et al., 2018) under drought stress, where the offspring of stressed parents presented attributes that improved their performance compared to the offspring of non-stressed parents, linked to metabolite changes. Considering that N plays a central role in plant metabolism, the understanding of how N affects maternal plant performance and of its effects on inter and transgenerational resistance

of offspring is crucial for the potential use of maternal environmental conditions as a tool to preconditioning.

Chenopodium quinoa Willd. (Amaranthaceae) is pseudocereal native of the Andean regions of South America, that has demonstrated to have considerable resilience to numerous abiotic stresses, including a notable tolerance to N-deficiency (Bascuñan-Godoy et al., 2018). Quinoa seeds have remarkable nutritional properties, including high protein content and the presence of all essential amino acids. This has led to its selection by the FAO as a crop with significant potential to contribute to global food security (Abugoch, 2009; Bazule et al., 2014; INIA, 2015; Nowak, et al., 2016). Considering its role in food security, enhancing N-deficit resistance through inter and transgenerational memory in quinoa is of high importance.

We recently reported that the maternal N supply in quinoa modulates the development and metabolic profile of their immediate offspring, being the maternal environment the regulator of the stress response of the first-generation offspring at seed and seedling stages (Castro et al., 2024). We

found that seeds from LN mother plants had higher lipid content and lower amino acids which were associated with a faster germination of the seeds. Additionally, seedling grown at LN presented a higher biomass, more root tips and an enhanced photosynthetic capacity associated with starch accumulation. All these changes suggested a maternal induction of tolerance to N-stress in their offspring.

To explore the potential stress memory inheritance beyond the maternal effect in quinoa, this study investigates the impact of maternal N supply on the physiological and molecular responses of its offspring across two generations. We hypothesize that the N deficiency condition in F0 plants has more importance than the current N grown conditions, affecting metabolomic profile and physiological performance, under N deficiency. These findings provide insights into how maternal N availability influences progeny performance, potentially through mechanisms of stress memory and transgenerational inheritance.

MATERIAL AND METHODS

Plant material and growth conditions (F1 and F2 seedlings and plants)

F1 seeds were obtained from previous work (Castro et al., 2024). Briefly, F0 plants were grown in 10 L pots filled with 5 Kg of substrate (80% sand and 20% perlite) supplemented with modified MS culture medium (Murashige and Skoog, 1962) without N at sowing, then at 4 true leaves, and at 8 true leaves stage. The substrate was supplemented with NH_4NO_3 to reach two N-level treatments at the same times as the MS supplementation: high nitrogen (HN_{F0}: 0.6 g of N per pot), which is the optimal N level for quinoa growth, and low nitrogen (LN_{F0}: 0.3 g N per pot) (See Pinto-Irish et al., 2020 for details about optimal and deficient N level for quinoa growth). Plants were maintained with optimal soil moisture until seed maturation when we collected F1 seeds.

The experiments for F1 were conducted in pots from September 2023 to February 2024 (at University of Concepción, Concepción, Chile) under greenhouse conditions. The environmental conditions were: 1200 μmol m^{-2} s^{-1} PAR at noon (natural light), maximum and minimum temperatures (daily ranges) of 25 ºC and 17 ºC respectively, 12 h day length, and 80% relative humidity. Seeds were directly germinated in pots of 1 L and 10 L filled with 1 and 5 kg of substrate, respectively, consisting of 80% sand and 20% perlite. One supplementation with modified MS culture medium (Murashige and Skoog, 1962) without N was administered at sowing for the 1 L pots, and three supplementations for the 10 L pots: at sowing, when plants developed 4 true leaves, and finally at the 8 true leaves stage. The substrate was supplemented with NH_4NO_3 as N source to reach two level treatment. Four groups conditions were obtained for F1 (Fig. 1): 1) Offspring of HN mother plants, grown at HN ($HN_{F0}HN_{F1}$); 2) Offspring of HN mother plants, grown at LN ($HN_{F0}LN_{F1}$); 3) Offspring of LN mother plants, grown at HN ($LN_{F0}HN_{F1}$); and 4) Offspring of LN mother plants, grown at LN ($LN_{F0}LN_{F1}$). Eight groups conditions were obtained for F2, and 4 were selected for analysis (Fig. 1): 1) Sustained HN control ($HN_{F0}HN_{F1}HN_{F2}$); 2) LN stress control ($HN_{F0}HN_{F1}LN_{F2}$); 3) Stress reversion ($LN_{F0}HN_{F1}LN_{F2}$); 4) Stress

maintenance ($LN_{F0}LN_{F1}LN_{F2}$). F1 and F2 plants in 1 L pots (1 per pot) were irrigated at field capacity every three days with water maintaining optimal soil moisture, until they had 4 true leaves (~20 days of growth). At this time, measurements of biomass, gas exchange, and chlorophyll *a* fluorescence parameters were performed, and samples were collected for analysis. F1 and F2 plants in 10 L pots (1 per pot) were irrigated to field capacity with water every three days maintaining optimal soil moisture until seed maturation stage. Measurements were performed after two weeks of panicle initiation (December 2023, grain filling stage).

Gas exchange measurements

Photosynthetic gas exchange measurements were conducted in healthy fully expanded leaves (third leaf from the top) (n=5) using a CIRAS-2 infrared gas analyzer system (PP SYSTEMS, MA, USA). Leaves were first equilibrated at a photon density flux of 1,200 μmol m^2 s^{-1} (slightly higher than light saturation point) for at least 10 min. CO_2 concentration was set at 400 ppm. Leaf temperature was maintained at 28 °C, and the leaf-to-air vapor pressure

deficit was kept between 1 and 1.3 kPa. Under these chamber conditions, we determined net photosynthesis (Pn), stomatal conductance (g_s), and transpiration rate (E).

Chlorophyll *a* fluorescence measurements

Chlorophyll (Chl) *a* fluorescence measurements were conducted with a portable fluorimeter (FMS 2, Hansatech Instruments Ltd., Norfolk, United Kingdom). Leaves from plants (third leaf from the top) of each group (n=3) were dark-adapted at ambient temperature for 30 min prior to measurements. The actinic light used for measurements was of 1,200 μmol photons m^2 s^{-1} following Bascuñán-Godoy et al. (2015). Fluorescence parameters including maximum photochemical efficiency of PSII (Fv/Fm) and non-photochemical quenching (NPQ) were calculated according to Maxwell and Johnson (2000), and the photochemical quenching (qL, that estimates the fraction of open PSII) according to Kramer et al. (2004). The data was obtained using the following formulas: $F_v/F_m = (F_m - F_O)/F_m$; $qL = ((F'_m - F_s)/(F'_m - F'_O)) \cdot (F'_O/F_s)$; $NPQ = (F_m - F'_m)/F'_m$.

Seed germination parameters

Fifty seeds from 5 different individuals from each treatment were placed in Petri dishes with tissue paper; 5 mL of distilled water was added as needed to maintain adequate moisture for germination. Seeds were incubated for 24 h at 25°C in the dark. The number of germinated seedlings was recorded every 2 h. Germination was considered completed when the radicle emerged from the seed. Germination percentage ([number of germinated seeds/number of total seeds] *100) was determined according to Scott et al. (1984). Mean germination time ($\sum_{i=1}^{k} ni * ti \,/\, \sum_{i=1}^{k} ni$; where ti = time since the beginning of the experiment; ni = number of germinated seeds at i time; and k = last germination time) was determined according to Ranal and Santana (2006).

Biochemical characterization of F1 and F2 seedlings

For biochemical determinations, 5 seedlings per treatment (n=5 for F1 and F2) were utilized. Protein quantification was performed using the Bradford method (1976), using BSA as standard protein. Total free amino acid content was determined by ninhydrin method, according to Sun et al. (2006). Total soluble sugars (TSS) were extracted with a methanol-chloroform-water solution (12:5:3 v:v:v) according to Dickinson (1979) and determined according to Chow and Landhäusser (2004) using phenol 2% and sulfuric acid. Starch content was determined according to Smith and Zeeman (2006) by solubilizing the starch, converting it quantitatively to glucose and assaying the glucose. Nitrate content was determined by reducing nitrate to nitrite using vanadium chloride (III) (VCl_3), followed by addition of sulfanilamide and dichloroiodate de N-(1-naftil)-ethylenediamine (NEDD) (Doane and Horwáth, 2003).

Metabolomic analyses of F1 and F2 seedlings

For the metabolomic profile analyses, leaves of F1 and F2 seedlings were frozen, ground to powder and lyophilized to generate 50 mg/sample of each treatment, with each treatment conducted in triplicate. Metabolite profiling and analysis was performed at Mass Spectrometry and Sequencing Unit (PUC, Santiago, Chile) using an untargeted global metabolomic platform that combined Gas Chromatography – Mass Spectrometry (GC-MS) and Ultra Performance Liquid Chromatography – Tandem Mass Spectrometer (UPLC/MS/MS) analyses. For the sample preparation, 500 µL of ACN:IPA:water (3:3:2) were added to each sample, and mixed in vortex for 30 s. Samples were incubated at -20°C for 1 h, then vortex for 30 s and 15 min in ultrasound on ice. Then centrifuged for 15 min at 13.000 g at 4°C to obtain the supernatant. The chromatography was performed in a Kinetex C18 column of 2.1 mm x 100 mm, with 1.7 u particle, and the solvents were water + 0.1% formic acid and 90% acetonitrile + 0.1% formic acid. Metabolites were identified using the Fiehnlib libraries (https://fiehnlab.ucdavis.edu/projects/fiehnlib). Metabolite processing and analysis were performed using MetaboScape 4.0 software (Bruker Daltonics). The data was preprocessed with a custom R script, handling missing values, median normalization and a pareto scaling. The *FactoMineR*

and *ggplot2* R packages were used to generate the PCA analysis and plots. The *pheatmap* R package with the default clustering method was applied to cluster metabolites based on their z-score normalized expression levels across samples. The ClassyFire online platform was used to assign the metabolites to a class according to their chemical properties (Djoumbou Feunang et al., 2016).

F1 plant yield and F2 plant biomass

Dry weight of leaves and roots were determined by drying the tissue at 60 °C for 48 h until constant weight was reached. Grain yield was determined as the total grain weight per plant at the end of the growth season.

Statistical analysis

Two-way ANOVA was used to study the effect of N supply in mothers (F0) and their impact on the offspring (F1) growing at different N conditions. One-way ANOVA was conducted to determine the effects of N in mother plants (F0) on the F2 offspring. For the assumption checking, Kolmogorov-Smirnov test was used for the normality testing and the equal variance was tested by checking the variability in the group means. Tukey HSD test (level of significance $p < 0.05$) was used as a post-hoc test, to explore evidence of significant differences. The statistical analyses were performed using the STATISTICA 11.0 software (StatSoft Inc., Tulsa, OK, USA).

RESULTS

Pn was dependent on N level of seedling, but maternal LN supply influences NPQ in F2 generation

F1 descendants of LN_{F0} have higher Pn when grown at LN_{F1} (Fig. 2A). This was statistically different compared to $HN_{F0}HN_{F1}$; and was correlated with higher gs and E in $LN_{F0}LN_{F1}$ seedlings. However, F2 descendants exhibit no significant differences in Pn between treatments (Fig. 2D), so no differences related to maternal N supply environment were observed.

Also, gs and E significantly increased in F1 descendants of LN_{F0} when grown at LN_{F1} (~40% higher for gs and ~ 30% higher for E) (Fig. 2B, C). The maximum quantum efficiency (Fv/Fm) was always higher than 0.8 (Fig. 2G, J), indicating no stress of the PSII, despite thermal dissipation (non-photochemical quenching, NPQ) tending to decrease in $LN_{F0}LN_{F1}$ (Fig. 2H). In F2, a statistically significant decrease in NPQ was observed in

$LN_{F0}LN_{F1}LN_{F2}$ compared to $HN_{F0}HN_{F1}LN_{F2}$ (Fig. 2K). Consistently, qL in $LN_{F0}LN_{F1}LN_{F2}$ tended to be higher than in the other treatments, but without statistically significant differences (Fig. 2L).

Sustained LN supply through generations increases starch content, but no differences in N related metabolites were evident

Offspring of LN_{F0} significantly increased their starch content, compared to the other treatments, when growing at LN in F1 (Fig. 3A). In F2, plants that were sustained at LN through generations have higher amount of starch than those that were submitted to N limitation just in the F2 generation (Fig. 3D). When comparing F1 and F2, a similar amount of starch was found in F1 and F2 seedlings between $LN_{F0}LN_{F1}$ and $LN_{F0}LN_{F1}LN_{F2}$ (Fig. 3A, D), and statistical differences were observed in F2 when plants were sustained at LN through generations compared to first generation at LN or when the mother (F1) was grown at HN (Fig. 3A, D).

Regarding TSS, statistically significant differences were observed in F1, when comparing $HN_{F0}HN_{F1}$ to LN_{F1} treatments ($HN_{F0}LN_{F1}$ and $LN_{F0}LN_{F1}$) (Fig. 3G). In contrast, no significant differences in TSS values between plant treatments were observed in F2. All treatments in F2 showed higher TSS values regarding F1 (Fig. 3J).

It was interesting that total protein was similar in both generations F1 and F2 and among seedling treatments. Statistical differences were observed in F1 in $HN_{F0}LN_{F1}$ and $LN_{F0}HN_{F1}$ in comparison to $HN_{F0}HN_{F1}$ (reduction of ~13%) (Fig. 3B, E).

On the other hand, free amino acids content decreased in both F1 and F2 when grown at LN, independent of the N of their ancestors (Fig. 3H, K). Nitrate content acted similarly to free amino acids content, heavily decreasing when either the mother has grown at LN_{F0}, or the seedling is growing at LN (F1 and F2) (Fig. 3C, F). Finally, nitrite content was more variable in F1, where statistical differences were observed when comparing one LN treatment ($HN_{F0}LN_{F1}$, $LN_{F0}HN_{F1}$) to sustain LN treatment

($LN_{F0}LN_{F1}$), here $LN_{F0}LN_{F1}$ reached similar levels than $HN_{F0}HN_{F1}$ (Fig. 3I), and showed no significant changes between treatments in F2 (Fig. 3L).

Maternal N supply (F0) influences the metabolic profile of their offspring at seedling stage (F1 and F2)

The metabolic profile of F1 seedlings yielded a total of 141 known metabolites (Fig. 4A) and the F2 metabolic profile yielded 107 known metabolites (Fig. 5A). Metabolites showing differences in abundance between treatments were categorized into seven classes: Carbohydrate, Flavonoid, Amino Acid, Lipid, Nucleotide, Terpene and Other (Table S1, S3). Additionally, each heatmap was divided into five and four clusters, respectively, to facilitate a more detailed description of the results. F1 showed a higher accumulation of overall metabolites in comparison to F2. The ANOVA analysis (Table S2, S4) helped identify key metabolites with significant changes across treatments, showing stress-induced metabolic shifts in each generation, with 74 metabolites for F1 seedlings and 56 metabolites for F2 that had p-values < 0.05.

The PCA analysis for both generations show a separation between treatments. The Principal Component 1 (PC1) explains 41% and 31.2% of the variability between treatments for F1 and F2 respectively, while PC2 explains 16% and 21% of the variability in F1 and F2, respectively. In $HN_{F0}HN_{F1}$ and $LN_{F0}LN_{F1}$ treatments cluster together separating from $HN_{F0}LN_{F1}$ and $LN_{F0}HN_{F1}$ in F1 (Fig. 4B). In F2, $LN_{F0}HN_{F1}LN_{F2}$ clusters differentially with both $HN_{F0}HN_{F1}HN_{F2}$ and $HN_{F0}HN_{F1}LN_{F2}$ (overlaps). Although $LN_{F0}HN_{F1}LN_{F2}$ has a high variability in their samples, it clusters together with the other LN_{F0} treatment, separating with a slight overlap from the HN_{F0} treatments (Fig. 5B), indicating that the treatments that come from a HN_{F0} have a similar metabolic pattern, different from the offspring of LN_{F0}.

For F1, cluster I showed that the metabolomic pattern follows the clustering of the PCA, where $HN_{F0}HN_{F1}$ and $LN_{F0}LN_{F1}$ treatments shared a similar accumulation of metabolites, likewise $HN_{F0}LN_{F1}$ and $LN_{F0}HN_{F1}$ (Fig. 4A). For the rest of the heatmap, $LN_{F0}LN_{F1}$ shows a high accumulation of metabolites in every cluster except cluster IV. These metabolites that accumulate correspond to mostly lipids, flavonoids and some amino acids

and terpenes. The metabolites that had significant differences accumulated in this treatment included kaempferol and quercetin derivates, linked to antioxidant defense (Singh et al., 2021), and lipids like phosphatidylinositol (PI 34:2) and diacylglycerols. LPE 16:0 and glutamate are some of the metabolites that had a lower accumulation in this treatment.

For F2, both treatments that are descendants of HN_{F0}, indistinctly the N treatment in which their mothers or themselves were grown, share a similar metabolic pattern, similarly to the LN_{F0} descendants, and corresponding to what we describe for the PCA, and showing particularly in cluster I and IV (Fig. 5B). The descendants of HN_{F0} showed an accumulation of amino acids like glutamic acid, glutamine, isoleucine and phenylalanine, crucial for protein synthesis and N metabolism. This treatments also accumulate fatty acids and lipids like MGMG 18:2, DGMG 18:3 and monopalmitin, Linolenic acid, 2-hidroxypalmitic acid and 9-HOTrE, involved in membrane structure and signaling pathways. $LN_{F0}LN_{F1}LN_{F2}$ accumulate metabolites that are in cluster III and include lipids (for example PI 34:2) and 2 flavonoids. For both treatments descendants of LN_{F0}, there is an accumulation of

glycerophospholipids and lysophospholipids, which are essential components for maintaining cellular structure under stress. Specifically, $LN_{F0}HN_{F1}LN_{F2}$ treatment showed a high variability between samples, so there is no clear pattern or metabolite to pinpoint in this treatment, consistent with the necessity to deal with changing N-conditions across generations.

N supply on mother plants (F0) induces changes in photosynthesis and chlorophyll *a* fluorescence parameters in their offspring at adult stage (F1)

At adult stage, F1 plants show no significant difference in Pn (Fig. 6A). Descendants of LN_{F0} decreased gs and E: these decreases are significant for plant growing at HN_{F1}, but not for plants growing at LN_{F1} (Fig. 6B, C). Fv/Fm and qL show no significant difference between treatments (Fig. 6D, F). However, $LN_{F0}LN_{F1}$ treatment displayed significantly lower values of NPQ than $HN_{F0}HN_{F1}$ treatment (Fig. 6E).

Effect of maternal N supply (F0) on yield and germination parameters of their offspring (F1 plant yield and F2 seed germination)

Offsprings of both HN_{F0} and LN_{F0} mother plants showed a decrease in their yield at LN_{F1} conditions in comparison with HN_{F1} conditions; this decrease was significant for both, a -14.2% for HN_{F0} descendants and a -29.3% for LN_{F0} descendants (Fig. 7A).

The descendant seeds (F2 seeds) of F1 plants at all treatments reached ~100% of germination (Fig. 7B); however, the descendants of LN_{F0} grown at HN_{F1} and LN_{F1} germinated slower than their HN_{F0} counterparts (~1.3 h difference in HN_{F1} and ~3.4 h difference in LN_{F1}) (Fig. 7C). F2 seeds obtained from the $HN_{F0}LN_{F1}$ treatment had significant lowest MGT than seeds from the other treatments (Fig. 7C).

Effect of N supply in F0 on F2 biomass

Phenotypically, the overall biomass was similar between descendants of $HN_{F0}HN_{F1}$ grown at both HN_{F2} and LN_{F2}, and between descendants grown at LN_{F2} that came from $LN_{F0}HN_{F1}$ and $LN_{F0}LN_{F1}$ plants, (Fig. 8A). Shoot biomass follow this pattern (Fig. 8B), also showing that descendants of LN_{F0} have a higher shoot biomass than HN_{F0} descendants. Comparing $HN_{F1}LN_{F2}$ treatments, there is a tendency to have higher biomass when it comes from LN_{F0}. For the root biomass, descendants grown at LN_{F2} that came from $LN_{F0}HN_{F1}$ and $LN_{F0}LN_{F1}$ plants have a higher biomass than the other treatments, but no significant difference between them were observed (Fig. 8C). On the other hand, descendants of $HN_{F0}HN_{F1}$ when grown at LN_{F2} have a higher root biomass than when grown at HN_{F2} (9.5%). Also, when comparing $HN_{F1}LN_{F2}$ treatments, they have a significantly higher root biomass when it comes from LN_{F0} (37.3%).

DISCUSSION

LN in mother plants induces a persistent tendency to reduce NPQ

The constant presence of LN across generations influences significantly the photosynthetic performance and chlorophyll *a* fluorescence parameters in seedlings. In F1 the increase in Pn in $LN_{F0}LN_{F1}$ was associated with a higher gs and E (Fig. 2A, B, C), suggesting that maternal stress primes their offspring to a physiological adjustment to optimize carbon gain and improve water use efficiency under N-limited conditions (Castro et al., 2024; de Camargo Santos et al., 2024). In contrast, F2 showed no significant differences in Pn among treatments, although gs and E remained elevated under LN_{F2} conditions regardless of ancestral N-supply (Fig. 2D, E, F).

Regarding NPQ, there is known that quinoa plants growing at LN increased NPQ (Bascuñan-Godoy et al., 2018, Cisse et al., 2020) as a photoprotective mechanism to dissipate excess light energy as heat to prevent photodamage

that can cause a decline of photosynthetic efficiency (Müller et al, 2001). Since 70% of leaf N is accumulated in chloroplast, the decrease of photosynthetic capacity, and thus the need to eliminate excess irradiated energy, can be attributed to a reduction in synthesis of key enzymes in the photosynthesis process, such as RuBisCO (Fathi and Zeidali, 2021; Murchie et al., 2005; Kasajima et al., 2011). This was observed in our prior investigation, where NPQ increased 2.4 times under LN regarding HN (Castro et al., 2024). Here, there is a tendency to be reduced in $LN_{F0}LN_{F1}$ (Fig. 2H) and significantly lower in $LN_{F0}LN_{F1}LN_{F2}$ (Fig. 2K), suggesting a reduced need for thermal dissipation of excess energy, possibly due to more efficient photosynthetic usage of absorbed light under constant N-deficiency across generations (Sahay et al., 2024), or to a lower light capture due to the reduced N accumulating in chloroplasts, thus a reduced quantity of reaction centers that captures light (Cisse et al., 2020).

In parallel to NPQ decrease in F2, qL showed a tendency to increase (Fig. 2L), which reflects an enhanced photochemical efficiency and electron transport rate, where more absorbed light energy is used for photochemistry

rather than being dissipated as heat, as seen in plants treated with reduced chlorophyll content (Sperdouli et al., 2024; Moustakas et al., 2022; Wang et al., 2022). These findings imply that maternal (F0) N-supply and the maintenance of N stress across generations influences not only stomatal behavior but also the regulation of energy dissipation processes in the photosystems under N-stress conditions, potentially as a transgenerational inherited trait, where in F1 there is a combined effect of the plant sensing of LN and the maternal effect that induces the changing, meanwhile in F2 the N status of the mother plant regulate the energy dissipation response.

Maintenance of protein content was independent of mother N supply, and is in detriment of free amino acids under LN

There is known that N is stored in photosynthetic compounds. The maintenance of Fv/Fm and qL (Fig. 2G, I, J, L) is indicative of the principal photosynthetic components that have been maintained spite the present LN conditions or sustained LN through generations (Wang et at., 2018; Kramer et al. 2004). This could be related to the unmodified content of total protein

observed in F1 and F2 that also remain unaltered spite LN (actual or generational) (Fig. 3B, E).

In both generations, there is an accumulation of lipids, crucial to maintaining the membrane integrity and signaling during stress, in contrast to amino acids like glutamic acid and glutamine that were diminished in treatments with one or more generation in LN (Fig. 3H, K), which indicates an adaptive strategy to manage N-limiting conditions. Both glutamine and glutamic acid are key metabolites in N metabolism, to maintain the N balance as they are involved in GS/GOGAT cycle, vital for N assimilation and essential to protein biosynthesis (Yin et al., 2022; Akhtar et al., 2024). The diminish in these amino acids in one or more generations in LN conditions, coupled with the maintenance in protein levels across treatments could indicate that to maintain N balance and biomass, this treatments assimilate all N available into protein and do not accumulate glutamine as N reservoir like HN_{F0} treatments in both generations, that accumulate these amino acids, being an adaptative strategy to maintain the C/N balance (Kan et al., 2015; Zayed et al., 2023).

Constant LN across generations compared to first time under LN increase carbohydrates, terpenes and lipids, which could be related to changes in gs

The effect of maternal (F0) N-supply on carbohydrate and nitrogen metabolism was evident in both generations (F1 and F2). The increased starch content in offspring of LN_{F0} and $LN_{F0}LN_{F1}$ likely serves as carbon reserve enhancing resilience to N-stress, and as an osmolyte contributing to plant water potential (Castro et al. 2024). It also relates with the increase in gs in both generations when grown at LN, where the maintenance of an open stomata induces more CO_2 fixation, therefore, more carbon reserve molecules like starch and lipids. The slight increase of TSS in F1 growing at HN when the ancestor was stress could be related to the same, suggesting that the maternal stress induces accumulation of carbon reserve molecules, that did not reflect in an increase of TSS in F2 growing at LN, likely due to the higher starch reservoir that soluble sugars. Total protein content in F1 decreases when growing at HN_{F1} in descendants of stress mothers, while in

F2 there is no difference between treatments. On the other hand, the decrease in free amino acid content in both F1 and F2 generations when grown at LN, independent of the N-state of their ancestors, could indicate that there is an efficient conversion of amino acids to proteins when the mother plant was stressed, also indicating N-remobilization to sustain growth under LN conditions (Batista-Silva et al., 2019; Hildebrandt, 2018).

The nitrate content was lower in LN_{F0} offspring or when grown at LN on both generations, suggesting an inherited N-use efficiency strategy (Fig. 3C, F). Conversely, nitrite content in F1 was significantly lower in HN_{F0} offspring under LN_{F1}, but higher in LN_{F0} offspring under the same F1 conditions (Fig. 3I). Finally, nitrite content in F2 was more variable in F1, decreasing at LN_{F1} when the mother grew at HN_{F0} and increasing at LN_{F1} when the mother grew at LN_{F0}, but it showed no change between treatments in F2 (Fig. 3I, L), this could indicate a differential N assimilation pathway in each generation, and a metabolic reprogramming in the offspring (Castro et al., 2024; Herman and Sultan, 2011).

The metabolomic profile of F1 seedlings revealed distinct patterns, with clusters enriched in lipids, amino acids, and flavonoids in treatments where maternal and offspring N supplies were the same (Fig. 4). F2 seedlings showed higher variability, particularly in treatments that came from LN_{F0} plants, suggesting a more complex integration of stress memory, incorporating both immediate and ancestral N environments into their metabolic patterns (Fig. 5). The increase levels of flavonoids and terpenes, particularly in treatments originating from LN conditions suggest and enhanced antioxidant and defense capacity, likely a protective mechanism to oxidative stress induced by N deficiency (Agati et al., 2020).

LN across generations accelerate growth

F1 plants showed no significant differences in Pn, but descendants of LN_{F0} decreased gs and E, particularly under HN_{F1} (Fig. 6A, B, C). This suggests a long-term adjustment in water exchange, potentially as a stress memory mechanism. In terms of chlorophyll *a* fluorescence parameters, no significant differences were observed in Fv/Fm and qL, suggesting that they were maintained across N conditions (Fig. 6D, F). However, NPQ decreased in

offspring growth at LN_{F1}, indicating reduced thermal dissipation of excess light energy, potentially due to more efficient photosynthesis light utilization in LN conditions (Fig. 6E). These findings suggest that maternal N influences carbon assimilation and energy dissipation, contributing to an adaptative strategy in different N conditions.

Biomass allocation in F2 plants showed that maternal (F0) N-supply influences shoot and root biomass, with higher shoot and root biomass in descendants of LN_{F0} (Fig. 8). Comparing $HN_{F1}HN_{F2}$ treatments, there is a tendency to have higher biomass when it comes from LN_{F0}, indicating a potential transgenerational effect on growth strategies under N-stress. Maternal N-deficit precondition offspring to have enhanced N-use efficiency and growth, supporting the hypothesis of transgenerational memory mechanisms.

Effect of maternal N supply (F0) on yield and germination of their progeny

Maternal N-supply affects yield and germination traits. F1 plants exhibited reduced yield under LN_{F1} conditions, more significantly in descendants of LN_{F0} mothers (Fig. 7A). This indicates that although physiological and metabolic adjustments occur, they may not fully offset growth limitations imposed by continuous nitrogen stress. In maize, N-deficit impairs chloroplast function and ultrastructure which, finally, decreases biomass and grain yield (Jin et al., 2015, Liu et al., 2018). Moreover, F2 seeds from LN_{F0} germinated more slowly, suggesting that maternal nitrogen stress can influence seed vigor and early developmental processes in progeny (Fig. 7C).

Finally, maternal N-stress induces metabolic and physiological adaptations in quinoa across generations. The trade-offs between early-stage vigor, metabolic priming and reproductive yield suggest a complex balance between stress resistance and resource allocation, with the descendants of LN_{F0} the offspring better prepared for external N limiting conditions.

This adaptation to LN is not only related with radicular development as we saw in Castro et al. (2024), but it also affects the metabolism which can be

seen to some extent in F2. This metabolomic reprogramming, which increases C assimilation and enhances biomass gain, could be a competitive strategy under LN conditions that shortens life cycle and reduces N fertilizer use, achieving similar production levels with lower N input as one time a year with an excess of N.

AUTHOR CONTRIBUTIONS

CC and LBG designed the assays and led the writing of the manuscript. CC, RSL, FA, JO, MPJ and EE performed the assays, measurements and data analysis. TCP, EOG and LBG edited the manuscript. All authors contributed to the article and approved the final version of the manuscript.

ACKNOLEDGEMENTS

This work was supported by ANID BECAS/DOCTORADO NACIONAL grant 21201031, ANID FONDECYT REGULAR 1220589 and ANID FONDECYT REGULAR Nº 1211473. The authors acknowledge the Fondequip EQM170172.

REFERENCES

Abugoch, L. (2009). Quinoa (Chenopodium quinoa Willd.): Composition, Chemistry, Nutritional, and Functional Properties. In *Advances in Food and Nutrition Research* (Vol. 58, pp. 1–31). Elsevier. https://doi.org/10.1016/S1043-4526(09)58001-1

Agati, G., Brunetti, C., Fini, A., Gori, A., Guidi, L., Landi, M., Sebastiani, F., & Tattini, M. (2020). Are Flavonoids Effective Antioxidants in Plants? Twenty Years of Our Investigation. *Antioxidants*, *9*(11), 1098. https://doi.org/10.3390/antiox9111098

Akhtar, K., Ain, N., Prasad, P. V. V., Naz, M., Aslam, M. M., Djalovic, I., Riaz, M., Ahmad, S., Varshney, R. K., He, B., and Wen, R. (2024). Physiological, molecular, and environmental insights into plant nitrogen uptake, and metabolism under abiotic stresses. *The Plant Genome*, 17, e20461. https://doi.org/10.1002/tpg2.20461

Bascuñán-Godoy, L., Sanhueza, C., Hernández, C. E., Cifuentes, L., Pinto, K., Álvarez, R., González-Teuber, M., and Bravo, L. A. (2018). Nitrogen Supply Affects Photosynthesis and Photoprotective Attributes During Drought-Induced Senescence in Quinoa. *Front Plant Sci*, **9**, 1–14. https://doi.org/10.3389/fpls.2018.00994

Bascuñán-Godoy, L., Alcaino, C., Carvajal, D. E., Sanhueza, C., Montecinos, S., and Maldonado, A. (2015). Ecophysiological responses to drought followed by re-watering of two native Chilean swamp forest plants: Myrceugenia exsucca (DC.) O. Berg and Luma chequen (Molina) A. Gray. *Gayana Bot*, **72**, 203–212. https://doi.org/10.4067/S0717-66432015000200004

Batista-Silva, W., Heinemann, B., Rugen, N., et al. (2019). The role of amino acid metabolism during abiotic stress release. *Plant Cell Environ*. 42: 1630–1644. https://doi.org/10.1111/pce.13518

Bazule, D., Bertero, D., and Nieto, C. (2014). Estado del arte de la quinua en el mundo en 2013. In *FAO (Santiago, Chile) CIRAD (Montpellier, France)*. https://doi.org/10.1016/0006-2952(67)90244-4

Bradford, M. M. (1976). A Rapid and Sensitive Method for the Quantitation of Microgram Quantities of Protein Utilizing the Principle of Protein-Dye Binding. *Anal Biochem*, **72**, 248–254.

Bruce, T. J. A., Matthes, M. C., Napier, J. A., and Pickett, J. A. (2007). Stressful "memories" of plants: Evidence and possible mechanisms. *Plant Sci*, **173**(6), 603–608. https://doi.org/10.1016/j.plantsci.2007.09.002

Castro, C., Rojas, J., Ortíz, J., Sanhueza-Lepe, R., Vergara, A., Poblete, F., Escobar, E., Coba de la Peña T., Ostria-Gallardo, E., Bascuñan-Godoy, L. (2024). Nitrogen Stress

Memory in Quinoa: Maternal Effects on Seed Metabolism and Offspring Growth and Physiology. *Physiol Plant*. 176(6):e14614. doi: 10.1111/ppl.14614. PMID: 39513412.

Chow, P. S., and Landhäusser, S. M. (2004). A method for routine measurements of total sugar and starch content in woody plant tissues. *Tree Physiology*, **24**(10), 1129–1136. https://doi.org/10.1093/treephys/24.10.1129

Cisse, A., Zhao, X., Fu, W., Kim, R. E. R., Chen, T., Tao, L., and Feng, B. (2020). Non-Photochemical Quenching Involved in the Regulation of Photosynthesis of Rice Leaves under High Nitrogen Conditions. *Int J Mol Sci.* **21**(6):2115. doi: 10.3390/ijms21062115

de Camargo Santos, A., Schaffer, B., Rowland, D., Bremgartner, M., Moon, P., Tillman, B., Rodrigues de Souza, E. and Bassil, E. (2024). Cross-Generational Effect of Water Deficit Priming on Physiology of Peanut Plants Under Water Stress. *J Agro Crop Sci*, 210: e12736. https://doi.org/10.1111/jac.12736

Dickinson, R. E. (1979). Analytical procedures for the sequential extraction of 14C-labeled constituents from leaves, bark and wood of cottonwood plants. *Physiologia Plantarum* **45**, 480-488. https://doi.org/10.1111/j.1399-3054.1979.tb02618.x

Djoumbou Feunang, Y., Eisner, R., Knox, C., Chepelev, L., Hastings, J., Owen, G., Fahy, E., Steinbeck, C., Subramanian, S., Bolton, E., Greiner, R., Wishart, D. S. (2016). ClassyFire: automated chemical classification with a comprehensive, computable taxonomy. *J Cheminform* **8**, 61. https://doi.org/10.1186/s13321-016-0174-y

Doane, T. A., and Horwáth, W. R. (2003). Spectrophotometric determination of nitrate with a single reagent. *Analytical Letters*, **36**(12), 2713–2722. https://doi.org/10.1081/AL-120024647

Dobin, A., Davis, C.A., Schlesinger, F., Drenkow, J., Zaleski, C., Jha, S., Batut, P., Chaisson, M., Gingeras, T.R. (2013) STAR: ultrafast universal RNA-seq aligner. *Bioinformatics* **29**(1): 15–21. https://doi.org/10.1093/bioinformatics/bts635

Fathi, A. and Zeidali, E. (2021). Conservation tillage and nitrogen fertilizer: a review of corn growth and yield and weed management. *Central Asian Journal of Plant Science Innovation*, *1*(3), 121-142. doi: 10.22034/CAJPSI.2021.03.01

Forster, J. C. (1995). Soil sampling, handling, storage and analysis. In K. Alef and P. Nannipieri (Eds.), *Methods in Applied Soil Microbiology and Biochemistry* (pp. 49–121). Academic Press Ltd. https://doi.org/10.1016/b978-012513840-6/50018-5

Gamir, J., Sánchez-Bel, P., and Flors, V. (2014). Molecular and physiological stages of priming: how plants prepare for environmental challenges. *Plant Cell Reports*, **33**(12), 1935–1949. https://doi.org/10.1007/s00299-014-1665-9

Gundel, P. E., Rudgers, J. A., and Whitney, K. D. (2017). Vertically transmitted symbionts as mechanisms of transgenerational effects. *American J Bot*, **104**(5), 787–792. https://doi.org/10.3732/ajb.1700036

Hatzig, S. V., Nuppenau, J. N., Snowdon, R. J., and Schießl, S. V. (2018). Drought stress has transgenerational effects on seeds and seedlings in winter oilseed rape (Brassica napus L.). *BMC Plant Biol*, **18**(1). https://doi.org/10.1186/s12870-018-1531-y

Herman, J. J. and Sultan, S. E. (2011) Adaptive transgenerational plasticity in plants: case studies, mechanisms, and implications for natural populations. *Front. Plant Sci.* **2**:102. doi: 10.3389/fpls.2011.00102

Hildebrandt, T.M. (2018). Synthesis versus degradation: directions of amino acid metabolism during Arabidopsis abiotic stress response. *Plant Mol Biol* **98**, 121–135. https://doi.org/10.1007/s11103-018-0767-0

Holeski, L. M., Jander, G., and Agrawal, A.A. (2012). Transgenerational defense induction and epigenetic inheritance in plants. *Trends Ecol Evol*. 27(11):618-26. doi: 10.1016/j.tree.2012.07.011.

INIA. (2015). Quínoa: Un súper Alimento Para Chile y el Mundo. *Tierra Adentro*, *N° 108*, 84. http://biblioteca.inia.cl/medios/revista-tierra-adentro/Tierra_Adentro_1_diciembre-Especial-Quinoa.pdf

Jin, X., Yang, G., Tan, C., & Zhao, C. (2015). Effects of nitrogen stress on the photosynthetic CO2 assimilation, chlorophyll fluorescence and sugar-nitrogen ratio in corn. *Scientific reports*, *5*(1), 9311.

Kasajima, I., Ebana, K., Yamamoto, T., Takahara, K., Yano, M., and Kawai-Yamada, M. (2011). Molecular distinction in genetic regulation of nonphotochemical quenching in rice. *Proc. Natl. Acad. Sci.* USA. **108**:13835–13840. doi: 10.1073/pnas.1104809108.

Kambona, C. M., Koua, P. A., Léon, J., and Ballvora, A. (2023). Stress memory and its regularion in plants experiencing recurrent drought conditions. *Theoretical and Applied Genetics* **136**, 26. https://doi.org/10.1007/s00122-023-04313-1Murphy, D., Rawsthorne, S., and Hills, M. (1993). Storage lipid formation in seeds. *Seed Science Research*, **3**(2), 79-95. doi:10.1017/S096025850000163X

Kan, C. C., Chung, T. Y., Juo, Y. A., and Hsieh, M. H. (2015). Glutamine rapidly induces the expression of key transcription factor genes involved in nitrogen and stress responses in rice roots. *BMC Genomics*. 16. 10.1186/s12864-015-1892-7.

Kramer, D. M., Johnson, G., Kiirats, O., and Edwards, G. E. (2004). New fluorescence parameters for the determination of QA redox state and excitation energy fluxes. Photosynth Res, **79**, 209–218. https://doi.org/doi:10.1023/B:PRES.0000015391.99477.0d

Li, H., Li, J., Zhang, X., Shi, T., Chai, X., Hou, P., & Wang, Y. (2021). Mesophyll conductance, photoprotective process and optimal N partitioning are essential to the maintenance of photosynthesis at N deficient condition in a wheat yellow-green mutant (Triticum aestivum L.). *J plant physiol*, 263, 153469. https://doi.org/10.1016/j.jplph.2021.153469.

Liu, Z., Gao, J., Gao, F., Liu, P., Zhao, B., & Zhang, J. (2018). Photosynthetic characteristics and chloroplast ultrastructure of summer maize response to different nitrogen supplies. *Frontiers in Plant Science*, *9*, 576.

Liu, H. P., Able, A. J., and Able, J. A. (2021) Nitrogen Starvation-Responsive MicroRNAs Are Affected by Transgenerational Stress in Durum Wheat Seedlings. *Plant (Basel)*, **10**(5), 826. doi: 10.3390/plants10050826

Love, M.I., Huber, W. & Anders, S. (2014). Moderated estimation of fold change and dispersion for RNA-seq data with DESeq2. *Genome Biol* **15**, 550. https://doi.org/10.1186/s13059-014-0550-8

Massaro, M., De Paoli, E., Tomasi, N., Morgante, M., Pinton, R., and Zanin, L. (2020). Transgenerational Response to Nitrogen Deprivation in *Arabidopsis thaliana*. *Int J Mol Sci,* **20**, 5587. doi: 10.3390/ijms20225587

Maxwell, K., and Johnson, G. N. (2000). Chlorophyll fluorescence - a practical guide. *J Exp Bot*, **51**, 659–668. https://doi.org/doi: 10.1093/jexbot/51.345.659

Moustakas, M., Sperdouli, I., Adamakis, I., Moustaka, J., İşgören, S., and Şaş, B. (2022). Harnessing the Role of Foliar Applied Salicylic Acid in Decreasing Chlorophyll Content to Reassess Photosystem II Photoprotection in Crop Plants. *International Journal of Molecular Sciences*, 23. https://doi.org/10.3390/ijms23137038.

Murashige, T. and Skoog, F. (1962), A Revised Medium for Rapid Growth and Bio-Assays with Tobacco Tissue Cultures. *Physiologia Plantarum* **15**: 473-497. https://doi.org/10.1111/j.1399-3054.1962.tb08052.x

Müller, P., Li, X. P., and Niyogi, K. K. (2001). Non-photochemical quenching. A response to excess light energy. *Plant physiology*, *125*(4), 1558-1566.

Murchie, S. H., Peng, S., and Horton, P. (2005). Acclimation of photosynthesis to high irradiance in rice: Gene expression and interactions with leaf development. *J. Exp. Bot.* **56**:449–460. doi: 10.1093/jxb/eri100

Nowak, V., Du, J., and Charrondière, U. R. (2016). Assessment of the nutritional composition of quinoa (Chenopodium quinoa Willd.). *Food Chem*, **193**, 47–54. https://doi.org/10.1016/j.foodchem.2015.02.111

Pinto-Irish, K., Coba de la Peña, T., Ostria-Gallardo, E., Ibáñez, C., Briones, V., Vergara, A., Alvarez, R., Castro, C., Sanhueza, C., Castro, P.A., Bascuñán-Godoy, L. (2020). Seed characterization and early nitrogen metabolism performance of seedlings from Altiplano and coastal ecotypes of Quinoa. BMC Plant Biol. 20(1):343. doi: 10.1186/s12870-020-02542-w.

Ranal, M. A., and Santana, D. G. (2006). How and why to measure the germination process? *Brazilian J Botany*, **29**, 1–11. https://doi.org/10.1590/S0100-84042006000100002

Racette, K., Zurweller, B., Tillman, B., and Rowland, D. (2020). Transgenerational stress memory of water deficit in peanut production. *Field Crops Research*, ***248***. https://doi.org/10.1016/j.fcr.2019.107712

Sahay S, Grzybowski M, Schnable JC, Głowacka K. (2024). Genotype-specific nonphotochemical quenching responses to nitrogen deficit are linked to chlorophyll a to b ratios. *J Plant Physiol*. 297: 154261. doi: 10.1016/j.jplph.2024.154261.

Scott, S. J., Jones, R. A., and Williams, W. A. (1984). Review of Data Analysis Methods for Seed Germination. *Crop Science*, **24**, 1192–1199.

Sharma, M., Kumar, P., Verma, V., Sharma, R., Bhargava, B., and Irfan, M. (2022). Understanding plant stress memory response for abiotic stress resilience: Molecular insights and prospects. *Plant Physiol and Biochem* 179, 10-24. https://doi.org/10.1016/j.plaphy.2022.03.004

Siddique, A. B., Parveen, S., Rahman, Z., and Rahman, J. (2024). Revisiting plant stress memory: mechanisms and contribution to stress adaptation. *Physiol and Mol Biol of Plants* **30**(2), 349-367. https://doi.org/10.1007/s12298-024-01422-z

Singh, P., Arif, Y., Bajguz, A., Hayat, S. (2021). The role of quercetin in plants. *Plant Physiol Biochem.* **166**:10-19. doi: 10.1016/j.plaphy.2021.05.023.

Smith, A. M., and Zeeman, S. C. (2006). Quantification of starch in plant tissues. *Nature Protocols*, **1**(3), 1342–1345. https://doi.org/10.1038/nprot.2006.232

Sperdouli, I., Panteris, E., Moustaka, J., Aydın, T., Bayçu, G., and Moustakas, M. (2024). Mechanistic Insights on Salicylic Acid-Induced Enhancement of Photosystem II Function in Basil Plants under Non-Stress or Mild Drought Stress. *International Journal of Molecular Sciences*, 25. https://doi.org/10.3390/ijms25115728.

Sun, S. W., Lin, Y. C., Weng, Y. M., and Chen, M. J. (2006). Efficiency improvements on ninhydrin method for amino acid quantification. *Journal of Food Composition and Analysis*, **19**(2–3), 112–117. https://doi.org/10.1016/j.jfca.2005.04.006

Wang, G., Zeng, F., Song, P., Sun, B., Wang, Q., and Wang, J. (2022). Effects of reduced chlorophyll content on photosystem functions and photosynthetic electron transport rate in rice leaves. *Journal of plant physiology*, 272, 153669. https://doi.org/10.1016/j.jplph.2022.153669.

Wang, X., Zhang, X., Chen, J., Wang, X., Cai, J., Zhou, Q., Dai, T., Cao, W., and Jiang, D. (2018). Parental Drought-Priming Enhances Tolerance to Post-anthesis Drought in Offspring of Wheat. *Front Plant Sci*, **9**:261. doi:10.3389/fpls.2018.00261

Wang, Z., Li, G., Sun, H., Ma, L., Guo, Y., Zhao, Z., Gao, H., & Mei, L. (2018). Effects of drought stress on photosynthesis and photosynthetic electron transport chain in young apple tree leaves. *Biology Open*, 7(11): bio035279. https://doi.org/10.1242/bio.035279.

Ye, J. Y., Tian, W. H. and Jin, C. W. (2022). Nitrogen in plants: from nutrition to the modulation of abiotic stress adaptation. *Stress Biology.* 2, 4. https://doi.org/10.1007/s44154-021-00030-1

Yin, H., Yang, F., He, X., Du, X., Mu, P., Ma, W. (2022). Advances in the functional study of glutamine synthetase in plant abiotic stress tolerance response. *The Crop Journal.*10(4), 917-923. https://doi.org/10.1016/j.cj.2022.01.003.

Zayed, O., Hewedy, O. A., Abdelmoteleb, A., Ali, M., Youssef, M. S., Roumia, A. F., Seymour, D., Yuan, Z. C. (2023). Nitrogen Journey in Plants: From Uptake to Metabolism, Stress Response, and Microbe Interaction. *Biomolecules*. 13(10):1443. doi: 10.3390/biom13101443.

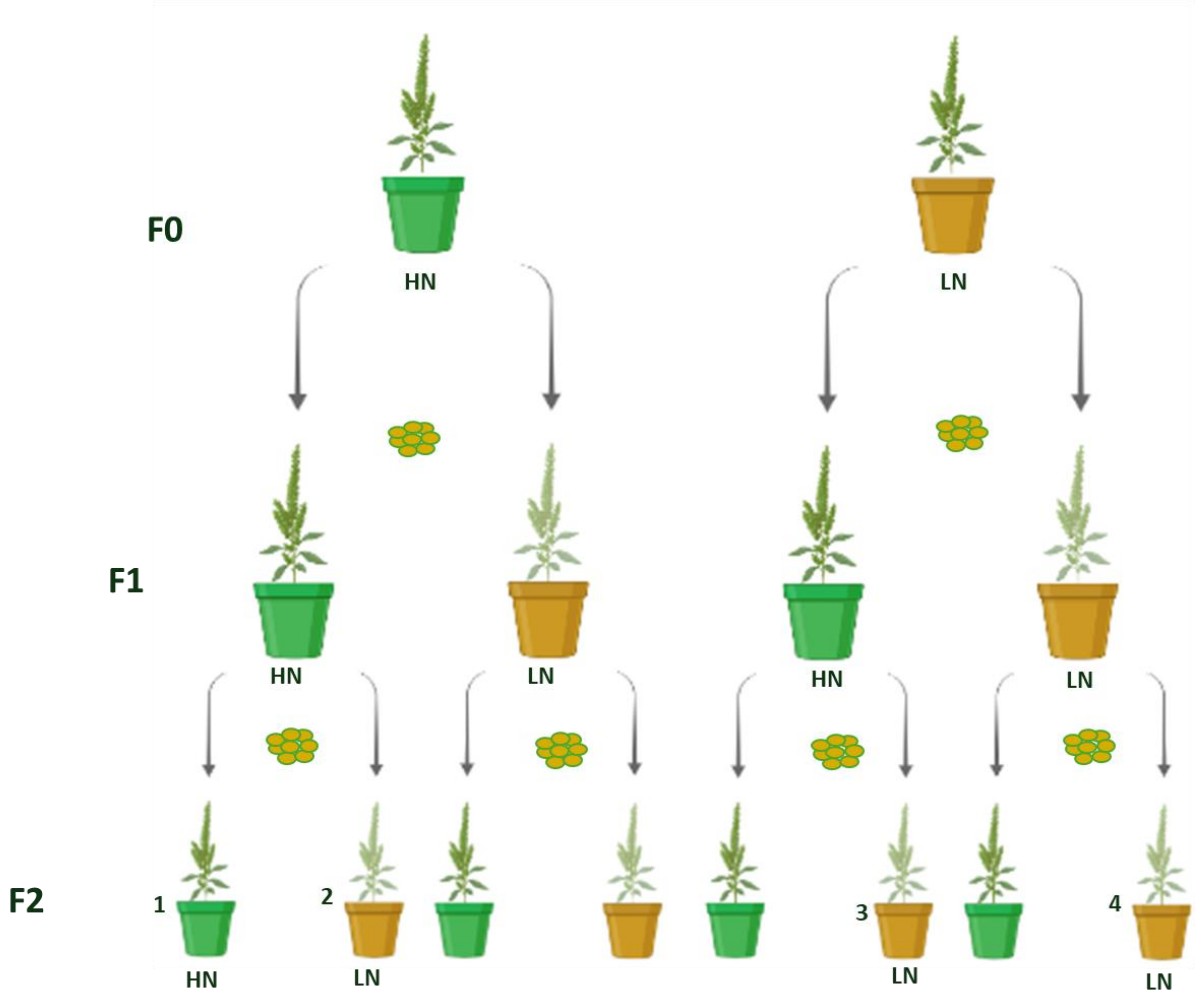

Figure 2.1. Experimental design. Growth conditions and selected treatments of F1 and F2 plants.

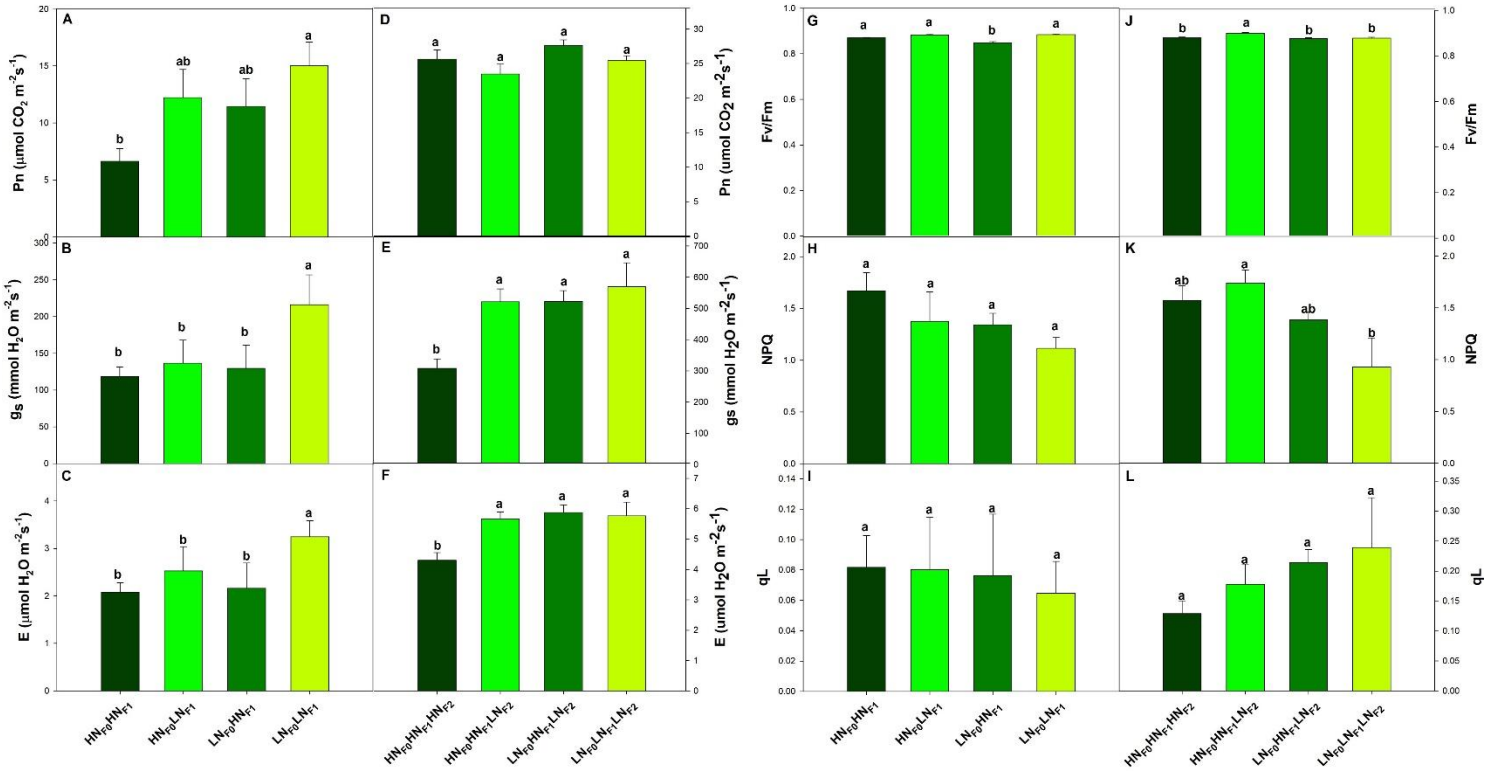

Figure 2.2. Photosynthetic parameters and Photochemical and nonphotochemical fluorescence parameters of 20-day-old F1 and F2 seedlings (descendants of F0 mother plants grown at HN and LN). A, D. Net photosynthetic rate (Pn). **B, E.** Stomatal conductance (gs). **C, F.** Transpiration rate (E). **G, J.** Maximum quantum efficiency (Fv/Fm)**. H, K.** Non-photochemical quenching (NPQ)**. I, L.** Photochemical quenching (qL). A-C and G-I correspond to F1 seedlings, D-F and J-L correspond to F2 seedlings. Results were calculated from four independent measurements of different individuals. Bars show mean values ± SE (n = 5). Common letters indicate no significant differences between treatments using two-way ANOVA for F1, which factors were N supply in F0 and N supply in seedlings, and one-way ANOVA for F2. Tukey HSD was used as a post hoc test ($p < 0.05$).

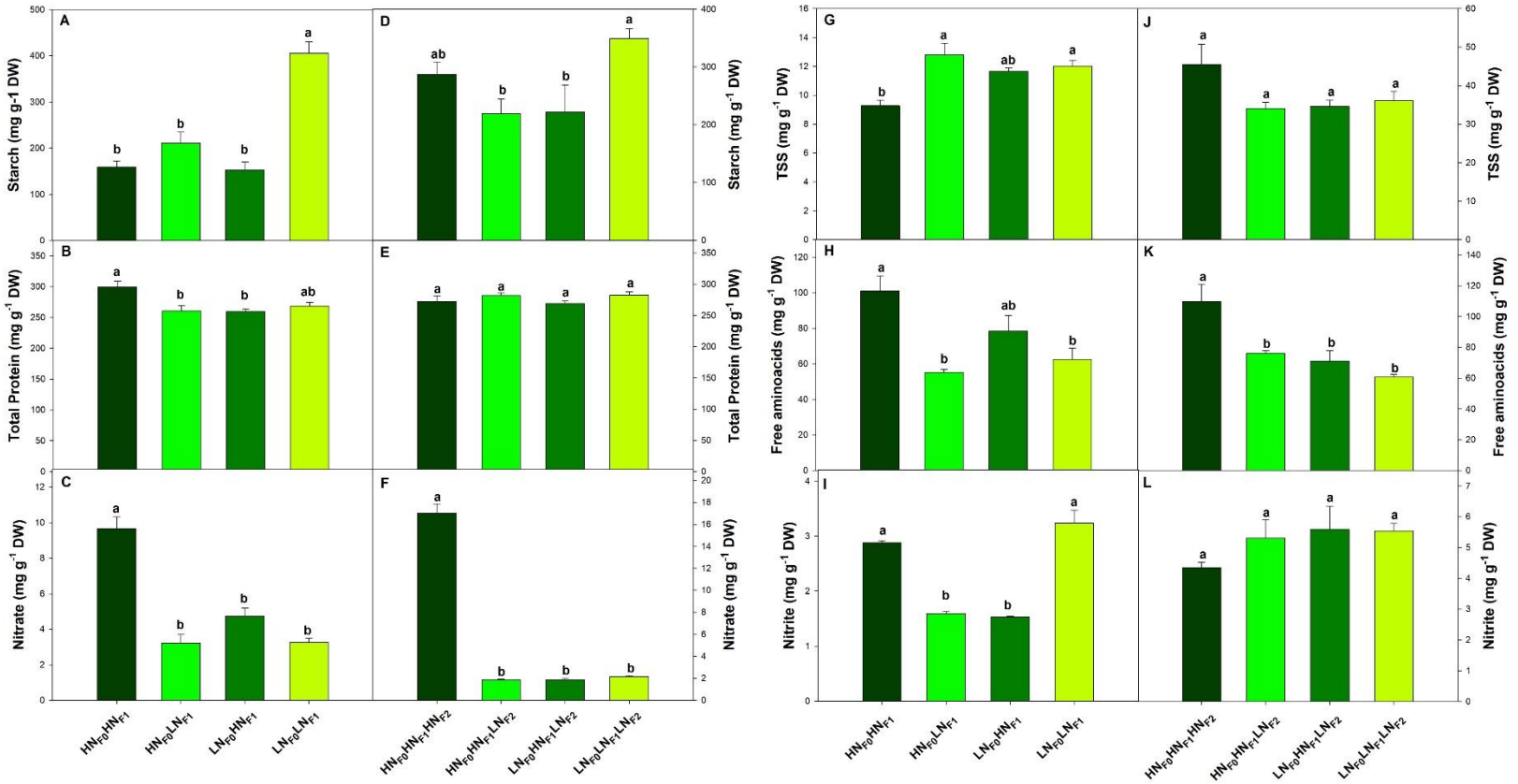

Figure 2.3. Carbohydrates and nitrogen compounds in shoots of 20-day-old F1 and F2 seedlings (descendants of HN_{F0} and LN_{F0} mother plants). A, D. Starch content. **B, E.** Total protein. **C, F.** Nitrate content. **G, J.** Total soluble sugars (TSS). **H, K.** Free amino acids. **I, L.** Nitrite content. A-C and G-I correspond to F1 seedlings, D-F and J-L correspond to F2 seedlings.Bars show mean values ± SE (n=5). Common letters indicate no significant differences between treatments using two-way ANOVA for F1, which factors were N supply in F0 and N supply in seedlings, and one-way ANOVA for F2. Tukey HSD was used as a post hoc test ($p < 0.05$).

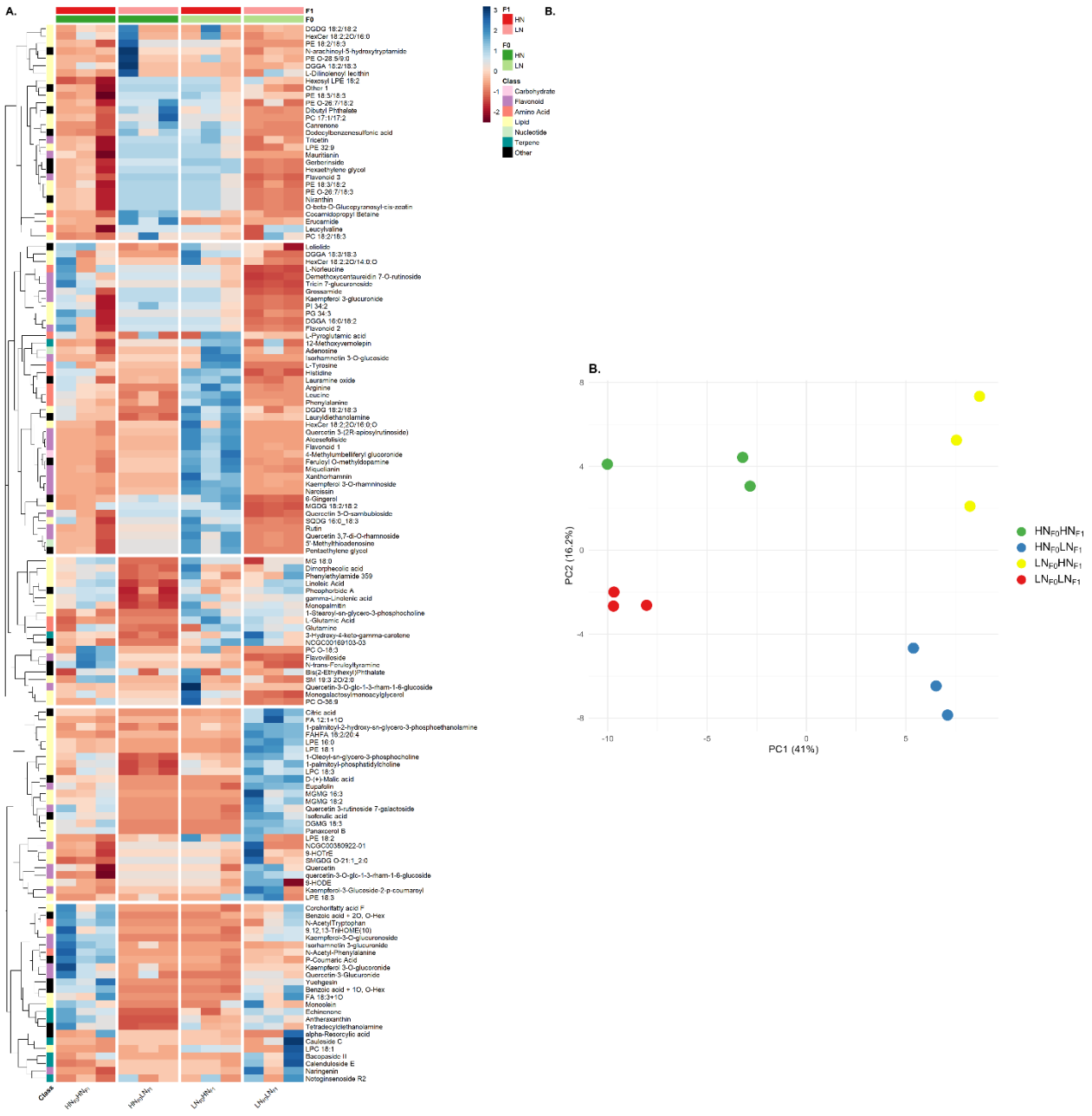

Figure 2.4. Metabolomics analysis in F1 seedlings (descendants of HN_{F0} and LN_{F0} mother plants) grown in HN and LN conditions. A. Heatmap of metabolites detected in the different treatments. **B.** Principal Component Analysis (PCA) of seedlings metabolites. Normalized measurements were scaled using z-scores and analyzed using heatmap and hierarchical clustering. A file containing detailed information for metabolites and their aliases is available in Table S1.

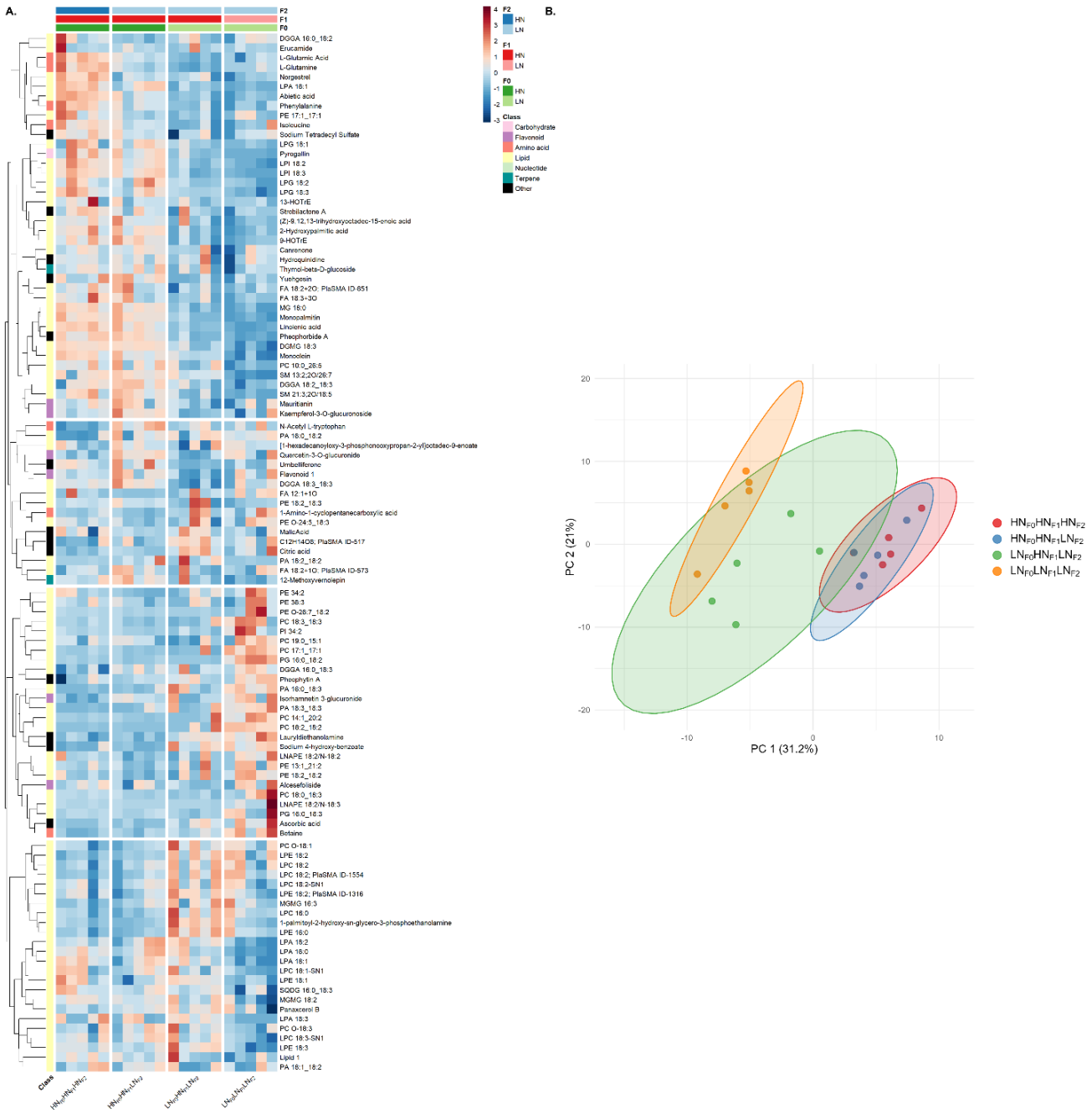

Figure 2.5. Metabolomics analysis in F2 seedlings (descendants of HN_{F0} and LN_{F0} mother plants). A. Heatmap of metabolites detected in the different treatments**. B.** Principal Component Analysis (PCA) of seedlings metabolites. Normalized measurements were scaled using z-scores and analyzed using heatmap and hierarchical clustering. A file containing detailed information on metabolites and their aliases is available in Table S3.

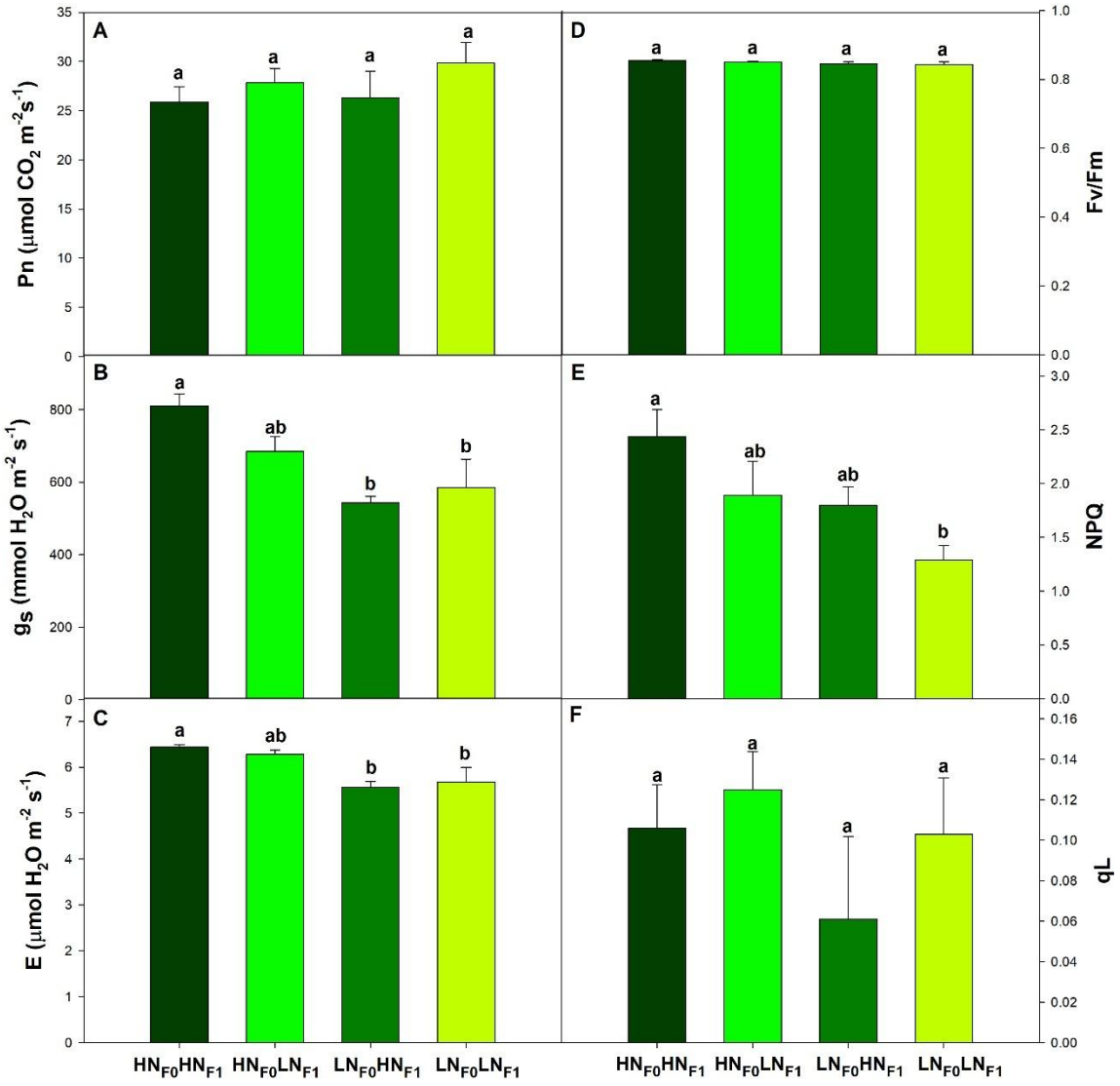

Figure 2.6. Photosynthetic parameters and photochemical and nonphotochemical fluorescence parameters of 60-day-old F1 plants (descendants of HN_{F0} and LN_{F0} mother plants) grown in HN and LN conditions. A. Net photosynthetic rate (Pn). **B.** Stomatal conductance (gs). C**.** Transpiration rate (E). **D.** Maximum quantum efficiency (Fv/Fm). **E.** Nonphotochemical quenching (NPQ). **F.** Photochemical quenching (qL). Results were calculated from five independent measurements of different individuals. Bars show mean values ± SE (n=5). Common letters indicate no significant differences between treatments using two-way ANOVA, which factors were N supply in F0 and N supply in seedlings. Tukey HSD was used as a post hoc test ($p < 0.05$).

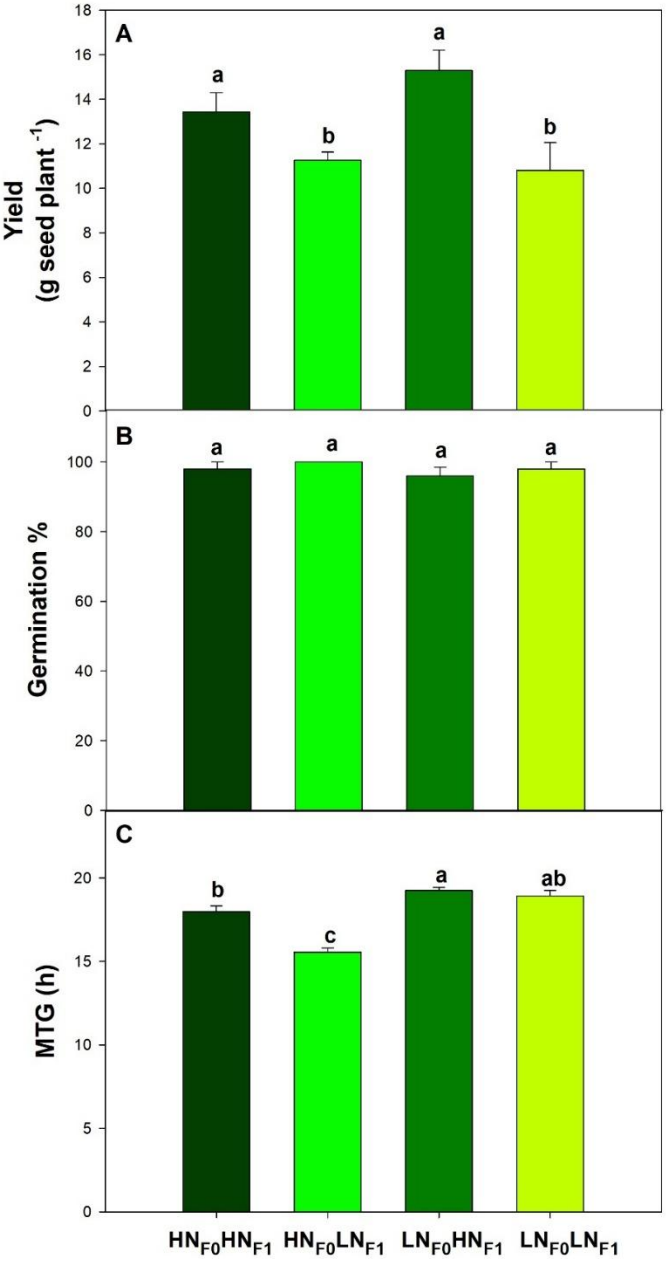

Figure 2.7. Yield of F1 plants and germination parameters of F2 seeds plants (descendants of HN_{F0} and LN_{F0} mother plants) grown in HN and LN conditions. A. Yield of F1 plants**. B.** Germination percentage. **C.** Mean Germination Time (MGT). For germination parameters, graphs show results from 50 seeds (distributed in 5 Petri dishes, with 10 seeds each). Bars show mean values ± SE (n=5). Common letters indicate no significant differences between treatments using two-way ANOVA, which factors were N supply in F0 and N supply in seedlings. Tukey HSD was used as a post hoc test ($p < 0.05$).

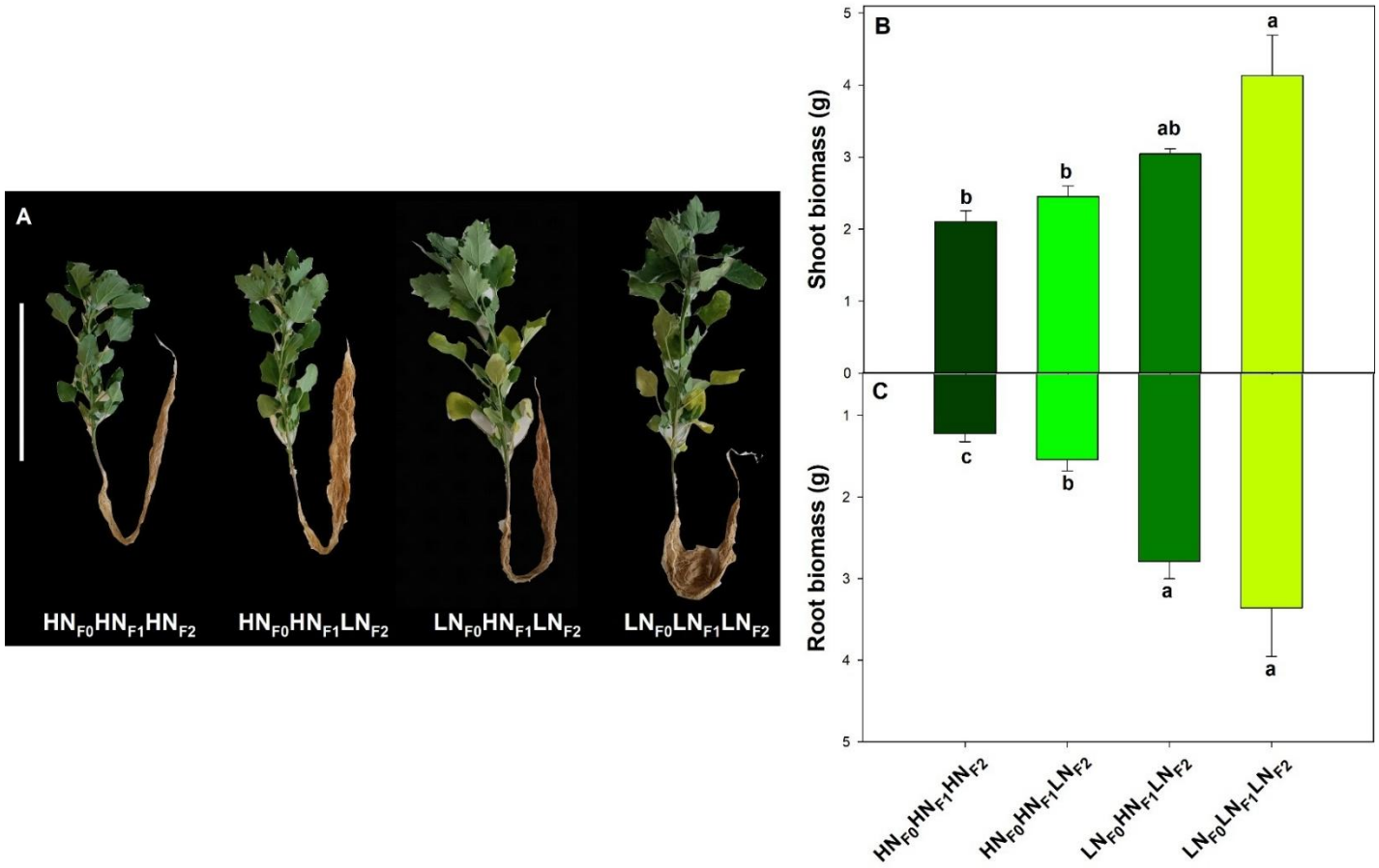

Figure 2.8. Phenotype and shoot and root biomass of 60-day-old F2 plants (descendants of HN_{F0} and LN_{F0} mother plants). A. 60-day-old F2 plants. White line indicates a 25 cm scale. **B.** Shoot biomass. **C.** Root biomass. Bars show mean values ± SE (n=5). Common letters indicate no significant differences between treatments using one-way ANOVA. Tukey HSD was used as a post hoc test ($p < 0.05$).

Supplemental Table 2.1. Metabolites and their aliases and class for F1 seedling metabolomic heatmap.

Metabolite	***Class***	***Alias***
12-Methoxyvernolepin	Terpene	
1-Oleoyl-sn-glycero-3-phosphocholine	Lipid	
1-palmitoyl-2-hydroxy-sn-glycero-3-phosphoethanolamine	Lipid	
1-palmitoyl-phosphatidylcholine	Lipid	
1-Stearoyl-sn-glycero-3-phosphocholine	Lipid	
3-Hydroxy-4-keto-gamma-carotene	Terpene	
4-Methylumbelliferyl glucoronide	Carbohydrate	
5'-Methylthioadenosine	Nucleotide	
6-Gingerol	Other	
13-TriHOME(10)	Lipid	9,12,13-TriHOME(10)
9-HODE	Lipid	
9-HOTrE	Lipid	
Adenosine	Nucleotide	
Alcesefoliside	Flavonoid	
alpha-Resorcylic acid	Other	
Antheraxanthin	Terpene	
Arginine	Amino Acid	
Bacopaside II	Terpene	
Benzoic acid + 1O, O-Hex	Other	
Benzoic acid + 2O, O-Hex	Other	
Bis(2-Ethylhexyl)Phthalate	Other	
Calenduloside E	Terpene	
Canrenone	Lipid	
Cauloside C	Terpene	
Citric acid	Other	
Cocamidopropyl Betaine	Amino Acid	
Corchorifatty acid F	Lipid	
D-(+)-Malic acid	Other	
Demethoxycentaureidin 7-O-rutinoside	Flavonoid	
DGDG 18:2/18:2	Lipid	
DGDG 18:2/18:3	Lipid	
DGGA 16:0/18:2	Lipid	
DGGA 18:2/18:3	Lipid	
DGGA 18:3/18:3	Lipid	
DGMG 18:3	Lipid	
Dibutyl Phthalate	Other	

Dimorphecolic acid	Lipid	
Dodecylbenzenesulfonic acid	Other	
Echinenone	Terpene	
Erucamide	Lipid	
Eupafolin	Flavonoid	
FA 12:1+1O	Lipid	
FA 18:3+1O	Lipid	
FAHFA 18:2/20:4	Lipid	
Feruloyl O-methyldopamine	Other	
2-(3,4-dihydroxyphenyl)-5,7-dihydroxy-3-[(2S,3R,4S,5S,6R)-3,4,5-trihydroxy-6-[[(2S,3R,4S,5R)-3,4,5-trihydroxyoxan-2-yl]oxymethyl]oxan-2-yl]oxychromen-4-one	Flavonoid	Flavonoid 1
3,4,5-trihydroxy-6-[5-hydroxy-2-(4-hydroxy-3-methoxyphenyl)-3-methoxy-4-oxochromen-7-yl]oxyoxane-2-carboxylic acid	Flavonoid	Flavonoid 2
3-[(2S,3R,4S,5S,6R)-4,5-dihydroxy-3-[(2R,3R,4R,5R,6S)-3,4,5-trihydroxy-6-methyloxan-2-yl]oxy-6-[[(2R,3R,4R,5R,6S)-3,4,5-trihydroxy-6-methyloxan-2-yl]oxymethyl]oxan-2-yl]oxy-5,7-dihydroxy-2-(4-hydroxyphenyl)-6-methoxychromen-4-one	Flavonoid	Flavonoid 3
Flavovilloside	Flavonoid	
gamma-Linolenic acid	Lipid	
Gerberinside	Other	
Glutamine	Amino Acid	
Grossamide	Flavonoid	
Hexaethylene glycol	Other	
HexCer 18:2;2O/14:0;O	Lipid	
HexCer 18:2;2O/16:0	Lipid	
HexCer 18:2;2O/16:0;O	Lipid	
Hexosyl LPE 18:2	Lipid	
Histidine	Amino Acid	
Isoferulic acid	Other	
Isorhamnetin 3-glucuronide	Flavonoid	
Isorhamnetin 3-O-glucoside	Flavonoid	
Kaempferol 3-glucuronide	Flavonoid	
Kaempferol 3-O-glucoronide	Flavonoid	
Kaempferol 3-O-rhamninoside	Flavonoid	
Kaempferol-3-Glucoside-2-p-coumaroyl	Flavonoid	
Kaempferol-3-O-glucuronoside	Flavonoid	

Lauramine oxide	Other	
Lauryldiethanolamine	Other	
L-Dilinolenoyl lecithin	Lipid	
Leucine	Amino Acid	
Leucylvaline	Amino Acid	
L-Glutamic Acid	Amino Acid	
Linoleic Acid	Lipid	
L-Norleucine	Amino Acid	
Loliolide	Other	
LPC 18:1	Lipid	
LPC 18:3	Lipid	
LPE 16:0	Lipid	
LPE 18:1	Lipid	
LPE 18:2	Lipid	
LPE 18:3	Lipid	
LPE 32:9	Lipid	
L-Pyroglutamic acid	Amino Acid	
L-Tyrosine	Amino Acid	
Mauritianin	Flavonoid	
MG 18:0	Lipid	
MGDG 18:2/18:2	Lipid	
MGMG 16:3	Lipid	
MGMG 18:2	Lipid	
Miquelianin	Flavonoid	
Monogalactosylmonoacylglycerol	Lipid	
Monoolein	Lipid	
Monopalmitin	Lipid	
N-Acetyl-Phenylalanine	Amino Acid	
N-AcetylTryptophan	Amino Acid	
N-arachinoyl-5-hydroxytryptamide	Other	
Narcissin	Flavonoid	
Naringenin	Flavonoid	
NCGC00169103-03_C19H18O6_Benz[3,4]anthra[1,2-b]oxirene-5,6-dione, 1a,2,3,4,5b,11,11a,11b-octahydro-10,11,11a-trihydroxy-3-methyl-	Other	NCGC00169103-03
NCGC00380922-01![6-[2-(3,4-dihydroxyphenyl)-8-hydroxy-4-oxochromen-7-yl]oxy-3,4,5-trihydroxyoxan-2-yl]methyl (E)-3-(4-hydroxyphenyl)prop-2-enoate	Flavonoid	NCGC00380922-01
Niranthin	Other	
Notoginsenoside R2	Terpene	

N-trans-Feruloyltyramine	Other	
O-beta-D-Glucopyranosyl-cis-zeatin	Lipid	
7-methoxy-6-(1,2,3-trihydroxy-3-methylbutyl)chromen-2-one	Other	Other 1
Panaxcerol B	Lipid	
PC 17:1/17:2	Lipid	
PC 18:2/18:3	Lipid	
PC O-18:3	Lipid	
PC O-36:9	Lipid	
P-Coumaric Acid	Other	
PE 18:2/18:3	Lipid	
PE 18:3/18:2	Lipid	
PE 18:3/18:3	Lipid	
PE O-26:7/18:2	Lipid	
PE O-26:7/18:3	Lipid	
PE O-28:5/9:0	Lipid	
Pentaethylene glycol	Other	
PG 34:3	Lipid	
Phenylalanine	Amino Acid	
Phenylethylamide 359	Lipid	
Pheophorbide A	Other	
PI 34:2	Lipid	
Quercetin	Flavonoid	
Quercetin 3-(2R-apiosylrutinoside)	Flavonoid	
Quercetin 3,7-di-O-rhamnoside	Flavonoid	
Quercetin 3-O-sambubioside	Flavonoid	
Quercetin 3-rutinoside 7-galactoside	Flavonoid	
Quercetin-3-Glucuronide	Flavonoid	
Quercetin-3-O-glc-1-3-rham-1-6-glucoside	Flavonoid	
quercetin-3-O-glc-1-3-rham-1-6-glucoside	Flavonoid	
Rutin	Flavonoid	
SM 19:3 2O/2:0	Lipid	
SMGDG O-21:1_2:0	Lipid	
SQDG 16:0_18:3	Lipid	
Tetradecyldiethanolamine	Other	
Tricetin	Flavonoid	
Tricin 7-glucuronoside	Flavonoid	
Xanthorhamnin	Flavonoid	
Yuehgesin	Other	

Supplemental Table 2.2. Two-way ANOVA analysis of F1 seedling metabolomic showing key metabolites with significant changes across treatments. Factors were N treatment in F0 and N treatment in F1.

Metabolite	***F0 (F.val)***	***F0 (raw.p)***	***F0 (adj.p)***	***F1 (F.val)***	***F1 (raw.p)***	***F1 (adj.p)***	***Interaction (F.val)***	***Interaction (raw.p)***	***Interaction (adj.p)***
Kaempferol 3-O-rhamninoside	144.46	2.12E-06	0.000277	147.06	1.98E-06	0.000251	170.24	1.13E-06	4.93E-05
Flavonoid 1	103.62	7.43E-06	0.000486	110.93	5.76E-06	0.000251	117.12	4.69E-06	0.0001536
D-(+)-Malic acid	53.31	8.38E-05	0.00365	50.385	0.000102	0.00267	312.21	1.08E-07	7.07E-06
Xanthorhamnin	44.964	0.000152	0.00497	45.95	0.000141	0.00307	51.418	9.51E-05	0.0010382
Lauryldiethanolamine	30.572	0.000554	0.0121	64.139	4.33E-05	0.00141	80.476	1.90E-05	0.000414
Demethoxycentaureidin 7-O-rutinoside	31.673	0.000494	0.0121	3.781	0.088	0.18012	2.506	0.152	0.2586
Miquelianin	25.561	0.000982	0.0142	28.325	0.000709	0.009956	34.726	0.000365	0.0031877
Isorhamnetin 3-glucuronide	25.728	0.000962	0.0142	2.801	0.133	0.24199	2.855	0.13	0.23014
N-trans-Feruloyltyramine	27.446	0.000784	0.0142	0.109	0.75	0.8073	0.018	0.896	0.92628
Tricin 7-glucuronoside	19.397	0.002	0.0238	0.839	0.386	0.47258	3.369	0.104	0.20035
P-Coumaric Acid	20.526	0.002	0.0238	0.843	0.385	0.47258	0.106	0.753	0.80198
Grossamide	16.939	0.003	0.0262	2.315	0.167	0.2717	6.23	0.037	0.086554
PI 34:2	17.163	0.003	0.0262	1.97	0.198	0.3016	3.798	0.087	0.17534
N-Acetyl-Phenylalanine	17.156	0.003	0.0262	1.21	0.303	0.40094	0.321	0.586	0.65056
Flavovilloside	18.42	0.003	0.0262	0.106	0.753	0.8073	0.129	0.728	0.78707
Cocamidopropyl Betaine	15.667	0.004	0.0308	16.747	0.003	0.028071	19.015	0.002	0.010077
1-palmitoyl-2-hydroxy-sn-glycero-3-phosphoethanolamine	15.74	0.004	0.0308	4.369	0.07	0.15283	2.929	0.125	0.22743

N-AcetylTryptophan	14.556	0.005	0.0363	2.423	0.158	0.26532	1.738	0.224	0.32971
1-Oleoyl-sn-glycero-3-phosphocholine	12.756	0.007	0.0416	2.859	0.129	0.23801	13.832	0.006	0.024562
Kaempferol-3-O-glucuronoside	13.199	0.007	0.0416	3.427	0.101	0.1965	0.967	0.354	0.45915
Yuehgesin	12.835	0.007	0.0416	2.745	0.136	0.24405	0.984	0.35	0.45915
Monopalmitin	12.961	0.007	0.0416	21.841	0.002	0.020154	0.019	0.894	0.92628
Erucamide	12.222	0.008	0.0419	11.479	0.01	0.051606	13.421	0.006	0.024562
L-Norleucine	12.403	0.008	0.0419	3.415	0.102	0.1965	7.705	0.024	0.0655
1-palmitoyl-phosphatidylcholine	12.495	0.008	0.0419	4.852	0.059	0.14053	2.85	0.13	0.23014
LPC 18:3	11.75	0.009	0.0453	3.471	0.099	0.1965	0.339	0.576	0.64492
Kaempferol 3-O-glucoronide	11.31	0.01	0.0485	0.027	0.874	0.89448	1.673	0.232	0.33769
Citric acid	10.694	0.011	0.049	8.734	0.018	0.05895	35.842	0.000328	0.0030691
4-Methylumbelliferyl glucoronide	10.654	0.011	0.0496	10.161	0.013	0.051606	27.424	0.000786	0.0054193
Panaxcerol B	10.588	0.012	0.0507	8.334	0.02	0.06093	715.21	4.11E-09	5.38E-07
DGGA 16:0/18:2	9.82	0.014	0.0524	5.09	0.054	0.131	10.161	0.013	0.039605
Flavonoid 2	9.82	0.014	0.0524	5.09	0.054	0.131	10.161	0.013	0.039605
Benzoic acid + 2O, O-Hex	7.659	0.024	0.0839	1.19	0.307	0.40217	19.482	0.002	0.010077
NCGC00380922-01	7.235	0.028	0.0894	8.694	0.018	0.05895	12.128	0.008	0.028324
Bis(2-Ethylhexyl)Phthalate	6.544	0.034	0.0989	4.425	0.069	0.15283	14.418	0.005	0.022586
PC O-36:9	6.536	0.034	0.0989	2.942	0.125	0.23393	12.433	0.008	0.028324
PC 18:2/18:3	6.484	0.034	0.0989	15.083	0.005	0.038529	7.133	0.028	0.07336
LPE 16:0	6.159	0.038	0.105	42.888	0.000179	0.003349	24.636	0.001	0.00655

Kaempferol-3-Glucoside-2-p-coumaroyl	5.779	0.043	0.114	10.213	0.013	0.051606	10.185	0.013	0.039605
Leucylvaline	5.758	0.043	0.114	10.249	0.013	0.051606	10.158	0.013	0.039605
Leucine	5.575	0.046	0.1205	19.07	0.002	0.020154	14.661	0.005	0.022586
Linoleic Acid	5.413	0.048	0.123	16.063	0.004	0.034933	2.665	0.141	0.24304
Quercetin 3-(2R-apiosylrutinoside)	5.122	0.053	0.123	5.914	0.041	0.10531	70.648	3.05E-05	0.0004994
FAHFA 18:2/20:4	5.047	0.055	0.126	12.425	0.008	0.045565	9.352	0.016	0.047636
Dibutyl Phthalate	4.955	0.057	0.128	4.49	0.067	0.15133	10.02	0.013	0.039605
quercetin-3-O-glc-1-3-rham-1-6-glucoside	4.79	0.06	0.133	12.737	0.007	0.043667	8.989	0.017	0.049489
Phenylalanine	4.571	0.065	0.139	10.904	0.011	0.051606	11.25	0.01	0.034474
gamma-Linolenic acid	4.17	0.075	0.155	13.352	0.006	0.043667	1.063	0.333	0.44513
MGMG 18:2	3.978	0.081	0.156	3.939	0.082	0.17326	55.342	7.34E-05	0.000874
Feruloyl O-methyldopamine	4.091	0.078	0.156	4.577	0.065	0.15133	39.327	0.00024	0.0024185
Histidine	4.079	0.078	0.156	113.91	5.21E-06	0.00025152	33.742	0.000401	0.0031979
Alcesefoliside	3.77	0.088	0.161	4.504	0.067	0.15133	72.614	2.76E-05	0.000499
Canrenone	3.753	0.089	0.161	3.885	0.084	0.17467	12.864	0.007	0.0262
Quercetin	3.829	0.086	0.161	12.665	0.007	0.043667	0.006	0.941	0.95864
Hexosyl LPE 18:2	3.646	0.093	0.166	12.576	0.008	0.045565	4.399	0.069	0.14556
Dodecylbenzenesulfonic acid	3.192	0.112	0.190	3.408	0.102	0.1965	17.299	0.003	0.014556
FA 12:1+1O	3.211	0.111	0.190	13.233	0.007	0.043667	6.53	0.034	0.085654
5'-Methylthioadenosine	2.378	0.162	0.251	1.888	0.207	0.30421	20.926	0.002	0.010077
Pentaethylene glycol	2.356	0.163	0.251	1.869	0.209	0.30421	20.991	0.002	0.010077
MGMG 16:3	2.384	0.161	0.251	2.589	0.146	0.25166	13.697	0.006	0.024562

DGDG 18:2/18:3	2.071	0.188	0.276	8.164	0.021	0.062523	32.416	0.000458	0.0033332
Quercetin 3,7-di-O-rhamnoside	2.076	0.188	0.276	1.621	0.239	0.33447	21.65	0.002	0.010077
DGMG 18:3	1.953	0.2	0.291	1.611	0.24	0.33447	80.944	1.86E-05	0.0004148
Calenduloside E	1.868	0.209	0.297	11.84	0.009	0.049125	2.061	0.189	0.30567
Narcissin	1.583	0.244	0.336	2.085	0.187	0.2882	64.348	4.28E-05	0.0006229
HexCer 18:2;2O/16:0;O	1.533	0.251	0.342	1.156	0.314	0.40727	21.981	0.002	0.010077
Rutin	1.102	0.325	0.421	1.518	0.253	0.34887	59.14	5.80E-05	0.0007598
PE 18:3/18:3	0.891	0.373	0.452	27.72	0.00076	0.009956	0.516	0.493	0.57617
LPE 18:1	0.581	0.468	0.542	21.745	0.002	0.020154	6.275	0.037	0.086554
Loliolide	0.125	0.732	0.804	30.927	0.000534	0.008744	0.642	0.446	0.53962
DGGA 18:3/18:3	0.033	0.86	0.908	4.075	0.078	0.16751	13.035	0.007	0.0262
Lauramine oxide	0.014	0.909	0.945	8.529	0.019	0.060707	33.39	0.000415	0.0031979
Isorhamnetin 3-O-glucoside	0.016	0.902	0.945	0.000588	0.981	0.981	12.964	0.007	0.0262
Naringenin	0.006	0.938	0.959	14.562	0.005	0.038529	0.394	0.548	0.62424

Supplemental Table 2.3. Metabolites and their aliases and class for F2 seedling metabolomic heatmap.

Metabolite	*Class*	*Alias*
(Z)-9,12,13-trihydroxyoctadec-15-enoic acid	Lipid	
[1-hexadecanoyloxy-3-phosphonooxypropan-2-yl]octadec-9-enoate	Lipid	
12-Methoxyvernolepin	Terpene	
13-HOTrE	Lipid	
1-Amino-1-cyclopentanecarboxylic acid	Amino acid	
1-palmitoyl-2-hydroxy-sn-glycero-3-phosphoethanolamine	Lipid	
2-Hydroxypalmitic acid	Lipid	
9-HOTrE	Lipid	
Abietic acid	Lipid	
Alcesefoliside	Flavonoid	
Ascorbic acid	Other	
Betaine	Amino acid	
C12H14O8; PlaSMA ID-517	Other	
Canrenone	Lipid	
Citric acid	Other	
DGGA 16:0_18:2	Lipid	
DGGA 16:0_18:3	Lipid	
DGGA 18:2_18:3	Lipid	
DGGA 18:3_18:3	Lipid	
DGMG 18:3	Lipid	
Erucamide	Lipid	
FA 12:1+1O	Lipid	
FA 18:2+1O; PlaSMA ID-573	Lipid	
FA 18:2+2O; PlaSMA ID-651	Lipid	
FA 18:3+3O	Lipid	
2-(3,4-dihydroxyphenyl)-5,7-dihydroxy-3-[(2S,3R,4S,5S,6R)-3,4,5-trihydroxy-6-[[(2S,3R,4S,5R)-3,4,5-trihydroxyoxan-2-yl]oxymethyl]oxan-2-yl]oxychromen-4-one	Flavonoid	Flavonoid 1
Hydroquinidine	Other	
Isoleucine	Amino acid	
Isorhamnetin 3-glucuronide	Flavonoid	
Kaempferol-3-O-glucuronoside	Flavonoid	
Lauryldiethanolamine	Other	
L-Glutamic Acid	Amino acid	

L-Glutamine	Amino acid	
Linolenic acid	Lipid	
[5-acetyloxy-3-(hydroxymethyl)-2-oxo-6-propan-2-ylcyclohex-3-en-1-yl] 3-methylbutanoate	Lipid	Lipid 1
LNAPE 18:2/N-18:2	Lipid	
LNAPE 18:2/N-18:3	Lipid	
LPA 16:0	Lipid	
LPA 16:1	Lipid	
LPA 18:1	Lipid	
LPA 18:2	Lipid	
LPA 18:3	Lipid	
LPC 16:0	Lipid	
LPC 18:1-SN1	Lipid	
LPC 18:2	Lipid	
LPC 18:2; PlaSMA ID-1554	Lipid	
LPC 18:2-SN1	Lipid	
LPC 18:3-SN1	Lipid	
LPE 16:0	Lipid	
LPE 18:1	Lipid	
LPE 18:2	Lipid	
LPE 18:2; PlaSMA ID-1316	Lipid	
LPE 18:3	Lipid	
LPG 18:1	Lipid	
LPG 18:2	Lipid	
LPG 18:3	Lipid	
LPI 18:2	Lipid	
LPI 18:3	Lipid	
MalicAcid	Other	
Mauritianin	Flavonoid	
MG 18:0	Lipid	
MGMG 16:3	Lipid	
MGMG 18:2	Lipid	
Monoolein	Lipid	
Monopalmitin	Lipid	
N-Acetyl L-tryptophan	Amino acid	
Norgestrel	Lipid	
PA 16:0_18:2	Lipid	
PA 16:0_18:3	Lipid	
PA 18:1_18:2	Lipid	
PA 18:2_18:2	Lipid	

PA 18:3_18:3	Lipid
Panaxcerol B	Lipid
PC 10:0_26:5	Lipid
PC 14:1_20:2	Lipid
PC 17:1_17:1	Lipid
PC 18:0_18:3	Lipid
PC 18:2_18:2	Lipid
PC 18:3_18:3	Lipid
PC 19:0_15:1	Lipid
PC O-18:1	Lipid
PC O-18:3	Lipid
PE 13:1_21:2	Lipid
PE 17:1_17:1	Lipid
PE 18:2_18:2	Lipid
PE 18:2_18:3	Lipid
PE 34:2	Lipid
PE 36:3	Lipid
PE O-24:5_18:3	Lipid
PE O-26:7_18:2	Lipid
PG 16:0_18:2	Lipid
PG 16:0_18:3	Lipid
Phenylalanine	Amino acid
Pheophorbide A	Other
Pheophytin A	Other
PI 34:2	Lipid
Pyrogallin	Carbohydrate
Quercetin-3-O-glucuronide	Flavonoid
SM 13:2;2O/26:7	Lipid
SM 21:3;2O/18:5	Lipid
Sodium 4-hydroxy-benzoate	Other
Sodium Tetradecyl Sulfate	Other
SQDG 16:0_18:3	Lipid
Strobilactone A	Other
Thymol-beta-D-glucoside	Terpene
Umbelliferone	Other
Yuehgesin	Other

Supplemental Table 2.4. One-way ANOVA analysis of F2 seedling metabolomic showing key metabolites with significant changes across treatments.

Metabolite	*f.value*	*p.value*	*(-LOG10(p))*	*FDR*
12-Methoxyvernolepin	5.4225	0.0091155	2.0402	0.023874
1-palmitoyl-2-hydroxy-sn-glycero-3-phosphoethanolamine	15.43	5.56E-05	4.2552	0.00047018
2-Hydroxypalmitic acid	7.3303	0.0026122	2.583	0.010262
9-HOTrE	9.7536	0.00067403	3.1713	0.0035306
Abietic acid	29.197	1.00E-06	5.9981	2.76E-05
Ascorbic acid	4.917	0.013132	1.8817	0.02778
DGGA 18:2_18:3	6.8962	0.0034159	2.4665	0.012017
DGGA 18:3_18:3	6.5928	0.0041422	2.3828	0.013807
DGMG 18:3	33.736	3.77E-07	6.4233	1.68E-05
Isoleucine	5.0985	0.011498	1.9394	0.027346
Kaempferol-3-O-glucuronoside	4.481	0.018231	1.7392	0.037137
L-Glutamic Acid	20.384	1.03E-05	4.9866	0.00010313
L-Glutamine	21.464	7.46E-06	5.1275	8.20E-05
Linolenic acid	21.695	6.97E-06	5.1569	8.20E-05
LPA 16:0	12.073	0.00022121	3.6552	0.0014314
LPA 16:1	14.624	7.58E-05	4.1202	0.00059574
LPA 18:1	6.9978	0.0032054	2.4941	0.011753
LPA 18:2	5.5598	0.008277	2.0821	0.022207
LPC 16:0	4.2143	0.022426	1.6493	0.044051
LPE 16:0	14.17	9.08E-05	4.0419	0.00066596
LPE 18:2	4.7676	0.014674	1.8334	0.030456
LPE 18:3	5.9103	0.006502	2.187	0.019867
LPG 18:2	7.8299	0.0019386	2.7125	0.0078979
LPG 18:3	17.36	2.76E-05	4.5586	0.00025329

LPI 18:2	25.626	2.38E-06	5.6229	4.37E-05
LPI 18:3	33.221	4.19E-07	6.3776	1.68E-05
MG 18:0	24.361	3.31E-06	5.4796	4.56E-05
MGMG 18:2	10.852	0.00039002	3.4089	0.002258
Monoolein	13.934	9.99E-05	4.0005	0.00068676
Monopalmitin	27.4	1.53E-06	5.8144	3.37E-05
N-Acetyl L-tryptophan	6.8594	0.0034958	2.4565	0.012017
Norgestrel	8.7379	0.0011575	2.9365	0.0055357
PA 16:0_18:3	5.7212	0.0074001	2.1308	0.020872
PA 18:3_18:3	5.8304	0.0068654	2.1633	0.020411
Panaxcerol B	5.6538	0.0077527	2.1105	0.02132
PC 14:1_20:2	5.0807	0.011648	1.9337	0.027346
PC 17:1_17:1	7.913	0.0018466	2.7336	0.0078124
PC 18:0_18:3	4.9497	0.01282	1.8921	0.027651
PC 18:2_18:2	8.3805	0.0014125	2.85	0.0062148
PC 18:3_18:3	7.1506	0.0029159	2.5352	0.01106
PC 19:0_15:1	4.9588	0.012734	1.895	0.027651
PE 13:1_21:2	4.1501	0.023589	1.6273	0.045523
PE 18:2_18:2	4.4508	0.018659	1.7291	0.037319
PE 36:3	5.0841	0.011619	1.9348	0.027346
PG 16:0_18:2	32.779	4.59E-07	6.3379	1.68E-05
Phenylalanine	10.463	0.00047139	3.3266	0.0025926
Pheophorbide A	24.846	2.92E-06	5.5353	4.56E-05
PI 34:2	5.292	0.010002	1.9999	0.025585
Pyrogallin	9.0699	0.00096606	3.015	0.0048303
Quercetin-3-O-glucuronide	6.0555	0.005895	2.2295	0.018527
SM 13:22O/26:7	11.571	0.00027791	3.5561	0.0016984
SM 21:32O/18:5	4.9602	0.012721	1.8955	0.027651

Sodium 4-hydroxy-benzoate	8.614	0.0012394	2.9068	0.0056808
SQDG 16:0_18:3	5.0764	0.011684	1.9324	0.027346
Umbelliferone	4.9886	0.012458	1.9045	0.027651
Yuehgesin	6.1149	0.0056651	2.2468	0.018328

CHAPTER 3:

Transcriptome related to transgenerational memory

Uncovering gene networks modules underlying transgenerational stress memory to N deficiency in *Chenopodium quinoa* Willd (Amaranthaceae)

Authors and addresses:

Catalina Castro[1], M. Paz Jerez[1], Elizabeth Escobar[1], Enrique Ostria-Gallardo[1], Ben Williams[2], Teodoro Coba de la Peña[3], Luisa Bascuñan-Godoy[1]

[1]Laboratorio de Fisiología Vegetal, Departamento de Botánica, Facultad de Ciencias Naturales y Oceanográficas, universidad de Concepción, Concepción, Chile

[2]Innovative Genomics Institute, University of California, Berkeley, CA 94720, USA

[3]Laboratorio de Recursos Naturales y Fitorremediación, Centro de Estudios Avanzados en Zonas Áridas (CEAZA), La Serena, Chile

ABSTRACT

Transgenerational stress memory enables plants to transmit stress-induced adaptations to their offspring, enhancing resilience to environmental challenges. While epigenetic mechanisms have been well-documented, the role of transcriptional regulation remains less explored, particularly under nitrogen (N) deficiency. In this study, we investigated the influence of maternal N availability (F0) on the transcriptomic profiles of quinoa (*Chenopodium quinoa*) offspring across two generations (F1 and F2), aiming to identify transcriptional patterns and regulatory networks associated with inter- and transgenerational adaptation to N-stress.

Using mRNA-seq, PCA-SOM clustering, and weighted gene co-expression network analysis, we identified differentially expressed genes (DEGs) influenced predominantly by F0 N conditions. In F1 seedlings, 106 DEGs were found, and 222 in F2, with 47 shared across generations. Transcriptional clusters were associated with key biological processes including photosynthesis, N metabolism, stress response, signaling, and developmental

regulation. Distinct co-expression modules revealed hub genes, such as *WRKY*s, *CRF*s, *MLP-like* proteins, glutamate decarboxylases, and leucine-rich repeat kinases, central to the inheritance and regulation of stress memory. F0-derived N conditions had a stronger influence than immediate N environments, demonstrating that transcriptional memory is maintained across generations.

Our results show that maternal N limitation triggers a persistent transcriptomic reprogramming in quinoa, priming progeny to cope with N deficiency through anticipatory gene expression patterns. This study highlights transcriptional memory as a crucial component of stress adaptation and provides valuable insights for improving nutrient use efficiency and resilience in crops through intergenerational priming strategies.

INTRODUCTION

Plants can display molecular mechanisms to resist abiotic stress, and this can be extended beyond the individual lifetime, transmitting these stress adaptations to next generations, known as transgenerational stress memory (Herman and Sultan, 2011; Holeski et al., 2012, Sharma et al., 2022). Among the most studied mechanisms of this response are epigenetic changes (histone acetylation and DNA methylation). However, other mechanisms could contribute to explaining the inheritance of stress memory, including the role of transcriptional regulation (Avramova, 2019). Studies have highlighted the importance of transcription factors not only in the initial stress response, but also in how stressful experiences are remembered and transmitted to future generations. Understanding how gene expressions respond to environmental conditions across generations is crucial for knowing the molecular basis of plant stress adaptation.

Nitrogen (N) is a critical macronutrient for plants growth and development, influencing primary metabolic pathways and cellular signaling (Ye et al., 2022). Parental nutrient availability not only influences the current generation but also affects the progeny through mechanisms of transgenerational memory, which enable plants to anticipate environmental stress based on ancestors' experiences to enhance their survival and reproductive success. Lamelas et al. (2024) found that seedlings that ancestors exposed to heat and drought stress, retained key proteins to cope with current heat stress. It also showed that seeds from stress plants presented differential gene expression, particularly microRNAs and stress response genes, and high levels of starch and secondary metabolites as biomarkers for stress memory. Li et al. (2022) studies in transgenerational memory in response to cadmium stress found that some genes maintained the same expression under normal conditions in the second generation that the stress parents. With that, they concluded that the accumulation of those genes in the offspring was potentially related to transgenerational memory. Research on both intergenerational and transgenerational memory related to N limitation has been scantily documented. In *Arabidopsis thaliana*, it has been shown that exposure to multigenerational stress enhances the nitrate uptake ability,

triggering a suite of responses to N-deficiency (Massaro et al., 2020). Additionally, Liu et al. (2021) showed cross-stress effects, demonstrating that progeny from water-stressed plants exhibited increased resistance to N starvation compared to offspring from well-watered plants. Zhao et al. (2024) transcription analysis showed upregulation of N transport-related proteins to increase the nitrogen absorption of plants, and found various transcription factors including *GRAS*, *MYB*, and *WRKY* upregulated to enhanced nitrogen uptake by expanding root absorption area.

*Chenopodium qui*noa Willd. is a highly resilient crop that has a considerable resistance to a numerous abiotic stresses, including a notable tolerance to N-deficit (Bascunan-Godoy et al., 2018). Recent studies have shown that the maternal N supply in quinoa modulates the development and metabolic profile of their offspring, highlighting the role of maternal environment in regulating the stress response of the 1rst generation offspring (Castro et al., 2024). However, it's not clear the extent to which these responses persist across generations and contribute to the inheritance of stress memory.

In this study, we investigate the impact of maternal N availability (F0) on transcriptomic profiles of their offspring across generations, to identify transcriptional patterns associated with N-stress adaptations and their maintenance across two generations (F1 and F2). We hypothesize that the N deficiency in mother plants (F0) influences the changes in transcriptional profiles, preparing the offspring to face stressful N conditions. These findings will contribute to a deeper understanding of plant stress adaptation and provide valuable insights for crop improvement strategies targeting enhanced nutrient use efficiency.

MATERIAL AND METHODS

Plant material and grown conditions

F1 and F2 seeds were obtained from previous work (Castro et al., 2024, Castro et al., unpublished). Briefly, F0 plants were grown in 10 L pots filled with 5 Kg of substrate (80% sand and 20% perlite) supplemented with modified MS culture medium (Murashige and Skoog, 1962) without N at sowing, then at 4 true leaves, and at 8 true leaves stage. The substrate was supplemented with NH_4NO_3 to reach two N-level treatments at the same times as the MS supplementation: high nitrogen (HN_{F0}: 0.6 g of N per pot), which is the optimal N level for quinoa growth, and low nitrogen (LN_{F0}: 0.3 g N per pot). Plants were maintained with optimal soil moisture until seed maturation, when we collected F1 seeds. The experiments were conducted in pots from August to December 2023 (at University of California, Berkeley, USA) under greenhouse conditions. The environmental conditions were: 1200 µmol m^{-2} s^{-1} PAR at noon (natural light), maximum and minimum temperatures (daily ranges) of 25 ºC and 17 ºC respectively, 12 h day length,

and 80% relative humidity. Seeds were directly germinated in pots of 1 L filled with 1 kg of substrate consisting of 80% sand and 20% perlite. One supplementation with modified MS culture medium (Murashige and Skoog, 1962) without N was administered at sowing. The substrate was supplemented with NH_4NO_3 as N source to reach two level treatment, four groups combining N conditions were obtained for F1: 1) Offspring of HN mother plants, grown at HN ($HN_{F0}HN_{F1}$); 2) Offspring of HN mother plants, grown at LN ($HN_{F0}LN_{F1}$); 3) Offspring of LN mother plants, grown at HN ($LN_{F0}HN_{F1}$); and 4) Offspring of LN mother plants, grown at LN ($LN_{F0}LN_{F1}$). Eight groups combining N conditions were obtained for F2, and four were selected for analysis (Fig. 1): 1) HN control ($HN_{F0}HN_{F1}HN_{F2}$); 2) LN stress control ($HN_{F0}HN_{F1}LN_{F2}$); 3) Stress reversion ($LN_{F0}HN_{F1}LN_{F2}$); 4) Stress maintenance ($LN_{F0}LN_{F1}LN_{F2}$). HN refers to high concentration of inorganic N in soil, but it is the optimal N conditions for growth in quinoa (Jerez et al., 2023). F1 and F2 plants were irrigated at field capacity every three days with water maintaining optimal soil moisture, until they had four true leaves (~20 days of growth). At this time samples were collected in liquid nitrogen for analysis.

mRNA-seq and DESeq analysis of seedlings (F1 and F2)

Leaf tissue from 20-day-old seedlings was collected and immediately frozen in liquid nitrogen. One leaf per sample was ground using a Qiagen TissueLyser II. Total RNA was insulated using Qiagen RNeasy Plant Mini Kit (QIAGEN) according to manufacturer's instructions. The yield and quality were determined by a Nanodrop spectrophotometer. RNA-seq was performed on an Illumina NovaSeq 6000 and X-Plus Sequencing Platform at Novogene Co. Inc. (Sacramento, CA, USA), obtaining 150 bp paired end reads. Prior to mapping, adapters were trimmed using Trim Galore (Babraham Bioinformatics), trimming 9 bp from the 5'-end of reads, and enforcing a 3'-end quality of >25%. Reads were mapped to the QQ74 *Chenopodium quinoa* genome using STAR, permitting 0.05 mismatches as a fraction of total read length and discarding reads that did not map uniquely (Dobin et al., 2013). Differentially expressed (DE) genes were identified by running *htseq-count* and DESeq2 in the *Savio* cluster at UC Berkeley, ensuring a p-value <0.05 for DE genes, and a minimum of two-fold change in expression and an adjusted p-value <0.05 for top DE genes. *pheatmap*,

FactoMineR and *ggplot2* R packages were used to generate the top DE genes heatmap and PCA analysis and plots.

Validation of DEG by qPCR analysis

Using a manual inspection of common genes between F1 and F2, we selected three genes based on their stress memory associated function to validate the repeatability of the RNA-seq data. cDNA was obtained from total leaf RNA from three biological replicates using the AffinityScript QPCR cDNA Synthesis kit according to manufacturer's instructions. qPCR reaction was performed in an AriaMx Real-time PCR system (Agilent Technologies) using a Brilliant III SYBR Green QPCR Master Mix reagent. The specific primers used for the qPCR analysis were designed using the Primer-BLAST tool (http://www.ncbi.nlm.nih.gov/tools/primer-blast). The gene *elongation factor 1 alpha* (*EF1a*) was used as internal reference to calculate the relative expression level, using the 2-ΔΔCt method (Livak & Schmittgen, 2001). Significant differences of gene expression were determined by an ANOVA test with *P*-value ≤ 0.05.

Principal component analysis (PCA) and self-organizing maps (SOM) clustering

To quantify transcript abundance, RNA-Seq counts were normalized by Trimmed Mean of *M*-values (TMM), and genes from the upper 75% quartile of coefficient of variation for expression across treatments were selected for further analysis. The scaled expression values within samples were used to cluster these genes for a multidimensional 2 x 3 hexagonal SOM using the *KOHONEN* R package (Wehrens and Buydens, 2007). One hundred training interactions were used during clustering with a decrease in the alpha learning rate in F1 from ca. 0.0070 to 0.0030 and in F2 from ca 0.0075 to 0.0035 (Fig. S2). SOM outcome was visualized into pie charts for codebook vectors to obtain the counts number and mean distance of genes assigned to each node (Fig. S3), and into a PCA space where PC values were calculated based on gene expression of samples across N treatments. Box plot option from *ggplot2* R package was used to visualize gene accumulation patterns associated to each treatment in each node.

Gene co-expression network analysis

To further explore the gene clusters generated by the PCA-SOM analysis, a Gene Regulatory Network (GNR)-based approach was used to study the interactions between gene expression and N availability treatments. From the PCA-SOM clustering method, we identify different nodes accumulating transcripts in relation to a given nitrogen treatment. For each node, we used those highly accumulated genes to construct a weighted gene co-expression network by using the Weighted Gene Co-expression Analysis (WGCNA; Langfelder & Horvath, 2008) and the *igraph* (Csardi & Nepusz, 2006) R packages for visualization. To calculate the adjacency matrix with the WGCNA package, a soft threshold (β) value was calculated for each node and was used to achieve the scale free topology criteria. We used the resources and algorithms of community structure functions of the *igraph* R package to explore network properties such as connectivity, centralization, modularity and community structure. Finally, we selected the 5% Hub genes (gene that is highly connected to other genes in a network, Table S1 for F1

hub genes, S2 for F2 hub genes) for each node to visualize the co-expression network of those genes using the *Kamada-Kawai* layout algorithm. Hub genes allowed us to identify key central genes regulating the responses of F1 and F2 to a given nitrogen availability treatment.

RESULTS

Maternal N supply (F0) influences transcriptomic profile of their offspring at seedling stage (F1 and F2)

For the F1 transcriptomic analysis, 106 genes were the top differentially expressed (DE). The differentiation was given by the F0 treatment, where 50 genes showed increased abundance in HN_{F0} offspring ($HN_{F0}HN_{F1}$ and $HN_{F0}LN_{F1}$) and 56 were increased in LN_{F0} offspring ($LN_{F0}HN_{F1}$ and $LN_{F0}LN_{F1}$) (Fig. 1A). In the case of F2, there were 222 top DE genes, showing a pattern not as marked as F1, but where F0 also influenced the expression of genes on the F2 (Fig. 2A). Here, 20 genes were decreased and

46 were increased in $HN_{F0}HN_{F1}LN_{F2}$, 71 genes were increased in both offsprings of LN_{F0} plants, and finally, 85 genes were increased in both descendants of HN_{F0} plants. Comparing F1 and F2 DE genes, 47 genes were common in both generations (Fig. S4, Table S2).

The PCA analysis for both generations show a separation between treatments. The Principal Component 1 (PC1) explains 71% and 62% of the variability between treatments for F1 and F2, respectively, while PC2 explains 7% and 17% of the variability in F1 and F2, respectively. In both F1 and F2 the treatments that come from the same F0 treatments cluster together, indicating that the transcriptomic pattern of seedlings that come from same F0 mother plant are similar.

Validation of RNA-Seq Gene Expression by qPCR

RNA-Seq methods are robust enough to not always require validation since studies show that about 80 – 85% of genes have consistent expression

measurements between RNAseq and qPCR, and discrepancies are more likely for genes with small fold changes (less than 2-fold) (Coenye, 2021; Everaert et al. 2017). We validate the RNA-Seq data by qPCR. The genes selected to validate the RNA-Seq were *Auxin efflux carrier* (*PIN7*), *Nitrate transporter 1.1* (*NRT1.1*) and a methyltransferase (*NTM1*). The correlation between RNA-Seq gene expression data and the relative abundance determined by qPCR of the selected genes was r = 0.927, indicating a high correlation (Fig. S1).

PSA-SOM analysis of F1 and F2 seedlings descendants of maternal plants grown at contrasting N supplies

From the full dataset of differentially expressed genes, we studied the dynamics of gene expression in seedlings of both generations. The PCA coupled with a SOM clustering analysis (PCA-SOM) revealed patterns of transcript accumulation (Fig. 3A, 4A). Clusters 1 and 2 show a contrasting pattern. Cluster 1 store genes up-regulated in HN_{F0} and down-regulated in LN_{F0}, while cluster 2 shows up-regulated genes in LN_{F0} and down-regulated

in HN_{F0} (without importance of F1 N-supply). Clusters 3 through 6 shows transcripts accumulating only in one treatment. Specifically, cluster 3 and 6 shows transcripts up-regulating in continuous HN or LN conditions over both generations $HN_{F0}HN_{F1}$ and $LN_{F0}LN_{F1}$, respectively. Finally, cluster 4 and 5 distinguish $HN_{F0}LN_{F1}$ and $LN_{F0}HN_{F1}$, respectively (Fig. 3B).

On the other hand, F2 genes show contrasting accumulation patterns between clusters. Clusters 1 and 2 have contrasting patterns in $HN_{F0}HN_{F1}LN_{F2}$ treatment, cluster 1 shows up-regulated genes and cluster 2 down-regulated genes in this treatment. Clusters 3 and 4 show genes with contrasting patterns in LN_{F0}, grown at LN_{F2} (without importance of F1 N-supply), cluster 3 contains up-regulated genes, while cluster 4 contains down-regulated genes in these treatments. Finally, clusters 5 and 6 display a contrasting pattern of accumulation in $LN_{F0}HN_{F1}LN_{F2}$ treatments, cluster 5 with up-regulated genes and cluster 6 showing down-regulated genes (Fig. 4B).

For each SOM node, we reviewed those genes associated with each treatment to find the predominant biological process of each cluster, according to their

gene ontology (GO). In F1 (Fig. 3), node 1 mainly contained genes related to carbohydrate, lipid and phosphate metabolism, node 2 include genes related to signaling transduction and cellular communication, node 3 contain transcripts related to photosynthesis and energy production, node 4 include genes related to stress response and transcription factors, node 5 also contains genes related to stress response, and signal transduction and, finally, node 6 includes genes related to lipid and carbohydrate metabolism, stress response and transcriptional regulation. For F2 (Fig. 4), node 1 principally includes genes related to photosynthesis and energy production, and nitrogen metabolism, node 2 includes genes related mostly to metabolism and transcriptional regulation and gene expression, node 3 mostly has genes related to lipid and carbohydrate metabolism, node 4 includes genes associated with hormone biosynthesis, nitrogen and carbohydrate metabolism and stress responses, node 5 includes genes associated to structural and developmental processes, and finally, node 6 includes genes related to metabolism, stress response and cell structure.

Gene co-expression networks in F1 and F2 seedlings descendants of maternal plants grown at contrasting N supplies

We used those highly accumulated transcripts from each node to construct a weighted gene co-expression network for F1 and F2. Then we selected central genes (hub genes), which present a higher number of connections and are the candidate genes for inheritance of N-deficiency stress memory.

For the F1 generation, **cluster 1** network consisted of 62 genes (up-regulated in HN_{F0} and down-regulated in LN_{F0} seedlings), and the top 5 genes with highest connections were: *MLP-Like Protein 1*, *Uridine Kinase/Uracil Phosphoribosyl transferase 1* (pyrimidine nucleotide biosynthesis), *Disease Resistance-Responsive family protein* (stress response), *Mannose-Binding Lectin Superfamily protein* (pathogen resistance), and *Calcaneurin-Like Metallo-Phosphoesterase Superfamily protein* (phosphorylation signaling). **Cluster 2** network consisted of 59 genes (up-regulated in LN_{F0} and down-regulated in HN_{F0} seedlings), and the top 5 genes with highest connections were: *SEC14p-Like Phosphatildyinositol Transfer family protein* (membrane

lipid transfer and metabolism), *SEC14P Cytosolic Factor Family protein/Phosphoglycerride Transfer Family protein*, *Proline Extensin-Like Receptor Kinase 1* (cell wall regulation, growth, stress signal), *Sugar Transporter 1*, and *Transducin Family protein/WD-40 repeat family protein* (signal transduction). **Cluster 3** network consisted of 55 genes (up-regulated in $HN_{F0}HN_{F1}$ seedlings), and the top 5 genes with highest connections were: *Riboflavin Kinase/FMN Hydrolase* (redox reactions), *Photosystem II Reaction Center protein D* (AUR62039623, AUR62039871), *Photosystem I, PsaA/PsaB protein*, and *RNA Polymerase Subunit Beta* (RNA synthesis and transcriptional control). **Cluster 4** network consisted of 66 genes (up-regulated in $HN_{F0}LN_{F1}$ seedlings), and the top 5 genes with highest connections were: *GOT1/SFT2-Like vescicle transport protein family* (regulates intracellular transport), *Peptidase S24/S26A/S26B/S26C family protein* (protein degradation and processing), *Multiprotein Bridgind factor 1C* (*MBF1c*, gene regulation, chromatin remodeling), *PDI-Like 1-2* (protein folding), and *UDP-Glycosyltransferase superfamily protein* (catalyze addition of sugars to lipophilic molecules). **Cluster 5** network consisted of 80 genes (up-regulated in $LN_{F0}HN_{F1}$ seedlings), and the top 5 genes with highest connections were: *Wall-Asociated Kinase 2* (*WAK2*, signaling

receptor), *Glutamate Decarboxylase* (*GAD*, decarboxylation of glutamate to gamma-aminobutyric acid (GABA)), *Alpha/Beta-Hydrolases superfamily protein* (epoxide hydrolase activity, cutin biosynthetic process), *Chitinase A* (biotic stress defense and cell wall degradation), and *Cysteine-Rich RLK (Receptor-Like Protein Kinase) 10* (plant development and stress adaptation). **Cluster 6** network consisted of 82 genes (up-regulated in $LN_{F0}LN_{F1}$ seedlings), and the top 5 genes with highest connections were: *O-Glycosyl Hydrolases family 17 protein* (degrades glycosidic bonds), *Plastidic Pyruvate Kinase Beta Subunit 1* (*PKpβ1*, AUR62031459, AUR62021072, generate ATP and carbon skeletons for nitrogen assimilation), *Pyruvate Kinase Family protein* (*PK*, converts phosphoenolpyruvate to pyruvate, linking nitrogen and carbon metabolism), and *Pentatricopeptide Repeat (PPR) Superfamily protein* (post-transcriptional regulation of gene expression in plastids and mitochondria) (Table S1).

For the F2 generation, **cluster 1** network consisted of 38 genes (up-regulated in $HN_{F0}HN_{F1}LN_{F2}$ seedlings), and the top 5 genes with highest connections were: *Nicotinamidase 1* (*NIC1*, NAD+ biosynthesis), *Osmotin 34* (positive

regulator in the generation of ABA responses), *CHITINASE FAMILY PROTEIN* (stress responses and structural modifications), *Oxophytodienoate-Reductase 3* (jasmonic acid biosynthesis), and *Hydorxyproline-Rich Glycoprotein Family protein* (*HRGP*, structural integrity, facilitate intercellular communication in roots, leaves and reproductive tissues). **Cluster 2** network consisted of 33 genes (down-regulated in $HN_{F0}HN_{F1}LN_{F2}$ seedlings) and the top 5 genes with highest connections were: *ENTH/VHS/GAT Family protein* (ubiquitin binding), *Uricase/Urate Oxidase/Nodulin 35, putative* (catalyzes the oxidative breakdown of uric acid in the purine degradation pathway), *FUS3-Complementing gene 2* (regulation of RNA splicing), *Tautomerase/MIF superfamily* (enzyme regulation and stress response), and *Sucrose Transporter 2* (*SUT2*, sucrose transport). **Cluster 3** network consisted of 69 genes (up-regulated in LN_{F0} grown at LN_{F2}) and the top 5 genes with highest connections were: *Plant protein of unknown function DUF869* (AUR62035737, AUR62035443), *Cupredoxin superfamily protein* (electron carrier in chloroplast), *Fatty acid hydroxylase superfamily* (cell wall integrity), and *Leucine-Rich Repeat Protein Kinase Family Protein* (signal transduction, regulate stress tolerance and development). **Cluster 4** network

consisted of 100 genes (down-regulated genes in LN_{F0} grown at LN_{F2}), and the top 5 genes with highest connections were: *Chaperone DnaJ-Domain Superfamily* (*Hsp40*, AUR62041900, AUR62035012, protein refolding and degradation during stress), *P-Loop Containing Nucleoside Triphosphate Hydrolases Superfamily protein* (ATP/GTP binding and signaling), *Dormancy-Associated Protein-Like 1* (*DRM1*, regulates seed dormancy and germination), and *Fatty Alcohol Oxidase 3* (*FAO3*, oxidization of fatty alcohols to produce fatty aldehydes). **Cluster 5** network consisted of 32 genes (up-regulated in $LN_{F0}HN_{F1}LN_{F2}$ seedlings), and the top 5 genes with highest connections were: *Eucaryotic Aspartyl Protease Family protein* (proteolysis), *Photosystem I subunit K* (organizing the peripheral light-harvesting complexes), *Haloacid Dehalogenase-Like Hydrolase (HAD) superfamily protein* (intracellular dephosphorylation and maintenance of phosphate homeostasis), *Chlorophyll a-b binding family protein* (part of light-harvesting complex), and *ATPase F1 Complex Gamma subunit protein* (ATP synthesis). **Cluster 6** network consisted of 30 genes (down-regulated in $LN_{F0}HN_{F1}LN_{F2}$ seedlings), and the top 5 genes with highest connections were: *Glutathione S-Transferase TAU9* (*GST*, detoxification and stress responses), *Cyclin family protein* (interacts with CDKs to ensure progression

of cell cycle, control cell division, proliferation and developmental transitions), *Chitinase A* (biotic stress response and cell wall degradation), *26S Proteosome Regulatory Complex* (targeted protein degradation and recycling of N-compounds), and *P450 Reductase 1* (xenobiotic detoxification) (Table S2).

DISCUSSION

Mother N-supply affects the transcriptomic profiles of seedlings

Transcriptomic analysis revealed differential gene expressions across generations, with 106 DEGs in F1 and 222 in F2, of which 47 were shared between both generations (Figure 1, 2, S4). The F0 N treatment influenced both generations' transcriptomic profiles more than the current N-condition in which the offsprings were grown. This aligns with findings in *A. thaliana* (Massaro et al., 2019) where multigenerational exposure to stress enhanced

the progeny's ability to respond to N deficiency, particularly by changes in the expression of N-responsive genes.

Some of the shared genes included genes related to N metabolism and stress responses and may constitute a core set of genes involved in mediating transgenerational responses to N stress due to their up-regulation in LN_{F0} descendants grown at any condition. These included: *Nitrate Transporter 1.1* (*NRT1.1*), a dual affinity nitrate transporter (Sun and Zheng, 2015); *Glutamate Receptor 2.1* (*GLR2.1*), a plasma membrane channel involved in plant growth and development, reproduction and defense mechanisms (Yu et al., 2022; Simon et al. 2023); *S-adenosyl-L-methionine-dependent Methyltransferases Superfamily protein* (*SAM-dependent MTase*), that plays a critical role in methylation processes affecting DNA, proteins and secondary metabolites (Struck et al., 2012); *Quinone Reductase* (*QR*), involved in resistance to oxidative damage (Song et al., 2016). Additionally, transcription factors like *E2F TF3*, which regulates cell cycle and DNA replication (Nisa et al., 2023), and *GRAS*, associated with development and hormone signaling, also appear to be critical in stress response mechanisms.

These findings underscore the complex interplay of nitrogen metabolism, stress response and developmental regulation in quinoa, offering potential targets for enhancing plant resistance and adaptation.

The PCA-SOM clustering identified distinctives accumulation patterns of transcripts across treatments, with maternal (F0) N-levels having a major influence on gene clustering (Fig. 3, 4). This analysis to identify and analyze gene expression clusters in response to environmental conditions is particularly effective in examining stress induced gene regulation and better understand the genetics behind plant adaptation to environmental conditions (Ostria-Gallardo et al., 2018; Lopez et al., 2023). Gene co-expression networks derived from the PCA-SOM analysis reveal how different N conditions experienced by mother plants influence the transcription profiles in both the F1 and F2 generations of *Chenopodium quinoa*. Hub genes identified in our study are likely key players in transmitting stress memory across generations. The connectivity of these hubs within the network suggests their central role in modulating physiological and molecular

responses to N stress, which could be critical for optimizing nutrient use efficiency and enhancing stress resilience in progeny.

Gene clustering, co-expression networks and regulatory hub genes in F1

The 1rst generation seedlings (F1, Fig. 3, 5) show a direct response to maternal N conditions, underpinning an intergenerational stress memory. The descendants of HN_{F0} (Fig. 3B, 5, **Cluster 1**) had up-regulated genes associated with photosynthesis and primary metabolism, which suggest a physiological adjustment of this offspring to enhance energy acquisition, storage and usage. This cluster shows that maternal N supply anticipates the offspring to optimize energy storage and utilization in environments mirroring maternal N. Also, this cluster presented hub genes like *MLP-Like Protein 1,* crucial for modulating the physiological activity of hydrophobic compounds in plant organs. It control growth and cell development of plants in vegetative stages through the induction of the downstream genes and is involved in stress responses to biotic and abiotic stress (Fujita and Inui, 2021). Another important hub gene found in cluster 1 is *Uridine Kinase*, as a

gene involved in pyrimidine metabolism, plays an important role in various aspects of plant development, such as germination, chloroplast biogenesis, response to stress (Dong et al., 2019). The accumulation of these two genes in this cluster demonstrate an integrated stress response with metabolic pathways. This suggests that these plants are transcriptionally prepared to optimize resource utilization where there is optimal N availability and managing stress while maintaining metabolic balance to efficient N use in stress conditions.

On the other hand, LN_{F0} offspring (Fig. 3B, 5, **Cluster 2**) had up-regulated genes related to signaling transduction and cellular communication, indicating the activation of signaling pathways that might be crucial for N-stress adaptation. The latest highlights the response to nutrient deficiency signals and enabling these plants to manage N uptake and stress signaling with more efficiency under N-limited conditions. *PITPenes* in this cluster, like *SEC14*p-*Like PITP*, play a crucial role in membrane lipid transfer and cellular signaling for chloroplast function, and to control the response to environmental conditions (Huang et al., 2016; Montag et al., 2023). This

suggests a mechanism to maintain cellular integrity and communication, preparing the seedling for survival in N deficient conditions, given by the mother LN conditions.

Each treatment also had a specific cluster of up-regulated genes. For instance, $HN_{F0}HN_{F1}$ (Fig. 3B, 5, **Cluster 3**) contained transcripts related to photosynthesis and energy production. This enhancement could reflect an adaptative strategy to maximize photosynthesis efficiency and energy capture, crucial for optimizing growth and development in environments where N is not a limiting factor. The hub genes in this cluster highlight the importance of photosynthesis-related genes which are vital for optimizing energy capture and utilization, indicating a sustained enhancement of robust growth and development, supporting the idea that these seedlings are primed to take full advantage of rich N environments.

In **cluster 4**, genes linked to stress response and various transcription factors were up-regulated in $HN_{F0}LN_{F1}$ (Fig. 3B, 5), indicating a strong transcriptional reprogramming to withstand stress at the first encounter. The

hub genes present here are likely involved in adaptive responses that enable plants to efficiently manage a sudden reduction in N availability, including stress mitigation and metabolic adjustment. These processes are vital for adapting to environmental inputs and managing internal resource allocation. One of those genes is *MBF1c*, which main function is in stress tolerance regulation, enhance the tolerance of plants with overexpression of this gene and improve the growth of plants in stressful conditions, participating in the prevention of damage caused by oxidative stress (Alavilli et al., 2017; Jaimes-Miranda and Chávez, 2020). Thus, the overexpression of *MBF1c* on this cluster is an indicative of the capacity of quinoa to adapt to sudden N-deficiency.

Similarly, $LN_{F0}HN_{F1}$ (Fig. 3B, 5 **Cluster 5**) also accumulates genes related to stress response and signaling transduction, pointing to a preparation through stress signaling from the LN in the previous generation to cope with any N condition it might encounter. Hub genes in Cluster 5 included *WAK2,* a cell wall receptor that acts regulating cell expansion and contributes to stress response (Yao et al., 2025). It shows that the accumulation of the gene

is given by the stressful growing conditions of the mother plants rather than the growing conditions of this plant. *Glutamate Decarboxylase*, another important hub gene in this cluster, in *A. thaliana* mediates GABA shunt upregulation during phosphate deprivation, a nutritional stress like N-deficiency, which is hypothesized to facilitate flux of TCA cycle and respiration (Benidickson et al., 2023). The upregulation of both genes might prepare the plant to rapidly assimilate and utilize the available N, reflecting a predisposition to benefit from resource abundance.

Finally, **cluster 6** includes genes involved in metabolic processes (lipid and carbohydrate metabolism) and stress responses, accumulating specifically in $LN_{F0}LN_{F1}$ seedlings, which indicate adjustment in gene expression to support metabolic efficiency and stress adaptation to expected environmental conditions based on maternal growing status, and the stress response of the seedling itself to cope with the N-deficit on its environment. This cluster involves hub genes such as *PKpβ1* and *PK*, that mainly generates pyruvate and ATP for N-assimilation, and its expression is involved in abiotic stress response and sustaining plant growth under stress conditions (Duan et al.

2025). Production of pyruvate is key to the regulation of different metabolic pathways, producing acetyl-CoA, hence maintaining the C/N balance under stress conditions (Le et al., 2021; Dong et al., 2022). This gene accumulation sustains the long-term strategies to cope with N-deficiency, enhancing stress resistance and resource-use efficiency.

Gene clustering, co-expression networks and regulatory hub genes in F2

In F2 generation, the gene expression demonstrates the lasting impact of maternal (F0) N-conditions (Fig. 4, 6), sustaining a transgenerational stress memory and adaptation to N deficiency.

First time of F2 seedlings under LN conditions: Clusters 1 and 2 showed the up and down regulation of genes in the first time of a generation experimenting N stress ($HN_{F0}HN_{F1}LN_{F2}$), respectively. Central to **cluster 1** are up-regulated hub genes involved in photosynthesis, energy production and nitrogen and carbohydrate metabolism. This suggest an efficiency in

energy production and nutrient management across generations, likely to rapid adaptation to better N conditions, perhaps by enhancing nutrient uptake and assimilation pathways. *Nicotinamidase 1* (*NIC1*) and *osmotin 34*, underlines the role of hormone biosynthesis and stress signaling in adapting to environmental stresses (Park and Kim, 2021). *NICs* specifically are involved in the biosynthesis and recycling of Nicotinamide adenine dinucleotide (NAD). NAD stimulates ROS accumulation by stimulating respiration fluxes and also induces genes coding for chitinases and cell wall-related metabolism (Pétriacq et al., 2016). This expression profile might involve mechanisms to increasingly refine nutrient use, ensuring survival and growth despite lower N availability. On the contrary, **cluster 2** shows down-regulated genes in the same offspring related with transcriptional regulation and gene expression, with genes like *Sucrose Transporter 2* and *Uricase* (that catalyzes the oxidation of uric acid to allantoin, in the purine degradation pathway), which illustrates the plant's capability to regulate metabolism and solute transport effectively, to modulate the growth and stress responses to a first-time encountering N deficit, ensuring that the energy and resources are allocated efficiently. In this case, these are not crucial in plants with a history of optimal N availability.

Priming memory of LN_{F0} in F2: Clusters 3 and 4 presented up and down regulated genes, respectively, in treatments where F0 and F2 were grown under stress conditions (LN), indistinctively from the F1 N-conditions ($LN_{F0}HN_{F1}LN_{F2}$ and $LN_{F0}LN_{F1}LN_{F2}$), and in a lower extent in plants exposed for the first time to LN ($HN_{F0}HN_{F1}LN_{F2}$). These genes represent those involved in transgenerational stress memory, where the regulation of these genes are dependent on the N conditions of F0 plants (independent of the N conditions of F1), more than the current N conditions. In Clusters 3 and 4 there are up-regulated genes related to lipid and carbohydrate metabolism, and down-regulated genes related to hormone biosynthesis, nitrogen and carbohydrate metabolism and stress responses, indicating adjustments in metabolic rates and storage strategies. **Cluster 3**, specific to up-regulation of genes in offspring of LN_{F0} plants grown at LN_{F2} ($LN_{F0}HN_{F1}LN_{F2}$ and $LN_{F0}LN_{F1}LN_{F2}$) and with the tendency to increase in first time in LN ($HN_{F0}HN_{F1}LN_{F2}$), accumulates hub genes related to metabolic processes and electron transport, specifically *Leucine Rich Repeat* (*LRR*) protein kinase family. This gene is involved in signal transduction, regulating stress tolerance and development (Zhiqi et al., 2025), pointing out the role of

metabolic adjustments in ensuring efficient energy use and structural integrity under varied nutrient conditions through generations. **Cluster 4**, on the other hand, contains genes that are downregulated in the same treatment, with genes like *Chaperone DnaJ-Domain* (*Hsp40*), and *Dormancy-Associated Protein-Like 1* (*DRM1*). *Hsp40* chaperone is involved in protein folding, preventing aggregation and assisting in the degradation of misfolded proteins under stress (Razzaq et al., 2023; Chen et al., 2021; Sarkar et al., 2013); and its downregulation could indicate a reduced need or capacity for protein quality control possibly due to a priming from the previously stress generations, maintaining cellular stability with fewer chaperones. It also could be a cost of transgenerational memory, where protective pathways are attenuated due to prolonged exposure to stress. In the case of *DRM1* it is associated with bud dormancy and repression of plant growth (Chen et al., 2023). The downregulation of a growth-repressive gene could reflect the deactivation of dormancy and repression mechanisms, promoting a faster development.

Memory reversion/persistence in F2: Finally, clusters 5 and 6 showed the regulation of genes in an intermedial stress-free generation condition ($LN_{F0}HN_{F1}LN_{F2}$). Specifically, this group includes genes that are not changed by first-time exposure to stress (similar expression between $HN_{F0}HN_{F1}HN_{F2}$ and $HN_{F0}HN_{F1}LN_{F2}$) but could be involved in a possible stress reversion condition and shown an opposite regulation to persistent LN through generations ($LN_{F0}LN_{F1}LN_{F2}$). Here there is an up-regulation of genes related to structural and developmental processes, and genes related to photosynthesis and energy production, and a down-regulation of genes related to metabolism, stress response and cell structure, indicating the importance of the photosynthetic machinery and nutrient assimilation processes to be efficient. **Cluster 5** involves up-regulated genes in $LN_{F0}HN_{F1}LN_{F2}$ and down-regulated in $LN_{F0}LN_{F1}LN_{F2}$, where there are genes associated with structural and developmental processes suggesting a genetic memory that perpetuates high resource utilization efficiency, optimizing growth and productivity in offspring where there is a generational alternation of N availability. All of this and the decrease in genes related to productivity suggest that there is a shift and tradeoff between productivity and growth, highlighting the high resource utilization efficiency of plants in reversion of

transgenerational stress memory. **Cluster 6** shows the opposite pattern, up-regulated genes in $LN_{F0}LN_{F1}LN_{F2}$ and down-regulated genes in $LN_{F0}HN_{F1}LN_{F2}$ and includes *GST* and Cyclin; *GST* is involved in responses to cope with oxidative stress, metabolizing ROS and acting in signal transduction pathways, upregulating protective and detoxification mechanisms under abiotic stress (Hernández and Rodriguez, 2020). Cyclin interacts with *CDK*s to ensure the progression of cell cycle, control cell division and proliferation and developmental transitions, functioning as a cell cycle regulator (Kitsios and Doonan, 2011; Malumbres, 2014). Another hub gene in this cluster is *26S proteosome,* involved in the degradation of ubiquitinated proteins in the cell (Bedford et al., 2010; Stone, 2014), and its upregulation leads to an increase in stress tolerance, alleviating the toxics effects of ROS (Kurepa et al., 2008). The up-regulation of these genes in $LN_{F0}LN_{F1}LN_{F2}$ reflects an adaptation to maintain cellular function and resilience under continuous generational stress, giving the plant capacity to reinforce its physiological defenses, helping in maintain adaptations to maximize resource use efficiency and recycling. These genes could play key roles in fine-tuning the plant's response to inherited and immediate N conditions, ensuring that energy and resources are allocated efficiently. The

persistence of these transcriptional signatures across generations indicates that progeny may retain an anticipatory advantage when faced with similar environmental conditions, thereby improving stress resistance.

Gene regulation in the inheritance of stress memory

Other important genes that could be involved in inheritance of stress memory are *CRFs* and are accumulating in $LN_{F0}LN_{F1}$ seedlings. This key transcription factor responds to oxidative stress, increasing their antioxidant capacity, and are also important in proper embryo formation, critical to formation of next generation seeds so its accumulation in these seedlings with high stress memory marks indicate the need to have a normal reproductive development (Shi et al., 2013; Hallmark and Rashotte, 2019; Gentile et al., 2024). *WRKY* transcription factors are crucial for regulating stress responses in plants and has been identified as a drought induce memory gene and has been found to be upregulated in N-stress plants to enhance the N uptake, contributing to plant memory and regulating the expression of its target upon repeated stress (Bakshi and Oelmüller, 2014; Nguyen et al., 2022; Zhao et al. 2024). This

response may be transmitted to generations of stress plants, like we observed here, where plants that come from LN stress mother grown at optimal N conditions show an accumulation of this transcription factor, which could be essential to possible stress conditions that the offspring plants could encounter. Also, as Li et al. (2022) found that if the gene expression of some genes is maintained in offspring at normal conditions, then those genes were potentially related to transgenerational memory. The observed transcriptomic changes across generations suggest that transgenerational N stress memory in quinoa may confer adaptive benefits by preconditioning offspring to LN environments, even if this offspring encounter optimal N conditions. This also affects the phenotype of the offspring, where there is a tendency to have higher plant biomass when plants are descendants of LN_{F0} plants, indicating that the maternal F0 N preconditions their offspring to have an enhanced N-use efficiency and growth both intergenerational in F1 and transgenerationally in F2. This memory effect may be relevant in populations facing recurrent nutrient limitations, where the ability to maintain metabolic and transcriptional homeostasis across generations could enhance plant fitness and productivity.

Finally, the identification of key transcriptional regulators, stress-responsive genes networks and gene expression patterns across generations and their links to environmental cues responses is crucial for uncovering the biological processes and molecular pathways that module the transgenerational stress adaptation to N-deficiency in quinoa.

REFERENCES

Alavilli, H., Lee, H., Park, M., and Lee, B-h. (2017). Antarctic Moss Multiprotein Bridging Factor 1c Overexpression in Arabidopsis Resulted in Enhanced Tolerance to Salt Stress. *Front. Plant Sci.* 8:1206. doi: 10.3389/fpls.2017.01206

Avramova, Z. (2019). Defence-related priming and responses to recurring drought: Two manifestations of plant transcriptional memory mediated by the ABA and JA signalling pathways. *Plant Cell Environ*. 42(3):983-997. doi: 10.1111/pce.13458.

Bakshi, M., & Oelmüller, R. (2014). WRKY transcription factors: Jack of many trades in plants. *Plant Signaling & Behavior*, *9*(2). https://doi.org/10.4161/psb.27700

Bascuñán-Godoy, L., Sanhueza, C., Hernández, C. E., Cifuentes, L., Pinto, K., Álvarez, R., González-Teuber, M., and Bravo, L. A. (2018). Nitrogen Supply Affects Photosynthesis and Photoprotective Attributes During Drought-Induced Senescence in Quinoa. *Front Plant Sci*, **9**, 1–14. https://doi.org/10.3389/fpls.2018.00994

Bedford, L., Paine, S., Sheppard, P. W., Mayer, R. J., Roelofs, J. (2010). Assembly, structure, and function of the 26S proteasome. *Trends Cell Biol*. 20(7): 391-401. doi: 10.1016/j.tcb.2010.03.007.

Benidickson, K. H., Raytek, L. M., Hoover, G. J., Flaherty, E. J., Shelp, B. J., Snedden, W. A. and Plaxton, W. C. (2023), Glutamate decarboxylase-1 is essential for efficient acclimation of *Arabidopsis thaliana* to nutritional phosphorus deprivation. *New Phytol,* 240: 2372-2385. https://doi.org/10.1111/nph.19300

Castro, C., Rojas, J., Ortíz, J., Sanhueza-Lepe, R., Vergara, A., Poblete, F., Escobar, E., Coba de la Peña T., Ostria-Gallardo, E., Bascuñan-Godoy, L. (2024). Nitrogen Stress Memory in Quinoa: Maternal Effects on Seed Metabolism and Offspring Growth and Physiology. *Physiol Plant*. 176(6):e14614. doi: 10.1111/ppl.14614. PMID: 39513412.

Chen, R., Luo, L., Li, K., Li, Q., Li, W., and Wang, X. (2023). Dormancy-Associated Gene 1 (OsDRM1) as an axillary bud dormancy marker: Retarding Plant Development, and Modulating Auxin Response in Rice (Oryza sativa L.). *Journal of plant physiology*, 291, 154117. https://doi.org/10.1016/j.jplph.2023.154117.

Chen, T., Xu, T., Zhang, T., Liu, T., Shen, L., Chen, Z., Wu, Y., and Yang, J. (2021). Genome-Wide Identification and Characterization of *DnaJ* Gene Family in Grape (*Vitis vinifera* L.). *Horticulturae*, *7*(12), 589. https://doi.org/10.3390/horticulturae7120589

Coenye, T. (2021). Do results obtained with RNA-sequencing require independent verification? Biofilm. 3:100043. doi: 10.1016/j.bioflm.2021.100043

Csardi, G., & Nepusz, T. (2006). The igraph software. *Complex syst*, *1695*, 1-9.

Dong, N., Chen, L., Ahmad, S., Cai, Y., Duan, Y., Li, X., Liu, Y., Jiao, G., Xie, L., Hu, S., Sheng, Z., Shao, G., Wang, L., Tang, S., Wei, X., Hu, P. (2022). Genome-Wide Analysis and Functional Characterization of Pyruvate Kinase (PK) Gene Family Modulating Rice Yield and Quality. *Int J Mol Sci*. 5;23(23):15357. doi: 10.3390/ijms232315357.

Dong, Q., Zhang, Y. X., Zhou, Q., Liu, Q. E., Chen, D. B., Wang, H., Cheng, S. H., Cao, L. Y., Shen, X. H. (2019). UMP Kinase Regulates Chloroplast Development and Cold Response in Rice. *Int J Mol Sci.* 20(9):2107. doi: 10.3390/ijms20092107.

Duan, X., Xu, Y., Zhang, K. *et al.* (2025). The pyruvate kinase gene family in soybean: genome-wide investigation and expression profiling. *Acta Physiol Plant.* **47**, 43. https://doi.org/10.1007/s11738-025-03792-7

Everaert, C., Luypaert, M., Maag, J. L. V., Cheng, Q. X., Dinger, M. E., Hellemans, J., Mestdagh, P. (2017). Benchmarking of RNA-sequencing analysis workflows using whole-transcriptome RT-qPCR expression data. *Sci Rep*. 7(1):1559. doi: 10.1038/s41598-017-01617-3.

Fujita, K., and Inui, H. (2021). Biological functions of major latex-like proteins in plants. *Plant Sci.* 306, 110856. https://doi.org/10.1016/j.plantsci.2021.110856.

Gentile, D., Serino, G., and Frugis, G. (2024). CRF transcription factors in the trade-off between abiotic stress response and plant developmental processes. *Front. Genet.* 15:1377204. doi: 10.3389/fgene.2024.1377204

Herman, J. J., and Sultan, S. E. (2011). Adaptive transgenerational plasticity in plants: Case studies, mechanisms, and implications for natural populations. *Front Plant Sci*, **2**, 1–10. https://doi.org/10.3389/fpls.2011.00102

Hernández Estévez, I., and Rodríguez Hernández, M. (2020). Plant Glutathione S-transferases: An overview. *Plant Gene*. 23, 100233. https://doi.org/10.1016/j.plgene.2020.100233.

Hallmark, H. T., Rashotte, A. M. (2019). Review – Cytokinin Response Factors: Responding to more than cytokinin. *Plant Science*. 289, 110251. https://doi.org/10.1016/j.plantsci.2019.110251.

Holeski, L. M., Jander, G., and Agrawal, A. A. (2012). Transgenerational defense induction and epigenetic inheritance in plants. *Trends in Ecology and Evolution*, **27**(11), 618–626. https://doi.org/10.1016/j.tree.2012.07.011

Huang, J., Ghosh, R., and Bankaitis, V. A. (2016). Sec14-like phosphatidylinositol transfer proteins and the biological landscape of phosphoinositide signaling in plants. *Biochim Biophys Acta*. 1861(9 Pt B):1352-1364. doi: 10.1016/j.bbalip.2016.03.027.

Jaimes-Miranda, F., Chávez Montes, R. A., (2020). The plant MBF1 protein family: a bridge between stress and transcription. *Journal of Experimental Botany*. 71, 6,1782–1791. https://doi.org/10.1093/jxb/erz525.

Jerez, M. P., Ortiz, J., Castro, C., Escobar, E., Sanhueza, C., Del-Saz, N. F., Ribas-Carbo, M., Coba de la Peña, T., Ostria-Gallardo, E., Fischer, S., Castro, P. A. and Bascunan-Godoy, L. (2023). Nitrogen sources differentially affect respiration, growth, and carbon allocation in Andean and Lowland ecotypes of *Chenopodium quinoa* Willd. *Front. Plant Sci.* 14:1070472. doi: 10.3389/fpls.2023.1070472

Kitsios, G., Doonan, J. H. (2014). Cyclin dependent protein kinases and stress responses in plants. *Plant Signal Behav*. 6(2):204-9. doi: 10.4161/psb.6.2.14835.

Kurepa, J., Toh-e, A. and Smalle, J.A. (2008), 26S proteasome regulatory particle mutants have increased oxidative stress tolerance. The Plant Journal, 53: 102-114. https://doi.org/10.1111/j.1365-313X.2007.03322.x

Lamelas, L., López-Hidalgo, C., Valledor, L., Meijón, M. and Cañal, M.J. (2024). Like mother like son: Transgenerational memory and cross-tolerance from drought to heat stress are identified in chloroplast proteome and seed provisioning in Pinus radiata. Plant, Cell and Environment, 47, 1640–1655. https://doi.org/10.1111/pce.14836

Langfelder, P., & Horvath, S. (2008). WGCNA: an R package for weighted correlation network analysis. *BMC bioinformatics*, *9*, 1-13.

Laitinen, R. A., and Nikoloski, Z. (2019). Genetic basis of plasticity in plants. *J. Exp. Bot*. 70, 739–745. doi: 10.1093/jxb/ery404

Li, G., Zhao, Y., Liu, F., Shi, M., Guan, Y., Zhang, T., Zhao, F., Qiao, Q., and Geng, Y. (2022). Transcriptional memory of gene expression across generations participates in transgenerational plasticity of field pennycress in response to cadmium stress. *Front. Plant Sci.* 13:953794. doi: 10.3389/fpls.2022.953794

Le, X. H., Lee, C. P., Millar, A. H. (2021). The mitochondrial pyruvate carrier (MPC) complex mediates one of three pyruvate-supplying pathways that sustain Arabidopsis respiratory metabolism, *The Plant Cell*. 33, 8, 2776–2793, https://doi.org/10.1093/plcell/koab148

Liu, H. P., Able, A. J., and Able, J. A. (2021) Nitrogen Starvation-Responsive MicroRNAs Are Affected by Transgenerational Stress in Durum Wheat Seedlings. *Plant (Basel)*, **10**(5), 826. doi: 10.3390/plants10050826

Livak, K. J., Schmittgen, T. D. (2001). Analysis of relative gene expression data using real-time quantitative PCR and the 2(-Delta Delta C(T)) Method. Methods. 25(4):402-8. doi: 10.1006/meth.2001.1262.

López, D., Larama, G., Sáez, P. L., Bravo, L. A. (2023). Transcriptome Analysis of Diurnal and Nocturnal-Warmed Plants, the Molecular Mechanism Underlying Cold Deacclimation Response in Deschampsia antarctica. *Int. J. Mol. Sci*. 24, 11211. https://doi.org/10.3390/ijms241311211

Malumbres, M. (2014) Cyclin-dependent kinases. *Genome Biol* **15**, 122. https://doi.org/10.1186/gb4184

Massaro, M., De Paoli, E., Tomasi, N., Morgante, M., Pinton, R., & Zanin, L. (2019). Transgenerational Response to Nitrogen Deprivation in *Arabidopsis thaliana*. *International Journal of Molecular Sciences*, *20*(22), 5587. https://doi.org/10.3390/ijms20225587

Montag, K., Ivanov, R., and Bauer, P. (2023). Role of SEC14-like phosphatidylinositol transfer proteins in membrane identity and dynamics. *Front. Plant Sci.* 14:1181031. doi: 10.3389/fpls.2023.1181031

Nguyen, N. H., Vu, N. T., & Cheong, J.-J. (2022). Transcriptional Stress Memory and Transgenerational Inheritance of Drought Tolerance in Plants. *International Journal of Molecular Sciences*, *23*(21), 12918. https://doi.org/10.3390/ijms232112918

Nisa, M., Eekhout, T., Bergis, C., Pedroza-Garcia, J. A., He, X., Mazubert, C., Vercauteren, I., Cools, T., Brik-Chaouche, R., Drouin-Wahbi, J., Chmaiss, L., Latrasse, D., Bergounioux, C., Vandepoele, K., Benhamed, M., De Veylder, L., Raynaud, C. (2023). Distinctive and complementary roles of E2F transcription factors during plant replication stress responses. *Mol Plant*. 7;16(8):1269-1282. doi: 10.1016/j.molp.2023.07.002.

Ostria-Gallardo, E., Ranjan, A., Ichihashi, Y., Corcuera, L. J., Sinha, N. R. (2018). Decoding the gene coexpression network underlying the ability of Gevuina avellana to live in diverse light conditions. New Phytol. 220(1):278-287. doi: 10.1111/nph.15278.

Park, E. J., and Kim, T. H. (2021). Arabidopsis *OSMOTIN 34* Functions in the ABA Signaling Pathway and Is Regulated by Proteolysis. *Int J Mol Sci*. 24;22(15):7915. doi: 10.3390/ijms22157915.

Pétriacq, P., Ton, J., Patrit, O., Tcherkez, G., and Gakière, B. (2016). NAD Acts as an Integral Regulator of Multiple Defense Layers. *Plant Physiology* 172(3), 1465–1479, https://doi.org/10.1104/pp.16.00780

Razzaq, M. K., Rani, R., Xing, G., Xu, Y., Raza, G., Aleem, M., Iqbal, S., Arif, M., Mukhtar, Z., Nguyen, H. T., Varshney, R. K., Siddique, K. H. M., & Gai, J. (2023). Genome-Wide Identification and Analysis of the Hsp40/J-Protein Family Reveals Its Role in Soybean (*Glycine max*) Growth and Development. *Genes*, *14*(6), 1254. https://doi.org/10.3390/genes14061254

Sarkar, K. S., Thapar, U., Kundnani, P., Panwar, P., and Grover, A. (2013). Functional relevance of J-protein family of rice (Oryza sativa), *Cell Stress and Chaperones.* **18:**3, 321-331, https://doi.org/10.1007/s12192-012-0384-9.

Sharma, M., Kumar, P., Verma, V., Sharma, R., Bhargava, B., and Irfan, M. (2022). Understanding plant stress memory response for abiotic stress resilience: Molecular insights and prospects. *Plant Physiol and Biochem* **179**, 10-24. https://doi.org/10.1016/j.plaphy.2022.03.004

Shi, X., Gupta, S., and Rashotte, A. M. (2013). Characterization of two tomato AP2/ERF genes, *SlCRF1* and *SlCRF2* in hormone and stress responses. *Plant Cell Rep* **33**, 35–45. https://doi.org/10.1007/s00299-013-1510-6

Simon, A. A., Navarro-Retamal, C., and Feijó, J. A. (2023). Merging Signaling with Structure: Functions and Mechanisms of Plant Glutamate Receptor Ion Channels. *Annu Rev Plant* Biol. 22; 74:415-452. doi: 10.1146/annurev-arplant-070522-033255.

Sommer, R. J. (2020). Phenotypic plasticity: From theory and genetics to current and future challenges. *Genetics* 215, 1–13. doi: 10.1534/genetics.120.30 3163

Song, X., Fang, J., Han, X., He, X., Liu, M., Hu, J., and Zhuo, R. (2016). Overexpression of quinone reductase from Salix matsudana Koidz enhances salt tolerance in transgenic Arabidopsis thaliana. *Gene*. 576; 1, 520-527. https://doi.org/10.1016/j.gene.2015.10.069.

Stone S. L. (2014). The role of ubiquitin and the 26S proteasome in plant abiotic stress signaling. Front Plant Sci. 16; 5:135. doi: 10.3389/fpls.2014.00135.

Struck, A. W., Thompson, M. L, Wong, L. S, and Micklefield, J. (2012). S-adenosyl-methionine-dependent methyltransferases: highly versatile enzymes in biocatalysis, biosynthesis and other biotechnological applications. *Chembiochem*. 21; 13(18):2642-55. doi: 10.1002/cbic.201200556.

Sun, J. and Zheng, N. (2015). Molecular Mechanism Underlying the Plant NRT1.1 Dual-Affinity Nitrate Transporter. *Front. Physiol*. 6:386. doi: 10.3389/fphys.2015.00386

Wehrens, R., & Buydens, L. M. C. (2007). Self- and Super-organizing Maps in R: The kohonen Package. *Journal of Statistical Software*, *21*(5), 1–19. https://doi.org/10.18637/jss.v021.i05

Yao, X., Humphries, J., Johnson, K. L., Chen, J., Ma, Y. (2025). Function of WAKs in Regulating Cell Wall Development and Responses to Abiotic Stress. *Plants (Basel)*. 23; 14(3):343. doi: 10.3390/plants14030343.

Ye, J. Y., Tian, W. H. and Jin, C. W. (2022). Nitrogen in plants: from nutrition to the modulation of abiotic stress adaptation. *Stress Biology*. 2, 4. https://doi.org/10.1007/s44154-021-00030-1

Yu, B., Liu, N., Tang, S., Qin, T., & Huang, J. (2022). Roles of Glutamate Receptor-Like Channels (GLRs) in Plant Growth and Response to Environmental Stimuli. *Plants*, *11*(24), 3450. https://doi.org/10.3390/plants11243450

Zhao, L., Cai, B., Zhang, X., Zhang, B., Feng, J., Zhou, D., Chen, Y., Zhang, M., Qi, D., Wang, W., et al. (2024). Physiological and Transcriptional Characteristics of Banana Seedlings in Response to Nitrogen Deficiency Stress. *Horticulturae* **10**, 290. https://doi.org/10.3390/ horticulturae10030290

Zhiqi, H., Tingyi, W., Dongdong, C., Lan, S., Guangheng, Z., Qian, Q., Li, Z. (2025). Leucine-Rich Repeat Protein Family Regulates Stress Tolerance and Development in Plants. *Rice Science*. 32, 1, 32-43. https://doi.org/10.1016/j.rsci.2024.12.003.

A


F1
F0
ferric reduction oxidase 2
ATP binding;nucleic acid binding;helicases
Glycosyl hydrolases family 32 protein
S-adenosyl-L-methionine-dependent methyltransferases superfamily protein
RING/U-box superfamily protein
AUR62033759
alpha/beta-Hydrolases superfamily protein
nucleolar essential protein-related
AUR62017405
AUR62020518
DNA-binding bromodomain-containing protein
C-8,7 sterol isomerase
AUR62040815
Ubiquitin-specific protease family C19-related protein
smr (Small MutS Related) domain-containing protein
AUR62026603
D-arabinono-1,4-lactone oxidase family protein
DNAse I-like superfamily protein
AUR62017404
carboxypeptidase D, putative
Tetratricopeptide repeat (TPR)-like superfamily protein
Pseudouridine synthase family protein
Tetratricopeptide repeat (TPR)-like superfamily protein
Ribonuclease E inhibitor RraA/Dimethylmenaquinone methyltransferase
cation/H+ exchanger 2
transcription regulatory protein SNF5, putative (BSH)
dihydroflavonol 4-reductase-like1
SEC14 cytosolic factor family protein / phosphoglyceride transfer family protein
ATP binding;nucleic acid binding;helicases
lysine histidine transporter 1
AUR62002384
nodulin MtN21 /EamA-like transporter family protein
AUR62010189
protein kinase family protein
high chlorophyll fluorescent 107
P-glycoprotein 11
Wall-associated kinase family protein
Auxin efflux carrier family protein
methyltransferases
ATP binding cassette subfamily B4
xylem cysteine peptidase 2
SAUR-like auxin-responsive protein family
FAR1-related sequence 5
N-MYC downregulated-like 1
zinc ion binding
NB-ARC domain-containing disease resistance protein
Protein of unknown function (duplicated DUF1399)
root hair specific 16
SUMO-activating enzyme 2
cyclic nucleotide-gated channel 18
Homeodomain-like superfamily protein
AUR62019928
P-loop containing nucleoside triphosphate hydrolases superfamily protein
Eukaryotic aspartyl protease family protein
Galactose oxidase/kelch repeat superfamily protein
Quinone reductase family protein
nitrate transporter 1.1
Pentatricopeptide repeat (PPR) superfamily protein
glucan synthase-like 4
CBL-interacting protein kinase 20
AUR62019314
uroporphyrinogen-III synthase family protein
RING/U-box superfamily protein
glutamate receptor 2.1
Galactose oxidase/kelch repeat superfamily protein
GRAS family transcription factor
AUR62016715
Galactose oxidase/kelch repeat superfamily protein
Ribonuclease E inhibitor RraA/Dimethylmenaquinone methyltransferase
Protein kinase superfamily protein
NB-ARC domain-containing disease resistance protein
E2F transcription factor 3
AUR62005651
ENTH/VHS/GAT family protein
AUR62007595
glycerol-3-phosphate acyltransferase 1
Pseudouridine synthase family protein
Restriction endonuclease, type II-like superfamily protein
NB-ARC domain-containing disease resistance protein
DP-E2F-like 1
P-loop containing nucleoside triphosphate hydrolases superfamily protein
AUR62016297
PYR1-like 2
Glycosyltransferase family 61 protein
hydroxycinnamoyl-CoA shikimate/quinate hydroxycinnamoyl transferase
UDP-Glycosyltransferase superfamily protein
protein arginine methyltransferase 6
PB1 domain-containing protein tyrosine kinase
Major facilitator superfamily protein
AUR62038166
AUR62017113
tubulin folding cofactor B
UDP-glucosyl transferase 85A7
squamosa promoter binding protein-like 7
TOPLESS-related 2
zinc finger (C2H2 type, AN1-like) family protein
AGC (cAMP-dependent, cGMP-dependent and protein kinase C) kinase family protein
peptide deformylase 1A
AUR62020563
actin-related protein 9
Haloacid dehalogenase-like hydrolase (HAD) superfamily protein
AUR62027400
Transcription elongation factor (TFIIS) family protein
Peroxidase superfamily protein
AMP-dependent synthetase and ligase family protein
NAD(P)-binding Rossmann-fold superfamily protein
3
2
1
0
-1
-2
F1
HN
LN
F0
HN
LN

B

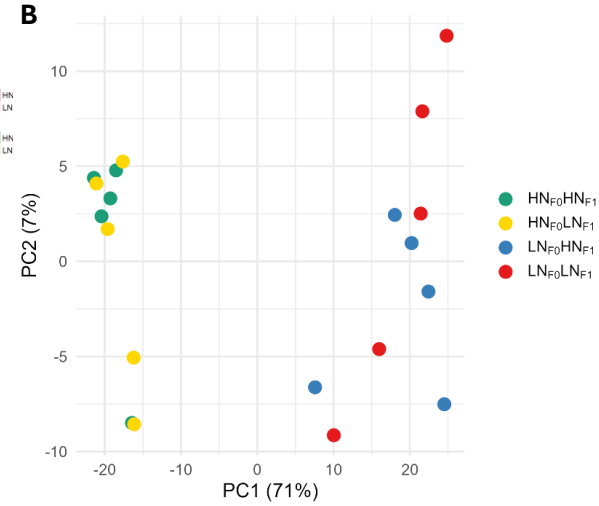
10
5
0
-5
-10
-20
-10
0
10
20
PC2 (7%)
PC1 (71%)
HN$_{F0}$HN$_{F1}$
HN$_{F0}$LN$_{F1}$
LN$_{F0}$HN$_{F1}$
LN$_{F0}$LN$_{F1}$

Figure 3.1. Top differentially expressed genes in F1 seedlings (descendants of HN_{F0} and LN_{F0} mother plants) grown at HN and LN. A. Heat map of F1 DE genes. Each column contains the measurements for gene expression change for a single sample. Relative gene expression is indicated by color: high-expression (red), median-expression (white), and low-expression (blue). **B.** Principal Component Analysis (PCA) of transcripts.

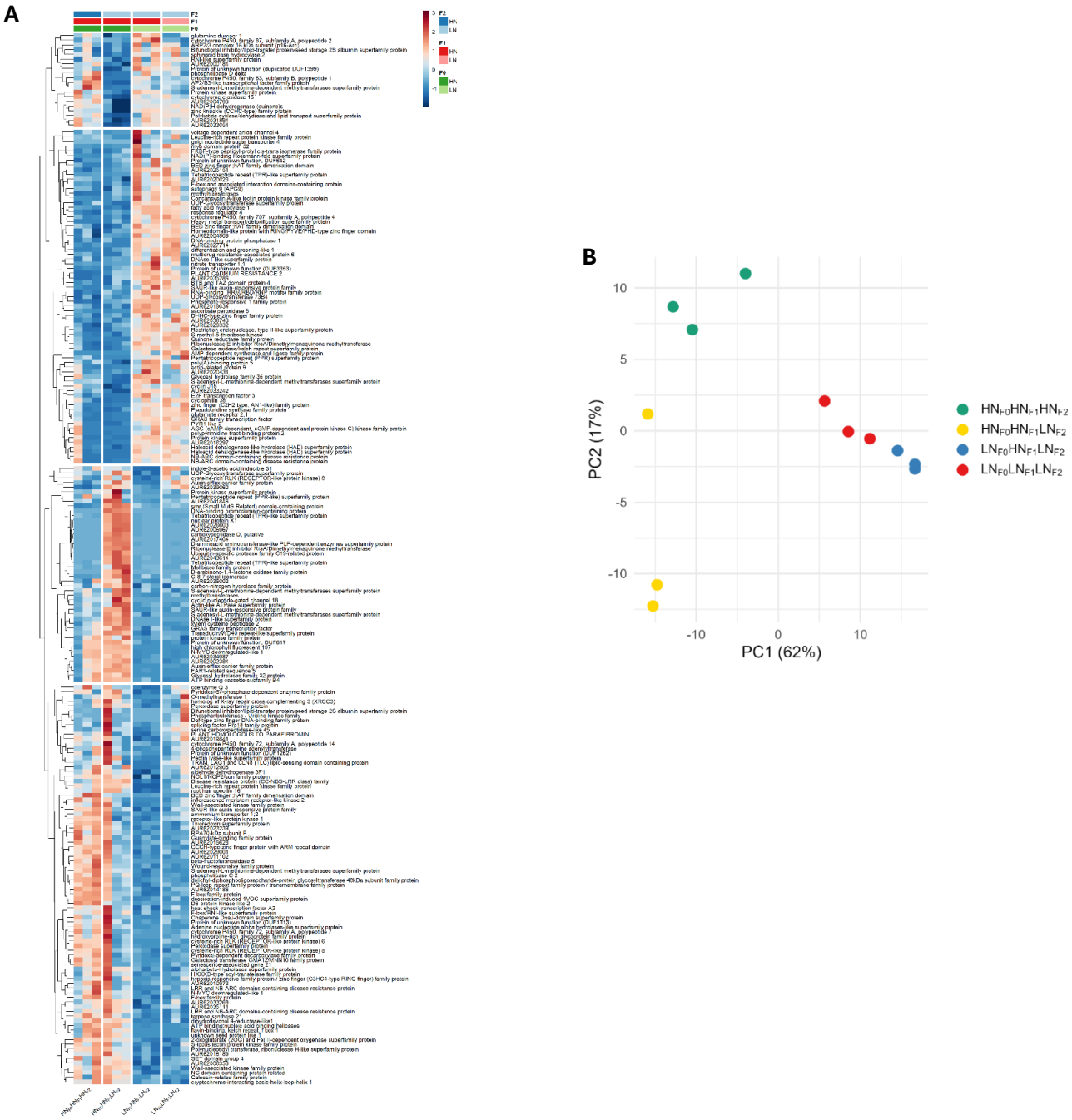

Figure 3.2. Top differentially expressed genes in F1 seedlings (descendants of HN$_{F0}$ and LN$_{F0}$ mother plants) grown at HN and LN. A. Heat map of F1 DE genes. Each column contains the measurements for gene expression change for a single sample. Relative gene expression is indicated by color: high-expression (red), median-expression (white), and low-expression (blue). **B.** Principal Component Analysis (PCA) of transcripts.

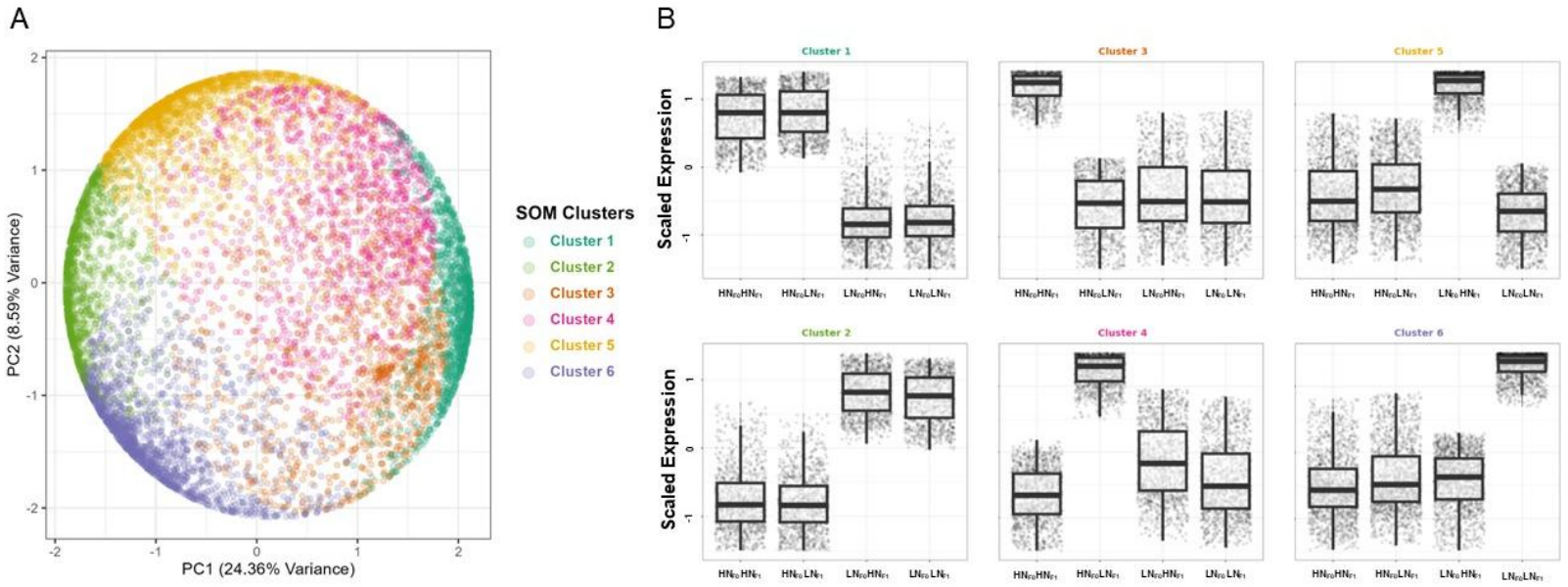

Figure 3.3. PCA-SOM analysis of DE genes in F1 seedlings. A. Principal component analysis (PCA) with self-organizing map (SOM) clustering for gene expression. **B.** Box plots of the specific accumulation pattern of transcripts for each treatment within each cluster defined by the PCA-SOM. PCA-SOM space shows two principal components (PC1, PC2) that explain the higher percentage of variance in the dataset and represent the clustering patterns of the transcriptional profile in the treatments (indicated by different colors). In each box plot the horizontal line indicates the median while bars represent the maximum and minimum values of the scaled transcript abundance.

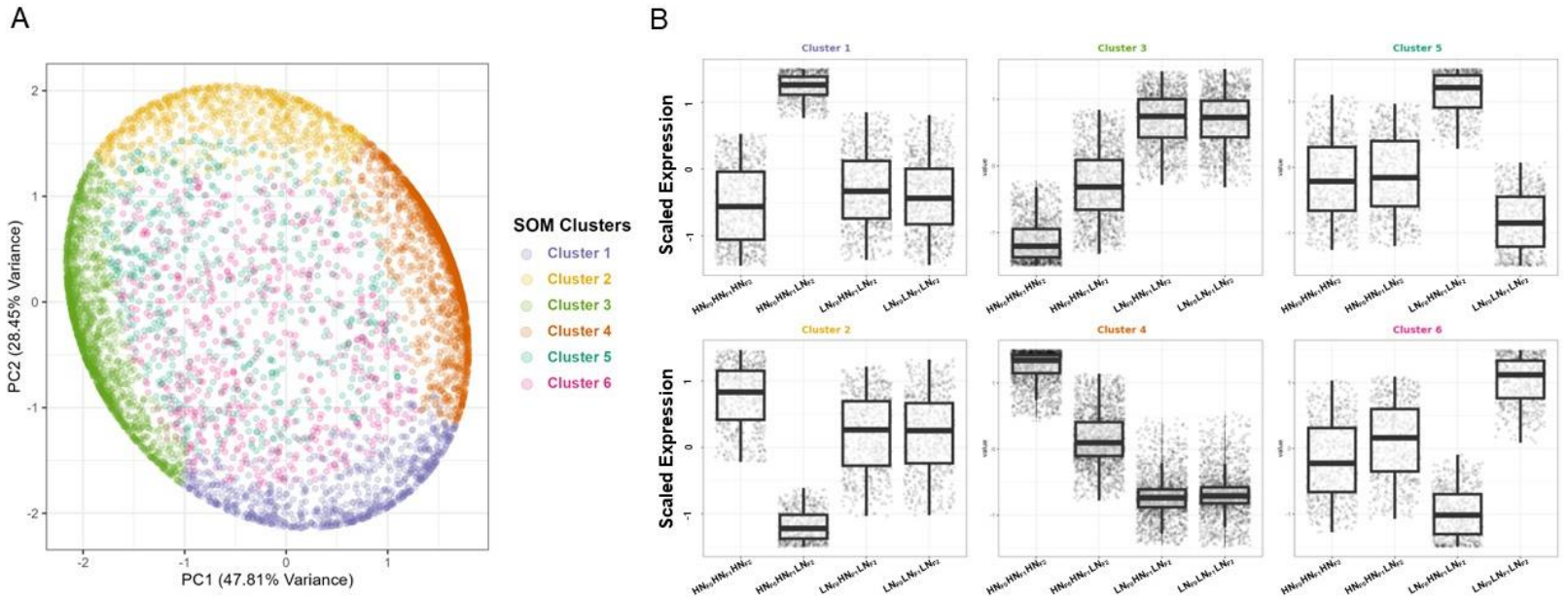

Figure 3.4. PCA-SOM analysis of DE genes in F2 seedlings. A. Principal component analysis (PCA) with self-organizing map (SOM) clustering for gene expression. **B.** Box plots of the specific accumulation pattern of transcripts for each treatment within each cluster defined by the PCA-SOM. PCA-SOM space shows two principal components (PC1, PC2) that explain the higher percentage of variance in the dataset and represent the clustering patterns of the transcriptional profile in the treatments (indicated by different colors). In each box plot the horizontal line indicates the median while bars represent the maximum and minimum values of the scaled transcript abundance.

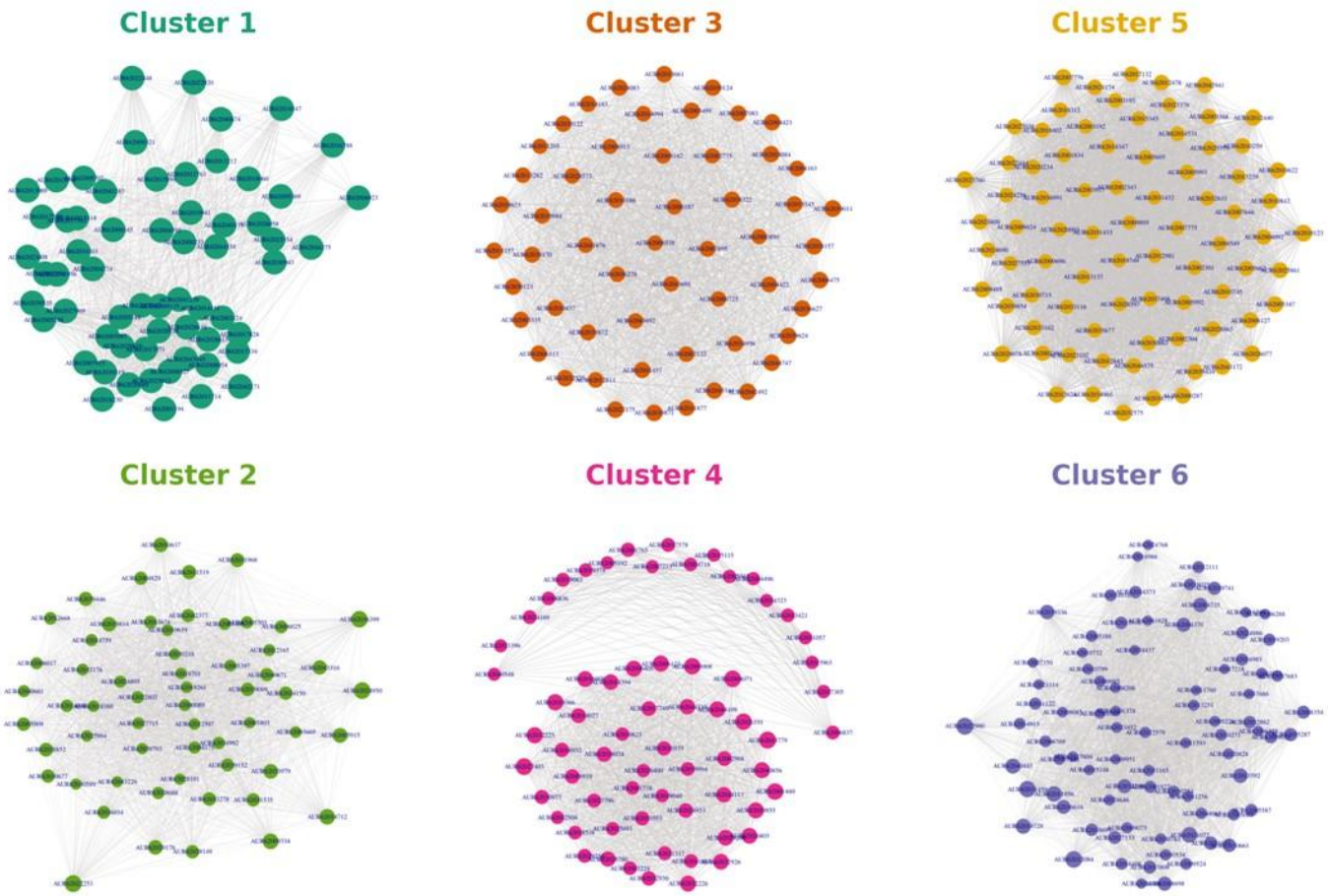

Figure 3.5. Gene co-expression networks of F1 hub genes. Gene co-expression networks of the hub genes for each PCA-SOM cluster. Colors correspond to the same clusters as the PCA-SOM.

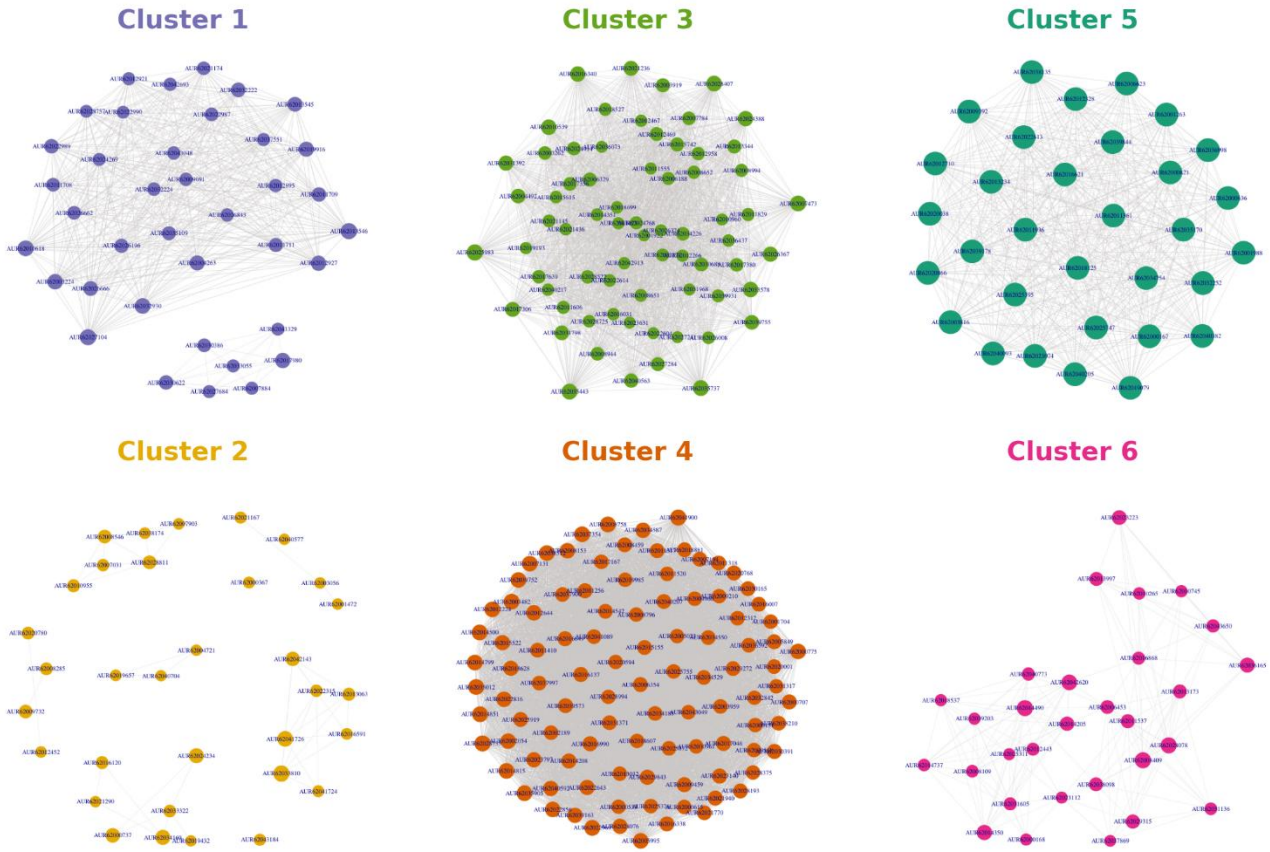

Figure 3.6. Gene co-expression networks of F2 hub genes. Gene co-expression networks of the hub genes for each PCA-SOM cluster. Colors correspond to the same clusters as the PCA-SOM.

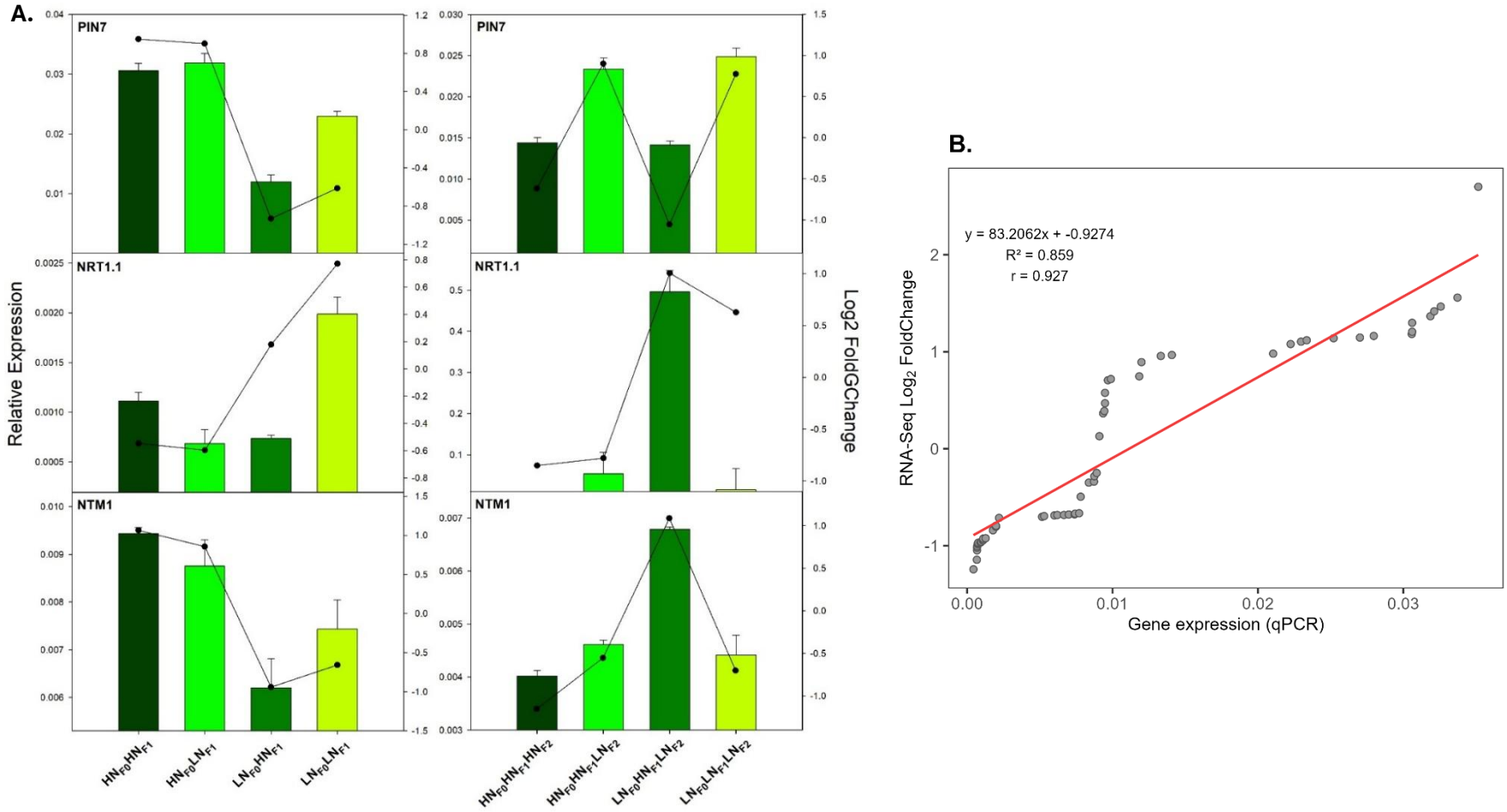

Supplemental Figure 3.1. Transcriptome validation. A. Relation between relative gene expressions evaluated by qPCR and Log_2 FoldChange of RNA-seq. Bars and dots show the mean ± standard error (n=3) for qPCR and RNA-seq, respectively. **B.** Pearson correlation between qPCR and RNA-seq of 3 differentially expressed genes.

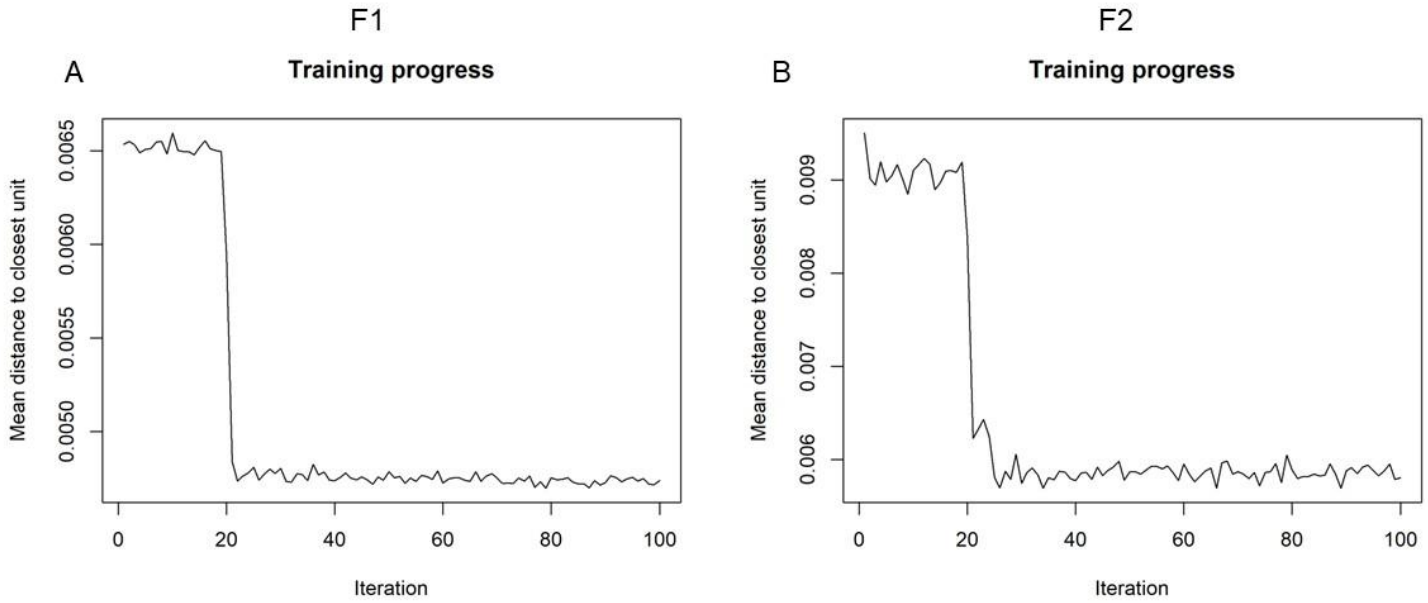

Supplemental Figure 3.2. Training progress of average distances between genes using self-organizing maps showing the effect of neighborhood shrinking to include the winning unit, i.e., when the vectors in the dataset reach the closest similarity.

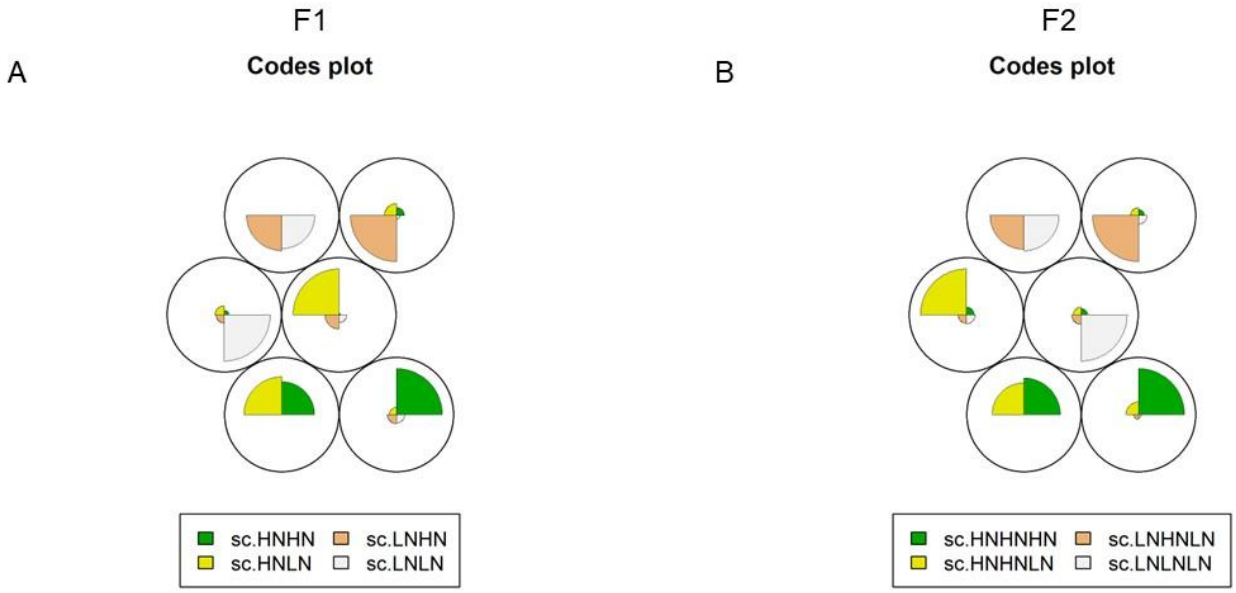

Supplemental Figure 3.3. Codebook vectors for F1 and F2 seedlings showing the clusters of differentially expressed genes with maximum neighboring after training process. The codebook vectors represent the expression profile of genes associated to a given state after the construction of the map.

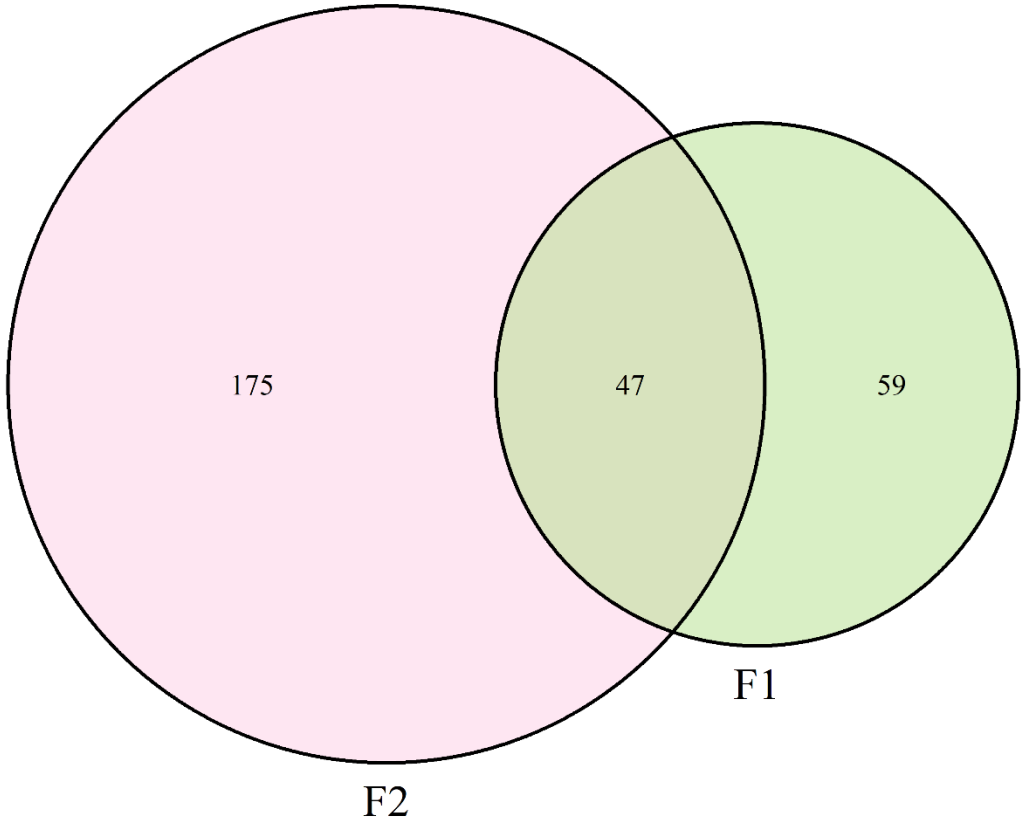

Supplemental Figure 3.4. Venn diagram of DE genes of F1 (green) and F2 (pink) seedlings and shared DE genes between them.

Supplemental Figure 3.5. Phenotype of 90-day-old F1 and 60-day-old F2 plants (descendants of HN_{F0} and LN_{F0} mother plants). A. 90-day-old F1 plants. **B.** 60-day-old F2 plants. White line indicates a 20 cm scale.

Supplemental Table 3.1. F1 seedlings hub genes by cluster/node

Cluster 1		
Gene	**Gene name**	**Hub value**
AUR62023008	MLP-like protein 28	91.81714954
AUR62018230	uridine kinase/uracil phosphoribosyltransferase 1	89.97155421
AUR62013069	Disease resistance-responsive (dirigent-like protein) family protein	89.58933259
AUR62015896	Mannose-binding lectin superfamily protein	87.89121116
AUR62039319	Calcineurin-like metallo-phosphoesterase superfamily protein	87.58062455
AUR62025812	sulfoquinovosyldiacylglycerol 2	87.29770169
AUR62008054	ribonuclease 2	87.18149702
AUR62020689	sulfoquinovosyldiacylglycerol 2	87.1443216
AUR62005239	phospholipase D P1	86.2418215
AUR62017828	DHBP synthase RibB-like alpha/beta domain	85.37723773
AUR62026058	NA	84.86669385
AUR62005369	equilibrative nucleotide transporter 1 (ENT1)	84.43572593
AUR62043945	sulfoquinovosyldiacylglycerol 1	84.23773444
AUR62044375	Cation efflux family protein	83.81978346
AUR62017971	MSCS-like 2	83.66415522
AUR62042171	phosphatidic acid phosphohydrolase 2	83.41028935
AUR62007915	Purple acid phosphatases superfamily protein	83.38386411
AUR62031956	actin binding protein family	82.49094854
AUR62014451	purple acid phosphatase 10	82.40761332
AUR62034303	Protein of unknown function (DUF179)	82.29684958
AUR62008927	purple acid phosphatase 15	82.11802636
AUR62020744	starch synthase 4	82.01604164
AUR62028630	ribonuclease 2	81.32458254
AUR62015894	NA	81.31180427
AUR62011714	Patched family protein	80.56195672
AUR62016788	purple acid phosphatase 10	80.26253074
AUR62018060	glycine-rich protein	80.15936067
AUR62001194	lipase class 3 family protein	79.84768219
AUR62017581	P-loop containing nucleoside triphosphate hydrolases superfamily protein	79.41544817
AUR62006923	SWIB/MDM2 domain	79.07705258
AUR62003124	Purple acid phosphatases superfamily protein	78.8857015
AUR62030943	Thioredoxin superfamily protein	78.37438058
AUR62009135	sulfoquinovosyldiacylglycerol 1	78.31767623
AUR62007354	alkenal reductase	78.00745647

AUR62034547	purple acid phosphatase 10	77.11341121
AUR62009321	MLP-like protein 31	77.02205262
AUR62015118	P-loop containing nucleoside triphosphate hydrolases superfamily protein	76.93971049
AUR62044534	NA	76.92881461
AUR62022920	UDP-glucose pyrophosphorylase 3	76.7338445
AUR62028615	phosphoribosylanthranilate isomerase 1	76.458187
AUR62039535	Phosphoglucomutase/phosphomannomutase family protein	76.39764192
AUR62027969	starch synthase 4	75.75234291
AUR62022448	Calcineurin-like metallo-phosphoesterase superfamily protein	74.91093787
AUR62041239	transcription regulators	74.36776889
AUR62004595	Major facilitator superfamily protein	74.10767781
AUR62011212	2-oxoglutarate (2OG) and Fe(II)-dependent oxygenase superfamily protein	74.03126712
AUR62012763	Plastid-lipid associated protein PAP / fibrillin family protein	73.78421677
AUR62029819	NA	73.56966296
AUR62041587	NA	73.55954039
AUR62000145	NAD kinase 1	73.49138315
AUR62023554	2-oxoglutarate (2OG) and Fe(II)-dependent oxygenase superfamily protein	73.46773501
AUR62019941	UDP-Glycosyltransferase superfamily protein	73.16856993
AUR62020539	thiazole biosynthetic enzyme, chloroplast (ARA6) (THI1) (THI4)	73.15846673
AUR62000233	cystatin B	73.13269576
AUR62040171	NA	72.83519862
AUR62003097	Purple acid phosphatases superfamily protein	72.74433226
AUR62004774	UDP-GLUCOSE PYROPHOSPHORYLASE 1	72.56821433
AUR62017334	D-isomer specific 2-hydroxyacid dehydrogenase family protein	72.40426101
AUR62009702	Polyketide synthase, enoylreductase family protein	72.39022141
AUR62007343	NA	72.2644384
AUR62040674	Putative lysine decarboxylase family protein	72.1735849
AUR62017799	potassium transporter 1	72.0622902

Cluster 2		
Gene	**Gene name**	**Hub value**
AUR62022253	Sec14p-like phosphatidylinositol transfer family protein	119.866529
AUR62024950	NA	118.341705
AUR62036399	SEC14 cytosolic factor family protein / phosphoglyceride transfer family protein	117.568148

AUR62009334	proline extensin-like receptor kinase 1	111.320546
AUR62014712	sugar transporter 1	110.637683
AUR62005915	Transducin family protein / WD-40 repeat family protein	105.515586
AUR62033979	beta glucosidase 13	104.190859
AUR62010637	ribosomal protein L24	103.577684
AUR62029178	Shugoshin C terminus	103.568208
AUR62019814	HMG (high mobility group) box protein	103.375334
AUR62043316	cyclin-dependent kinase B2	101.995004
AUR62011519	phosphatidic acid phosphatase-related / PAP2-related	100.994915
AUR62039446	Leucine-rich repeat protein kinase family protein	100.951724
AUR62031968	Sec14p-like phosphatidylinositol transfer family protein	99.3927062
AUR62028852	serine carboxypeptidase-like 45	98.3030536
AUR62033278	Leucine-rich repeat (LRR) family protein	96.0268731
AUR62005909	NA	95.5429312
AUR62030677	NA	95.4847345
AUR62024150	Microtubule associated protein (MAP65/ASE1) family protein	95.4708867
AUR62019089	P-loop containing nucleoside triphosphate hydrolases superfamily protein	95.3434979
AUR62028149	Transducin family protein / WD-40 repeat family protein	95.0986432
AUR62031535	Bifunctional inhibitor/lipid-transfer protein/seed storage 2S albumin superfamily protein	94.7018315
AUR62040671	Kinesin motor family protein	94.3018298
AUR62004829	NA	94.1695823
AUR62042377	NA	93.7480685
AUR62039152	NA	92.6071577
AUR62036034	Sec14p-like phosphatidylinositol transfer family protein	92.36624
AUR62013674	NA	91.6593782
AUR62006025	syntaxin of plants 111	91.5148538
AUR62012668	beta glucosidase 46	90.2784734
AUR62014040	Plant protein of unknown function (DUF936)	88.683237
AUR62034992	NA	87.8687702
AUR62028688	XH/XS domain-containing protein	87.421413
AUR62005703	serine carboxypeptidase-like 45	87.3039841
AUR62022802	ROP guanine nucleotide exchange factor 5	87.2355712
AUR62004175	Plant-specific transcription factor YABBY family protein	86.7929986
AUR62040661	zinc finger protein-related	86.3350791
AUR62014759	NA	86.3336451
AUR62024805	early nodulin-like protein 15	86.1122197
AUR62005105	basic helix-loop-helix (bHLH) DNA-binding superfamily protein	86.0766635

AUR62006017	IQ-domain 18	85.6304302
AUR62012165	ROP guanine nucleotide exchange factor 5	84.8911436
AUR62027715	Protein kinase family protein	84.7946524
AUR62005397	Pectin lyase-like superfamily protein	84.5692392
AUR62032176	Aldolase-type TIM barrel family protein	84.0041348
AUR62010639	IQ-domain 22	83.8710103
AUR62000089	Leucine-rich repeat (LRR) family protein	83.8066808
AUR62019261	Leucine-rich repeat (LRR) family protein	82.9898711
AUR62003669	Xanthine/uracil permease family protein	82.7516313
AUR62018380	Cyclin family protein	82.6575481
AUR62025964	Leucine-rich repeat protein kinase family protein	81.8078123
AUR62012597	cysteine-rich RLK (RECEPTOR-like protein kinase) 10	81.6659631
AUR62018701	basic helix-loop-helix (bHLH) DNA-binding superfamily protein	81.2531808
AUR62030218	Cytochrome b561/ferric reductase transmembrane protein family	80.5450726
AUR62005803	galactosyltransferase1	80.2625638
AUR62028101	Heavy metal transport/detoxification superfamily protein	79.9503422
AUR62043226	NA	79.423914
AUR62039793	structural maintenance of chromosome 3	79.3482744
AUR62030589	NA	79.2648473

Cluster 3		
Gene	**Gene name**	**Hub value**
AUR62039011	riboflavin kinase/FMN hydrolase	288.112673
AUR62039623	photosystem II reaction center protein D	285.337677
AUR62022175	Photosystem I, PsaA/PsaB protein	284.063031
AUR62042492	RNA polymerase subunit beta	284.002147
AUR62039871	photosystem II reaction center protein D	283.431737
AUR62038157	Survival protein SurE-like phosphatase/nucleotidase	283.176961
AUR62011157	photosynthetic electron transfer A	282.613035
AUR62006475	photosystem II reaction center protein B	282.28577
AUR62044747	Photosystem I, PsaA/PsaB protein	282.276258
AUR62032525	ribulose-bisphosphate carboxylases	282.184565
AUR62005499	sulfur E2	282.155274
AUR62024084	photosystem II reaction center protein D	281.782689
AUR62036627	Photosystem I, PsaA/PsaB protein	281.714523
AUR62013661	SPX domain gene 3	280.971902
AUR62043344	photosystem II reaction center protein A	280.854249
AUR62039624	Photosystem I, PsaA/PsaB protein	280.80849

AUR62004423	nicotinate/nicotinamide mononucleotide adenyltransferase	280.7589
AUR62006113	ribulose-bisphosphate carboxylases	280.425043
AUR62030124	RNA polymerase subunit beta	280.083091
AUR62030123	DNA-directed RNA polymerase family protein	278.907259
AUR62024083	RNA polymerase subunit beta	278.515669
AUR62015545	NAD(P)H dehydrogenase subunit H	277.815832
AUR62003335	VPS35 homolog B	277.634634
AUR62014183	NA	276.846446
AUR62041457	DNA-binding protein phosphatase 1	276.082203
AUR62010437	purple acid phosphatase 10	275.962617
AUR62038322	phosphate starvation-induced gene 2	275.76487
AUR62030122	DNA-directed RNA polymerase family protein	275.494797
AUR62030170	DNA-directed RNA polymerase family protein	275.473951
AUR62039872	photosystem II reaction center protein C	274.528934
AUR62011877	phosphate transporter 1	273.103282
AUR62010186	Uncharacterised conserved protein (UCP030210)	272.206557
AUR62034956	DNA-directed RNA polymerase family protein	271.912811
AUR62007083	pyrophosphorylase 3	270.785635
AUR62007895	PLC-like phosphodiesterases superfamily protein	270.033064
AUR62004422	Histone superfamily protein	269.933895
AUR62019984	phosphate starvation-induced gene 2	269.695357
AUR62004163	SPX domain gene 3	269.255494
AUR62028573	NAD(P)H dehydrogenase subunit H	268.152831
AUR62014094	DNA-directed RNA polymerase family protein	267.903132
AUR62000187	RING/U-box superfamily protein	267.512764
AUR62012811	Inositol monophosphatase family protein	267.167372
AUR62013282	monogalactosyldiacylglycerol synthase 2	267.080525
AUR62002132	phosphoenolpyruvate carboxylase kinase 1	266.159982
AUR62043691	photosystem II reaction center protein C	264.129877
AUR62036278	ankyrin repeat family protein / regulator of chromosome condensation (RCC1) family protein	263.623194
AUR62043692	photosystem II reaction center protein D	263.160321
AUR62009162	ARM repeat superfamily protein	263.020179
AUR62041876	ribosomal protein S2	262.846691
AUR62011205	monogalactosyldiacylglycerol synthase 2	261.627604
AUR62002775	photosystem II reaction center protein B	261.438923
AUR62006538	Calcium-dependent lipid-binding (CaLB domain) family protein	261.097676
AUR62000850	Major facilitator superfamily protein	260.925588
AUR62000725	phospholipase D P1	260.618291

AUR62008915	NA	259.542961

Cluster 4		
Gene	**Gene name**	**Hub value**
AUR62007213	Got1/Sft2-like vescicle transport protein family	83.8111732
AUR62040548	Peptidase S24/S26A/S26B/S26C family protein	83.8974283
AUR62033396	multiprotein bridging factor 1C	83.9609438
AUR62014323	PDI-like 1-2	84.2503245
AUR62012504	UDP-Glycosyltransferase superfamily protein	84.3023305
AUR62005192	Heat shock protein 70 (Hsp 70) family protein	84.3680546
AUR62013963	endoplasmic reticulum oxidoreductins 1	84.4650497
AUR62015115	PDI-like 2-2	84.7001521
AUR62005565	multidrug resistance-associated protein 3	85.0352871
AUR62004496	phosphoinositide 4-kinase gamma 4	85.1103607
AUR62025693	Terpenoid cyclases family protein	85.4559359
AUR62026400	NA	85.4807612
AUR62004718	glycine-rich protein	85.6712537
AUR62037305	zinc finger protein-related	85.7617308
AUR62019040	basic chitinase	85.8613703
AUR62010621	osmotin 34	85.9103543
AUR62011057	NA	86.3805384
AUR62041738	alpha/beta-Hydrolases superfamily protein	86.3967104
AUR62018538	PHYTOCYSTATIN 2	86.8969895
AUR62006836	NAC domain containing protein 103	86.9298077
AUR62019378	OBP3-responsive gene 1	86.9983787
AUR62019994	cytochrome P450, family 88, subfamily A, polypeptide 3	87.6113343
AUR62003224	Chitinase family protein	87.7096262
AUR62013421	heavy metal atpase 2	87.9559307
AUR62006837	NAC domain containing protein 82	88.150082
AUR62024169	multidrug resistance-associated protein 3	88.3264139
AUR62041884	Leucine-rich repeat transmembrane protein kinase	88.4628114
AUR62031317	homolog of carrot EP3-3 chitinase	88.5250511
AUR62029256	terpene synthase 21	88.6147938
AUR62017578	PDI-like 2-2	88.8435043
AUR62027796	EXORDIUM like 2	88.9032986
AUR62019063	PDI-like 1-2	89.1675966
AUR62001765	SCARECROW-like 14	89.9787376
AUR62030977	polyamine oxidase 1	90.5378422
AUR62010155	EXORDIUM like 2	90.7644778

AUR62031053	alpha-L-arabinofuranosidase 2	90.8465151
AUR62016932	F-box and associated interaction domains-containing protein	91.4840263
AUR62032930	NA	91.8647838
AUR62009919	jasmonate-zim-domain protein 1	92.1795257
AUR62002968	Protein of unknown function (DUF1262)	92.9008434
AUR62024953	methyl esterase 17	92.9132312
AUR62017740	NA	93.0661987
AUR62014027	NA	94.5533683
AUR62038074	NAD(P)-binding Rossmann-fold superfamily protein	96.1156833
AUR62028780	Kunitz family trypsin and protease inhibitor protein	96.8593607
AUR62044110	Kunitz family trypsin and protease inhibitor protein	97.9878302
AUR62044113	Kunitz family trypsin and protease inhibitor protein	97.9878302
AUR62014394	cytochrome P450, family 83, subfamily B, polypeptide 1	98.2878542
AUR62029269	NA	99.7891219
AUR62032926	NA	100.063805
AUR62026803	plantacyanin	100.2581
AUR62016608	NA	100.347197
AUR62032226	Serine protease inhibitor, potato inhibitor I-type family protein	100.740561
AUR62040856	NA	101.013666
AUR62039855	beta-1,3-glucanase 1	101.297679
AUR62006405	NA	101.610504
AUR62044109	Kunitz family trypsin and protease inhibitor protein	101.864622
AUR62006123	Phosphorylase superfamily protein	101.928492
AUR62032225	Serine protease inhibitor, potato inhibitor I-type family protein	102.41226
AUR62019366	Phosphorylase superfamily protein	103.763831
AUR62003008	cytochrome P450, family 71, subfamily B, polypeptide 10	104.143816
AUR62026191	NA	104.514438
AUR62001460	Subtilase family protein	104.673314
AUR62004071	Peroxidase superfamily protein	105.850302
AUR62027403	homolog of carrot EP3-3 chitinase	106.192332
AUR62043779	Kunitz family trypsin and protease inhibitor protein	107.191844

Cluster 5		
Gene	**Gene name**	**Hub value**

AUR62023760	wall-associated kinase 2	225.469734
AUR62010123	glutamate decarboxylase	225.011092
AUR62032575	alpha/beta-Hydrolases superfamily protein	222.115541
AUR62028078	chitinase A	221.905214
AUR62012624	cysteine-rich RLK (RECEPTOR-like protein kinase) 10	219.268952
AUR62026077	UDP-Glycosyltransferase superfamily protein	218.597059
AUR62012440	SPFH/Band 7/PHB domain-containing membrane-associated protein family	218.572901
AUR62000287	calreticulin 3	217.288842
AUR62007776	Protein of unknown function (DUF1262)	216.99266
AUR62042941	PAR1 protein	216.360083
AUR62005347	Eukaryotic aspartyl protease family protein	216.321963
AUR62010622	osmotin 34	214.746529
AUR62009489	reversibly glycosylated polypeptide 2	213.756947
AUR62043172	beta-1,3-glucanase 1	213.729304
AUR62008127	Bifunctional inhibitor/lipid-transfer protein/seed storage 2S albumin superfamily protein	213.132479
AUR62034775	phosphate transporter 3	212.990931
AUR62034965	cytochrome P450, family 81, subfamily D, polypeptide 8	212.297786
AUR62025861	lysine histidine transporter 1	211.710475
AUR62023809	homolog of carrot EP3-3 chitinase	210.754599
AUR62039410	UDP-glucosyl transferase 74B1	209.714199
AUR62012478	WRKY DNA-binding protein 40	208.391797
AUR62027038	CAP (Cysteine-rich secretory proteins, Antigen 5, and Pathogenesis-related 1 protein) superfamily protein	208.023926
AUR62010842	NA	207.809239
AUR62017132	cytochrome P450, family 72, subfamily A, polypeptide 15	207.068463
AUR62002303	LRR family protein	206.762564
AUR62004092	cytochrome BC1 synthesis	206.566165
AUR62039854	Glycosyl hydrolase superfamily protein	206.412009
AUR62033162	glutathione S-transferase phi 8	205.993002
AUR62010259	UDP-glucosyl transferase 73B3	205.899509
AUR62021174	PAR1 protein	204.11187
AUR62018312	P-loop containing nucleoside triphosphate hydrolases superfamily protein	203.055372
AUR62044575	Ankyrin repeat family protein	202.981029
AUR62018402	Acyl-CoA N-acyltransferases (NAT) superfamily protein	202.812294
AUR62003568	NA	202.684335
AUR62024690	XB3 ortholog 4 in Arabidopsis thaliana	202.613565
AUR62028863	GRAM domain family protein	202.043644
AUR62020234	Aluminium activated malate transporter family protein	201.853705

AUR62005993	chitinase A	201.482982
AUR62030715	syntaxin of plants 121	201.266855
AUR62030863	NA	200.360435
AUR62010745	Heavy metal transport/detoxification superfamily protein	198.944025
AUR62005662	MAC/Perforin domain-containing protein	198.923481
AUR62022444	phospholipase A 2A	198.043097
AUR62023102	AGAMOUS-like 15	198.031878
AUR62014531	PLANT CADMIUM RESISTANCE 2	197.06441
AUR62003195	ankyrin repeat family protein	196.616896
AUR62037498	benzoyloxyglucosinolate 1	196.303511
AUR62024256	Protein of unknown function (DUF707)	196.032444
AUR62012843	Pollen Ole e 1 allergen and extensin family protein	195.516591
AUR62005992	chitinase A	195.472506
AUR62002343	chitinase A	195.375611
AUR62009424	AGAMOUS-like 15	195.172808
AUR62035677	cytochrome P450, family 72, subfamily A, polypeptide 15	193.850829
AUR62007646	ferulic acid 5-hydroxylase 1	193.436554
AUR62027553	AWPM-19-like family protein	193.420747
AUR62005695	GRAM domain family protein	193.351833
AUR62003192	ankyrin repeat family protein	193.043333
AUR62002304	LRR family protein	192.771725
AUR62000696	Calmodulin-binding protein	192.749776
AUR62002301	LRR family protein	192.421193
AUR62004549	NA	192.103885
AUR62033116	multidrug resistance-associated protein 10	191.79327
AUR62001834	C2H2-type zinc finger family protein	191.237706
AUR62020003	receptor like protein 13	191.217583
AUR62014347	NB-ARC domain-containing disease resistance protein	190.905357
AUR62032633	sigma factor binding protein 1	190.68595
AUR62015345	O-methyltransferase family protein	190.004241
AUR62007775	Protein of unknown function (DUF1262)	189.842397
AUR62036991	NAC domain containing protein 90	189.442973
AUR62031433	NAD(P)-binding Rossmann-fold superfamily protein	188.996245
AUR62013137	Protein kinase superfamily protein	188.225586
AUR62013239	UDP-glucosyl transferase 73C6	188.000094
AUR62028597	Galactose oxidase/kelch repeat superfamily protein	187.762783
AUR62003917	UDP-glycosyltransferase 73B4	187.656349
AUR62025570	NA	186.73831
AUR62023376	Protein kinase superfamily protein	185.804778
AUR62009895	Cytochrome P450 superfamily protein	185.756333

AUR62012981	F-box family protein with a domain of unknown function (DUF295)	185.214942
AUR62031432	DNA primases	184.914237
AUR62019749	NA	184.900373

Cluster 6		
Gene	**Gene name**	**Hub value**
AUR62022980	NA	96.0129896
AUR62012084	O-Glycosyl hydrolases family 17 protein	94.4861143
AUR62031459	plastidic pyruvate kinase beta subunit 1	92.9469409
AUR62021072	plastidic pyruvate kinase beta subunit 1	88.7896592
AUR62011956	Pyruvate kinase family protein	87.9668036
AUR62019729	Pentatricopeptide repeat (PPR) superfamily protein	85.7032516
AUR62040443	Peroxidase superfamily protein	85.18012
AUR62013592	Cupredoxin superfamily protein	82.9412707
AUR62004735	AMP-dependent synthetase and ligase family protein	82.4527464
AUR62039336	branched-chain amino acid transaminase 2	82.0740041
AUR62004370	cytochrome P450, family 86, subfamily A, polypeptide 8	80.6386706
AUR62008698	glycosyl hydrolase 9B13	80.4477227
AUR62032269	Pyruvate kinase family protein	80.0805582
AUR62036616	NOD26-like intrinsic protein 1	78.5685312
AUR62030661	Ran BP2/NZF zinc finger-like superfamily protein	76.9977239
AUR62023157	Pollen Ole e 1 allergen and extensin family protein	76.3067588
AUR62035287	Eukaryotic aspartyl protease family protein	75.4657693
AUR62019741	Pectin lyase-like superfamily protein	75.3099
AUR62013804	Fatty acid hydroxylase superfamily	74.7634651
AUR62008354	Major facilitator superfamily protein	74.0028996
AUR62027133	flavin-dependent monooxygenase 1	73.970357
AUR62019035	Eukaryotic aspartyl protease family protein	73.6527445
AUR62024886	Ran BP2/NZF zinc finger-like superfamily protein	72.1266238
AUR62018699	NAD(P)-binding Rossmann-fold superfamily protein	71.4390166
AUR62013916	cinnamyl alcohol dehydrogenase 9	71.3637281
AUR62032862	phosphofructokinase 2	70.933529
AUR62005587	NA	70.7894951
AUR62014373	Leucine-rich repeat protein kinase family protein	70.2922422
AUR62001922	ralf-like 34	69.8486799
AUR62016985	CBS domain-containing protein	69.3661421
AUR62019203	Leucine-rich repeat protein kinase family protein	69.314386
AUR62031122	GDSL-like Lipase/Acylhydrolase superfamily protein	69.0836261
AUR62012111	FIZZY-related 3	68.3225646

AUR62016408	NA	68.1571105
AUR62014916	GDSL-like Lipase/Acylhydrolase superfamily protein	68.0580262
AUR62005085	Protein kinase superfamily protein	67.4091327
AUR62010271	CYCLIN D3	67.0275373
AUR62006769	Protein of unknown function, DUF538	66.8119637
AUR62018025	Glucose-methanol-choline (GMC) oxidoreductase family protein	66.7788626
AUR62009524	basic helix-loop-helix (bHLH) DNA-binding superfamily protein	66.7240896
AUR62030754	SEC14 cytosolic factor family protein / phosphoglyceride transfer family protein	66.4802317
AUR62005188	NAD(P)-binding Rossmann-fold superfamily protein	66.2570117
AUR62014915	GDSL-like Lipase/Acylhydrolase superfamily protein	66.2122685
AUR62044065	TRICHOME BIREFRINGENCE-LIKE 22	65.3960774
AUR62037683	Peroxidase superfamily protein	65.1024465
AUR62031165	Tetratricopeptide repeat (TPR)-like superfamily protein	65.0102033
AUR62030534	inflorescence meristem receptor-like kinase 2	64.8762229
AUR62009985	SKU5 similar 5	64.3873442
AUR62022579	cytochrome P450, family 86, subfamily A, polypeptide 8	63.8521164
AUR62043823	O-acyltransferase (WSD1-like) family protein	63.8120558
AUR62009075	Leucine-rich receptor-like protein kinase family protein	63.6848433
AUR62013251	CYCLIN D3	63.2581576
AUR62031256	N-MYC downregulated-like 1	63.1662052
AUR62024646	Calcium-dependent phosphotriesterase superfamily protein	63.0855539
AUR62010799	cytokinin response factor 2	63.0018551
AUR62020828	Carbohydrate-binding X8 domain superfamily protein	62.971615
AUR62030761	inflorescence meristem receptor-like kinase 2	62.8432821
AUR62007346	homeobox-7	62.7158436
AUR62005226	alpha/beta-Hydrolases superfamily protein	62.6086197
AUR62023452	Eukaryotic aspartyl protease family protein	62.4073748
AUR62011593	Phototropic-responsive NPH3 family protein	62.012859
AUR62017604	protodermal factor 1	60.975632
AUR62006329	3-ketoacyl-CoA synthase 2	60.9320806
AUR62004206	Leucine-rich repeat protein kinase family protein	60.263879
AUR62006288	methyltransferases	60.1587322
AUR62016396	HCO3- transporter family	60.055251
AUR62001029	Duplicated homeodomain-like superfamily protein	60.0171051
AUR62009085	S-adenosyl-L-methionine-dependent methyltransferases superfamily protein	59.7237376
AUR62015148	protodermal factor 1	59.6113814
AUR62037686	Protein of unknown function (DUF1336)	59.4247666

AUR62034437	myb domain protein 16	59.180568
AUR62010732	Pectin lyase-like superfamily protein	59.0604224
AUR62001378	TRICHOME BIREFRINGENCE-LIKE 22	58.9783024
AUR62023314	3-ketoacyl-CoA synthase 6	58.9663598
AUR62041628	3-ketoacyl-CoA synthase 19	58.9487917
AUR62009951	Subtilase family protein	58.9117567
AUR62024768	Peroxidase superfamily protein	58.2807345
AUR62024606	AMP-dependent synthetase and ligase family protein	58.2736755
AUR62007350	Tyrosine transaminase family protein	58.2590946
AUR62016986	Cystathionine beta-synthase (CBS) family protein	58.1145836
AUR62017218	UDP-Glycosyltransferase superfamily protein	57.9997853
AUR62011760	AMP-dependent synthetase and ligase family protein	57.8826121

Supplemental Table 3.2. F2 seedlings hub genes by cluster/node

Cluster 1		
Gene	**Gene name**	**Hub value**
AUR62013546	NA	49.5120841
AUR62027104	nicotinamidase 1	49.2186442
AUR62010618	osmotin 34	48.5192858
AUR62032930	NA	47.6004535
AUR62003224	Chitinase family protein	47.4145452
AUR62017980	oxophytodienoate-reductase 3	46.7569518
AUR62012927	hydroxyproline-rich glycoprotein family protein	46.6203248
AUR62019916	Protein of unknown function, DUF538	46.4053021
AUR62004263	2-oxoglutarate (2OG) and Fe(II)-dependent oxygenase superfamily protein	45.8009894
AUR62013545	NA	45.7761141
AUR62026666	Peroxidase superfamily protein	45.0885028
AUR62032222	Serine protease inhibitor, potato inhibitor I-type family protein	44.7453598
AUR62011709	hydroxyproline-rich glycoprotein family protein	44.4762824
AUR62030622	expansin A8	44.4499848
AUR62022989	Peroxidase superfamily protein	44.3588048
AUR62026196	BED zinc finger	43.3643265
AUR62011711	hydroxyproline-rich glycoprotein family protein	43.2319966
AUR62035109	NA	42.9621375
AUR62011708	hydroxyproline-rich glycoprotein family protein	42.3284278
AUR62026662	Peroxidase superfamily protein	42.1287107
AUR62030386	NA	42.1200339
AUR62022987	Peroxidase superfamily protein	42.007464
AUR62021174	PAR1 protein	41.9101698
AUR62012895	NA	41.4725187
AUR62032224	Serine protease inhibitor, potato inhibitor I-type family protein	41.2305388
AUR62009691	Thioredoxin superfamily protein	41.1061715
AUR62043048	gamma vacuolar processing enzyme	40.9637915
AUR62026843	annexin 8	40.8930025
AUR62042693	Pyridoxal phosphate (PLP)-dependent transferases superfamily protein	40.8766567
AUR62037551	RmlC-like cupins superfamily protein	40.3372036
AUR62012921	hydroxyproline-rich glycoprotein family protein	40.329004
AUR62027684	NA	40.2093696
AUR62033055	uridylyltransferase-related	40.175002

AUR62007884	Ribonuclease E inhibitor RraA/Dimethylmenaquinone methyltransferase	40.1485584
AUR62024269	receptor serine/threonine kinase, putative	39.9486853
AUR62043329	Cysteine proteinases superfamily protein	39.9376265
AUR62022990	Peroxidase superfamily protein	39.4755901
AUR62028757	S-locus lectin protein kinase family protein	39.442994

Cluster 2		
Gene	**Gene name**	**Hub value**
AUR62033810	NA	2.70572091
AUR62041726	ENTH/VHS/GAT family protein	2.60998354
AUR62034169	uricase / urate oxidase / nodulin 35, putative	2.50237124
AUR62024234	FUS3-complementing gene 2	2.49661735
AUR62000737	NA	2.42641591
AUR62042143	Tautomerase/MIF superfamily protein	2.40375893
AUR62028811	sucrose transporter 2	2.31701147
AUR62008546	Nuclear transport factor 2 (NTF2) family protein with RNA binding (RRM-RBD-RNP motifs) domain	2.28240237
AUR62009732	Insulinase (Peptidase family M16) family protein	2.27886068
AUR62013063	AGAMOUS-like 24	2.18202663
AUR62010955	RNA-binding protein-related	2.17052978
AUR62016120	PAPA-1-like family protein / zinc finger (HIT type) family protein	2.15572102
AUR62008285	aldehyde dehydrogenase 10A8	2.14839102
AUR62020780	GLN phosphoribosyl pyrophosphate amidotransferase 1	2.13126275
AUR62033322	Cleavage/polyadenylation specificity factor, 25kDa subunit	2.11116179
AUR62022315	nucleolar essential protein-related	2.08476878
AUR62007031	BTB/POZ domain-containing protein	2.06834811
AUR62021167	cleavage and polyadenylation specificity factor 100	2.04656988
AUR62043184	ARM repeat protein interacting with ABF2	2.03031576
AUR62000367	Alpha-1,4-glucan-protein synthase family protein	2.0035052
AUR62041724	Tesmin/TSO1-like CXC domain-containing protein	1.9974031
AUR62016591	early nodulin-like protein 17	1.9697515
AUR62038174	kinase associated protein phosphatase	1.96759202
AUR62012452	aspartate aminotransferase 5	1.95667536
AUR62019657	trehalose-6-phosphatase synthase S4	1.94509933
AUR62003056	Prolyl oligopeptidase family protein	1.94059608
AUR62007903	Protein kinase superfamily protein	1.93807508
AUR62001472	cell division cycle 48C	1.92741362
AUR62004721	Pyridoxal phosphate (PLP)-dependent transferases superfamily protein	1.92056343

AUR62021290	DEAD box RNA helicase (PRH75)	1.91129468
AUR62040577	RNA-binding KH domain-containing protein	1.90312665
AUR62019432	proton pump interactor 1	1.89490561
AUR62040704	Tetratricopeptide repeat (TPR)-like superfamily protein	1.89429405

Cluster 3		
Gene	**Gene name**	**Hub value**
AUR62025983	NA	194.976725
AUR62035443	Plant protein of unknown function (DUF869)	191.918039
AUR62007473	Cupredoxin superfamily protein	191.121284
AUR62035737	Plant protein of unknown function (DUF869)	189.640319
AUR62028407	Fatty acid hydroxylase superfamily	189.178374
AUR62010539	Leucine-rich repeat protein kinase family protein	185.727679
AUR62033578	GATA transcription factor 2	185.157648
AUR62016340	fatty acid desaturase 5	184.950578
AUR62024388	NA	183.777821
AUR62026367	3-ketoacyl-CoA synthase 2	181.895051
AUR62031392	HXXXD-type acyl-transferase family protein	181.562907
AUR62021236	BCL-2-associated athanogene 1	181.508536
AUR62017306	Glucose-methanol-choline (GMC) oxidoreductase family protein	180.193398
AUR62004492	O-acyltransferase (WSD1-like) family protein	176.454809
AUR62031798	cytochrome B5 isoform B	176.356078
AUR62039755	Fatty acid hydroxylase superfamily	176.1808
AUR62040563	Plant invertase/pectin methylesterase inhibitor superfamily	171.924866
AUR62003919	Leucine-rich repeat protein kinase family protein	170.483711
AUR62015742	fatty acid desaturase A	169.012698
AUR62027284	cytochrome P450, family 706, subfamily A, polypeptide 6	168.975764
AUR62013344	Tetratricopeptide repeat (TPR)-like superfamily protein	168.838902
AUR62006329	3-ketoacyl-CoA synthase 2	168.641926
AUR62012469	aldehyde dehydrogenase 11A3	167.976718
AUR62030688	FASCICLIN-like arabinogalactan protein 17 precursor	167.402556
AUR62017356	Leucine-rich repeat protein kinase family protein	165.90713
AUR62024414	guanylate kinase	165.382865
AUR62008944	TRICHOME BIREFRINGENCE-LIKE 19	165.075161
AUR62017380	sterol-4alpha-methyl oxidase 1-1	164.292084
AUR62007784	Adenosylmethionine decarboxylase family protein	164.0945
AUR62017639	Ribosomal protein L12/ ATP-dependent Clp protease adaptor protein ClpS family protein	163.534394
AUR62034226	Protein of unknown function (DUF1218)	163.288758

AUR62003262	Protein of unknown function (DUF3550/UPF0682)	163.005773
AUR62028522	alpha carbonic anhydrase 1	162.221642
AUR62012958	SAUR-like auxin-responsive protein family	160.588158
AUR62008652	multidrug resistance-associated protein 4	159.149893
AUR62011606	AUX/IAA transcriptional regulator family protein	158.998468
AUR62011829	Heat shock protein DnaJ with tetratricopeptide repeat	158.648897
AUR62018527	xyloglucan endotransglucosylase/hydrolase 24	158.575854
AUR62006188	alpha carbonic anhydrase 1	158.538358
AUR62024768	Peroxidase superfamily protein	158.230332
AUR62008994	ribulose bisphosphate carboxylase small chain 1A	158.186205
AUR62031871	delta tonoplast integral protein	156.472014
AUR62039931	Cupredoxin superfamily protein	156.071037
AUR62021145	HXXXD-type acyl-transferase family protein	155.294281
AUR62008651	multidrug resistance-associated protein 4	155.015636
AUR62026008	guanylate kinase	154.479588
AUR62014351	HXXXD-type acyl-transferase family protein	153.265486
AUR62015615	protein kinase family protein	153.193386
AUR62022614	Heavy metal transport/detoxification superfamily protein	153.033722
AUR62028725	NA	152.732858
AUR62036437	NOD26-like intrinsic protein 6	151.389066
AUR62021436	Integrase-type DNA-binding superfamily protein	151.323509
AUR62016031	BCL-2-associated athanogene 1	151.101468
AUR62018699	NAD(P)-binding Rossmann-fold superfamily protein	150.433726
AUR62042913	Homeodomain-like superfamily protein	149.971841
AUR62012467	ARM repeat superfamily protein	149.298568
AUR62040217	phosphofructokinase 3	149.180539
AUR62012266	Plant protein of unknown function (DUF828)	148.81943
AUR62019193	Bifunctional inhibitor/lipid-transfer protein/seed storage 2S albumin superfamily protein	148.79114
AUR62026374	Arabidopsis protein of unknown function (DUF241)	148.692303
AUR62041421	GATA transcription factor 4	148.299511
AUR62011555	aspartate-glutamate racemase family	146.437455
AUR62010960	2Fe-2S ferredoxin-like superfamily protein	145.386164
AUR62031968	Sec14p-like phosphatidylinositol transfer family protein	144.907426
AUR62022604	Protein kinase superfamily protein	144.752894
AUR62001922	ralf-like 34	144.649898
AUR62023631	camphor resistance CrcB family protein	144.627523
AUR62027241	homolog of Synechocystis YCF37	144.298501
AUR62036073	alpha/beta-Hydrolases superfamily protein	144.278922

Cluster 4		
Gene	**Gene name**	**Hub value**
AUR62041900	Chaperone DnaJ-domain superfamily protein	629.546436
AUR62028735	P-loop containing nucleoside triphosphate hydrolases superfamily protein	625.28702
AUR62014851	dormancy-associated protein-like 1	617.189564
AUR62035012	Chaperone DnaJ-domain superfamily protein	615.564246
AUR62014500	NA	615.199327
AUR62008758	fatty alcohol oxidase 3	614.329471
AUR62037354	RING membrane-anchor 3	613.613031
AUR62022969	PLAC8 family protein	613.204779
AUR62014815	RING membrane-anchor 3	611.184096
AUR62014799	RING/U-box superfamily protein	611.12978
AUR62038512	Chaperone DnaJ-domain superfamily protein	610.790444
AUR62035905	NA	610.221319
AUR62005995	pseudo-response regulator 5	610.109534
AUR62012224	Tetratricopeptide repeat (TPR)-like superfamily protein	608.389841
AUR62007131	nudix hydrolase homolog 8	608.030009
AUR62003482	peptide transporter 2	607.834283
AUR62039752	Plant protein of unknown function (DUF828) with plant pleckstrin homology-like region	607.293111
AUR62000775	respiratory burst oxidase homologue D	606.806957
AUR62002054	Transmembrane amino acid transporter family protein	603.346792
AUR62022816	heat shock protein 18.2	602.522466
AUR62012644	Ankyrin repeat family protein	601.939118
AUR62022856	Tetratricopeptide repeat (TPR)-like superfamily protein	601.008416
AUR62008153	ferric reduction oxidase 8	601.002159
AUR62034587	transducin family protein / WD-40 repeat family protein	597.956141
AUR62015522	Plant invertase/pectin methylesterase inhibitor superfamily protein	597.119451
AUR62039163	NA	596.970234
AUR62040592	NA	596.41463
AUR62022643	Chaperone DnaJ-domain superfamily protein	595.003816
AUR62023797	RING/FYVE/PHD zinc finger superfamily protein	593.065286
AUR62029843	Chaperone DnaJ-domain superfamily protein	591.602111
AUR62018628	Protein of unknown function (DUF760)	590.079254
AUR62030391	dehydration-induced protein (ERD15)	589.815319
AUR62028076	pseudo-response regulator 9	588.959605
AUR62014208	Chaperone DnaJ-domain superfamily protein	588.325446
AUR62011256	Protein kinase superfamily protein with octicosapeptide/Phox/Bem1p domain	587.403524

AUR62016990	RING/U-box superfamily protein	586.47329
AUR62021940	Ubiquitin-like superfamily protein	586.034563
AUR62017046	dormancy-associated protein-like 1	585.873963
AUR62020768	GTP binding Elongation factor Tu family protein	585.850844
AUR62023140	DNA/RNA polymerases superfamily protein	585.778973
AUR62009459	DNA/RNA polymerases superfamily protein	584.904819
AUR62005849	NA	583.414826
AUR62016137	beta-xylosidase 1	582.820389
AUR62016338	post-illumination chlorophyll fluorescence increase	582.586201
AUR62008459	CCT motif -containing response regulator protein	582.296802
AUR62016649	maternal effect embryo arrest 14	582.051591
AUR62000707	Chaperone DnaJ-domain superfamily protein	581.249794
AUR62039573	cytochrome P450, family 72, subfamily A, polypeptide 15	580.705269
AUR62030165	dual specificity protein phosphatase (DsPTP1) family protein	579.594799
AUR62011318	cold, circadian rhythm, and rna binding 2	579.06944
AUR62006354	saposin B domain-containing protein	577.924979
AUR62018881	nudix hydrolase homolog 8	577.489351
AUR62025919	RNA-metabolising metallo-beta-lactamase family protein	575.835379
AUR62007194	Histone H3 K4-specific methyltransferase SET7/9 family protein	575.181438
AUR62038210	Eukaryotic aspartyl protease family protein	574.944323
AUR62011410	maternal effect embryo arrest 14	574.743053
AUR62029272	Uncharacterised conserved protein (UCP012943)	574.717952
AUR62028193	heat shock factor 3	574.516473
AUR62016007	Sugar isomerase (SIS) family protein	574.375867
AUR62040207	Zinc finger C-x8-C-x5-C-x3-H type family protein	574.215227
AUR62021770	winged-helix DNA-binding transcription factor family protein	573.724581
AUR62011317	cold, circadian rhythm, and rna binding 2	573.710515
AUR62031371	Xanthine/uracil permease family protein	572.895644
AUR62015155	putative mitochondrial RNA helicase 2	572.720716
AUR62041089	B-box type zinc finger protein with CCT domain	571.12261
AUR62034529	ubiquitin-conjugating enzyme 16	571.117122
AUR62036592	maternal effect embryo arrest 18	571.065127
AUR62003959	transducin family protein / WD-40 repeat family protein	570.938651
AUR62014542	vacuolar protein sorting 46.1	570.573421
AUR62034550	Papain family cysteine protease	570.51529
AUR62017167	Chaperone DnaJ-domain superfamily protein	570.178126
AUR62002189	Plant invertase/pectin methylesterase inhibitor superfamily protein	568.411587

AUR62034188	Duplicated homeodomain-like superfamily protein	568.333903
AUR62020001	serine-rich protein-related	567.169601
AUR62004966	Major facilitator superfamily protein	567.082821
AUR62000151	NA	566.878793
AUR62025872	Chaperone DnaJ-domain superfamily protein	566.771517
AUR62039518	phosphoglucomutase, putative / glucose phosphomutase, putative	566.254992
AUR62037900	Pyruvate kinase family protein	566.193129
AUR62037997	NA	566.040139
AUR62012312	Integrase-type DNA-binding superfamily protein	565.850749
AUR62025376	heptahelical transmembrane protein2	565.849859
AUR62025755	BTB and TAZ domain protein 2	565.441093
AUR62000615	Transmembrane CLPTM1 family protein	565.432192
AUR62019985	myb-like transcription factor family protein	563.985795
AUR62028375	heptahelical transmembrane protein2	563.859387
AUR62020594	NA	563.778608
AUR62011520	post-illumination chlorophyll fluorescence increase	563.315813
AUR62001704	maternal effect embryo arrest 59	563.111369
AUR62043049	alpha-vacuolar processing enzyme	562.072922
AUR62031317	homolog of carrot EP3-3 chitinase	561.949259
AUR62008796	Tetratricopeptide repeat (TPR)-like superfamily protein	561.832531
AUR62030961	similar to RCD one 5	561.45343
AUR62009210	Zinc finger C-x8-C-x5-C-x3-H type family protein	561.331386
AUR62028994	RING/U-box superfamily protein	560.951112
AUR62018607	DEA(D/H)-box RNA helicase family protein	560.720789
AUR62005023	NA	560.164186
AUR62032842	NA	560.031834
AUR62013032	farnesylated protein 6	559.815822
AUR62000533	NA	559.565114

Cluster 5		
Gene	**Gene name**	**Hub gene**
AUR62009392	Eukaryotic aspartyl protease family protein	160.261828
AUR62038135	photosystem I subunit K	159.380446
AUR62003816	Haloacid dehalogenase-like hydrolase (HAD) superfamily protein	159.310796
AUR62019079	Chlorophyll A-B binding family protein	157.379858
AUR62012710	ATPase, F1 complex, gamma subunit protein	155.472368
AUR62040382	glutamine synthetase 2	155.004006
AUR62000167	ALBINA 1	154.405879

AUR62036998	NA	154.290994
AUR62020866	photosystem I subunit G	153.907227
AUR62001988	Haloacid dehalogenase-like hydrolase (HAD) superfamily protein	153.316994
AUR62040093	cytochrome b6f complex subunit (petM), putative	153.179141
AUR62034754	DegP protease 1	152.652981
AUR62032252	photosystem II reaction center W	151.560632
AUR62018125	Domain of unknown function (DUF3598)	150.12097
AUR62006623	2-phosphoglycolate phosphatase 1	149.905637
AUR62020038	Major facilitator superfamily protein	149.605121
AUR62001263	Haloacid dehalogenase-like hydrolase (HAD) superfamily protein	149.245066
AUR62023074	Eukaryotic aspartyl protease family protein	149.221593
AUR62039178	phosphoglycerate kinase 1	148.659421
AUR62000821	Metallopeptidase M24 family protein	148.305118
AUR62011936	photosystem II reaction center W	147.203822
AUR62040205	photosystem I light harvesting complex gene 2	145.191898
AUR62011361	cytochrome c biogenesis protein family	145.151739
AUR62022613	light harvesting complex of photosystem II 5	144.564656
AUR62025395	photosystem I subunit E-2	144.425169
AUR62016621	presequence protease 1	144.388161
AUR62039844	ALBINA 1	144.308558
AUR62000636	NA	143.347337
AUR62012328	Glycine cleavage T-protein family	143.296153
AUR62012478	WRKY DNA-binding protein 40	143.155987
AUR62035170	Photosystem II reaction center PsbP family protein	142.36498
AUR62025747	Haloacid dehalogenase-like hydrolase (HAD) superfamily protein	141.911361

Cluster 6		
Gene	**Gene name**	**Hub value**
AUR62008409	glutathione S-transferase tau 9	12.6662401
AUR62014490	Cyclin family protein	12.574186
AUR62028078	chitinase A	12.4807282
AUR62040773	26S proteasome regulatory complex, non-ATPase subcomplex, Rpn2/Psmd1 subunit	12.2086859
AUR62014350	P450 reductase 1	12.0081095
AUR62036165	PLANT CADMIUM RESISTANCE 2	11.7253524
AUR62023223	Malectin/receptor-like protein kinase family protein	11.5801779
AUR62014205	FORMS APLOID AND BINUCLEATE CELLS 1C	11.2467071

AUR62029315	ARF-GAP domain 5	11.1704079
AUR62011537	Peptidase S24/S26A/S26B/S26C family protein	10.9848842
AUR62013997	Eukaryotic aspartyl protease family protein	10.9639159
AUR62013173	Calcium-binding EF hand family protein	10.9104528
AUR62010799	cytokinin response factor 2	10.8881825
AUR62037869	sodium/calcium exchanger family protein / calcium-binding EF hand family protein	10.8746753
AUR62042620	Beta-glucosidase, GBA2 type family protein	10.4394662
AUR62039203	proton pump interactor 1	10.3148204
AUR62031605	Actin-binding FH2 (Formin Homology) protein	10.2886502
AUR62016868	HXXXD-type acyl-transferase family protein	10.2290085
AUR62012443	NA	10.1462452
AUR62008109	XH/XS domain-containing protein	9.96199098
AUR62031136	IQ-domain 9	9.93610816
AUR62014737	Protein of unknown function (DUF300)	9.85533748
AUR62010265	Leucine-rich repeat (LRR) family protein	9.76228078
AUR62010745	Heavy metal transport/detoxification superfamily protein	9.62665063
AUR62038098	chloride channel D	9.61318056
AUR62018537	Tetratricopeptide repeat (TPR)-like superfamily protein	9.56326985
AUR62000168	DNA binding	9.53342734
AUR62025311	HEAT/U-box domain-containing protein	9.44501286
AUR62023112	pheophytinase	9.4381657
AUR62043650	amino acid permease 8	9.43131853

Supplemental Table 3.3. List of shared DE genes between F1 and F2 seedlings.

Shared genes F1 and F2
Pentatricopeptide repeat (PPR) superfamily protein
Protein kinase superfamily protein
E2F transcription factor 3
Quinone reductase family protein
Pseudouridine synthase family protein
ATP binding nucleic acid binding helicases
S-adenosyl-L-methionine-dependent methyltransferases superfamily protein
smr (Small MutS Related) domain-containing protein
Tetratricopeptide repeat (TPR)-like superfamily protein
Ribonuclease E inhibitor RraA/Dimethylmenaquinone methyltransferase
SAUR-like auxin-responsive protein family
xylem cysteine peptidase 2
FAR1-related sequence 5
C-8,7 sterol isomerase
Actin-like ATPase superfamily protein
dihydroflavonol 4-reductase-like1
AMP-dependent synthetase and ligase family protein
high chlorophyll fluorescent 107
actin-related protein 9
AUR62016297
Galactose oxidase/kelch repeat superfamily protein
AUR62017404
Restriction endonuclease, type II-like superfamily protein

AUR62020559
AUR62020560
AUR62020564
NB-ARC domain-containing disease resistance protein
N-MYC downregulated-like 1
PYR1-like 2
Auxin efflux carrier family protein
zinc finger (C2H2 type, AN1-like) family protein
DNA-binding bromodomain-containing protein
Calcium-dependent protein kinase (CDPK) family protein
protein kinase family protein
cyclic nucleotide-gated channel 18
carboxypeptidase D, putative
Ubiquitin-specific protease family C19-related protein
ATP binding cassette subfamily B4
AGC (cAMP-dependent, cGMP-dependent and protein kinase C) kinase family protein
GRAS family transcription factor
glutamate receptor 2.1
nitrate transporter 1.1
DNAse I-like superfamily protein
methyltransferases
D-arabinono-1,4-lactone oxidase family protein
Glycosyl hydrolases family 32 protein
Haloacid dehalogenase-like hydrolase (HAD) superfamily protein

GENERAL DISCUSSION

Inheritance of Stress Memory in Quinoa

Diverse studies have demonstrated that plants can transmit information about environmental conditions to their offspring, a phenomenon called "stress memory" that might confer adaptative advantages under similar stress conditions in future generations (Herman and Sultan, 2011; Rasmann et al., 2012; Kambona et al., 2023; Pissolato et al., 2024). In this work we studied transmission of memory in the offspring of *Chenopodium quinoa* plants exposed to N deficit. In this work we used the concept of stress memory suggested by Lämke and Bäurle (2017) and Pissolato et al. (2024). *C. quinoa*, a species renowned for its resistance to abiotic stress, may exhibit enhanced N-use efficiency. Mother plants of quinoa exposed to LN exhibited a reduced yield and lower Pn and gs, along with an increased NPQ. These changes suggest that under N-deficit, maternal plants (F0) shifts their metabolism from carbon fixation to photoprotection and nutrient remobilization (Castro

et al., 2024; Bascuñan-Godoy et al., 2018). This was reflected in the biochemical and metabolic remodeling of seeds derived from LN mother plants, with lower nitrate and amino acids but higher starch, sugars and lipids (like PE, PI 34:2). These are known to play roles in osmoprotection and energy supply during germination under stress (Kou et al., 2011). These findings suggest that the maternal N stress changes the compounds of seeds, and these shifts can influence the germination time, accelerating the germination of LN seeds. This could be an important trait in competitive environments like N deficiency, leaving a metabolic imprint in the seeds that can act as an anticipatory signal to future environments (Lemaitre et al., 2008; Hou et al., 2012).

Influence of maternal environment on first generation offspring (F1) development

Seedlings from LN mothers showed an enhanced growth compared to seedlings descendants of HN mother plants, as evidenced by grater biomass, longer primary roots, and higher number of root tips. The increased root

biomass and modified root architecture observed in seedlings are indicative of strategic developmental adjustments aimed at optimizing nutrient acquisition. Together with the higher gs in $LN_{F0}LN_{F1}$ seedlings, root traits correlated strongly with higher starch and TSS (carbohydrate reserves). The higher gs in these seedlings could be related to a diminution of the synthesis (through nitrate reductase) of nitric oxide (NO), which induces stomatal closure, due to a low availability of the precursor (NO_3^-) (Neill et al., 2003; Neill et al., 2008). This could lead to an increase in carbon fixation (thus TSS and starch production) to sustain plant growth under limiting N conditions, (Huertas et al., 2024; Prescott et al., 2020). Our results show that the offspring can alter both metabolism and growth (and architecture) to increase carbon and N acquisition anticipating the stressful environmental conditions

Additionally to de accumulation of protective metabolites, daughter seedlings of stressed mothers are able to upregulate genes linked to carbohydrate metabolism (*GAD*), lipid remodeling, stress signaling (*WAK2*, *PIN7*) and N assimilation (*NRT1.1*, *PK*s) (Alavilli et al., 2017; Jaimes-Miranda and Chávez, 2020). These findings revealed physiological changes

are related to a transcriptional reprogramming initiated in mother plants, to optimize N use and stress tolerance in the offspring (Herman and Sultan, 2011).

These findings provide evidence that the maternal N environment critically shapes the expression of genes, metabolic profiles and growth physiology of offspring in *C. quinoa*. These adjustments highlight the plant's capacity to use environmental cues from previous generations to anticipate and prepare for similar challenges to its descendance.

Persistence of stress responses into second generation offspring (F2)

In the second generation (F2), similar physiological and biochemical traits were observed, suggesting the persistence of a stress memory beyond the first generation.

The metabolomic analysis shows that F2 seedlings maintain higher levels of metabolites associated with N-stress response compared to F1, including amino acids, sugars and secondary metabolites that are crucial to energy storage, osmotic adjustment and stress defense (Heman and Sultan, 2011). This suggests that there is an enhanced metabolomic adaptation, potentially facilitating a better grown and survival under N deficiency (Castro et al., 2024, Herman and Sultan, 2011). It also highlighted an improvement in photosynthesis and chlorophyll *a* parameters in F2 seedlings, a lower NPQ and a slightly elevated qL under stress conditions. These traits indicate a more efficient energy management and photoprotective mechanism of plants that its ancestor grown at LN conditions. These responses are also related to an up-regulation of genes related to photosynthesis, electron transport and energy production in descendants of stress mothers (F0). These enhancements suggest that F2 plants are not only absorbing and utilizing N more effectively but are also optimizing light energy conversion under stress. This strategy is crucial for maintaining growth and productivity as seen in plants with reduced chlorophyll content (Sperdouli et al., 2024; Moustakas et al., 2022; Wang et al., 2022; Sahay et al., 2024). While NPQ increased in mother plants at LN conditions, a reduction in NPQ was observed in daughter

and granddaughter seedlings derived from LN-treated mothers when grown at LN, suggesting a transgenerational acclimation that reduced the need for thermal energy dissipation (Müller et al., 2001; Bascuñan-Godoy et al., 2018a). This may be attributed to the reduced N and protein accumulation in chloroplasts, which limits the energy absorbed by the reaction centers (Cisse et al., 2020). Consistent with this, an upregulation of genes associated with electron transport (*Cupredoxin*) and to light-harvesting complexes (*Photosystem 1 subunit K*) under sustained N deficiency across generations (Sahay et al., 2024), indicate a capacity for anticipatory acclimation through modulation of energy acquisition pathways. The increased store of different antioxidant compounds like flavonoids and terpenes, and other metabolites related to N remobilization in LN_{F2}, shows an improved capacity to mitigate oxidative stress caused by nutrient deficiency without depending as much in heat dissipation, compared to HN descendants.

Transcriptomic analysis revealed 222 DEGs influenced more by F0 N status than by current N conditions, with 47 genes shared between F1 and F2 generations. Key clusters in F2 showed regulation of genes involved in

photosynthesis, structural development, detoxification, and hormonal balance (Zhao et al., 2024; Hernández and Rodríguez, 2020). Further, we observed upregulation of genes related to maintain metabolic processes and electron transport in LN environments in descendants of LN_{F0}. This indicates a transgenerational stress memory mechanism where sustained maternal stress alters the transcriptional baseline of descendants, enabling plastic responses to fluctuating environments (Li et al., 2022).

We found two genes that were upregulated in the offspring of LN_{F0} that also form part of the regulatory genes in both generations. *Cytokinin response factor* (*CRF*s) is a transcription factor that responds to oxidative stress, increasing the antioxidant capacity of the plant. Also, they are important in proper embryo development, critical to the formation of the next generation (Shi et al., 2013; Hallmark and Rashotte, 2019; Gentile et al., 2024). Its upregulation in seedlings exposed to persistent LN across generations ($LN_{F0}LN_{F1}$ and $LN_{F0}LN_{F1}LN_{F2}$ seedlings) indicate the need to have a normal reproductive development to properly form the next generation. *WRKY* transcription factors on the other hand were upregulated in seedlings

descendants of LN_{F0}, when F1 was grown at HN ($LN_{F0}HN_{F1}$ and $LN_{F0}HN_{F1}LN_{F2}$ seedlings). This transcription factor has been found to be upregulated in N-stress to enhance N uptake, contributing to plant memory and regulating the expression of its target genes upon repeated stress (Bakshi and Oelmüller, 2014; Nguyen et al., 2022; Zhao et al. 2024). As seen by Li et al. (2022), if the gene expression of some genes is maintained in offspring even when grown at optimal conditions, then those genes were potentially related to transgenerational memory. These two genes, highly important in stress responses, and their maintenance through both offspring generations suggest that there is a transference of stress memory to the offspring.

These results demonstrate that quinoa not only inherit but also amplify the beneficial adaptations to N deficiency across two generations. These adaptations manifest through shifts in metabolic profiles, physiological growth traits and biochemical markers, contributing to the overall resistance of the plant. The increased efficiency in N assimilation suggests that the stress memory effects may be accumulated in successive generations, supposing a

rapid evolutionary mechanism where plants exposed to consistent environmental stressors could exhibit increasing resistance.

Integrating physiology, metabolic and molecular insights into transgenerational memory

Our genetic and physiological findings studied in Chapters 1, 2 and 3, provided a more comprehensive understanding of how *C. quinoa* manages to sustain enhanced performance under N-deficient conditions across generations. The close relation between the upregulated genes and the enhanced root architecture and biomass observed in F1 and F2 generations suggests that these genetic changes are directly contributing to the phenotypic traits associated with improved N efficiency and stress adaptation.

Chapter 1 establishes the foundation that maternal N conditions alter seed metabolism and growth physiology of F1 generation, crucial for the plant's immediate response to environmental stress and priming for long-term

adaptations. Chapter 2 demonstrates that the physiological traits not only persist into F2 generations but also appear to be amplified, suggesting a cumulative effect of the stress memory, in which each generation further optimizes the physiological response based on inherited stress memory. Finally, chapter 3 provides the molecular insights necessary to understand the genetic basis of these observed physiological changes.

The metabolic adjustments noted in Chapter 1, such as changes in metabolite profiles in seeds from N stressed plants, are likely to prepare the seedlings for enhanced survival under similar conditions. These metabolic changes correlate with the genetic findings in Chapter 3, where genes involved in metabolite processing and stress response are upregulated in descendants of stress mothers. This suggests that the metabolic pre-conditioning observed in seeds may be driven by genetic alterations that prime the seedlings at a molecular level, for a more efficient response to environmental stress. Moreover, the genetic data from Chapter 3 not only explains the metabolic and physiological adaptations but also provides a deeper understanding of how these adaptive responses are maintained and amplified across

generations, supporting the notion of a genetically encoded memory that influences both immediate and long-term responses to nitrogen deficiency.

Integrating these findings, the thesis illustrates a complex interplay that together facilitates a transgenerational memory of nitrogen stress in quinoa (Fig. 1). The consistency of adaptive traits across generations underscores the potential for maternal environmental conditions to prime offspring for enhanced performance. Moreover, the amplification of these traits in successive generations suggests an adaptive mechanism that may allow *C. quinoa* to progressively adjust to recurring environmental challenges over the time.

Expanding on the genetic aspects of transgenerational memory could yield valuable insights. Future research should delve deeper into the epigenetic mechanisms that may underpin stress memory, such as DNA methylation patterns, histone modifications, and RNA-mediated processes. Identifying specific epigenetic markers associated with stress memory could facilitate the development of breeding strategies that harness these natural adaptations.

In conclusion, this thesis demonstrates that *Chenopodium quinoa* possess the ability to inherit a stress memory according to Bruce et al. (2007) across generations which manifests through various beneficial adaptations to N availability. These findings not only add to our understanding of plant adaptive mechanisms but also suggest practical approaches to enhancing crop resilience and productivity under poor soils environments. The insights gained from this study pave the way for further research into the genetic and epigenetic mechanisms underlying transgenerational stress memory, offering promising prospects for sustainable agriculture.

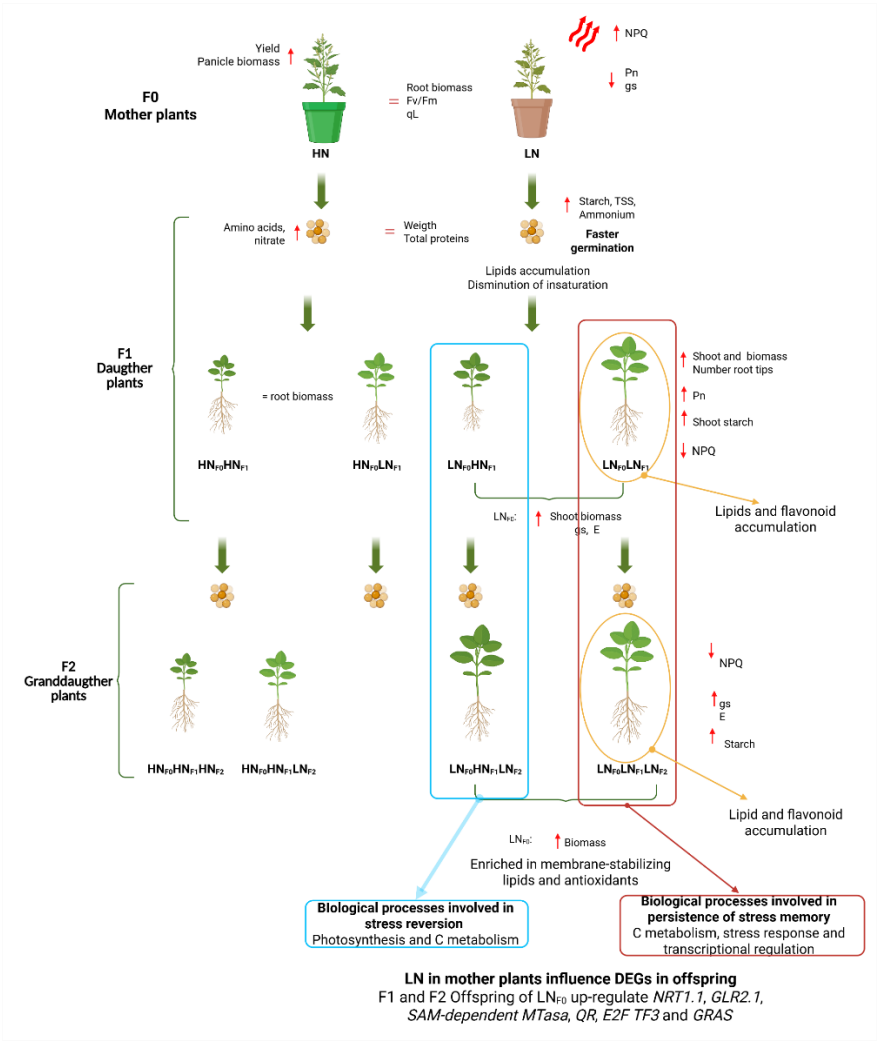

Figure 4.1. Overview of the responses associated with the inheritance of stress memory by N deficiency in *C. quinoa*. In F0 generation, clear physiological differences were observed between plants grown under optimal N (HN) conditions and those exposed to N deficiency (LN). LN_{F0} plants showed higher heat dissipation and a decrease in photosynthesis and stomatal conductance. Seeds from plants subjected to HN and LN showed changes in the accumulation of lipids, starch and soluble sugars. Seeds from plants exposed for the first time to LN (LN_{F0} and $HN_{F0}LN_{F1}$ seeds) showed a faster germination. Seedlings of F1 and F2 generation ($LN_{F0}LN_{F1}$ and $LN_{F0}LN_{F1}LN_{F2}$), exhibit increased growth, higher stomatal conductance and reduced heat dissipation. Amino acid level was similar among seedlings growing at LN, but an elevated accumulation of starch, lipids and flavonoids was observed in LN descendants. Within both generations F1 and F2 an increased expression of genes related to N acquisition and DNA methylation was highlighted.

REFERENCES

Abugoch, L. (2009). Quinoa (Chenopodium quinoa Willd.): Composition, Chemistry, Nutritional, and Functional Properties. In *Advances in Food and Nutrition Research* (Vol. 58, pp. 1–31). Elsevier. https://doi.org/10.1016/S1043-4526(09)58001-1

Alves de Freitas Guedes, F., Menezes-Silva, P.E., DaMatta, F.M. *et al.* Using transcriptomics to assess plant stress memory. *Theor. Exp. Plant Physiol.* **31**, 47–58 (2019). https://doi.org/10.1007/s40626-018-0135-0

Avramova, Z. (2019). Defence-related priming and responses to recurring drought: Two manifestations of plant transcriptional memory mediated by the ABA and JA signalling pathways. *Plant Cell Environ*. 42(3):983-997. doi: 10.1111/pce.13458.

Bakshi, M., and Oelmüller, R. (2014). WRKY transcription factors: Jack of many trades in plants. *Plant Signaling & Behavior*, *9*(2). https://doi.org/10.4161/psb.27700

Bascuñán-Godoy, L., Reguera, M., Abdel-Tawab, Y. M., and Blumwald, E. (2016). Water deficit stress-induced changes in carbon and nitrogen partitioning in Chenopodium quinoa Willd. *Planta*, *243*(3), 591–603. https://doi.org/10.1007/s00425-015-2424-z

Bascuñán-Godoy, L., Sanhueza, C., Hernández, C. E., Cifuentes, L., Pinto, K., Álvarez, R., González-Teuber, M., and Bravo, L. A. (2018a). Nitrogen supply affects photosynthesis and photoprotective attributes during drought-induced senescence in quinoa. *Frontiers in Plant Science*, *9*(July). https://doi.org/10.3389/fpls.2018.00994

Bascuñán-Godoy, L., Sanhueza, C., Pinto, K., Cifuentes, L., Reguera, M., Briones, V., Zurita-silva, A., Álvarez, R., Morales, A., and Silva, H. (2018b). Nitrogen physiology of contrasting genotypes of Chenopodium quinoa Willd. (Amaranthaceae). *Scientific Reports*, 1–12. https://doi.org/10.1038/s41598-018-34656-5

Bazile, D., Martínez, E. A., and Fuentes, F. (2014). Diversity of quinoa in a biogeographical Island: A review of constraints and potential from arid to temperate regions of Chile. *Notulae Botanicae Horti Agrobotanici Cluj-Napoca*, *42*(2), 289–298. https://doi.org/10.1583/nbha4229733

Bazule, D., Bertero, D., and Nieto, C. (2014). Estado del arte de la quinua en el mundo en 2013. In *FAO (Santiago, Chile) CIRAD (Montpellier, France)*. https://doi.org/10.1016/0006-2952(67)90244-4

Bedi, S., Mehta, S., Sharma, S., and Vashist, K. K. (2009). Nitrogen nutrition and efficiency of seed reserve mobilization during germination in winter Maize cv. "Buland." *Journal of New Seeds*, *10*(1), 57–61. https://doi.org/10.1080/15228860802716184

Bendevis, M. A., Sun, Y., Rosenqvist, E., Shabala, S., Liu, F., and Jacobsen, S. E. (2014). Photoperiodic effects on short-pulse 14C assimilation and overall carbon and nitrogen allocation patterns in contrasting quinoa cultivars. *Environmental and Experimental Botany*, *104*, 9–15. https://doi.org/10.1016/j.envexpbot.2014.03.002

Berti, M., Wilckens, R., Hevia, F., Serri, H., Vidal, I., and Méndez, C. (2000). Fertilización Nitrogenada en Quinoa (Chenopodium quinoa Willd). *Ciencia e Investigación Agraria*, *27*(2), 81–90. https://doi.org/10.7764/rcia.v27i2.999

Bewley, J. D. (1997). Seed germination and dormancy. *Plant Cell*, *9*(7), 1055–1066. https://doi.org/10.1105/tpc.9.7.1055

Borisjuk, L., Rolletschek, H., Radchuk, R., Weschke, W., Wobus, U., and Weber, H. (2004). Seed development and differentiation: A role for metabolic regulation. *Plant Biology*, *6*(4), 375–386. https://doi.org/10.1055/s-2004-817908

Brevedan, R. E. (1980). Influencia del Nitrógeno en el aborto de flores y frutos de la soja y en su rendimiento en distintos niveles del canopeo. *Rev. Facultad de Agronomía*, *1*(1), 117–128.

Broncano, M. J., Riba, M., and Retana, J. (1998). Seed germination and seedling performance of two Mediterranean tree species, holm oak (Quercus ilex L.) and Aleppo pine (Pinus halepensis Mill.): A multifactor experimental approach. *Plant Ecology*, *138*(1), 17–26. https://doi.org/10.1023/A:1009784215900

Bruce, T. J. A., Matthes, M. C., Napier, J. A., and Pickett, J. A. (2007). Stressful "memories" of plants: Evidence and possible mechanisms. *Plant Science*, *173*(6), 603–608. https://doi.org/10.1016/j.plantsci.2007.09.002

Burrieza, H. P., López-Fernández, M. P., and Maldonado, S. (2014). Analogous reserve distribution and tissue characteristics in quinoa and grass seeds suggest convergent evolution. *Frontiers in Plant Science*, *5*(OCT), 1–11. https://doi.org/10.3389/fpls.2014.00546

Caliskan, S., and Makineci, E. (2015). Effects of carbon and nitrogen content on seed germination of calabrian pine (Pinus brutia) populations Efectos. *Bosque*, *36*(3), 435–443. https://doi.org/10.4067/S0717-92002015000300010

Caliskan, S., and Makineci, E. (2020). Carbon and nitrogen of seed and some germination parameters at different test temperatures in Anatolian black pine populations. *Journal of Sustainable Forestry*, *39*(1), 23–34. https://doi.org/10.1080/10549811.2019.1608451

Castro, C., Rojas, J., Ortíz, J., Sanhueza-Lepe, R., Vergara, A., Poblete, F., Escobar, E., Coba de la Peña, T., Ostria-Gallardo, E., Bascuñan-Godoy, L. (2024). Nitrogen Stress

Memory in Quinoa: Maternal Effects on Seed Metabolism and Offspring Growth and Physiology. *Physiol Plant*. 176(6):e14614. doi: 10.1111/ppl.14614. PMID: 39513412.

Chapin, F. S., Bloom, A. J., Field, C. B., and Waring, R. H. (1987). Plant Responses to Multiple Environmental Factors. *BioScience*, *37*(1), 49–57.

Ciampitti, I. A., Murrell, S. T., Camberato, J. J., Tuinstra, M., Xia, Y., Friedemann, P., and Vyn, T. J. (2013). Physiological dynamics of maize nitrogen uptake and partitioning in response to plant density and nitrogen stress factors: II. Reproductive phase. *Crop Science*, *53*(6), 2588–2602. https://doi.org/10.2135/cropsci2013.01.0041

Cisse, A., Zhao, X., Fu, W., Kim, R. E. R., Chen, T., Tao, L., and Feng, B. (2020). Non-Photochemical Quenching Involved in the Regulation of Photosynthesis of Rice Leaves under High Nitrogen Conditions. *Int J Mol Sci.* **21**(6):2115. doi: 10.3390/ijms21062115

Cong, W., Miao, Y., Xu, L., Zhang, Y., Yuan, C., Wang, J., Zhuang, T., Lin, X., Jiang, L., Wang, N., Ma, J., Sanguinet, K. A., Liu, B., Rustgi, S., and Ou, X. (2019). Transgenerational memory of gene expression changes induced by heavy metal stress in rice (Oryza sativa L.). *BMC Plant Biology*, *19*(1), 1–14. https://doi.org/10.1186/s12870-019-1887-7

Crawford, N. M., and Forde, B. G. (2002). Molecular and developmental biology of inorganic nitrogen nutrition. *The Arabidopsis Book*, *1*, e0011. https://doi.org/doi:10.1199/tab.0011

Donohue, K., and Schmitt, J. (1998). Maternal environmental effects in plants. In T. M. and C. Fox (Ed.), *Maternal Effects as Adaptations* (pp. 137–158). Oxford University Press, New York.

Falconer, D. S. (1981). *Introduction to Quantitative Genetics* (2nd Editio). Longman Group Ltd., London.

Fait, A., Angelovici, R., Less, H., Ohad, I., Urbanczyk-Wochniak, E., Fernie, A. R., and Galili, G. (2006). Arabidopsis seed development and germination is associated with temporally distinct metabolic switches. *Plant Physiology*, *142*(3), 839–854. https://doi.org/10.1104/pp.106.086694

Fenner, M. (2010). Environmental Influences on Seed Size and Composition. In *Horticultural Reviews* (Vol. 13). https://doi.org/10.1002/9780470650509.ch5

Fraire-Velázquez, S., and Balderas-Hernández, V. E. (2013). Abiotic Stress in Plants and Metabolic Responses. In K. Vahdati and C. Leslie (Eds.), *Abiotic Stress - Plant Responses and Applications in Agriculture*. IntechOpen.

Fuentes, S. I., Allen, D. J., Ortiz-Lopez, A., and Hernández, G. (2001). Over-expression of cytosolic glutamine synthetase increases photosynthesis and growth at low nitrogen concentrations. *Journal of Experimental Botany*, *52*(358), 1071–1081. https://doi.org/10.1093/jexbot/52.358.1071

Gan, S., and Amasino, R. M. (1997). Making sense of senescence: Molecular genetic regulation and manipulation of leaf senescence. *Plant Physiology*, *113*(2), 313–319. https://doi.org/10.1104/pp.113.2.313

Gamir, J., Sánchez-Bel, P., and Flors, V. (2014). Molecular and physiological stages of priming: how plants prepare for environmental challenges. *Plant Cell Reports*, *33*(12), 1935–1949. https://doi.org/10.1007/s00299-014-1665-9

Gargiulo, L., Grimberg, Å., Repo-Carrasco-Valencia, R., Carlsson, A. S., and Mele, G. (2019). Morpho-densitometric traits for quinoa (Chenopodium quinoa Willd.) seed phenotyping by two X-ray micro-CT scanning approaches. *Journal of Cereal Science*, *90*(May), 102829. https://doi.org/10.1016/j.jcs.2019.102829

Gazzarrini, S., Lejay, L., Gojon, A., Ninnemann, O., Frommer, W. B., and Von Wirén, N. (1999). Three functional transporters for constitutive, diurnally regulated, and starvation-induced uptake of ammonium into Arabidopsis roots. *Plant Cell*, *11*(5), 937–947. https://doi.org/10.1105/tpc.11.5.937

Gaufichon, L., Reisdorf-Cren, M., Rothstein, S. J., Chardon, F., and Suzuki, A. (2010). Biological functions of asparagine synthetase in plants. *Plant Science*, *179*(3), 141–153. https://doi.org/10.1016/j.plantsci.2010.04.010

Gentile, D., Serino, G., and Frugis, G. (2024). CRF transcription factors in the trade-off between abiotic stress response and plant developmental processes. *Front. Genet.* 15:1377204. doi: 10.3389/fgene.2024.1377204

Gu, R., Duan, F., An, X., Zhang, F., von Wirén, N., and Yuan, L. (2013). Characterization of AMT-mediated high-affinity ammonium uptake in roots of maize (Zea mays L.). *Plant and Cell Physiology*, *54*(9), 1515–1524. https://doi.org/10.1093/pcp/pct099

Gundel, P. E., Rudgers, J. A., and Whitney, K. D. (2017). Vertically transmitted symbionts as mechanisms of transgenerational effects. *American Journal of Botany*, *104*(5), 787–792. https://doi.org/10.3732/ajb.1700036

Hara, Y., and Toriyama, K. (1998). Seed nitrogen accelerates the rates of germination, emergence, and establishment of rice plants. *Soil Science and Plant Nutrition*, *44*(3), 359–366. https://doi.org/10.1080/00380768.1998.10414457

Herman, J. J., and Sultan, S. E. (2011). Adaptive transgenerational plasticity in plants: Case studies, mechanisms, and implications for natural populations. *Frontiers in Plant Science*, *2*(DEC), 1–10. https://doi.org/10.3389/fpls.2011.00102

Hernández Estévez, I., and Rodríguez Hernández, M. (2020). Plant Glutathione S-transferases: An overview. *Plant Gene*. 23, 100233. https://doi.org/10.1016/j.plgene.2020.100233.

Huertas, R., Ding, N., Scheible, W., and Udvardi, M. (2024). Transcriptional, Metabolic, Physiological and Developmental Responses to Nitrogen Limitation in Switchgrass (Panicum virgatum). *Environmental and Experimental Botany*. **222**, 105770. https://doi.org/10.1016/j.envexpbot.2024.105770.

INIA. (2015). Quínoa: Un súper Alimento Para Chile y el Mundo. *Tierra Adentro*, *N° 108*, 84.

Jacobsen, E. E., Skadhauge, B., and Jacobsen, S. E. (1997). Effect of dietary inclusion of quinoa on broiler growth performance. *Animal Feed Science and Technology*, *65*(1–4), 5–14. https://doi.org/10.1016/S0377-8401(96)01082-6

Jacobsen, S.-E., and Stølen, O. (1993). Quinoa - Morphology, phenology and prospects for its production as a new crop in Europe. *European Journal of Agronomy*, *2*(1), 19–29. https://doi.org/10.1016/s1161-0301(14)80148-2

Kambona, C. M., Koua, P. A. Léon, J., and Ballvora, A. (2023). Intergenerational and Transgenerational Effects of Drought Stress on Winter Wheat (Triticum aestivum L.). *Physiologia plantarum*. 175. e13951. 10.1111/ppl.13951.

Kou, H. P., Li, Y., Song, X. X., Ou, X. F., Xing, S. C., Ma, J., Von Wettstein, D., and Liu, B. (2011). Heritable alteration in DNA methylation induced by nitrogen-deficiency stress accompanies enhanced tolerance by progenies to the stress in rice (Oryza sativa L.). *Journal of Plant Physiology*, *168*(14), 1685–1693. https://doi.org/10.1016/j.jplph.2011.03.017

Krapp, A., Berthomé, R., Orsel, M., Mercey-Boutet, S., Yu, A., Castaings, L., Elftieh, S., Major, H., Renou, J. P., and Daniel-Vedele, F. (2011). Arabidopsis roots and shoots show distinct temporal adaptation patterns toward nitrogen starvation. *Plant Physiology*, *157*(3), 1255–1282. https://doi.org/10.1104/pp.111.179838

Krasensky, J., and Jonak, C. (2012). Drought, salt, and temperature stress-induced metabolic rearrangements and regulatory networks. *Journal of Experimental Botany*, *63*(4), 1593–1608. https://doi.org/10.1093/jxb/err460

Kronzucker, H. J., Schjoerring, J. K., Enter, Y., Kirk, G. J. D., Yaeesh Siddiqi, M., and Glass, A. D. M. (1998). Dynamic interactions between root NH4+ influx and long-

distance N translocation in rice: Insights into feedback processes. *Plant and Cell Physiology*, *39*(12), 1287–1293. https://doi.org/10.1093/oxfordjournals.pcp.a029332

Lamelas, L., López-Hidalgo, C., Valledor, L., Meijón, M. and Cañal, M.J. (2024). Like mother like son: Transgenerational memory and cross-tolerance from drought to heat stress are identified in chloroplast proteome and seed provisioning in Pinus radiata. *Plant, Cell and Environment*, 47, 1640–1655. https://doi.org/10.1111/pce.14836

Lämke, J., and Bäurle, I. (2017). Epigenetic and chromatin-based mechanisms in environmental stress adaptation and stress memory in plants. *Genome Biology*, *18*(1), 1–11. https://doi.org/10.1186/s13059-017-1263-6

Lea, P. J., and Forde, B. G. (1994). The use of mutants and transgenic plants to study amino acid metabolism. *Plant Cell Environ.*, *17*, 541–556.

Lea, P. J., and Miflin, B. J. (2011). Nitrogen Assimilation and its Relevance to Crop Improvement. In *Nitrogen Metabolism in Plants in the Post-genomic Era* (Vol. 42, pp. 1–40). https://doi.org/10.1002/9781444328608.ch1

Lee, R. B., and Rudge, K. A. (1986). Effects of nitrogen deficiency on the absorption of nitrate and ammonium by barley plants. *Annals of Botany*, *57*(4), 471–486. https://doi.org/10.1093/oxfordjournals.aob.a087129

Li, G., Meng, X., Zhu, M., and Li, Z. (2019). Research progress of betalain in response to adverse stresses and evolutionary relationship compared with anthocyanin. *Molecules*, *24*(17). https://doi.org/10.3390/molecules24173078

Li, G., Zhao, Y., Liu, F., Shi, M., Guan, Y., Zhang, T., Zhao, F., Qiao, Q., and Geng, Y. (2022). Transcriptional memory of gene expression across generations participates in transgenerational plasticity of field pennycress in response to cadmium stress. *Front. Plant Sci.* 13:953794. doi: 10.3389/fpls.2022.953794

Liss, P. S., and Slater, P. G. (1974). Alternative rute for nitrogen assimilation in higher plants. *Nature*, *251*, 614–616.

Liu, H. P., Able, A. J., and Able, J. A. (2021). Nitrogen Starvation-Responsive MicroRNAs Are Affected by Transgenerational Stress in Durum Wheat Seedlings. *Plant (Basel)*, **10**(5), 826. doi: 10.3390/plants10050826

Liu, Y., and von Wirén, N. (2017). Ammonium as a signal for physiological and morphological responses in plants. *Journal of Experimental Botany*, *68*(10), 2581–2592. https://doi.org/10.1093/jxb/erx086

López, M. E., Denoyes, B., and Bucher, E. (2024). Epigenomic and transcriptomic persistence of heat stress memory in strawberry (*Fragaria vesca*). *BMC Plant Biol* **24**, 405. https://doi.org/10.1186/s12870-024-05093-6

López-Fernández, M. P., and Maldonado, S. (2013). Programmed cell death during quinoa perisperm development. *Journal of Experimental Botany*, *64*(11), 3313–3325. https://doi.org/10.1093/jxb/ert170

Luo, J., Li, H., Liu, T., Polle, A., Peng, C., and Luo, Z. B. (2013). Nitrogen metabolism of two contrasting poplar species during acclimation to limiting nitrogen availability. *Journal of Experimental Botany* **64**(14), 4207–4224. https://doi.org/10.1093/jxb/ert234

Lu, Y., Gao, L., Hu, J., Liu, X., Jiang, D., Cao, W., Dai, T., and Tian, Z. (2024). Low nitrogen priming improves nitrogen uptake and assimilation adaptation to nitrogen deficit stress in wheat seedling. *Planta*, **259**, 107. https://doi.org/10.1007/s00425-024-04385-3

Mäck, G., and Tischner, R. (1994). Constitutive and Inducible net NH+4 Uptake of Barley (Hordeum vulgare L.) Seedlings. *Journal of Plant Physiology*, *144*(3), 351–357. https://doi.org/10.1016/S0176-1617(11)81198-3

Marek, L. F., and Stewart, C. R. (1992). Photosynthesis and photorespiration in presenescent, senescent, and rejuvenated soybean cotyledons. *Plant Physiology*, *98*(2), 694–699. https://doi.org/10.1104/pp.98.2.694

Marschner, H. (2012). *Marschner's Mineral Nutrition of Higher Plants* (2nd ed.). Elsevier Science.

Martínez, E. A., Veas, E., Jorquera, C., San Martín, R., and Jara, P. (2009). Re-introduction of Quínoa into arid Chile: Cultivation of two lowland races under extremely low irrigation. *Journal of Agronomy and Crop Science*, *195*(1), 1–10. https://doi.org/10.1111/j.1439-037X.2008.00332.x

Masclaux-Daubresse, C., Daniel-Vedele, F., Dechorgnat, J., Chardon, F., Gaufichon, L., and Suzuki, A. (2010). Nitrogen uptake, assimilation and remobilization in plants: Challenges for sustainable and productive agriculture. *Annals of Botany*, *105*(7), 1141–1157. https://doi.org/10.1093/aob/mcq028

Massaro, M., De Paoli, E., Tomasi, N., Morgante, M., Pinton, R., and Zanin, L. (2019). Transgenerational Response to Nitrogen Deprivation in *Arabidopsis thaliana*. *Int J Mol Sci,* **20**, 5587. doi: 10.3390/ijms20225587

Miller, A. J., Fan, X., Orsel, M., Smith, S. J., and Wells, D. M. (2007). Nitrate transport and signalling. *Journal of Experimental Botany*, *58*(9), 2297–2306. https://doi.org/10.1093/jxb/erm066

Moll, R. H., Kamprath, E. J., and Jackson, W. A. (1982). Analysis and Interpretation of Factors Which Contribute to Efficiency of Nitrogen Utilization. *Agronomy Journal*, *74*(3), 562–564. https://doi.org/10.2134/agronj1982.00021962007400030037x

Mousseau, T. A., and Fox, C. W. (1998). The adaptive significance of maternal effects. *Trends in Ecology and Evolution*, *13*(10), 403–407.

Mu, X., Chen, Q., Chen, F., Yuan, L., and Mi, G. (2018). Dynamic remobilization of leaf nitrogen components in relation to photosynthetic rate during grain filling in maize. *Plant Physiology and Biochemistry*, *129*(December 2017), 27–34. https://doi.org/10.1016/j.plaphy.2018.05.020

Naing, A. H., and Kim, C. K. (2021). Abiotic stress-induced anthocyanins in plants: Their role in tolerance to abiotic stresses. *Physiologia Plantarum*, *172*(3), 1711–1723. https://doi.org/10.1111/ppl.13373

Neill, S.J., Desikan, R. and Hancock, J.T. (2003), Nitric oxide signalling in plants. New Phytologist, 159: 11-35. https://doi.org/10.1046/j.1469-8137.2003.00804.x

Neill, S., Barros, R., Bright, J., Desikan, R., Hancock, J., Harrison, J., Morris, P., Ribeiro, D., and Wilson, I. (2008). Nitric oxide, stomatal closure, and abiotic stress, *Journal of Experimental Botany*, Volume 59, Issue 2, February 2008, Pages 165–176, https://doi.org/10.1093/jxb/erm293

Nowak, V., Du, J., and Charrondière, U. R. (2016). Assessment of the nutritional composition of quinoa (Chenopodium quinoa Willd.). *Food Chemistry*, *193*, 47–54. https://doi.org/10.1016/j.foodchem.2015.02.111

O'Brien, J. A. A., Vega, A., Bouguyon, E., Krouk, G., Gojon, A., Coruzzi, G., and Gutiérrez, R. A. A. (2016). Nitrate Transport, Sensing, and Responses in Plants. *Molecular Plant*, *9*(6), 837–856. https://doi.org/10.1016/j.molp.2016.05.004

Pissolato, M. D., Martins, T. S., and Fajardo, Y. C. G. *et al.* (2024). Stress memory in crops: what we have learned so far. *Theor. Exp. Plant Physiol.* **36**, 535–565. https://doi.org/10.1007/s40626-024-00315-6

Prescott, C., Grayston, S., Helmisaari, H., Kaštovská, E., Körner, C., Lambers, H., Meier, I., Millard, P., and Ostonen, I. (2020). Surplus Carbon Drives Allocation and Plant-Soil Interactions. *Trends in ecology & evolution*. https://doi.org/10.1016/j.tree.2020.08.007.

Putnam, H. M., and Gates, R. D. (2015). Preconditioning in the reef-building coral *Pocillopora damicornis* and the potential for trans-generational acclimatization in coral larvae under future climate change conditions. *Journal of Experimental Biology*, *218*(15), 2365–2372. https://doi.org/10.1242/jeb.123018

Rasmann, S., De Vos, M., Casteel, C. L., Tian, D., Halitschke, R., Sun, J. Y., Agrawal, A. A., Felton, G. W., and Jander, G. (2012). Herbivory in the previous generation primes plants for enhanced insect resistance. *Plant Physiology*, *158*(2), 854–863. https://doi.org/10.1104/pp.111.187831

Raven, J. A., and Farquhar, G. D. (1981). Methylammonium Transport in Phaseolus vulgaris Leaf Slices. *Plant Physiology*, *67*(4), 859–863. https://doi.org/10.1104/pp.67.4.859

Rawat, S. R., Silim, S. N., Kronzucker, H. J., Siddiqi, M. Y., and Glass, A. D. M. (1999). AtAMT1 gene expression and NH4+ uptake in roots of Arabidopsis thaliana: Evidence for regulation by root glutamine levels. *Plant Journal*, *19*(2), 143–152. https://doi.org/10.1046/j.1365-313X.1999.00505.x

Roach, D. A., and Wulff, R. D. (1987). Maternal effects in plants. *Annual Review of Ecology and Systematics. Vol. 18*, *18*(1987), 209–235. https://doi.org/10.1146/annurev.es.18.110187.001233

Sahay, S., Grzybowski, M., Schnable, J. C., Głowacka, K. (2024). Genotype-specific nonphotochemical quenching responses to nitrogen deficit are linked to chlorophyll a to b ratios. *J Plant Physiol*. 297: 154261. doi: 10.1016/j.jplph.2024.154261.

Schmidt, D. D., and Baldwin, I. T. (2006). Transcriptional responses of Solanum nigrum to methyl jasmonate and competition: A glasshouse and field study. *Functional Ecology*, *20*(3), 500–508. https://doi.org/10.1111/j.1365-2435.2006.01122.x

Shahri, W. (2011). Senescence: Concepts and Synonyms. *Asian Journal of Plant Sciences*, *10*(1), 24–28. https://doi.org/10.3923/ajps.2011.24.28

Shi, X., Gupta, S., and Rashotte, A. M. (2013). Characterization of two tomato AP2/ERF genes, *SlCRF1* and *SlCRF2* in hormone and stress responses. *Plant Cell Rep* **33**, 35–45. https://doi.org/10.1007/s00299-013-1510-6

Soriano, D., Orozco-Segovia, A., Mrquez-Guzmn, J., Kitajima, K., Gamboa-De Buen, A., and Huante, P. (2011). Seed reserve composition in 19 tree species of a tropical deciduous forest in Mexico and its relationship to seed germination and seedling growth. *Annals of Botany*, *107*(6), 939–951. https://doi.org/10.1093/aob/mcr041

Sultan, S. E. (1996). Phenotypic plasticity for offspring traits in Polygonum persicaria. *Ecology*, *77*, 1791–1807.

Thanos, C. A., and Rundel, P. W. (1995). Fire-Followers in Chaparral: Nitrogenous Compounds Trigger Seed Germination. *The Journal of Ecology*, *83*(2), 207. https://doi.org/10.2307/2261559

Ullrich, W. R., Larsson, M., Larsson, C.-M., Lesch, S., and Novacky, A. (1984). Ammonium uptake in Lemna gibba G 1, related membrane potential changes, and inhibition of anion uptake. *Physiol. Plant.*, *61*, 369–376.

Von Wirén, N., Gazzarrini, S., and Frommer, W. B. (1997). Regulation of mineral nitrogen uptake in plants. In *Plant and Soil* (Vol. 196, Issue 2, pp. 191–199). https://doi.org/10.1023/A:1004241722172

Wang, M. Y., Siddiqi, M. Y., Ruth, T. J., and Glass, A. D. M. (1993). Ammonium uptake by rice roots. I. Fluxes and Subcellular Distribution of 13NH4+. *Plant Physiology*, *103*, 1249–1258. https://doi.org/10.1104/pp.104.3.899

Wen, D., Xu, H., Xie, L., He, M., Hou, H., and Zhang, C. (2017). A loose endosperm structure of wheat seed produced under low nitrogen level promotes early germination by accelerating water uptake. *Scientific Reports*, *7*(1), 1–11. https://doi.org/10.1038/s41598-017-03333-4

Yin, J., Zhou, M., Lin, Z., Li, Q. Q., and Zhang, Y. Y. (2019). Transgenerational effects benefit offspring across diverse environments: a meta-analysis in plants and animals. *Ecology Letters*, *22*(11), 1976–1986. https://doi.org/10.1111/ele.13373

Zhao, L., Cai, B., Zhang, X., Zhang, B., Feng, J., Zhou, D., Chen, Y., Zhang, M., Qi, D., Wang, W., et al. (2024). Physiological and Transcriptional Characteristics of Banana Seedlings in Response to Nitrogen Deficiency Stress. *Horticulturae* **10**, 290. https://doi.org/10.3390/ horticulturae10030290